

IP3
FSAR UPDATE

CHAPTER 2

SITE AND ENVIRONMENT

2.1 SUMMARY OF CONCLUSIONS

This Chapter sets forth the site and environmental data which together formed the basis for many of the criteria for designing the facility and for evaluating the routine and accidental releases of radioactive liquids and gases to the environment. These data support the conclusion that there will be no undue risk to public health and safety due to plant operation. The strength of this conclusion rests with these data and the determinations (also included in this report) of several independent consultants, each speaking within a particular area of expertise - health physics, demography, geology, seismology, hydrology or meteorology, as the case may be.

The task of evaluating the environmental characteristics of the area was facilitated by the fact that more than 12 years of studies and measurements of environmental characteristics were undertaken. For over twenty years, measurements have been made of the effects on the environment of releases from at least one operating nuclear power facility at the Indian Point Site.

Conservative projections have been made of the growth of population in the area and these projections have been taken into account in plant design and operation as to control the effects of accidents. Population estimates are presented in subchapter 2.4.

The census data for 1990 reveals that the population within a 10-mile radius of the site was approximately 238,043 whereas the 2000 estimated population is 564,200. The land is now zoned principally for residential and state park usage although there is some industrial activity and a little agricultural and grazing activity. The projections do not indicate that the land usage within this radius will shift appreciably during the period of plant operation.

Geologically, the site consists of a hard limestone formation in a jointed condition which provides a solid bed for the plant foundation. The bedrock is sufficiently sound to support any loads up to 50 tons per square foot, which is far in excess of any load imposed by the plant. Although it is hard, the jointed limestone formation is permeable to water. Thus, if water from the plant should enter the ground (an improbable event since the plant is designed to preclude any leakage into the ground) it would percolate to the river rather than enter any ground water supply. Additional studies by the geology consultant, Thomas W. Fluhr, and examination of soil borings confirmed the above conclusions.

In the Hudson River, about 80,000,000 gallons of water flow past the plant each minute during the peak tidal flow. This flow provides additional mixing and dilution for liquid discharges from the facility. Plant design was based on the conservative assumption that the river water is used for drinking, thus radioactive discharges are reduced by dilution with ordinary plant effluent to concentrations that would be tolerable for drinking water. There is very little danger of flooding at the site.

Significant seismic activity in the Indian Point area is rare and no damage has resulted therefrom. As stated by the consultant on seismology, the site is "practically non-seismic" and is as safe as any area, at present known." Notwithstanding such assurance, the plant is designed to withstand an earthquake of the highest intensity ever recorded in this area.

IP3 FSAR UPDATE

Meteorological conditions in the area of the site were determined during a two-year test program (1955 to 1957). The validity of these conclusions was verified by a test program completed in October 1970. The meteorological analysis also includes data from periods of November 26, 1969 through October 1, 1970, and January 1, 1970 through December 31, 1971. These data were used in evaluating the effects of gaseous discharges from the plant during normal operations and during a postulated Loss-of-Coolant Accident. In addition, data supplied by the U.S. Weather Bureau at the Bear Mountain Station, regarding the meteorological conditions during periods of precipitation, have been used to evaluate the rainout of fission gases into surface water reservoirs following a postulated Loss-of-Coolant Accident. The evaluations indicate that the site meteorology provides adequate diffusion and dilution of any released gases.

Environmental radioactivity has been measured at the site and surrounding area for nearly twenty years in association with the operation of Indian Point 1, and the construction and operation of Indian Point 2 and 3. These measurements are being continued and reported as dictated by the Technical Specifications and ODCM. The radiation measurements of fallout, water samples, vegetation, marine life, etc. have shown no perceptible post-operative increase in radioactivity due to plant operations. Noticeable increases in fallout have coincided with weapons testing programs and appear to be related almost entirely to those programs. The New York State Department of Health, in an independent two-year post-operative study⁽¹⁾, found that environmental radioactivity in the vicinity of the site is no higher than anywhere else in the State of New York.

Consultants who participated in the preparation of the various reports, measurements and conclusions appearing in this Chapter included Dr. Merrill Eisenbud, then Director of Environmental Radiation Laboratory, Institute of Industrial Medicine, New York University; Dr. Benjamin Davidson (deceased), Meteorologist and Director, Geophysical Science Laboratory, New York University College of Engineering; Dr. James Halitski, then Senior Research Scientist, Department of Meteorology and Oceanography, New York University, College of Engineering; Dr. Edgar M. Hoover, then at the Regional Economic Development Institute, Inc.; Metcalf & Eddy Engineers, hydrology specialists; Rev. J. J. Lynch, S. J., then Director of the Seismic Observatory, Fordham University; Mr. Sidney Paige, then Consulting Geologist; Quirk, Lawler and Matusky Engineers, Environmental Science and Engineering Consultants; Mr. Karl R. Kennison, Consulting Civil and Hydraulic Engineer; Mr. Thomas W. Fluhr, P.E., Consulting Engineering Geologist; Reports by Captain Elliott B. Roberts, Chief of the Geophysics Division, U.S. Department of Commerce and by Mr. James Dorman, then at the Lamont Geologist Observatory, Columbia University. And also, Reports by Parsons, Brincherhoff, Quade and Douglas Inc., Engineers; Dames & Moore, Consultants; and Woodward-Clyde, Consultants.

References

- 1) Consolidated Edison Indian Point Reactor Post Operational Survey - August, 1965, Division of Environmental Health Services, New York State Department of Health, Hollis S. Ingraham, M.D., Commissioner.
- 2) Consolidated Edison Indian Point Reactor Environmental and Post Operation Survey - July, 1966, Division of Environmental Health Services, New York State Department of Health, Hollis S. Ingraham, M.D., Commissioner.

2.2 LOCATION

2.2.1 General

The Indian Point site comprises approximately 239 acres of land on the east bank of the Hudson River at Indian Point, Village of Buchanan, in upper Westchester County, New York. Indian Point 3 is located adjacent to and south of Unit No. 1 with Indian Point 2 adjacent to and north of Unit No. 1, which has been retired. The site is about 24 miles north of the New York City boundary line. The nearest city is Peekskill, 2.5 miles northeast of Indian Point. [Deleted]

The minimum distance from the Indian Point 3 reactor center line to the boundary of the site exclusion area and the outer boundary of the low population zone, as defined in 10 CFE 100.3 and 10 CFR 100.11, is 350 meters and 1100 meters, respectively.

2.2.2 Site Ownership and Control

Entergy is the sole owner of the Indian Point 3 Nuclear Power Plant. Figure 2.2-2 shows the land owned by Entergy at the Indian Point site. Plant Drawing 9321-F-64513 [Formerly Figure 2.2-3] shows a plot plan of Indian Point 3 and the boundary line and the Hudson River. Figure 2.2-4 shows the Indian Point Energy Center site ownership boundaries, the location of surrounding communities, and the Low Population Zone for Indian Point 3.

The Georgia – Pacific Corporation has an easement, (approximately 1610 feet long and 30 feet wide), along Entergy's southerly property line. The Georgia – Pacific easement is used for overhead electrical power and telephone lines, and for underground gas, water and sewer lines. These easements permit Entergy to determine all activities within the right-of-way in order to ensure safe operation of the Units.

As shown in Figure 2.2-2, the Algonquin Gas Transmission Company has a 26 inch gas mainline and a 30 inch gas main line on a right-of-way (approximately 1350 feet long and 65 feet wide) running east to west through Entergy's property. One 30 inch main and two 24 inch mains pass under the river to a pipeline facilities station on the easement near the river. One 24 inch main is available as a bypass alternative and ends in the pipeline facilities station while the other two continue as the 30 and 26 inch mains. The threats posed by the rupture of these pipelines and the release of natural gas (essentially methane) from them were addressed in Item 7 of Supplement 1 to the original FSAR. The September 21, 1973 SER concluded the failure of these gas lines would not impair the safe operation of the plant.

A subsequent evaluation in 2008 (Reference 1) discussed the consequences of fire and explosion due to a pipeline rupture. The hazards created by a breach and explosion of the pressurized above ground portions of the pipeline include:

- a. potential missiles,
- b. an over-pressurization event,
- c. a vapor cloud or flash fire,
- d. a hypothetical vapor cloud explosion, and
- e. a jet fire

A simultaneous rupture and ignition of both gas mains at the above ground locations inside the owner controlled area (OCA) is postulated to be the worst case scenario since this event will result in the most significant release of gas volume and have the potential to contribute to the largest potential fire. An attempt to uncover, breach and ignite a buried portion of the pipeline

IP3 FSAR UPDATE

was not considered feasible. The report concluded that the rupture of the natural gas pipelines that cross the Indian Point site and subsequent ignition of the methane released will result in a jet fire and injury or death to any people exposed to flames or intense thermal radiation. It will not, however, damage any safety related structure. Even in the unlikely event of a hypothetical vapor cloud explosion, structural damage to buildings other than the waterfront warehouse adjacent to the pipelines will not occur. A flammable vapor cloud fire that engulfs the plant is improbable because the turbulent momentum with which the methane exits the pipeline will confine flammable methane concentrations to the point of release.

The Algonquin Gas Transmission Company has installed a 42 inch gas pipeline that crosses the Hudson south of the site property and turns north. It passes through the easternmost corner of the site and then crosses Broadway between the Switchyard and the GT 2 / 3 fuel oil storage tank. The 42 inch gas line joins the 30 inch and 26 inch gas pipelines north of the switchyard and east of the site. A safety evaluation performed for the proposed pipeline and the juncture with the 30 and 26 inch pipelines concluded that the failure of these gas lines would not impair the safe operation of the plant because the effects are acceptable or can be excluded by probability (Reference 2).

An additional analysis (Reference 3) of a potential rupture of the underground portions of the existing pipeline was subsequently performed using the same methodology as for the 42 inch pipeline. This was requested due to allegations. It was concluded that safe operation would not be impaired since the plant would be able to safely shutdown following any affects such as damage to overhead transmission lines and that the probability of ruptures were sufficiently remote that ruptures could be excluded based on probability. During operation of the 42 inch pipeline the 26 inch pipeline will normally be idled (at normal operating pressure but no gas flow) which further restricts probability.

The Indian Point 3 protected area is enclosed by a chain link type security fence surmounted by three-strand barbed wire as indicated in Entergy's Security Plan. Appropriate control is maintained by Entergy at all access points into the Indian Point 3 security protected area. In addition, some areas within the protected area are designated as "vital areas" and access is controlled by a system of identification badges/card keys, locks and alarms.

Employees, who would need access to or through any portions of Entergy property, are required to adhere to the security provisions and check points operated and controlled by Entergy's security force. Details of Entergy's security program are given in the Security Plan for Indian Point Energy Center.

2.2.3 Access

The site is accessible by several roads in the Village of Buchanan. Two paved roads link the eastern boundary of the site to the existing plant. The site is not served by rail. The Indian Point 3 protected area is bounded by chain link-type fencing, or the equivalent, and contains an interior roadway system, access to which is under the control of Entergy's Guard Force.

IP3 FSAR UPDATE

2.2.4 Control of Exclusion and Restricted Area

In the event of an emergency situation at any of the Indian Point Units, the person in charge at that Unit shall immediately inform the person in charge at the other units. Further action, evaluation or institution of the offsite emergency plan will then depend on the seriousness of the emergency situation. Further details are provided in the Indian Point Energy Center Emergency Plan.

Control of the Indian Point Site Restricted Area to exclude unauthorized personnel at all times is controlled by IPEC. IPEC has responsibility for maintaining direct and continuous control over the persons on its property.

2.2.5 Activities on the Site

The principal activities on the site are the generation, transmission and distribution of electrical energy; associated service activities; activities relating to the controlled conversion of the nuclear energy of fuel to heat energy by the process of nuclear fission; and the storage, utilization and production of special nuclear, source and by-product materials.

2.3 TOPOGRAPHY

The Indian Point Site is surrounded on almost all sides by high ground ranging from 600 to 1000 feet above sea level. The site is located on the east bank of the Hudson River, which runs northeast to southwest at this point but turns sharply northwest approximately two miles northeast of the plant. The west bank of the Hudson is flanked by the steep, heavily wooded slopes of the Dunderberg and West Mountains to the northwest (elevations 1086 feet and 1257 feet respectively) and Buckberg Mountain to the west-southwest (elevation 793 feet). These peaks extend to the west by other names and gradually rise to slightly higher peaks.

The general orientation of this mass of high ground is northeast to southwest. One mile northwest of the site, Dunderberg bulges to the east, and north of Dunderberg and the site, high ground reaching 800 feet forms the east bank of the Hudson as the river makes a sharp turn to the northwest. To the east of the site, peaks are generally lower than those to the north and west. Spitzenberg and Blue Mountains average about 600 feet in height and there is a weak, poorly defined series of ridges which again seem to run in a north-northeast direction. The river south of the site makes another sharp bend to the southeast and the widens as it flows past Croton and Haverstraw.

[Deleted]

2.4 POPULATION

2.4.1 General

An initial report was prepared by Environmental Analysis, Inc. in June 1972. The report, which is included herein (see pages 2.4.P-1 to 2.4.P-42), used the 1970 population census to update population estimates and population projections to the year 2010, in 10-year intervals, for an area within a sixty-mile radius of the Indian Point Nuclear Power Plant Site at Buchanan, New York.

IP3
FSAR UPDATE

The resident population distribution, based on a May 1970 report was presented graphically by indicating the population estimated for each of the individual area segments of the selected grid system. The population distribution for a 55 mile radius is presented in Figure 2.4-1. The grid was centered on the reactor facility and extended radially for a distance of 55 miles. This area was subdivided by concentric circles with radii of 15, 25, 35, 45, and 55 miles, and by equally spaced radial lines.

The grid system, superimposed on the geographical area surrounding the site, for a 60-mile radius, is shown in Figure 2.4-2. Each sector of 22.5° was based on a line segment 11.25° from north (resulting in two subdivisions of the north bisected 22.5° sector); the others were designed in a clockwise fashion. The number of persons residing in each segment, based on the 1972 report, is presented in Figures 2.4-3 and 2.4-4 for the 5-mile and 60-mile radii, respectively.

Table 2.4-1, based on the June 1972 report, is a summary of the cumulative ring population estimates for the years 1970 to 2010, in 10 year increments, for complete ring zones up to sixty miles from the site.

In 1992, the Authority submitted new demographic and population distribution data on the Nuclear Regulatory Commission as part of its License Extension Request. This data shows that the projections performed in 1972 by Environmental Analysts were quite realistic, although slightly conservative. The rate of growth within the 50 mile radius was slightly slower than projected. Projections through 2010 should, thus, be viewed as conservative.

In 2003, KLD Associates, Inc. updated population distribution data for the 50 mile radius surrounding Indian Point using 2000 Census data. Table 2.4-2 summarizes this data by Zone. Tables 2.4-3 through 2.4-18 show population distribution by sector and zone. Table 2.4-19 shows population by segment. A comparison of the 1972 projections with 2000 Census data continues to show that projections through 2010 should be viewed as conservative.

A comparison of the 1972 projections found in Table 2.4-1 with 1990 and 2000 Census data is shown below:

	1990 Projection from 1972 Study	1990 Census	2000 Projection from 1972 Study	2000 Census
0-2 miles	15,673	16,774	20,698	12,442
0-5 miles	84,512	73,935	129,397	77,619
0-10 miles	408,198	237,338	564,220	257,475

Projections through 2010 should thus be viewed as conservative.

2.4.2 Population Centers

The closest population centers (defined in 10 CFR 100 as containing more than 25,000 residents) are Newburgh, N.Y. and White Plains, N.Y., both approximately 17 miles from the plant site. However, based on projected populations, the outer boundary of the more densely populated area of the City of Peekskill has been conservatively selected as the closest population center.

2.4.3 Low Population Zone

The Code of Federal Regulations, Title 10, Part 100 requires that a reactor be so situated that there is no population center, which is defined as a city of no less than 25,000 people, having its nearest boundary closer than 1-1/3 times the low population zone radius. Based on the 10 CFR 100 definition, and the outer boundary of the more densely populated area of the City of Peekskill as the population center, the low population zone (LPZ) for the plant is 1100 meters. (See Figure 2.2-4)

About 50 people reside within the low population zone, all of them to the east-southeast. This estimate of 50 people (a number which is expected to remain fairly static) is based on a survey of the area conducted by Consolidated Edison in September 1971.

2.4.4 Exclusion Area

The exclusion area for Indian Point 3 is shown in Figure 2.2-2. The minimum distance from the reactor containment to the boundary of the exclusion area is 350 meters. This exclusion area satisfied both 10 CFR 100.3 and 10 CFR 100.11.

2.4.5 Land Usage

Figures 2.4-6, 2.4-7, and 2.4-8 show, respectively, the land usage based upon official zoning maps, areas served by public utilities and areas served by sewage systems. The area surrounding the Indian Point Site is generally residential with some large parks and military reservations. The majority of the area to the east of the river within 15 miles of the site is zoned for residential usage as shown on the map in Figure 2.4-6. West of the river, within a fifteen-mile radius, the Palisades Interstate Park and residential areas are the dominant land usage. The only agricultural areas within fifteen miles are south and northwest of the plant, on the west side of the river.

References

- 1) IP-RPT-08-00032, "Consequences of Fire and Explosion Following the Release of Natural Gas from Pipelines Adjacent to Indian Point," by David Allen, Risk Research Group, August 2008
- 2) Entergy letter NL-15-030, "Revised 10 C.F.R. 50.59 Safety Evaluation and Supporting Analyses Prepared in Response to the Algonquin Incremental Market Natural Gas Project," dated April 8, 2015
- 3) IP-RPT-15-00048, "Consequences of a Postulated Fire or Explosion Following the Release of Natural Gas from the Existing 26" and 30" Pipelines Near IPEC," David Allen, Risk Research Group, October, 2015

IP3
FSAR UPDATE

Table 2.4-1

SUMMARY OF CUMULATIVE RING POPULATION ESTIMATES
(JUNE 1972)

<u>Radius of the Ring in Miles</u>	<u>Cumulative Ring Population Estimates</u>				
	1970	1980	1990	2000	2010
Half	21	31	45	65	88
One	745	1,008	1,375	1,891	2,453
Two	9,255	11,981	15,673	20,698	26,016
Three	20,318	25,747	33,045	42,926	53,349
Four	34,553	44,338	57,544	75,482	94,451
Five	52,683	70,053	94,512	129,397	168,164
Ten	218,398	297,459	408,198	564,220	734,682
Fifteen	450,207	603,034	814,078	1,107,195	1,423,387
Twenty	888,163	1,179,611	1,577,851	2,125,429	2,711,048
Thirty	3,984,844	4,637,627	5,480,207	6,584,630	7,724,505
Forty	11,659,574	12,882,240	14,403,268	16,333,563	18,276,655
Fifty	17,471,479	18,991,980	20,923,966	23,400,331	25,899,727
Sixty	19,510,656	21,383,172	23,821,556	26,997,743	30,235,074

IP3
FSAR UPDATE

Table 2.4-2

2000 Population Estimates By 360 Degree Zone

ZONE	2000 Population	Accumulated Totals
0-1 mile	1,971	
1-2 miles	10,471	
2-3 miles	19,516	
3-4 miles	18,791	
4-5 miles	26,870	77,619 (within 5 miles)
5-6 miles	27,674	
6-7 miles	21,404	
7-8 miles	25,688	
8-9 miles	49,767	
9-10 miles	55,323	257,475 (within 10 miles)
10-15 miles	398,447	
15-20 miles	460,697	
20-25 miles	1,116,848	2,233,467 (within 25 miles)
25-30 miles	2,205,078	
30-35 miles	2,544,937	
35-40 miles	3,734,393	
40-45 miles	3,833,427	
45-50 miles	2,232,598	16,783,900 (within 50 miles)

IP3
FSAR UPDATE

Table 2.4-3

2000 Population Estimates
Population Distribution By Sector and Zone

SECTOR: 1 (North)

<u>Zone</u>	<u>2000 Population</u>
0-1 mile	0
1-2 miles	11
2-3 miles	109
3-4 miles	183
4-5 miles	343
5-6 miles	300
6-7 miles	1,322
7-8 miles	2,395
8-9 miles	7,460
9-10 miles	182
10-15 miles	1,366
15-20 miles	43,748
20-25 miles	32,751
25-30 miles	54,348
30-35 miles	48,971
35-40 miles	18,752
40-45 miles	20,142
45-50 miles	41,358

IP3
FSAR UPDATE

Table 2.4-4
2000 Population Estimates
Population Distribution By Sector and Zone

SECTOR: 2 (North-Northeast)

<u>Zone</u>	<u>2000 Population</u>
0-1 mile	0
1-2 miles	0
2-3 miles	314
3-4 miles	661
4-5 miles	1,716
5-6 miles	921
6-7 miles	1,044
7-8 miles	340
8-9 miles	838
9-10 miles	1,235
10-15 miles	2,453
15-20 miles	4,967
20-25 miles	23,111
25-30 miles	22,593
30-35 miles	8,417
35-40 miles	10,711
40-45 miles	8,153
45-50 miles	2,859

IP3
FSAR UPDATE

Table 2.4-5

2000 Population Estimates
Population Distribution By Sector and Zone

SECTOR: 3 (Northeast)

<u>Zone</u>	<u>2000 Population</u>
0-1 mile	17
1-2 miles	3,439
2-3 miles	9,774
3-4 miles	4,510
4-5 miles	2,973
5-6 miles	3,823
6-7 miles	3,356
7-8 miles	1,760
8-9 miles	1,196
9-10 miles	1,097
10-15 miles	14,549
15-20 miles	14,593
20-25 miles	14,498
25-30 miles	11,974
30-35 miles	18,004
35-40 miles	18,775
40-45 miles	6,511
45-50 miles	7,254

IP3
FSAR UPDATE

Table 2.4-6

2000 Population Estimates
Population Distribution By Sector and Zone

SECTOR: 4 (East-Northeast)

<u>Zone</u>	<u>2000 Population</u>
0-1 mile	7
1-2 miles	1,653
2-3 miles	2,841
3-4 miles	3,238
4-5 miles	2,178
5-6 miles	3,683
6-7 miles	2,473
7-8 miles	4,797
8-9 miles	6,936
9-10 miles	6,915
10-15 miles	24,469
15-20 miles	13,258
20-25 miles	20,375
25-30 miles	89,902
30-35 miles	35,294
35-40 miles	21,347
40-45 miles	22,265
45-50 miles	78,210

IP3
FSAR UPDATE

Table 2.4-7

2000 Population Estimates
Population Distribution By Sector and Zone

SECTOR: 5 (East)

<u>Zone</u>	<u>2000 Population</u>
0-1 mile	334
1-2 miles	315
2-3 miles	24
3-4 miles	950
4-5 miles	594
5-6 miles	620
6-7 miles	1,545
7-8 miles	1,355
8-9 miles	3,224
9-10 miles	3,426
10-15 miles	15,387
15-20 miles	8,093
20-25 miles	26,346
25-30 miles	22,542
30-35 miles	22,092
35-40 miles	172,384
40-45 miles	167,423
45-50 miles	88,353

IP3
FSAR UPDATE

Table 2.4-8

2000 Population Estimates
Population Distribution By Sector and Zone

SECTOR: 6 (East-Southeast)

<u>Zone</u>	<u>2000 Population</u>
0-1 mile	251
1-2 miles	192
2-3 miles	757
3-4 miles	656
4-5 miles	918
5-6 miles	304
6-7 miles	75
7-8 miles	319
8-9 miles	626
9-10 miles	2,113
10-15 miles	19,280
15-20 miles	11,355
20-25 miles	34,346
25-30 miles	141,922
30-35 miles	61,824
35-40 miles	18,609
40-45 miles	3,254
45-50 miles	29,437

IP3
FSAR UPDATE

Table 2.4-9

2000 Population Estimates
Population Distribution By Sector and Zone

SECTOR: 7 (Southeast)

<u>Zone</u>	<u>2000 Population</u>
0-1 mile	807
1-2 miles	922
2-3 miles	1,543
3-4 miles	2,490
4-5 miles	694
5-6 miles	4,590
6-7 miles	2,630
7-8 miles	3,004
8-9 miles	10,085
9-10 miles	6,001
10-15 miles	37,224
15-20 miles	18,930
20-25 miles	101,556
25-30 miles	37,702
30-35 miles	12,330
35-40 miles	80,302
40-45 miles	239,071
45-50 miles	309,332

IP3
FSAR UPDATE

Table 2.4-10

2000 Population Estimates
Population Distribution By Sector and Zone

SECTOR: 8 (South-Southeast)

<u>Zone</u>	<u>2000 Population</u>
0-1 mile	435
1-2 miles	2,042
2-3 miles	868
3-4 miles	136
4-5 miles	217
5-6 miles	0
6-7 miles	90
7-8 miles	0
8-9 miles	3,864
9-10 miles	9,817
10-15 miles	21,348
15-20 miles	116,963
20-25 miles	218,703
25-30 miles	295,031
30-35 miles	258,202
35-40 miles	603,637
40-45 miles	756,484
45-50 miles	464,715

IP3
FSAR UPDATE

Table 2.4-11

2000 Population Estimates
Population Distribution By Sector and Zone

SECTOR: 9 (South)

<u>Zone</u>	<u>2000 Population</u>
0-1 mile	68
1-2 miles	541
2-3 miles	0
3-4 miles	0
4-5 miles	1,229
5-6 miles	5,661
6-7 miles	942
7-8 miles	4,716
8-9 miles	7,829
9-10 miles	7,864
10-15 miles	45,274
15-20 miles	47,358
20-25 miles	354,441
25-30 miles	926,582
30-35 miles	1,620,749
35-40 miles	2,099,064
40-45 miles	1,934,401
45-50 miles	743,893

IP3
FSAR UPDATE

Table 2.4-12

2000 Population Estimates
Population Distribution By Sector and Zone

SECTOR: 10 (South-Southwest)

<u>Zone</u>	<u>2000 Population</u>
0-1 mile	52
1-2 miles	604
2-3 miles	420
3-4 miles	2,853
4-5 miles	10,900
5-6 miles	5,970
6-7 miles	3,378
7-8 miles	3,778
8-9 miles	6,101
9-10 miles	10,856
10-15 miles	106,089
15-20 miles	68,692
20-25 miles	160,698
25-30 miles	437,592
30-35 miles	325,993
35-40 miles	529,035
40-45 miles	452,790
45-50 miles	351,395

IP3
FSAR UPDATE

Table 2.4-13

2000 Population Estimates
Population Distribution By Sector and Zone

SECTOR: 11 (Southwest)

<u>Zone</u>	<u>2000 Population</u>
0-1 mile	0
1-2 miles	0
2-3 miles	2,115
3-4 miles	2,486
4-5 miles	3,853
5-6 miles	626
6-7 miles	4,496
7-8 miles	3,090
8-9 miles	1,388
9-10 miles	2,955
10-15 miles	17,690
15-20 miles	40,837
20-25 miles	48,470
25-30 miles	69,388
30-35 miles	49,562
35-40 miles	98,399
40-45 miles	139,699
45-50 miles	58,048

IP3
FSAR UPDATE

Table 2.4-14

2000 Population Estimates
Population Distribution By Sector and Zone

SECTOR: 12 (West-Southwest)

<u>Zone</u>	<u>2000 Population</u>
0-1 mile	0
1-2 miles	457
2-3 miles	518
3-4 miles	628
4-5 miles	221
5-6 miles	433
6-7 miles	48
7-8 miles	134
8-9 miles	0
9-10 miles	5
10-15 miles	5,052
15-20 miles	4,381
20-25 miles	17,860
25-30 miles	15,165
30-35 miles	23,446
35-40 miles	22,991
40-45 miles	52,496
45-50 miles	27,668

IP3
FSAR UPDATE

Table 2.4-15

2000 Population Estimates
Population Distribution By Sector and Zone

SECTOR: 13 (West)

<u>Zone</u>	<u>2000 Population</u>
0-1 mile	0
1-2 miles	295
2-3 miles	154
3-4 miles	0
4-5 miles	0
5-6 miles	0
6-7 miles	0
7-8 miles	0
8-9 miles	0
9-10 miles	20
10-15 miles	6,164
15-20 miles	11,313
20-25 miles	17,014
25-30 miles	9,836
30-35 miles	18,522
35-40 miles	15,831
40-45 miles	11,592
45-50 miles	5,663

IP3
FSAR UPDATE

Table 2.4-16

2000 Population Estimates
Population Distribution by Sector and Zone

SECTOR: 14 (West-Northwest)

<u>Zone</u>	<u>2000 Population</u>
0-1 mile	0
1-2 miles	0
2-3 miles	19
3-4 miles	0
4-5 miles	0
5-6 miles	0
6-7 miles	0
7-8 miles	0
8-9 miles	217
9-10 miles	1,633
10-15 miles	36,983
15-20 miles	10,970
20-25 miles	14,136
25-30 miles	47,249
30-35 miles	12,119
35-40 miles	6,654
40-45 miles	3,682
45-50 miles	6,307

IP3
FSAR UPDATE

Table 2.4-17

2000 Population Estimates
Population Distribution By Sector and Zone

SECTOR: 15 (Northwest)

<u>Zone</u>	<u>2000 Population</u>
0-1 mile	0
1-2 miles	0
2-3 miles	60
3-4 miles	0
4-5 miles	192
5-6 miles	0
6-7 miles	0
7-8 miles	0
8-9 miles	3
9-10 miles	1,204
10-15 miles	9,477
15-20 miles	10,441
20-25 miles	12,645
25-30 miles	10,588
30-35 miles	15,017
35-40 miles	9,956
40-45 miles	6,814
45-50 miles	14,385

IP3
FSAR UPDATE

Table 2.4-18

2000 Population Estimates
Population Distribution By Sector and Zone

SECTOR: 18 (North-Northwest)

<u>Zone</u>	<u>2000 Population</u>
0-1 mile	0
1-2 miles	0
2-3 miles	0
3-4 miles	0
4-5 miles	842
5-6 miles	743
6-7 miles	5
7-8 miles	0
8-9 miles	0
9-10 miles	0
10-15 miles	35,642
15-20 miles	34,798
20-25 miles	19,898
25-30 miles	12,664
30-35 miles	14,395
35-40 miles	7,946
40-45 miles	8,650
45-50 miles	3,721

IP3
FSAR UPDATE

TABLE 2.4-19

PERMANENT RESIDENT
POPULATION BY SEGMENT

Segment	Ring (Miles)	Residential Population
1-N	0-2	11
2-NNE	0-2	0
3-NE	0-2	3,456
4-ENE	0-2	1,660
5-E	0-2	649
6-ESE	0-2	443
7-SE	0-2	1,729
8-SSE	0-2	2,477
9-S	0-2	609
10-SSW	0-2	656
11-SW	0-2	0
12-WSW	0-2	457
13-W	0-2	295
14-WNW	0-2	0
15-NW	0-2	0
16-NNW	0-2	0
Ring 0-2 Miles		12,442
1-N	2-5	635
2-NNE	2-5	2,691
3-NE	2-5	17,257
4-ENE	2-5	8,257
5-E	2-5	1,568
6-ESE	2-5	2,331
7-SE	2-5	4,727
8-SSE	2-5	1,221
9-S	2-5	1,229
10-SSW	2-5	14,173
11-SW	2-5	8,454
12-WSW	2-5	1,367
13-W	2-5	154
14-WNW	2-5	19
15-NW	2-5	252
16-NNW	2-5	842
Ring 2-5 Miles		65,177

IP3
FSAR UPDATE

Segment	Ring (Miles)	Residential Population
N	5-10	11,659
NNE	5-10	4,378
NE	5-10	11,232
ENE	5-10	24,804
E	5-10	10,170
ESE	5-10	3,437
SE	5-10	26,310
SSE	5-10	13,771
S	5-10	27,012
SSW	5-10	30,083
SW	5-10	12,555
WSE	5-10	620
W	5-10	20
WNW	5-10	1,850
NW	5-10	1,207
NNW	5-10	748
Ring 5-10 Miles		163,403
Cumulative Totals		
Total 0-2 Miles		12,442
Total 0-5 Miles		77,619
Total 0-10 Miles		257,475

IP3
FSAR UPDATE

[Historical Information]

POPULATION ESTIMATES FOR 1970
and
THE POPULATION PROJECTIONS TO 2010
for
SPECIFIED ZONES WITHIN A SIXTY-MILE RADIUS
of
INDIAN POINT NUCLEAR POWER PLANT SITE

FOR

CONSOLIDATED EDISON COMPANY OF NEW YORK, INC.
4 Irving Place
New York, New York 10003

Prepared by

ENVIRONMENTAL ANALYSTS, INC.
224 Seventh Street
Garden City, New York 11530

June, 1972

2.4.P-1

IP3
FSAR UPDATE

TABLE OF CONTENTS

<u>SECTION</u>	<u>TITLE</u>	<u>PAGE</u>
I	INTRODUCTION	1
II	1970 POPULATION ESTIMATION METHODS	4
III	POPULATION ESTIMATES FOR THE YEAR 1970	6
IV	METHODS OF POPULATION PROJECTION	11
V	POPULATION PROJECTIONS FOR THE YEAR 1980	12
VI	POPULATION PROJECTIONS FOR THE YEAR 1990	17
VII	POPULATION PROJECTIONS FOR THE YEAR 2000	22
VIII	POPULATION PROJECTIONS FOR THE YEAR 2010	27
XI	APPENDIX	33
X	REFERENCES	40

INTRODUCTION

This report provides the 1970 population estimates and the population projections for the years 1980, 1990, 2000 and 2010 for the area within a sixty-mile radius of the Indian Point Nuclear Power Plant site at Buchanan, New York.

The area encompassed by the sixty-mile radius circle was divided into 16 sectors of $22^{\circ} - 30'$. The north oriented sector is formed by two radii, $11^{\circ} - 15'$ on either side of the true north as shown in Figure 1. This sector is referred to as sector "A" and succeeding sectors, B through P are drawn in the clockwise direction.

The area within the sixty-mile radius was further divided by 13 rings drawn about the Indian Point Nuclear Power Plant site as follows:

- Two rings, each at a half-mile interval, for the first mile from the site.

- Four rings, each at a one-mile interval, from one mile to five miles from the site.

- Three rings, each at a five-mile interval, from five miles to twenty miles from the site.

- Four rings, each at a ten-mile interval, from twenty to sixty miles from the site.

The population estimates for the year 1970 and the population projection for the years 1980, 1990, 2000 and 2010 for each of the 208 zones formed by the sectors and the rings are given in this report.

The summary of cumulative ring population estimations for the years 1970, 1980, 1990, 2000 and 2010 is given in Table 1.

2.4.P-3

Figure 1. Ring and Sector Orientation

Table I

SUMMARY OF CUMULATIVE RING POPULATION ESTIMATES

RADIUS OF THE
RING IN MILES CUMULATIVE RING POPULATION ESTIMATES

	1970	1980	1990	2000	2010
Half	21	31	45	65	88
One	745	1,008	1,375	1,891	2,453
Two	9,255	11,981	15,673	20,698	26,016
Three	20,318	25,747	33,045	42,926	53,349
Four	34,553	44,338	57,544	75,482	94,451
Five	52,683	70,053	94,512	129,397	168,164
Ten	218,398	297,459	408,198	564,220	734,682
Fifteen	450,207	603,035	814,078	1,107,195	1,423,387
Twenty	888,163	1,179,611	1,577,851	2,125,429	2,711,048
Thirty	3,984,844	4,637,627	5,480,207	6,584,630	7,724,505
Forty	11,659,574	12,882,240	14,403,268	16,333,563	18,276,655
Fifty	17,471,479	18,991,980	20,923,966	23,400,331	25,899,727
Sixty	19,510,656	21,383,172	23,821,556	26,997,743	30,235,074

2.4.P-5

II. 1970 POPULATION ESTIMATION METHODS

The area within a 60-mile radius is divided by rings and sectors, into 208 zones. For the purpose of estimating 1970 population, the zones were divided into three categories. The first category included the 32 zones within the initial one-mile radius. The second consisted of the 64 zones between the one and five-mile radii. The third category consisted of the remaining 112 zones between the five and 60-mile radii.

The zones in the first category are relatively small. Those within a half-mile radius of the Indian Point have an area of approximately 0.05 square miles. The land area of the zones between the one-half mile and one-mile radii is approximately 0.15 square miles. There is a substantial possibility of error in estimating population for these small zones because census data on such a fine scale is not always available. For this reason, Consolidated Edison made a door-to-door survey to determine the exact population within a one-half mile radius of the site. In addition, a field observation of the area within a one-mile radius, including an actual count of dwelling units, was made on January 26, 1972. The population within one mile of the site was estimated on the basis of the data collected by Consolidated Edison, the field observations, and 1970 census tracts shown in the New York-Northeastern New Jersey Metropolitan Map Series.

The zones in the second category are somewhat larger. Their land area ranges from approximately 0.6 square miles, for the zones between the one and two mile radii, to approximately 1.8 miles for the zones between the four and five mile radii. Where census data was available for tracts or communities within zones, these data were used. Elsewhere within the second category zones, population was estimated by use of maps and field

inspection. In localities where large areas are fully developed with single-family dwellings, the total length of residential streets was measured by the use of a "map reader" The street length was then divided by 100 feet, which was the average plot width observed during the field survey, and multiplied by 3.5 persons per household, a figure obtained from the Bureau of the Census.

The zones in the third category are five to 60 miles from the plant site. The land area of each zone ranges from approximately 15 square miles, for zones between the 5 and 10 mile radii, to 216 square miles for zones between the 50 and 60 mile radii.

Because the outermost zones are so large, some villages, towns, cities, etc. are entirely located within a single zone. Therefore, the entire population of these communities, taken from the census population tables, could be ascribed to these zones.

For communities or census tracts located in more than one zone, the population was assumed to be distributed uniformly. The portion of the community or tract lying within each zone was determined by the use of a planimeter and a corresponding portion of its population was then attributed to that zone.

It should be emphasized that, for any given zone of the third category, the bulk of the population estimate is based on whole-tract or whole-community figures taken directly from the 1970 census tables. The component of the population estimate based on a real measurement is relatively minor. Therefore, the margin of error in these population estimates is considered to be small.

2.4.P-7

III. POPULATION ESTIMATES FOR THE 1970

The population estimates for the 13 rings are presented in Table 2 and the population estimates for the 208 specified zones are presented in Table 3.

Table 2

Ring Population Estimates for the Year 1970

Radius of the Ring in Miles	1970 Population Estimates
Half	21
One	724
Two	8,460
Three	11,063
Four	14,235
Five	18,130
Ten	165,715
Fifteen	231,809
Twenty	437,956
Thirty	3,096,681
Forty	7,674,730
Fifty	5,811,905
Sixty	2,039,177

IP3
FSAR UPDATE

Table 3

SPECIFIED ZONE POPULATION

BASED ON 1970 CENSUS

RING	SECTOR A	SECTOR B	SECTOR C	SECTOR D
0- ½ MILE	0	0	0	0
½- 1 MILE	0	0	0	18
1 - 2 MILES	0	0	1,050	1,470
2 - 3 MILES	158	840	2,880	1,890
3 - 4 MILES	280	875	2,135	1,855
4 - 5 MILES	525	2,240	2,660	2,100
5- 10 MILES	7,451	2,072	4,372	14,880
10 - 15 MILES	6,598	2,775	6,714	5,560
15 - 20 MILES	25,952	4,349	9,110	10,821
20 - 30 MILES	59,527	29,306	13,369	19,730
30 - 40 MILES	78,736	17,647	22,693	86,058
40 - 50 MILES	44,339	14,303	11,763	58,647
50 - 60 MILES	41,954	9,115	55,709	352,482
SECTOR TOTALS	265,520	83,522	132,455	555,511

2.4.P-9

IP3
FSAR UPDATE

Table 3 (Cont'd)

SPECIFIED ZONE POPULATION

BASED ON 1970 CENSUS

RING	SECTOR E	SECTOR F	SECTOR G	SECTOR H
0- ½ MILE	0	14	7	0
½- 1 MILE	280	62	140	210
1 - 2 MILES	630	630	910	1,470
2 - 3 MILES	263	298	683	1,068
3 - 4 MILES	980	1,085	1,190	595
4 - 5 MILES	875	385	1,190	385
5- 10 MILES	9,453	8,356	28,570	3,744
10 - 15 MILES	9,167	20,394	30,102	20,221
15 - 20 MILES	12,206	36,683	46,182	86,421
20 - 30 MILES	34,037	305,998	83,399	786,120
30 - 40 MILES	263,030	78,656	74,226	1,170,810
40 - 50 MILES	425,957	25,822	505,957	1,209,558
50 - 60 MILES	485,949	103,058	238,010	9,938
SECTOR TOTALS	1,242,827	581,441	1,010,566	3,290,540

2.4.P-10

IP3
FSAR UPDATE

Table 3 (Cont'd)

SPECIFIED ZONE POPULATION

BASED ON 1970 CENSUS

RING	SECTOR I	SECTOR J	SECTOR K	SECTOR L
0- ½ MILE	0	0	0	0
½- 1 MILE	14	0	0	0
1 - 2 MILES	680	910	10	300
2 - 3 MILES	53	263	840	350
3 - 4 MILES	105	1,610	1,505	560
4 - 5 MILES	245	2,415	945	560
5- 10 MILES	23,003	32,853	10,329	4,508
10 - 15 MILES	35,324	39,018	25,566	8,116
15 - 20 MILES	55,912	80,640	27,058	5,766
20 - 30 MILES	985,563	539,709	121,568	19,934
30 - 40 MILES	3,612,246	2,039,326	147,590	39,326
40 - 50 MILES	2,477,415	727,826	207,086	57,451
50 - 60 MILES	60,320	531,848	97,847	23,871
SECTOR TOTALS	7,255,880	3,996,418	640,344	160,742

2.4.P-11

IP3
FSAR UPDATE

Table 3 (Cont'd)

SPECIFIED ZONE POPULATION

BASED ON 1970 CENSUS

RING	SECTOR M	SECTOR N	SECTOR O	SECTOR P
0- ½ MILE	0	0	0	0
½- 1 MILE	0	0	0	0
1 - 2 MILES	420	0	0	30
2 - 3 MILES	504	98	595	280
3 - 4 MILES	0	0	1,155	305
4 - 5 MILES	630	875	840	1,260
5- 10 MILES	421	2,289	6,138	7,276
10 - 15 MILES	2,469	8,939	3,017	7,829
15 - 20 MILES	6,545	3,878	6,293	20,140
20 - 30 MILES	10,527	40,661	15,053	32,180
30 - 40 MILES	11,445	8,574	12,553	11,814
40 - 50 MILES	9,290	4,287	19,665	12,539
50 - 60 MILES	146	6,330	11,601	5,999
SECTOR TOTALS	42,397	75,931	76,910	99,652

2.4.P-12

IV. METHODS OF POPULATION PROJECTIONS

In May, 1970, Regional Economic Development Institute, Inc. (REDI) prepared a report entitled, "Population Estimates for 1960 and 2000 for the Specified Zones in a 60-Mile Area Around Indian Point New York", for the Consolidated Edison Company of New York, Inc. The various methods of population projection used by REDI, Inc. are presented in the appendix of this report.

For this report, it is assumed that the population growth between 1970 and the year 2010 will be the same as the growth projected by REDI, Inc. for the forty-year period between 1960 and the year 2000. Hence, the ratio of the population of the year 2000 to the population of the year 1960 was calculated for each specified zone by using REDI, Inc. data. These ratios were multiplied by the 1970 population to project the population for the year 2010 in each specified zone.

The population for the years 1980, 1990 and 2000 was projected by assuming a linear growth rate between the years 1970 and 2010.

V. POPULATION PROJECTIONS FOR THE YEAR 1980

The population projections for the 13 rings is presented in Table 4 and the population projections for the 208 specified zones is presented in Table 5.

IP3
FSAR UPDATE

Table 4

Ring Population Projections for the Year 1980

Radius of the Ring in Miles	Population Projected for the Year 1980
Half	31
One	977
Two	10,973
Three	13,766
Four	18,591
Five	25,715
Ten	227,406
Fifteen	305,576
Twenty	576,576
Thirty	3,458,016
Forty	8,244,613
Fifty	6,109,740
Sixty	2,391,193

2.4.P-14

IP3
FSAR UPDATE

Table 5

SPECIFIED ZONE POPULATION

PROJECTED FOR THE YEAR 1980

RING	SECTOR A	SECTOR B	SECTOR C	SECTOR D
0- ½ MILE	0	0	0	0
½- 1 MILE	0	0	0	21
1 - 2 MILES	0	0	1,149	1,608
2 - 3 MILES	210	1,121	3,140	2,057
3 - 4 MILES	408	1,275	2,333	2,278
4 - 5 MILES	700	3,265	4,690	3,061
5- 10 MILES	10,407	3,205	6,569	22,169
10 - 15 MILES	9,420	3,781	9,855	8,283
15 - 20 MILES	34,219	6,965	13,765	15,766
20 - 30 MILES	77,309	46,669	20,419	25,993
30 - 40 MILES	108,058	25,776	31,217	129,318
40 - 50 MILES	54,497	19,933	15,110	76,898
50 - 60 MILES	57,349	12,419	37,400	428,480
SECTOR TOTALS	352,577	124,409	145,647	715,932

2.4.P-15

IP3
FSAR UPDATE

Table 5 (Cont'd)

SPECIFIED ZONE POPULATION

PROJECTED FOR THE YEAR 1980

RING	SECTOR E	SECTOR F	SECTOR G	SECTOR H
0- ½ MILE	0	20	10	0
½- 1 MILE	335	89	204	306
1 - 2 MILES	821	862	1,314	1,962
2 - 3 MILES	383	434	1,025	1,426
3 - 4 MILES	1,198	1,581	1,635	794
4 - 5 MILES	1,275	551	1,517	514
5- 10 MILES	14,124	12,220	34,059	5,020
10 - 15 MILES	13,167	27,158	40,157	23,322
15 - 20 MILES	17,427	53,074	56,279	103,985
20 - 30 MILES	50,326	357,186	98,194	840,603
30 - 40 MILES	296,179	94,020	99,455	1,214,673
40 - 50 MILES	504,338	38,066	390,456	1,249,092
50 - 60 MILES	543,492	153,458	173,378	11,301
SECTOR TOTALS	1,443,065	738,719	897,683	3,452,998

2.4.P-16

IP3
FSAR UPDATE

Table 5 Cont'd)

SPECIFIED ZONE POPULATION

PROJECTED FOR THE YEAR 1980

RING	SECTOR I	SECTOR J	SECTOR K	SECTOR L
0- ½ MILE	0	0	0	0
½- 1 MILE	20	0	0	0
1 - 2 MILES	907	1,282	14	422
2 - 3 MILES	74	370	1,017	493
3 - 4 MILES	124	1,994	2,117	790
4 - 5 MILES	258	2,989	1,327	747
5- 10 MILES	30,901	44,980	14,625	6,019
10 - 15 MILES	42,392	52,052	32,874	10,779
15 - 20 MILES	70,628	104,318	37,016	8,401
20 - 30 MILES	1,027,136	586,325	160,145	27,571
30 - 40 MILES	3,781,447	2,139,556	210,150	57,226
40 - 50 MILES	2,540,338	790,690	291,572	79,766
50 - 60 MILES	99,923	687,334	122,455	33,942
SECTOR TOTALS	7,594,148	4,411,890	873,312	226,156

2.4.P-17

IP3
FSAR UPDATE

Table 5 Cont'd)

SPECIFIED ZONE POPULATION

PROJECTED FOR THE YEAR 1980

RING	SECTOR M	SECTOR N	SECTOR O	SECTOR P
0- ½ MILE	0	0	0	0
½- 1 MILE	0	0	0	0
1 - 2 MILES	583	0	0	42
2 - 3 MILES	711	130	794	373
3 - 4 MILES	0	0	1,627	430
4 - 5 MILES	841	1,168	1,121	1,682
5- 10 MILES	562	3,056	8,914	10,567
10 - 15 MILES	2,084	13,580	4,813	11,849
15 - 20 MILES	10,074	5,675	9,503	29,473
20 – 30 MILES	15,490	55,759	23,063	45,820
30 – 40 MILES	15,793	11,315	15,647	14,775
40 – 50 MILES	11,592	5,652	24,759	16,973
50 – 60 MILES	173	7,626	14,189	8,265
SECTOR TOTALS	57,903	103,961	104,430	140,249

2.4.P-18

V. POPULATION PROJECTIONS FOR THE YEAR 1990

The population projections for the 13 rings is presented in Table 6 and the population projections for the 208 specified zones is presented in Table 7.

Table 6

Ring Population Projections for the Year 1990

Radius of the Ring in Miles	Population Projected for the Year 1980
Half	45
One	1,330
Two	14,298
Three	17,372
Four	24,499
Five	36,968
Ten	313,686
Fifteen	405,880
Twenty	763,773
Thirty	3,902,356
Forty	8,923,061
Fifty	6,520,698
Sixty	2,897,591

IP3
FSAR UPDATE

Table 7

SPECIFIED ZONE POPULATION

PROJECTED FOR THE YEAR 1990

RING	SECTOR A	SECTOR B	SECTOR C	SECTOR D
0- ½ MILE	0	0	0	0
½- 1 MILE	0	0	0	25
1 - 2 MILES	0	0	1,258	1,761
2 - 3 MILES	281	1,497	3,424	2,239
3 - 4 MILES	595	1,859	2,550	2,798
4 - 5 MILES	935	4,761	8,270	4,463
5- 10 MILES	14,536	4,959	9,872	33,031
10 - 15 MILES	13,450	5,151	14,467	12,342
15 - 20 MILES	45,119	11,157	20,800	22,972
20 – 30 MILES	100,403	74,321	31,187	34,244
30 – 40 MILES	148,301	37,651	42,944	194,324
40 – 50 MILES	66,983	27,779	19,410	100,830
50 – 60 MILES	78,394	16,922	25,109	520,865
SECTOR TOTALS	468,997	186,057	179,291	929,894

2.4.P-20

IP3
FSAR UPDATE

Table 7 (Cont'd)

SPECIFIED ZONE POPULATION

PROJECTED FOR THE YEAR 1990

RING	SECTOR E	SECTOR F	SECTOR G	SECTOR H
0- ½ MILE	0	29	14	0
½- 1 MILE	402	128	297	446
1 - 2 MILES	1,070	1,180	1,900	2,620
2 - 3 MILES	559	633	1,538	1,904
3 - 4 MILES	1,465	2,306	2,248	1,060
4 - 5 MILES	1,859	791	1,935	686
5- 10 MILES	21,105	17,872	40,603	6,733
10 - 15 MILES	18,914	36,167	53,573	26,900
15 - 20 MILES	24,882	76,789	68,584	125,120
20 – 30 MILES	74,412	416,938	115,614	898,863
30 – 40 MILES	333,506	112,386	133,260	1,260,179
40 – 50 MILES	597,142	56,115	301,323	1,289,919
50 – 60 MILES	607,850	228,507	126,297	12,851
SECTOR TOTALS	1,683,166	949,841	847,186	3,627,281

2.4.P-21

IP3
FSAR UPDATE

Table 7 (Cont'd)

SPECIFIED ZONE POPULATION

PROJECTED FOR THE YEAR 1990

RING	SECTOR I	SECTOR J	SECTOR K	SECTOR L
0- ½ MILE	0	0	0	0
½- 1 MILE	29	0	0	0
1 - 2 MILES	1,212	1,806	20	595
2 - 3 MILES	105	521	1,233	694
3 - 4 MILES	148	2,470	2,979	1,114
4 - 5 MILES	273	3,700	1,863	998
5- 10 MILES	41,511	61,585	20,709	8,037
10 - 15 MILES	50,875	59,441	42,273	14,316
15 - 20 MILES	89,218	134,949	50,640	12,240
20 – 30 MILES	1,070,462	636,968	210,965	38,135
30 – 40 MILES	3,958,574	2,244,713	299,229	83,275
40 – 50 MILES	2,604,850	858,985	410,528	110,748
50 – 60 MILES	152,859	888,277	153,251	48,263
SECTOR TOTALS	7,970,125	4,893,415	1,193,690	318,415

2.4.P-22

IP3
FSAR UPDATE

Table 7 (Cont'd)

SPECIFIED ZONE POPULATION

PROJECTED FOR THE YEAR 1990

RING	SECTOR M	SECTOR N	SECTOR O	SECTOR P
0- ½ MILE	0	0	0	0
½- 1 MILE	0	0	0	0
1 - 2 MILES	810	0	0	59
2 - 3 MILES	1,003	174	1,060	499
3 - 4 MILES	0	0	2,292	607
4 - 5 MILES	1,123	1,559	1,497	2,246
5- 10 MILES	750	4,080	12,948	15,348
10 - 15 MILES	1,760	20,632	7,678	17,934
15 - 20 MILES	15,507	8,304	14,352	43,131
20 - 30 MILES	22,794	76,464	35,336	65,242
30 - 40 MILES	21,794	14,933	19,503	18,480
40 - 50 MILES	14,466	7,452	31,174	22,974
50 - 60 MILES	206	9,188	17,256	11,388
SECTOR TOTALS	80,213	142,786	143,196	197,908

2.4.P-23

VII. POPULATION PROJECTIONS FOR THE YEAR 2000

The population projections for the 13 rings is presented in Table 8 and the population projections for the 208 specified zones is presented in Table 9.

Table 8

Ring Population Projections for the Year 2000

Radius of the Ring in Miles	Population Projected for the Year 2000
Half	65
One	1,826
Two	18,807
Three	22,228
Four	32,556
Five	53,915
Ten	434,823
Fifteen	542,975
Twenty	1,018,234
Thirty	4,459,201
Forty	9,748,933
Fifty	7,066,768
Sixty	3,597,413

2.4.P-24

IP3
FSAR UPDATE

Table 9

SPECIFIED ZONE POPULATION

PROJECTED FOR THE YEAR 2000

RING	SECTOR A	SECTOR B	SECTOR C	SECTOR D
0- ½ MILE	0	0	0	0
½- 1 MILE	0	0	0	31
1 – 2 MILES	0	0	1,377	1,927
2 – 3 MILES	376	1,999	3,734	2,437
3 – 4 MILES	867	2,711	2,787	3,438
4 – 5 MILES	1,249	6,941	14,582	6,507
5- 10 MILES	20,303	7,672	14,834	49,213
10 – 15 MILES	19,203	7,019	21,236	18,388
15 – 20 MILES	59,492	17,870	31,429	33,471
20 – 30 MILES	130,396	118,356	47,634	45,115
30 – 40 MILES	203,530	54,996	59,077	292,008
40 – 50 MILES	82,329	38,715	24,934	132,210
50 – 60 MILES	107,162	23,058	16,857	633,170
SECTOR TOTALS	624,907	279,337	238,481	1,217,915

2.4.P-25

IP3
FSAR UPDATE

Table 9 (Cont'd)

SPECIFIED ZONE POPULATION

PROJECTED FOR THE YEAR 2000

RING	SECTOR E	SECTOR F	SECTOR G	SECTOR H
0- ½ MILE	0	43	21	0
½- 1 MILE	481	184	434	650
1 – 2 MILES	1,396	1,616	2,745	3,499
2 – 3 MILES	815	923	2,309	2,542
3 – 4 MILES	1,792	3,362	3,091	1,416
4 – 5 MILES	2,711	1,134	2,468	916
5- 10 MILES	31,535	26,138	48,404	9,029
10 – 15 MILES	27,169	48,164	71,470	31,027
15 – 20 MILES	35,526	111,102	83,580	150,551
20 – 30 MILES	110,026	468,686	136,125	961,161
30 – 40 MILES	375,538	134,339	178,554	1,307,391
40 – 50 MILES	707,024	82,724	232,536	1,332,080
50 – 60 MILES	679,829	340,259	92,001	14,614
SECTOR TOTALS	1,973,842	1,236,674	853,738	3,814,876

2.4.P-26

IP3
FSAR UPDATE

Table 9 (Cont'd)

SPECIFIED ZONE POPULATION

PROJECTED FOR THE YEAR 2000

RING	SECTOR I	SECTOR J	SECTOR K	SECTOR L
0- ½ MILE	0	0	0	0
½- 1 MILE	43	0	0	0
1 – 2 MILES	1,618	2,545	29	839
2 – 3 MILES	148	735	1,494	979
3 – 4 MILES	176	3,060	4,191	1,573
4 – 5 MILES	288	4,581	2,617	1,333
5- 10 MILES	55,765	84,318	29,324	10,731
10 – 15 MILES	61,055	92,638	54,358	19,014
15 – 20 MILES	112,701	174,575	69,279	17,835
20 – 30 MILES	1,115,616	691,985	277,911	52,746
30 – 40 MILES	4,143,998	2,355,039	426,066	121,182
40 – 50 MILES	2,681,019	933,179	578,015	153,765
50 – 60 MILES	233,837	1,147,965	191,794	68,626
SECTOR TOTALS	8,406,264	5,490,620	1,635,078	448,623

2.4.P-27

IP3
FSAR UPDATE

Table 9 (Cont'd)

SPECIFIED ZONE POPULATION

PROJECTED FOR THE YEAR 2000

RING	SECTOR M	SECTOR N	SECTOR O	SECTOR P
0- ½ MILE	0	0	0	0
½- 1 MILE	0	0	0	0
1 - 2 MILES	1,126	0	0	84
2 - 3 MILES	1,415	230	1,416	666
3 - 4 MILES	0	0	3,230	857
4 - 5 MILES	1,499	2,082	1,999	2,999
5- 10 MILES	1,002	5,449	18,806	22,292
10 - 15 MILES	1,486	31,345	12,250	27,143
15 - 20 MILES	23,870	12,153	21,675	63,118
20 - 30 MILES	33,541	104,858	54,141	92,987
30 - 40 MILES	30,074	19,708	24,311	23,113
40 - 50 MILES	18,052	9,826	39,251	31,099
50 - 60 MILES	244	11,070	21,229	15,690
SECTOR TOTALS	112,309	196,721	198,308	279,958

2.4.P-28

VIII. POPULATION PROJECTIONS FOR THE YEAR 2010

The population projections for the 13 rings is presented in Table 10 and the population projections for the 208 specified zones is presented in Table 11.

Table 10

Ring Population Projections for the Year 2010

Radius of the Ring in Miles	Population Projected for the Year 1980
Half	88
One	2,365
Two	23,563
Three	27,333
Four	41,102
Five	73,713
Ten	566,518
Fifteen	688,705
Twenty	1,287,661
Thirty	5,013,456
Forty	10,552,150
Fifty	7,623,072
Sixty	4,335,347

IP3
FSAR UPDATE

Table 11

SPECIFIED ZONE POPULATION

PROJECTED FOR THE YEAR 2010

RING	SECTOR A	SECTOR B	SECTOR C	SECTOR D
0- ½ MILE	0	0	0	0
½- 1 MILE	0	0	0	36
1 – 2 MILES	0	0	1,481	2,072
2 – 3 MILES	474	2,520	4,003	2,608
3 – 4 MILES	1,173	3,666	2,993	4,053
4 – 5 MILES	1,575	9,386	22,955	8,799
5- 10 MILES	26,526	10,878	20,548	67,704
10 – 15 MILES	25,534	8,991	28,870	25,298
15 – 20 MILES	74,223	26,050	43,728	45,232
20 – 30 MILES	160,723	171,733	66,845	56,248
30 – 40 MILES	262,191	74,470	76,248	404,473
40 – 50 MILES	97,102	50,490	30,466	164,212
50 – 60 MILES	137,609	29,533	12,256	740,212
SECTOR TOTALS	787,130	387,717	310,393	1,520,947

2.4.P-30

IP3
FSAR UPDATE

Table 11 (Cont'd)

SPECIFIED ZONE POPULATION

PROJECTED FOR THE YEAR 2010

RING	SECTOR E	SECTOR F	SECTOR G	SECTOR H
0- ½ MILE	0	59	29	0
½- 1 MILE	557	246	587	880
1 – 2 MILES	1,726	2,079	3,686	4,410
2 – 3 MILES	1,102	1,249	3,196	3,204
3 – 4 MILES	2,106	4,546	3,987	1,785
4 – 5 MILES	3,666	1,513	2,999	1,155
5- 10 MILES	43,483	35,429	55,712	11,419
10 – 15 MILES	36,301	60,570	90,005	34,780
15 – 20 MILES	47,237	149,300	97,906	174,570
20 – 30 MILES	150,444	550,796	155,124	1,014,094
30 – 40 MILES	412,947	154,952	225,647	1,346,431
40 – 50 MILES	809,318	112,842	188,999	1,366,800
50 – 60 MILES	743,502	467,883	71,403	16,198
SECTOR TOTALS	2,252,389	1,541,464	899,280	3,975,726

2.4.P-31

IP3
FSAR UPDATE

Table 11 (Cont'd)

SPECIFIED ZONE POPULATION

PROJECTED FOR THE YEAR 2010

RING	SECTOR I	SECTOR J	SECTOR K	SECTOR L
0- ½ MILE	0	0	0	0
½- 1 MILE	59	0	0	31
1 – 2 MILES	2,040	3,349	39	1,104
2 – 3 MILES	196	967	1,742	1,288
3 – 4 MILES	202	3,632	5,508	2,072
4 – 5 MILES	301	5,434	3,435	1,680
5- 10 MILES	70,619	108,414	38,733	13,524
10 – 15 MILES	70,648	116,663	66,471	23,861
15 – 20 MILES	135,866	214,502	89,020	24,102
20 – 30 MILES	1,153,108	739,401	346,468	68,374
30 – 40 MILES	4,298,572	2,447,191	565,270	163,597
40 – 50 MILES	2,725,156	997,122	760,005	199,929
50 – 60 MILES	328,559	1,409,397	229,498	90,948
SECTOR TOTALS	8,785,326	6,046,072	2,106,189	590,479

2.4.P-32

IP3
FSAR UPDATE

Table 11 (Cont'd)

SPECIFIED ZONE POPULATION

PROJECTED FOR THE YEAR 2010

RING	SECTOR M	SECTOR N	SECTOR O	SECTOR P
0- ½ MILE	0	0	0	0
½- 1 MILE	0	0	0	0
1 – 2 MILES	1,466	0	0	111
2 – 3 MILES	1,865	294	1,785	840
3 – 4 MILES	0	0	4,250	1,129
4 – 5 MILES	1,890	2,625	2,520	3,780
5- 10 MILES	1,263	6,867	25,350	30,049
10 – 15 MILES	1,298	43,801	17,800	37,814
15 – 20 MILES	33,706	16,482	30,143	85,595
20 – 30 MILES	45,687	134,995	76,168	123,249
30 – 40 MILES	38,913	24,607	28,997	27,644
40 – 50 MILES	21,552	12,260	47,196	39,623
50 – 60 MILES	281	12,850	24,942	20,276
SECTOR TOTALS	147,921	254,780	259,151	370,110

2.4.P-33

APPENDIX A

Methods of population projections used by
R.E.D.I., Inc. for their May 1970 Report
"Population Estimates for 1960 and 2000
for Specified Zones
in a 60-Mile Area Around Indian Point"

2.4.P-34

METHOD OF POPULATION PROJECTIONS USED BY R.E.D.I., INC.

In summary, the estimating method consisted of these two major steps:

Projections of total population in the year 2000, by counties, or parts of counties located within 60 miles from the site, were disaggregated by municipality or other minor civil divisions comprising the county, by two different equations, from which a compromise estimate was determined, and Population of municipalities or other minor civil divisions as reported in the 1960 Census of Population and the 2000 projected compromise estimate derived as above were allocated to the specified zone on the basis of the area and land use of the portion of the one or more municipalities lying in part in the given zone.

PROJECTING MUNICIPALITY POPULATION

Since the projection of population requires long and costly re-search, it was decided to utilize larger area projections made by a responsible agency in the area. Among projections of this nature reviewed were those made by the Regional Plan Association of New York, National Planning Association of Washington, D.C. and the Tri-State Transportation Commission. In terms of area coverage and time span,

2.4.P-35

those made by the Regional Plan Association (RPA) were found to be most suitable to the purposes of this study.

These RPA projections are the result of over fifteen years of study following the initial findings in the New York Metropolitan Region Study by Harvard University. The set used actually represents the estimates presently being utilized by the Association.

This RPA set required additional development of population estimates and projections for counties, or at least parts of counties, lying in the 60-mile area around the site but not covered by the RPA projections. The latest RPA set consists of New York City and 26 counties around New York City (5 of these counties were divided into two sub-areas to reflect major differences in density). Two of these are entirely outside of the 60-mile area around the site, but this area includes parts of 4 other counties not included in the RPA set. In summary, the 60-mile circle is made up of 36 areas, which may be classified into following sets: a) 23 full RPA-areas (representing 19 full counties); b) 9 areas that are portions of RPA-areas or counties; c) 4 areas that are parts of counties not belonging to the RPA Set.

The 2000 projections for those of these RPA counties which lie on the periphery of the 60-mile area around the site, were then scaled down to totals for only the municipalities or other minor civil divisions lying within or partially in this site-circumscribed area on the basis of their 1960 population as a per cent of the county total then.

2.4.P-36

IP3
FSAR UPDATE

For the four parts of counties in the site-circumscribed area but not in the RPA set, the 1960-2000 growth rates estimated for adjacent counties in the RPA set were used. The counties involved were,

Sullivan, New York
Columbia, New York
Pike, Pennsylvania
Hartford, Connecticut

It may be noted that since the parts of counties within the site-circumscribed area generally involved only a small strip of municipalities or other minor civil divisions, it is not unreasonable to assume that their growth patterns will approximate those of adjacent counties within the area.

The 1960 population and the 2000 projected estimates for the 36 counties and parts of counties used as control totals in the subsequent projections of municipality population, are reported in Table 3*.

The ordering of areas in this table is that in the latest RPA population projections study and is centered on Manhattan. This order was merely adopted for convenience and has no bearing on the subsequent development of estimates by zones within the site-circumscribed area.

*Six counties or parts of counties consist of a single municipality. Therefore, municipal disaggregation of county projections were not needed in these instances. Note that the population totals for the entire area reported in Table 3 are greater than those reported in Tables 1 and 2 because of municipalities on the fringe falling only partially within the 60-mile radius.

2.4.P-37

Using these county control totals, population in the constituent 638 municipalities or other minor civil divisions were projected to 2000 by the techniques developed in our 1965 study for the Indian Point site. The following repeats the description of these techniques, drawn from that study, with revision to fit the present exercise.

A. Extrapolative Projection. Our first set of projections is based on the assumption that places which grew faster than their counties in the 1950's will continue to do so, and that those which lagged behind their counties' growth in the 1950's will continue to lag for the balance of this century. Specifically, each municipality's population was first projected linearly to 2000, simply extending the 1950-1960 growth rate for another 40 years. This extrapolation was done on an arithmetic basis (using the 1950-1960 increase rate in persons per annum)*. The extrapolated figures for all the municipalities in each county or part of county were then totaled, and adjusted up or down pro rata to make the total conform to the RPA or other total already established for the county or part, as reported in Table 3.

* Geometric extrapolations would result in obviously unrealistic projections.

B. Density-Based Projection. One quite obvious shortcoming of the extrapolative technique just described is that it takes no account of restraints upon growth arising from the filling up of developable space. We sought, therefore, to develop an alternative set of projections which would incorporate the hypothesis that percentage rates of growth of individual communities slacken off with higher population densities per square mile.

In our earlier study, investigation disclosed a marked relationship of the expected sort in the 1950-1960 growth and density rate for municipalities. It appeared also that a straight-line regression relation between the logarithms of (1) the growth ratio and (2) the density of population at the beginning of the time interval provided a more appropriate formulation than a single linear relation.

Accordingly, the data on 1950 and 1960 population and land area for all municipalities were processed so as to yield a statistically fitted regression formula for municipalities in each county, relating rate of population growth to density of population. In fitting the equation, the data for individual municipalities were weighted according to population, giving larger places a proportionately greater influence on the formula.

2.4.P-39

These regression equations were generally associated with a high degree of correlation so as to leave little doubt as to the usefulness of this approach as a guide to relative rates of expected population growth.

The projections produced by this method for individual municipalities were then totaled for each county and adjusted to make the county totals conform to the RPA or other total already established for that county, or part of county, just as was done with the first or extrapolative set of projections.

C. Compromise Projection. The two alternative sets of projections just described rest on entirely different principles, each of which (the continuity of growth differentials, and the inverse relation of growth rate to density) has demonstrable validity but falls short of complete adequacy. Consequently, it seemed appropriate to combine the two types of projections into a third, incorporating both the continuity and the density effects.

To get this third set, labeled “com promise” projections, we took for each municipality the geometric mean between the adjusted extrapolative and the adjusted density-based projection. Then the “compromise” projections for the municipalities of each county were added up and adjusted to make the county total conform, as in the two previous cases, to the RPA or other total already established for the county or part of county.

The averaging procedure allows each of the two effects (growth-continuity and density) to exert an effect on the compromise projec-

tions. Where the extrapolative and the density-based projections were in close agreement, they reinforce each other in projecting differentiation of growth rates in different parts of a county; where the extrapolative and density-based projections give sharply differing answers, they tend to cancel one another out in terms of such differentiation, leading to compromise projections which show relatively little dissimilarity in growth rates among the part of a county. This seems appropriate – where the two approaches we have tried give very different results, we are well advised to take both of them less seriously and have less occasion for diverging very far from the simple assumption that all parts of any given county will grow at equal rates.

The geometric mean was chosen in preference to the arithmetic as a way of still further toning-down the most extreme variations of growth rates. It seems to us that the compromise projections are the “best” of the three so far as anyone can judge in advance. However, all three sets of projections are available for inspection should users of these reported results desire to make their own evaluations and decisions.

2.4.P-41

IP3
FSAR UPDATE

REFERENCES

1970 Census of Population of New York, New Jersey, Connecticut
and Pennsylvania

Vicinity Map Sheets of Poughkeepsie, Dutchess County, New York and Danbury,
Fairfield County, Connecticut

Census Tract Outline Maps for Patterson, New Jersey, New York
City, New York, Stamford, Norwalk and Bridgeport, Connecticut

County Map Sheets for Westchester, Putnam, Orange, Rockland,
Ulster County, New York and Fairfield County, Connecticut

Selected Sheets of New York, Northeast New Jersey Metropolitan
Map Series

100-Percent Tract Tables for the Areas Within the Sixty-Mile
Radius of Indian Point Nuclear Power Plant

1970 Census of Population and Housing, Master Enumeration
District – List

R.E.D.I., Incl., Population Estimates for 1960 and 2000 for Specified
Zones in a 60-Mile Area Around Indian Point New York, May, 1970

2.4.P-42

ENVIRONMENTAL ANALYSTS, INC. 226 Seventh Street, Garden City, New York 11530 • (516) 741-3061

2.5 HYDROLOGY

Between 2005 and 2007, GZA GeoEnvironmental (GZA), performed a comprehensive hydrogeologic investigation of the site. This investigation was initiated to understand groundwater flow and contaminant transport. During this investigation numerous borings were advanced to study the site geology, hydrology and aquifer properties. Details of the geology, hydrology and aquifer properties can be found in the GZA report (Reference 1).

[Historical]The hydrological features of the Indian Point site are relevant to the analysis of radioactive liquid and gaseous discharges from the plant. During normal plant operation, liquid wastes are discharged to the Hudson River through the Indian Point 3 circulating water discharge tunnel into the common discharge canal for Units 1, 2, and 3. Discharges are limited in accordance with the State Pollutant Discharge Elimination System Permit. The sources of ground water will not be susceptible to contamination from accidental ground seepage or leakage from the plant because of the permeability of the bedrock and the higher elevation of the plant relative to the river. Gaseous releases from the plant following a hypothetical accident have been studied for possible deposition of contaminants into surrounding surface water reservoirs. Therefore, the hydrological features are categorized by the Hudson River, ground water and wells, and surface water reservoirs. Two consultants have studied the hydrology of the Indian Point site. In 1955, prior to construction of Unit No. 1, Mr. Karl R. Kennison reported the flow characteristics of the river at the site. In 1965, the firm of Metcalf and Eddy reviewed Mr. Kennison's report and further reported the ground water hydrology and surface water reservoirs. The report by Metcalf and Eddy is included in this section, appended by the Kennison report (see pages S-1 to S-35).

Flow in the Hudson River is controlled more by the tides than by the runoff from the tributary watershed. Opposite the plant, the width of the river is 4500 to 5000 feet with a depth of 55 to 75 feet less than 1000 feet offshore. Total flow past the plant during the peak tidal flow is about 80,000,000 gallons per minute about 80 percent of the time, and it has been estimated that about 500 feet off the shore line, flow is at least 9,000,000 gallons per minute in a section 500-600 feet wide. This large flow assures adequate dilution and complete mixing of the discharge from the plant. The plant was designed and operates such that discharges into the river do not prevent using the river water for drinking purposes.

The net mean downstream flow due to runoff is as follows:

11,700,000 gpm may be expected to be exceeded 20 percent of the time;

4,710,000 gpm may be expected to be exceeded 60 percent of the time;

1,800,000 gpm may be expected to the exceeded 98 percent of the time.

The history of river flow for a 17-year period, presented in tables in both the Kennison and the Metcalf and Eddy reports, is for the net river runoff flow.

Within a five-mile radius of the plant only one municipal water supply utilizes ground water. Other wells are for industrial and commercial usage. The rock formations in the area, and the elevations of wells relative to the plant are such that accidental ground leakage or seepage percolating into the ground at Indian Point will not reach these sources of ground water but will flow to the river. This subjects is discussed further in Section 2.7.

Only two reservoirs within a five-mile radius of the site are used for municipal water supplies. The Camp Field Reservoir is the raw-water receiving basin for the City of Peekskill with the Catskill Aqueduct and Montrose Water District as alternate supplies. The impounding reservoir for the Stony Point water system serves the towns of Stony Point and Haverstraw, and the villages of Haverstraw and West Haverstraw. The Stony Point system is connected to the Spring Valley Water Company to provide an alternate source of supply. A third reservoir within five miles of the plant, Queensboro Lake, supplies water to a state park area only. The location of these reservoirs and those within a fifteen-mile radius are shown on Figure 2.5-1.

The City of New York's Chelsea Pumping Station is located about one mile north of Chelsea, New York, on the east bank of the Hudson River. Water can be pumped from intakes in the river at the rate of 100 million gallons per day into the city reservoir system, as required to supplement the primary supply from watersheds. The pumping station is 22 miles upriver from Indian Point measured along the centerline of the river as shown on Figure 2.5-2.

Discharge of any contaminant to a tidal estuary will result in its distribution throughout the estuary. Factors affecting this distribution include: tidal amplitude and current, river geometry, salinity distribution, and fresh water discharge. Quirk, Lawler and Matusky Engineers, Environmental Science and Engineering Consultants, of New York City, made extensive studies of the influence of these factors and assisted in the study of contaminant transport in the river. A report of this study is included in this section (see pages S-36 to S-69). This study served to determine the effect of radioactive discharges on overall river contamination, and specifically conditions at Chelsea pumping station, as discussed in detail in Section 14.3.2. During normal operation, discharges do not result in river concentrations that exceed Maximum Permissible Concentrations (MPC) at the Indian Point discharge canal.

Flooding at the site has been nonexistent. The highest recorded water elevation at the site was 7.4 feet above mean sea level during an exceptionally severe hurricane in November, 1950. Subsequent to that occurrence, the highest water elevation recorded at the site was 9-ft 8-in above mean sea level, which occurred during the extra-tropical Superstorm Sandy in November 2012.

Since the river water elevation would have to reach 15'-3" above mean sea level before it would seep into the lowest floor elevation of any of the Indian Point buildings, the potential for any flooding damage at the site appears to be extremely remote.

However, in order to determine the maximum probable elevation that the Hudson River could reach, the firm of Quirk, Lawler and Matusky was commissioned to make an in-depth study of the river under various flooding conditions. A report of this study, dated April, 1970, is included in this section (see pages I-1 to D-3).

Seven different flooding conditions governing the maximum water elevation at the site were investigated, (See Table V-4 on page V-50 of the April 1970 report) including the following:

- a) Flooding resulting from runoff generated by a Probable Maximum Precipitation over the entire Hudson River drainage basin upstream of the site.
- b) Flooding caused by the concurrent of an upstream dam failure concurrent with heavy runoff generated by a Standard Project Flood.

IP3
FSAR UPDATE

- c) Flooding due to the occurrence of a Probable maximum Hurricane concurrent with a spring high tide in the Hudson River.

The severest flooding condition revealed by the study is a result of the simultaneous occurrence of a Standard Project Flood, a failure of the Askokan Dam and a storm surge in New York Harbor at the mouth of the Hudson River resulting from a standard project hurricane. The water level under these conditions would reach 14 feet above mean sea level. Local wave action due to wind effects has been determined to add 1 foot to the river elevation, producing a maximum water elevation of 15 feet above mean sea level at the Indian Point site.

Since this maximum water elevation is 3 inches lower than the critical elevation of 15'-3" noted earlier, it is reasonable to conclude that flooding in the Hudson River will not present a hazard to the safe operation of Indian Point 3.

In response to the Atomic Energy Commission (AEC) questions during the review of the original FSAR, a number of additional reviews were performed. These were documented in the responses to AEC Questions Q2.7 through Q2.11 in Supplement 10 (January 1973) to the IP3 FSAR (Reference 2). In particular, the responses to Q2.9 and Q2.11 provided additional information regarding potential wind generated wave action and hurricane surge attenuation.

The response to Q2.11, regarding maximum hurricane surges during spring tides, reevaluated earlier work using consideration of estuary effects in the Hudson River from a surge at the mouth, the Battery. The study considered variations along the Hudson River in channel geometry, friction coefficient, and hurricane stages at the Battery as a function of time. The river is about 5,000 feet wide at Indian Point and the maximum water surface elevation at this location from hurricanes, wind surges, and high tides was determined to be 12.4 feet above mean sea level (Reference 2). In addition, the response to Q2.11 also provided a range of wind generated wave action during a probable maximum hurricane. The significant wave run-up was estimated to vary from less than 2.5 feet to 4.1 feet, dependent on the forward speed of the hurricane.

Since wind generated wave action in conjunction with extreme flooding conditions could raise the flooding level above plant grade in the vicinity of the service water pumps, the AEC concluded in their original Safety Evaluation Report (SER) for the Indian Point Unit No. 3 Operating License (Reference 3) that Technical Specification requirements were warranted to protect the service water pumps and shutdown the plant based on rising river water levels. Thus, the Staff concluded in Reference 3 that the combination of the elevation of the plant structures, the load-bearing capacity of the intake structure and the Technical Specification requirements on plant operation and service water pump protection, result in acceptable conditions to protect the plant against flooding. (Note: The requirements which were contained in the original Technical Specifications, Section 6.12 are currently contained in the IP3 Technical Requirements Manual, Section 3.7.E).

Additional Hudson River Hydrodynamic Studies

During the mid- and late-1970's, many hydrological studies of the Hudson River were conducted by electric utilities both in the vicinity of Indian Point and over the entire tidal portion of the estuary from the George Washington Bridge to the Albany dam. Consolidated Edison and the Power Authority have transmitted the results of these studies to the Nuclear Regulatory Commission over the years, some as part of the Environmental Technical Specifications report requirements, and others as part of applications for license amendments. Because the results

of both the data acquisition and the hydro-dynamic modeling studies generally support the earlier studies already described, these results will be reviewed very briefly:

The La Salle Hydraulic Model Study of Hudson River Flows Around Cooling Water Intakes, 1976

The purpose of the La Salle study was to estimate the range of the proportion of cooling water which recirculated from the discharge back into the intakes of Indian Point 2 and 3. Data were acquired by physical modelling and by use of neutral buoyancy drogues released in front of the intakes and the discharge. In addition, observation of patterns of turbulence and flow direction and strength were also made during all tidal stages and aided in interpretation of the quantitative data.

The study concluded that, over the whole tidal cycle, an average of 7.7 percent of the discharge water was recirculated. When the flood tide is running, the effluent creates a large eddy in front of the intakes, such that water drawn in actually comes from the upstream direction. The effluent itself, during a flood, goes around the outside of the eddy in front of the intakes, continuing upstream in a relatively wide, turbulent, diffused zone reaching up to 700 feet out from the east shore before arriving at Peekskill Bay. During ebb tide, all water comes to the intakes from a narrow 200 to 250 foot wide zone along the east shore. The effluent goes downstream in a zone 400 to 500 feet out from the east shore. During slack water, water is drawn into the intakes from the area just in front of the plants or from upstream because the effluent cuts off the flow from downstream. Various mixing processes during the different tidal stages result in fairly complete mixing of water in front of the intakes, minimizing saline and thermal stratification.

Influence of Indian Point Unit 2 and Other Stream Electric Generating Plants on the Hudson River Estuary, 1977

This report, edited by James T. McFadden, includes contributions by Texas Instruments and Lawler, Matusky and Shelly Engineers on the Hydrodynamics of the Hudson Estuary. Over a 57-year period, the long-term annual average freshwater flow at Green Island was estimated to be 13,268 cubic feet/second. However, during the early-to-mid 1970's, the annual average ranged from a low of 14,547 in 1971 to a high of 19,077 in 1973. Monthly average flows ranged from a low of 5,591 cubic feet per second in August 1973 to a high of 40,520 in May 1972. Tidal flows determine the overall flow regime of the Indian Point reach of the estuary, reaching 100,000 to 200,000 cubic feet per second. Only extreme freshwater inflows such as those which occurred in storms on March 28, 1913 and March 19, 1936 have suppressed tidal flows below the Albany dam. This suppression extended 48 Km below the dam.

During times of low freshwater flow, the salt front ascends the estuary to as far north as Newburgh. In drought, it may even reach Poughkeepsie. The presence of saline and fresh waters in the same river reach induces density- dependent turbulences and mixing. During these periods, tidal and vertical turbulences act to produce mixing and water mass transport motions. The ratio of tidal flow (Q_t) to freshwater flow update (Q_f) yields the vertical stratification factor, which at Indian Point ranges from a low of 3.3 in spring to a high of 23 in summer.

Conclusion

In the event of a radiological discharge into the Hudson River estuary, the turbulence caused by the discharge velocity itself plus the natural mixing processes described by the La Salle and the McFadden reports would determine the rapidity of mixing, of dilution, and of transport and diffusion. Mixing processes are at work at all times. The two reports, the major contributors in near-field and far-field hydrodynamics for Indian Point, support the findings of the earlier Indian Point hydrodynamic studies.

REFERENCES FOR SECTION 2.5

- 1) GZA, Hydrogeologic Site Information Report for the Indian Point Energy Center, January 7, 2008.
- 2) Original IP3 FSAR Chapter 2 Questions and Answers Q2.7 through Q2.11, IP3 FSAR Supplement 10 – January 1973.
- 3) Safety Evaluation Report By The Directorate of Licensing U.S. Atomic Energy Commission In The Matter Of Consolidated Edison Company of New York, Inc., Indian Point Nuclear Generating Unit No. 3, Docket 50-286, September 21, 1973.

IP3
FSAR UPDATE

HYDROLOGY OF INDIAN POINT SITE
AND SURROUNDING AREA

METCALF & EDDY ENGINEERS
OCTOBER, 1965

REPORT PREPARED BY GEORGE P. FULTON
UNDER DIRECTION OF HARRY L. KINSEL, P. E.

ACKNOWLEDGEMENTS

We acknowledge with thanks the assistance of many public officials, including the following, in furnishing data for this report:

Mr. Alfred Morgan, Chief Engineer
Palisades Interstate Park Commission

Mr. George O'Keefe, Director, Division
of Environmental Sanitation, Rockland
County Health Department

Mr. George Natt, Director,
Westchester County Water Agency

Mr. Michael Frimpter, U. S.
Geological Survey, Middletown, New York

S-2

INTRODUCTION

The hydrological features of the Indian Point site have been studied in three categories; the Hudson River, ground water and surface water reservoirs. Flow data and the flood history of the Hudson River in the vicinity of the Indian Point plant are discussed. Ground water sources within the area are generally used for industrial or commercial purposes with some limited residential usage on the west side of the river. The surface water reservoirs in the surrounding area that are used for water supplies and sources of alternate water supplies are also described.

S-3

-2-

HUDSON RIVER

General

The Consolidated Edison Indian Point plant is situated on the east bank of the Hudson River below Peekskill, just above Verplancks Point. In the general area of the plant, water from the Hudson River is used only for industrial cooling purposes. The nearest community utilizing the Hudson River for a public water supply at the present time is Poughkeepsie, some 30 miles upstream from the plant site.

Flow

Flow data for the Hudson River were abstracted from a previous report of Mr. K. Kennison, submitted to Consolidated Edison on November 18, 1958 (included as an appendix to the section on hydrology). Flood data were obtained from the Survey Division of the Corps of Engineers in New York City.

In the vicinity of Indian Point, the width of the Hudson River ranges from 4,500 to 5,000 feet with maximum depths of from 55 to 75 feet. Cross sectional areas of the river from a point three quarters of a mile upstream from the plant site to a mile downstream are in the order of from 165,000 to 170,000 square feet.

S-4

-3-

Flow duration records of the Hudson River for a 17-year period preceding 1930 show the following:

<u>Rate of Flow</u> c.f.s.	<u>Percent of Time</u> <u>Exceeded</u>
26,000	20%
15,250	40%
10,500	60%
7,000	80%
4,000	98%

It is evident that even the highest rates of flow expected will influence depth of flow in the river to only a small degree in the vicinity of the plant. This is due to the relatively high available flow section and the width of the river. River depth is affected more by the tidal influence than it can be by any anticipated flood flows.

The Hudson River is tidal as far upstream as Troy, some 100 miles from Indian Point. The elevation of the water surface in the vicinity of the plant is so responsive to the tidal cycle that average rate of flow has little effect on depth of flow or velocity of flow.

Flood History

Tide elevations vary both daily and seasonally and, in addition, can be affected by atmospheric conditions such as can exist during extreme storms or hurricanes. The atmospheric conditions can cause a surge which, added to the normal tide, establishes water elevation.

S-5

-4-

The highest water elevation at the U.S.G.S. station at Verplancks Point, one-half mile below Indian Point, was 7.4 feet above MSL (mean sea level) recorded in the year 1950. A higher surge occurred in 1960, but the normal tide stage was such that actual water elevation was somewhat less than the 1950 record.

in an earlier period, before 1935, the highest recorded elevation was 4.75 ft. above MSL at Verplancks Point on August 24, 1933.

Mean water elevations at Verplancks Point are just below 1.0 (MSL). The mean range of water depth stages is about 3.0 ft.. With high runoff in the Hudson River Basin, the mean range at times averages a half a foot higher during the spring period.

The highest river elevation, recorded in 1950, was about 6.5 feet higher than average river levels, or some 5.0 feet higher than average high river stages. Considering past flood history and the fact that flood stages are primarily the effect of tidal influence, flooding of the Indian Point plant site appears to be a highly unlikely possibility.

Contamination Potential

The hazards of contamination of water supplies by discharge of water borne wastes from the Consolidated Edison Indian point plant are almost minimal. In the reach of the Hudson River that could be affected, river water is used only for industrial cooling.

S-6

IP3
FSAR UPDATE

-5-

It should be mentioned that the City of New York is now in the process of constructing a river water pumping station at Chelsea in Putnam County below Poughkeepsie. The intent is to pump Hudson River water into the City system.

S-7

-6-

WELLS AND GROUND WATER

General

Within a five-mile radius of the plant the only public water supply using ground water is the Stony Point system of Utilities and Industries located in Rockland County across the river from Indian Point. Reports on ground water resources within this five-mile radius indicate the existence of numerous other wells. These wells are for industrial and commercial usage and for individual water supplies for private residences. Residential usage, however, is almost entirely confined to the area on the west side of the Hudson River.

Ground Water Geology

Water bearing strata in the area within a five-mile radius of Indian Point can be divided into unconsolidated surface deposits and consolidated bedrock. Unconsolidated deposits cover most of the bedrock in this area and range in thickness from a few feet in the hills to several hundred feet in the larger valleys. Unconsolidated deposits range from clays, which produce only meager quantities of water, to coarse sand and gravel capable of yielding several hundred gallons per minute to a well.

The bedrock underlies the unconsolidated deposits and, where these are absent, crops out at the surface. Ground water in bedrock occurs principally in fractures and solution channels.

S-8

-7-

Thus, the water bearing characteristics are generally similar, although the rocks differ widely in mineral composition and water yield.

Bedrock in Westchester County is, for the most part, metamorphic in character and includes schist and gneiss, with smaller amounts of limestone, quartzite and slate. Small injections of granite can also be found. Only minimal yields of ground water can be obtained from bedrock formations in Westchester County.

Consolidated rocks are the chief source of water in Rockland County. Principal rock units include the following:

- a) Newark Group; - sandstone, shale and conglomerate.
- b) Palisade Diabase – diabase with some basalt.
- c) Cambrian and Ordovician Rocks – quartzite, limestone and dolomite.
- d) Precambrian Rocks – granite, gneiss, with some schist and diorite.

The Newark group provides the greatest source of ground water supply in Rockland County. The other units of bedrock yield only minimal quantities, as in Westchester County.

A small area of Orange County lies within the 5-mile radius being considered. Wells in this area have been drilled in bedrock formations similar to those in Westchester County where the water yield is small.

S-9

-8-

Well Supplies

As mentioned before, the only public water supply served by wells in the 5-mile radius of Indian Point is the Stony Point System. This system serves the Villages of Haverstraw and West Haverstraw as well as portions of the Towns of Haverstraw and Stony Point. The Stony Point supply wells are located in stratified drift, an unconsolidated formation. These wells are relatively shallow, the greatest depth about 35 ft. Total yield of the wells to the system averages about 550 gpm.

Other wells in Rockland County, in the area being considered, include some wells for commercial and industrial use and many private wells serving individual residences. These wells are located in bedrock for the most part and range from 100 to 300 ft. in depth. Consumption of water from wells serving private homes will vary from 100 to 1,000 gpd (gallons per day), depending on the number of persons using the supply and the facilities using water.

There are only a few wells still in use in Westchester County within the 5-mile radius. Almost all the wells within 2 to 3 miles of Indian Point have been abandoned and connections have been made to public water systems for supply. At the fringes of the area a few private wells are used for individual residences. These wells are mostly in unconsolidated deposits with depths less than 50 ft. Some wells exist in bedrock with depths varying up to several hundred feet.

S-10

-9-

A small portion of the community of Fort Montgomery in Orange County lies within 5 miles of the plant. Homes in this community are served entirely by individual private wells in bedrock. Depth of the wells vary up to several hundreds of feet.

Contamination Potential

The bedrock formation is such that it is highly unlikely that wastes percolating into the ground from the Indian Point site will reach the water bearing formations used for water supply on the west side of the river in Rockland and Orange Counties. Most of the wells in Westchester County are shallow, in unconsolidated formations with ground surface elevations considerably higher than at the plant site. This situation would preclude the possibility of contamination of the supply through ground water flow. Bedrock wells in Westchester County are similarly at higher elevations and, for the most part, are drilled in different rock formations than exists at the plant site.

S-11

-10-

SURFACE WATER RESERVOIRS

General

The major sources of water supply in the Indian Point area are lakes and surface water reservoirs. The reservoirs within a 15-mile radius of the plant site are tabulated in Tables 1-7 along with the users, capacities and distances from Indian Point. A detailed analysis of the reservoirs within 5 miles of the plant describes alternate sources of supply to those communities served by the reservoirs.

City of Peekskill-Camp Field Reservoir

The 54-million gallon Camp Field Reservoir of the City of Peekskill system, located 2.9 miles from Indian Point, is a raw-water receiving basin for the water treatment plant. Water is pumped into this basin from Peekskill Hollow Brook. For the most part, the water supply is the continuous flow of this brook. At times of low flow the supply can be supplemented by releasing water into the stream from holding reservoirs in Wicopee (Putnam County) some 11.7 miles from Indian Point or from the Catskill Aqueduct of the City of New York, located a short distance upstream from the pump intake.

The City of Peekskill system is divided into two service pressure areas. Water for the low-pressure area flows by gravity from Camp Field Reservoir through a bank of slow-sand filters

S-12

-11-

into the system. No additional storage is provided for this section of the system. Water for the high-service area flows from the reservoir through two diatomaceous earth filters by gravity and then is pumped to a pair of elevated storage tanks with a total capacity of 800,00 gallons. The high-service system serves approximately 25 percent of the Peekskill area. The remaining area, including Standard Brands and most of the other industrial consumers, is served by the low-pressure system.

Total water consumption in Peekskill averages about 5 mgd. The largest single user is Standard Brands, at an average rate of 1.5 mgd. All water is supplied from Peekskill Hollow Brook. Two connections to other systems are available for emergency conditions. One is the above-mentioned Catskill Aqueduct connection which discharges into Peekskill Hollow Brook. This flow must be processed through the two treatment facilities for use. The other emergency connection is to the Montrose Water District system which can supply between 1.0 and 1.25 mgd from the Catskill Aqueduct to the low-service section of the Peekskill system.

Since no piping is installed to bypass Camp Field Reservoir, contamination of this basin would deprive Peekskill of its normal source of supply. Installation of a bypass would involve some 800 lin. ft. of 24-in. pipe between the inlet force mains and the outlet lines to the two filter facilities. With such a

S-13

-12-

bypass, it would be possible to take water directly to the filters from Peekskill Hollow Brook after the passage of contaminated water in the event of prolonged contamination of Camp Field Reservoir. It might be necessary to accelerate flushing out of the brook and the impoundment at the pumping station in such a situation by releasing water from either the Catskill Aqueduct or the Wicopee reservoirs.

Peekskill most likely could not depend on the Montrose connection alone. This can supply less than one-half the normal demands of the low-service system even with the assumption that Standard Brands would not operate during the emergency. The high-service system has only 800,000-gallon storage, which would last less than 24 hours after shutting down the Peekskill Hollow Brook supply.

As presently arranged, the City of Peekskill would be practically deprived of a water supply with elimination of Peekskill Hollow Brook as a source. A study will soon be made under the auspices of the Westchester County Water Agency and the State of New York to determine the feasibility of connecting the Peekskill system to a proposed transmission main crossing northern Westchester County from the Delaware Aqueduct of the City of New York. This proposal could furnish an independent source of water in sufficient supply to serve all the needs of the City of Peekskill in the event of an emergency.

S-14

-13-

Palisades Interstate Park Commission – Queensboro Lake

Queensboro Lake, some 5 miles from Indian Point, serves as the year-round water supply for Bear Mountain Inn. The inn facilities include the offices of the Palisades Interstate Park commission as well as a hotel and restaurant. Three other lakes feed into Queensboro Lake through stream flow or by pipe connection. Only Queensboro Lake is connected directly to the water system and no bypass is available to route water around the lake from a more distant location.

In case of contamination of Queensboro Lake, Bear Mountain Inn would be deprived of its water supply. A neighboring community, Fort Montgomery, is served entirely by individual private wells. This would seem to indicate that installation of an emergency well supply for Bear Mountain Inn would be feasible.

Stony Point Water System – Utilities and Industries

The Stony Point supply of Utilities and Industries, and investor-owned water company, serves the towns of Stony Point and Haverstraw as well as the villages of Haverstraw and West Haverstraw. Total average consumption is about 1.18 mgd with 1.0 mgd from a surface supply and 0.8 mgd from wells.

The impounding reservoir of the surface supply of 4.5 million gallon capacity is located some 3.5 miles from Indian Point 3 Point. With contamination of this supply, the system would be left with only the wells which furnish about 45 percent of total consumptions.

S-15

-14-

Negotiations are now under way for purchase of the Stony Point supply by the Spring Valley Water Company, an investor-owned utility serving most of the remaining areas of Rockland County. This company derives water from a well system of 13 to 15 mgd capacity and up to 7 mgd from De Forest Lake outflow some 10.8 miles from Indian Point. Plans have been completed for construction this fall of a connection between the Spring Valley Water Company system and the Stony Point system. This connection will furnish well water from the Spring Valley supply to the Stony Point network.

As far as can be ascertained from public records, the above three systems comprise the only surface water usage within a 5-mile radius of the Indian Point power plant except for industrial cooling water usage of the Hudson River. All other supplies are reported as originating in wells or from surface storage outside the 5-mile limit.

S-16

IP3
FSAR UPDATE

TABLE 1
WATER STORAGE RESERVOIRS
WITHIN 15 MILE RADIUS OF INDIAN PONT
WESTCHESTER COUNTY

<u>Code</u>	<u>Reservoir</u>	<u>User</u>	<u>Capacity Million Gallons</u>	<u>Distance Miles</u>	<u>Surface Acres</u>
W-8	Indian Brook	Ossining WB.	101	6.5	17
W-18	Pocantico Lake	New Rochelle Wat. Co.	200	11.9	63
W-14	Ferguson Lake	Pocantico Hills Est.	40 *	13.5	28
W-13	Tarrytown Res.	Tarrytown	313	14.0	85
W-13	Open Res. – 2	Tarrytown	1.75 & 1.10	14.0	1
W-1	Croton Res.	New York City (See List)	65,300 (Inside 15 mi.)		4059
W-10	Whippoorwill La.	New Castle Wat. Co.	25 *	13.3	8
W-11	Byram Lake	Mt. Kisco	950	15.0	133
W-11	Open Res.	Mt. Kisco	10 *	14.0	2
W-5	Lake Shenorock	Amawalk-Shenorock WD.	90 *	11.1	16
W-6	Open Res.	Lincoln Hall School	25 *	11.9	6
W-1A	Amawalk	NYC (See List)	10,000 (Included in W-1)	11.6	588
W-4	Camp Field Res.	Peekskill	54	2.9	11
* Estimated					

IP3
FSAR UPDATE

TABLE 2

WATER STORAGE RESERVOIRS

WITHIN 15 MILE RADIUS OF INDIAN PONT

PUTNAM COUNTY

<u>Code</u>	<u>Reservoir</u>	<u>User</u>	<u>Capacity Million Gallons</u>	<u>Distance Miles</u>	<u>Surface Acres</u>
P-20	Lake Mahopac	See List	5,000 *	12.7	577
P-10	Oscawanna Lake	See List	3,500 *	9.5	362
P-21	Pelton Pond	N.Y.S. Fahnestock Park	125 *	14.0	11
P-6	Cold Spring	Cold Spring	150 *	13.0	25
B-3	Cargill Res.	Beacon	160	15.0	22
B-2	Mt. Beacon Res.	Beacon	180	14.5	17
B-1	Melzingah Res.	Beacon	60	13.3	8
W-4	Wicopee	Peekskill	1,200	11.7	166
P-5	Lake Secor	Carmel WD #5	350 *	10.8	50

*Estimated

IP3
FSAR UPDATE

TABLE 3
WATER STORAGE RESERVOIRS
WITHIN 15 MILE RADIUS OF INDIAN PONT
ORANGE COUNTY

<u>Code</u>	<u>Reservoir</u>	<u>User</u>	<u>Capacity</u> <u>Million Gallons</u>	<u>Distance</u> <u>Miles</u>	<u>Surface</u> <u>Acres</u>
0-11	Lusk Res.	U.S. M.A.	50 *	7.5	16
0-4	Intake Res.	Highland Falls	2.5	6.5	
	Bog Meadow	" "	80	8.3	43
	Little Bog	" "	4.5	7.5	2
	Jims Pond	" "	40	8.4	16
0-12	Turkey Hill La.	Palisades Int. Park	150	5.9	58
	Nawahunta La.	" "	22	6.7	16
0-20	Silvermine La.	Palisades Int. Park	456	6.0	84
	Queensboro La.	" "	56	5.0	37
0-16	Lake Stahahe	Palisades Int. Park	230	11.1	90
0-16	Summit Lake	Palisades Int. Park	110	8.3	34
	Barnes La.	Pal. Int. Pk. & U.S.M.A.	24	8.0	18
	Te'ata La.	Pal. Int. Pk.	77	7.7	32
	Upper Twin La.	" " "	105	7.7	24
	Lower Twin La.	" " "	88	7.6	26
	Massawiepa La.	" " "	104	7.7	29
0-17	Lake Tiorati	Pal. Int. Pk., Tiorati	1,500	6.7	296
0-10	Crowmwell Lake	Woodbury	80	11.2	55
0-2	Walton Lake	Chester	300	14.6	129
0-5	Lake Mombasha	Monroe	1,750	13.0	324
0-1	Echo Lake	Arden Farms	40 *	9.5	30
0-7	Op Res.	Sterling Forest	60 *	13.7	42

IP3
FSAR UPDATE

ORANGE COUNTY (CONT'D.)

TABLE 3 (CONT'D)

<u>Code</u>	<u>Reservoir</u>	<u>User</u>	<u>Capacity Million Gallons</u>	<u>Distance Miles</u>	<u>Surface Acres</u>
0-8&9	Tuxedo Lake	Tuxedo & Tuxedo Pk.	2,500	14.5	294
0-3	Alex Meadow	Cornwall	23	9.2	9
	Arthur's Pond	Cornwall	115	9.2	20

* Estimated

IP3
FSAR UPDATE

TABLE 4

WATER STORAGE RESERVOIRS

WITHIN 15 MILE RADIUS OF INDIAN PONT

ROCKLAND COUNTY

<u>Code</u>	<u>Reservoir</u>	<u>User</u>	<u>Capacity Million Gallons</u>	<u>Distance Miles</u>	<u>Surface Acres</u>
R-14	Lake Sebago	Sebago Lake, Pal. Int. Pk	1,100	10.8	300
R-18	Lake Welch	Welch Lake	1,000	7.2	209
R-13	Breakneck Pond	Breakneck Lake, Pal. Int. Pk.	100	9.2	63
R-3	Sec. & Third Res.	Letchworth Vill.	100	8.5	40
R-1	Open Res.	Utilities & Ind.	4.5	.3.5	5
R-7	Hillburn Res.	Hillburn	1.0	14.7	4
R-6	Deforest Lake	Hackensack Wat. Co. Spring Val. Wat. Co.	5,500	10.8	960

-20-

TABLE 5

MULTIPLE USERS OF WATER SUPPLY SYSTEMS

WITHIN 15 MILE RADIUS OF INDIAN POINT

WESTCHESTER COUNTY

New Croton Aqueduct (New York City)

Ossining Water Board

Sing Sing Prison

Village of North Tarrytown

New Rochelle Water Company

Village of Bronxville

Town of Eastchester

Village of North Pelham

Village of Pelham

Village of Pelham Manor

Village of Tuckahoe

Village of Irvington

Village of Briarcliff Manor

New Castle Water District #1

Village of Tarrytown

Old Croton Aqueduct (New York City)

Ossining Water Board

Village of Ossining

Town of Ossining

Sing Sing Prison

S-22

-21-

Kensico Reservoir (New York City)

City of White Plains

North Castle District #1

Westchester Joint Water Works No. 1

Village of Mamaroneck

Town of Harrison

Town of Mamaroneck

City of Rye

City of New Rochelle

Village of Larchmont

Village of Scarsdale

Village of Pelham Manor

Harrison District #1

Catskill Aqueduct (New York City)

Grasslands (Westchester Co.)

Hawthorne Improvement District

Hawthorne

Town of Mt. Pleasant

Valhalla W D

Valhalla

Town of Mt. Pleasant

City of Yonkers

Village of Scarsdale

New Rochelle Wat. Co (same as Pocantico Lake)

S-23

QUIRK, LAWLER & MATUSKY ENGINEERS

-22-

Amawalk Reservoir (New York City)

Yorktown W S D D

Amawalk Heights W D

Town of Somers

Town of Yorktown (13 Water Districts)

Peekskill System (City of Peekskill)

City of Peekskill

Village of Buchanan

Town of Cortlandt

Indian Brook Reservoir (Ossining Water Board)

Village of Ossining

Town of Ossining

Sing Sing Prison

Whippoorwill Lake (New Castle Water Co.)

Town of New Castle (Part)

Town of North Castle (Part)

Pocantico Lake (New Rochelle Water Co.)

Village of Ardsley

Village of Dobbs Ferry

Town of Greenburgh

Village of Hastings

Village of Scarsdale

Village of Eastchester

S-24

QUIRK, LAWLER & MATUSKY ENGINEERS

-23-

Tarrytown Reservoir

Village of Tarrytown

Glenville W D

Town of Greenburgh

Eastview

Town of Mount Pleasant

Village of North Tarrytown

S-25

-24-

TABLE 6
MULTIPLE USERS OF WATER SUPPLY SYSTEMS
WITHIN 15 MILE RADIUS OF INDIAN POINT
PUTNAM COUNTY

Lake Oscawanna

Hiawatha Improvement Co.

Hilltop W D

Wildwood Knolls W D

Oscawanna Lake (Private Homes)

Lake Mahopac

Lake Gardens

Lake Mahopac Woods

Mahopac Hills

Mahopac Old Village

Lake Mahopac (Private Homes)

Lake Mahopac Ridge

Lake View Park

Mahopac School

S-26

- 25 -

TABLE 7

MULTIPLE USERS OF WATER SUPPLY SYSTEMS
WITHIN 15 MILE RADIUS OF INDIAN POINT
ROCKLAND COUNTY

De Forest Lake

Hackensack Water Co.

Spring Valley Water Co.

Town of Clarkstown (Part)

Town of Ramapo

Town of Orangetown

Nyack

Village of Nyack

Village of South Nyack

Upper Nyack

Town of Clarkstown (Part)

Stony Point Supply (Utilities and Industries)

Town of Stony Point

Town of Haverstraw

Village of West Haverstraw

S-27

QUIRK, LAWLER & MATUSKY ENGINEERS

KARL R. KENNISON
CIVIL AND HYDRAULIC ENGINEER
361 CLINTON AVE., BROOKLYN, N.Y.

Mr. G. R. Milne Nov. 18, 1955
Mechanical Engineer
Cons. Edison Co. of N.Y.
4 Irving Place
New York 3, N. Y.

Dear Sir :

You have described to me the general features of the atomic-energy power plant which you are planning to construct on the east bank of the Hudson River below Peekskill. I understand that you wish me to report on such hydrologic features of the site as may effect your plans.

From the information that you have made available to me I conclude that the most useful information I can give you is that which relates to the amount and character of the flow in the river. At the proposed site the river has a width of about 4500 to 5000 feet, a maximum depth of 55 to 75 feet at less than 1000 feet off shore, and a cross-sectional area of about 165,000 to 170,000 square feet. Sheet 1 shows a number of cross sections of the river, plotted from the U.S.C. &G.S. charts, at intervals of 1500 feet, from 3750 feet upstream to 5250 feet downstream from the proposed plant.

At this site the effect of the tides is all important and so far outweighs any other consideration that, at least for present purposes, the information already available on the day-by-day variation of the runoff from the tributary watershed is adequate.

On Sheet 2 I have plotted an approximate flow-duration curve from data I had already calculated covering a period of

S-28

- 2 -

17 years.

An average rate of about 26000 cfs may be expected to be exceeded 20% of the time

"	"	"	"	"	15250	"	"	"	40%	"	"	"
"	"	"	"	"	10500	"	"	"	60%	"	"	"
"	"	"	"	"	7000	"	"	"	80%	"	"	"

for say 2 % of the time the rate may be as low as 4000 cfs

However as above indicated the ebb and flow of the tide is the all important consideration. The river is tidal to as far upstream as Troy. Its hourly behavior in the tidal range varies throughout its length. The U. S. Coast & Geodetic Survey has tabulated a great deal of information from which a general picture of conditions off the shore at the proposed site can be obtained.

On Sheet 3 I have plotted the data, as they are applicable to this particular site. This indicates that the elevation of the water surface is so responsive to the tidal cycle that the average rate of flow, or runoff from the tributary watershed, has relatively little effect on the velocity past the site. I conclude that it is this velocity and the resulting volume of flow available for mixing and dilution in which you are primarily interested. In the limited time at my disposal I can only draw general conclusions. These may be adequate for present purposes. You could obtain better information by running a series of tests on surface and sub-surface floats, at varying distances off shore, throughout the tidal cycle.

The velocity recorded by the U.S.C.&G.S. is that in midstream at or near the surface. In order to be on the safe side in drawing conclusions, I have assumed that 80 % of this velocity represents the average vertically from surface to bottom, and that 80 % also represents the average horizontally from side to

S-29

side, hence that roughly 64 % represents the average over the entire cross section. I have also assumed that 15 % of the total cross section, or a stretch about five or six hundred feet wide off shore, is all that should be used in considering the initial mixing or diluting effect. In making this assumption I am governed to some extent by Hazen's studies relative to the off-shore distance of Poughkeepsie's water intake to avoid direct contamination by its sewage. I have further assumed that the velocity in this off-shore stretch is only 60% of the midstream velocity, hence that roughly 48% represents the average over the cross section of this off-shore stretch.

On Sheet 4 I have shown the result of these assumptions, which, as above stated, are believed to be on the safe side in considering the direct effect of mixing or dilution of your wastes. This emphasizes the all-important effect of the tides, the quantity available for dilution varying in about three hours from a maximum of eight or ten million gallons per minute to nothing.

Although you will have to put up with this variation as far as your continuous cooling water circulation is concerned, it does point to the desirability of incorporating in your design a method of controlling the time for the discharge into the cooling water outlet of any and all waste that is to any extent radioactive. I would say that this should be done in any event for the drainage from your routine and emergency demineralizers, and it might well be done also for drainage from all areas liable to accidental contamination.

From your estimate of the extent of dilution already
S-30

accomplished in the demineralizer waste overflow, I trust you can get an approximate figure for the dilution that may result in the river off shore, and can compare this with what you may find necessary or desirable for adequate protection of fish life or of the fish eating public.

As far as the effect on public water supplies is concerned, the use of the Hudson River for water supply, other than condenser cooling, is very limited. The nearest municipality involved is Poughkeepsie, 30 miles or more upstream, and even at that distance threatened at times with the problem of salinity. There is no likelihood that in the future any nearer municipality will take its domestic water supply from the Hudson. In fact the tendency is the other way, and the more remote municipalities of Catskill and Hudson have abandoned earlier supplies taken from the river.

As far as the effect on ground water is concerned, you have acquired an ample area of surrounding land. I can see no possibility of any deleterious effect.

I trust that this information which I have assembled in the limited time available will be helpful to you. If from these approximate figures there appears to be any question as to the adequacy of the safety factor in dilution, you may, as above stated, require additional information from float test.

From what you have told me about your proposed designs and methods of operation, I suspect that there is no real question of safety but only one of public relations – avoidance of even the appearance of danger.

Very truly yours,

S-31
S-32
S-33
S-34
S-35

TRANSPORT OF CONTAMINANTS
IN THE HUDSON RIVER
ABOVE INDIAN POINT STATION

QUIRK, LAWLER AND MATUSKY ENGINEERS
Environmental Science and Engineering Consultants
New York, New York

BASIS FOR ANALYSIS

Transport of any substance in a tidal estuary is governed by the Law of Conservation of Mass. Figure 1 illustrates the application of this law in an estuary. After discharge to the estuary, waste particles are carried downstream, in the movement of upland runoff toward the ocean. This phenomenon is known as convection. The rate of convective mass transport across any river section is equal to the product of fresh water runoff, Q , and contaminant concentration, c .

Besides convection, particles are transported in an estuary by longitudinal mixing. Longitudinal mixing, or dispersion, is a complex function of reversing tidal currents and salinity-induced circulation. Dispersive transport occurs only in the presence of a concentration gradient of the material being transported. The rate of dispersive transport is equal to the product of the dispersion coefficient, E , and the negative of the longitudinal concentration gradient, dc/dx . The dispersion coefficient, E , is a measure of the estuary's ability to transport material in the presence of a concentration gradient, and is a quantitative function of tidal current and salinity-induced circulation.

The concentration profile in Figure 1 indicates how convection and dispersion distribute estuarine contaminants. Since only contaminants that decay or, at best, are conserved, are being considered, the maximum containment concentration must occur at the point of introduction of the contaminant to the estuary. In the case of saline contamination, the salt is introduced at the mouth of the estuary so that the maximum salinity occurs here; in the case of discharge of radioactive contaminants at Indian Point, the maximum concentration of radioactivity will exist in this vicinity, as shown on Figure 1.

The concentration in the region downstream of the point of discharge, ($x = 0$), decays less rapidly than does its counterpart in the upstream region. This is so because in the downstream region, dispersion, in moving material in the direction of decreasing concentration, aids convection. More material is transported downstream than upstream, so, at the same absolute distance from the point of discharge, the upstream concentration is lower than the downstream concentration.

A mass balance over the incremental volume, $A\Delta x$, in Figures 1 is written:

$$\text{Inflow} - \text{Outflow} + \text{Production} = \text{Accumulation} \quad \dots \dots \dots (1)$$

S-37

S-38

Figure 1

Algebraic summation of the individual contributions, shown in Figure 1 to

Equation 1 gives:

$$\left[Qc - EA \frac{dc}{dx} \right]_x - \left[Qc - EA \frac{dc}{dx} \right]_{x+\Delta x} - KCA\Delta x = \frac{d}{dt} [CA\Delta x] \quad \dots \dots \dots (2)$$

in which:

c = contaminant concentration, ML^{-3}

x = distance along longitudinal axis of the estuary, L

t = time, T

A = cross-sectional area of the estuary, L^2

Q = fresh water flow (upland runoff), L^3T^{-1}

E = longitudinal dispersion coefficient, L^2T^{-1}

K = first order decay constant, T^{-1}

The production, or in this case, decay, term is the rate at which material is produced or consumed by physical, chemical, biochemical or nuclear reaction within the volume element.

For decay according to first order kinetics, the usual kinetics of radioactive decay, this rate of consumption of contaminant is equal to the product of the unit rate, Kc , times the volume, $A\Delta x$, within which the reaction is taking place.

The accumulation term completes the inventory by accounting for the net rate of increase or decrease of material upon summation of the rate of inflow, outflow and production. This is equal to the time rate of change of total contamination mass within the reactor volume, $A\Delta x$.

The parameters, Q , A , E and K , in most estuaries are functions of space and time. To avoid tenuous mathematical complexity, these parameters are often considered to be constants. This approach, justification of which appears in a later section of the report, has been selected for the analysis used in this report. For the case of constant Q , E , A and K , Equation 2 rearranges to:

$$E \left[\frac{\frac{dc}{dx} \Big|_{x+\Delta x} - \frac{dc}{dx} \Big|_x}{\Delta x} \right] - \frac{Q}{A} \left[\frac{c \Big|_{x+\Delta x} - c \Big|_x}{\Delta x} \right] - Kc = \frac{dc}{dt} \quad \dots \dots \dots 3$$

The bracketed terms are average rates of change with respect to x . The limit of Equation 3, as Δx approaches zero, is as follows:

S-39

2

$$E \frac{d^2c}{dx^2} - U \frac{dc}{dx} - Kc = \frac{dc}{dt} \quad \dots\dots (4)$$

U is equal to Q/A and is the average fresh water velocity. Equation 4 is a linear partial differential equation in x and t and is often referred to as the convection-diffusion equation for non-conservative substances. It has been selected as the defining equation for all subsequent analyses presented in this report.

At this juncture, it is important to note that the concentration, c , is actually a tidal smoothed, area averaged concentration. This means that rather than attempt to define local behavior at any point within a cross-section and during a tidal cycle, the analyst looks at the average concentration over an entire cross-section over a full tidal cycle. Justification of this procedure is given by Kent (1), Harleman and Holley (2), and Lawler (3).

This justification proceeds by starting with the equation of continuity of a single chemical specie (4), in which contaminant concentration is a function of three space dimensions and real time. Dependence on the lateral and vertical space coordinates is replaced by dependence on total cross-sectional area by integrating over the total width and depth. The resulting equation is then integrated over a tidal cycle and change with respect to real time replaced by change with respect to tidal cycle units of time.

In the course of these integrations, several new terms are generated, all of which contribute to the dispersion phenomenon. These are eventually replaced by the overall dispersion flux, $E \frac{dc}{dx}$.

Once contaminants are dispersed over the river channel, the various concentrations at specific points within the cross-section and tidal cycle can be expected to be less than 20% of the tidal smoothed, area averaged value. Figures 2 through 7 illustrate this for salt. The actual variation of salinity across various cross-sections within the reach between Indian Point and Chelsea is shown on Figures, 2, 4 and 6. Figures 3, 5 and 7 show the sinusoidal variation of the area averaged salinity at these sections over a tidal cycle, as well as a linearized plot of this variation.

S-40	3
S-41	Figure 2
S-42	Figure 3
S-43	Figure 4
S-44	Figure 5
S-45	Figure 6
S-46	Figure 7

II. SELECTION OF NUMERICAL VALUES OF PARAMETERS

Numerical values of the parameters E , U and K , which appear in the defining differential equation and therefore control the distribution of any contamination in the estuary, must be chosen for the Hudson River.

1. FRESH WATER DISCHARGE

Fresh water velocity, U , is obtained by dividing fresh water discharge by the river cross-sectional area, A . Fresh water flow into the Hudson is measured at Green Island, at mile point 152, where the tributary drainage area totals 8090 square miles. The drainage area of the Hudson Basin, tributary to the entire River, is approximately 13,370 square miles. Over 95% of this area is located north of Indian Point. Because of the inability to measure directly fresh water flow in tidal waters, the Green Island gage issued to establish lower River discharges. The ratio of tributary drainage areas between Indian Point and the gage is 1.57. Analysis of data developed by the United States Geological Survey (USGS) indicates a most probable value for yield factor of 1.22. All values of lower River flow referred to in this report were established using this ratio, i.e., lower River flow is equal to Green Island gaged flow times 1.22.

The pattern of the long-term monthly flows, shown in Figure 8, is indicative of the general variation of River discharge. During the months of March through May, the flow averaged 29,000 cfs or almost 3.5 times the average discharge during the months from June through October. This is equivalent to the statement that the volume of fresh water discharged during the spring months is in excess of twice the volume discharge during the subsequent five-month period.

Figure 1 and Equation 4 indicate that as fresh water velocity decreases, given a fixed value of the longitudinal dispersion coefficient, the dispersion effect increases. Therefore, contaminant concentration values in the region above Indian Point can be expected to increase as flow decreases. Furthermore, due to increased salinity intrusion during periods of low fresh water flow, the longitudinal dispersion coefficient, which is strongly dependent on salinity-induced circulation, can be expected to increase in the upper region of the River. For these reasons, analysis of the effect of pollutants on the River require that drought flows be selected in assigning values of U .

S-48 Figure 8

Figure 9 shows a statistical analysis of Hudson River drought flows for the years 1918 through 1964. For drought durations of one week (seven consecutive days), and one month, a plot of flow versus the percent of the time such flow can be expected to occur is given. For example, Figure 9 indicates, for a duration of one week, a flow of 2630 cfs can be expected to occur 5% of the time or once in 20 years.

It should be noted that the response of the Hudson to area-wide droughts is significantly different from that of individual, smaller-sized basins in the region. The difference can be attributed to the size and number of sub-drainage areas within the overall basin and the degree of regulation obtained from up-River storage facilities, such as the Sacandaga and Indian Lake reservoirs.

2. CROSS-SECTIONAL AREA

Figure 10 shows the variation of cross-sectional area with distance above the Battery. Variation is erratic and as such is not amenable to simple mathematical description; i.e., as an elementary function of distance. Between Indian Point and Chelsea, the area varies from a minimum of 120,000 square feet just north of Bear Mountain Bridge to a maximum of 175,000 square feet at the mouth of Newburgh Bay. The average area over this 22 mile river reach is 140,000 square feet; this number has been selected as the value of the constant parameter, A, in Equation 3.

3. LONGITUDINAL DISPERSION COEFFICIENT

The value of the longitudinal dispersion coefficient at any point within the salt-intruded reach of the River can be conveniently obtained by analysis of salinity profiles. The limiting form of Equation 2 for the case of a conservative substance such as salt, and non-constant values of Q, A and E, is:

$$\frac{1}{A} \frac{d}{dx} \left[EA \frac{dc}{dx} - Qc \right] = \frac{dc}{dt} \quad \dots\dots (5)$$

If the variation of salinity with x and t is known, the derivatives $\frac{\partial c}{\partial x}$ and $\frac{\partial c}{\partial t}$ may be obtained graphically or numerically. Equation 5 can then be used

to compute the value of E at any point within the saline reach of the River.

This procedure requires that a number of profiles be available so that the time derivative, $\frac{\partial c}{\partial t}$, can be computed and also requires that the value of Q, now a time and distance dependent function, controlling the intrusion, be known. This

S-49 5

S-50 Figure 9

S-51 Figure 10

latter requirement poses some difficult in evaluating Hudson River dispersion. Fresh water flow can only be measured at Green Island, above the tidal region, and the attenuating effect of tidal mixing on time-variable flows is not known.

These difficulties have been avoided by recognizing that drought flows in the Hudson remain relatively constant for extended periods of time; Q , and therefore U , are known and the steady Q gives rise to steady salinity profiles during these periods. Under these conditions, the net flux of salt in the River must be zero since there is no sink or source of salt within the estuary. Equation 5 then reduces to:

$$E \frac{dc}{dx} - U c = 0 \quad \dots\dots (6)$$

Rearrangement of Equation 6 yields a solution for the dispersion coefficient.

$$E = U \left[2.303 \frac{d \log c}{dx} \right]^{-1} \quad \dots\dots (7)$$

Numerical values of $\frac{d \log c}{dx}$ may be obtained by graphical differentiation

of a semi-logarithmic plot of salinity versus distance. $U(x)$ is equal to the flow associated with that profile, divided by the area, $A(x)$, at the point in question. Typical steady state salinity profiles are shown in Figure 11. Values of E , computed as described above, are shown in Figure 12 for these and several other drought profiles.

Figure 12 indicates that the dispersion coefficient at some points may increase as flow decreases whereas, at other points, the reverse may occur. For example, at mile point 20, the value of E , during the 1964 drought flow of 4100 cfs, was 12,000 sf/sec and, during the 1959 drought flow of 8700 cfs, was 6000 sf/sec. On the other hand, at mile point 50, E in 1964 was 4200 sf/sec and, in 1959, was 5000 sf/sec.

These phenomena can be explained in terms of the mechanisms contributing to longitudinal dispersion. In the lower part of the saline region, under drought conditions (less than 12,000 cfs), salinity-induced circulation, which depends strongly on the salt concentration, is the predominating mechanism, whereas, toward the end of the intrusion, this saline effect is less predominant and also less variable. The relative contribution of fresh water flow to the dispersion characteristics of the River increase as the absolute contribution of the salinity

S-53 Figure 11

S-54 Figure 12

decreases. Thus, increases in fresh water flow can, under some conditions, outweigh the corresponding decrease in salinity, the net effect being an increase in the dispersion coefficient.

Under other conditions, the reverse is true and a decrease in the dispersion coefficient in the presence of an increased flow will be observed. Details for these phenomena and a quantitative method for the prediction of $E(x)$ in the Hudson River as a function of flow are more fully discussed in previous reports (5), (6).

The determination of E as a function of x has been presented to justify the use and selection of constant values of E in this report. A choice of E equal to the maximum value of $E(x)$ within the reach between Indian Point and Chelsea will result in a conservative analysis for the following reasons:

- (1) As Chelsea is approached, the true value of E will fall below this maximum, causing the actual contaminant concentration to be lower than that predicted by constant parameter analysis.
- (2) The predicted downstream flux will be less than the actual downstream flux because the true E values, in this region, are larger than the constant E . Thus, the predicted value of the fraction of total contamination discharge moving upstream will be greater than the actual value of this fraction.

These qualitative statements can be seen more clearly by reference to Figure 1.

Figure 12 indicates that maximum E in the reach between Indian Point and Chelsea occurs between mile points 45 and 50. Accordingly, the values of E for this analysis have been selected by obtaining the average E between mile points 45 and 50 for any given flow. A second choice of E has been made by obtaining the average between mile point 43 and 65 (Indian Point and Chelsea).

The average value of E over a finite length of River is obtained by application of the mean value theorem for derivatives to Equation 7. This yields:

$$\left[\frac{E}{U} \right]_{AVG} = \left[2.303 \frac{\Delta \log c}{\Delta k} \right]^{-1} \quad \dots \dots (8)$$

$$E_{AVG} = U_{AVG} \left[2.303 \frac{\Delta \log c}{\Delta k} \right]^{-1} \quad \dots \dots (9)$$

A correlation of all available Hudson River salinity and flow data is shown on Figure 13. Values of E used in this report have been computed by application S-55 7

S-56 Figure 13

of Equation 9 to these data. For example, at a flow of 4000 cfs, the computation for average E between mile points 43 and 65 is:

$$E = \left[\frac{4000}{141,300} \right] \cdot \left[\frac{2.303 (\log 7000 - \log 2200)}{[-43(-65)] 5280} \right]^{-1}$$

$$= 2830 \text{ sq. ft/sec}$$

$$= 8.74 \text{ sq. mile/day}$$

Correspondingly, for the same flow, the average E between mile points 45 and 50 is:

$$E = \left[\frac{4000}{123,500} \right] \cdot \left[\frac{2.303 (\log 6500 - \log 5400)}{-45 - (-50)} \right]^{-1}$$

$$= 4640 \text{ sq. ft/sec}$$

$$= 14.3 \text{ sq. mile/day}$$

Figure 14 shows the variation, with flow, of average E, computed by Equation 9 as shown above.

S-57 8

S-58

Figure 14

III. EFFECT OF CONTINUOUS DISCHARGE ON CHELSEA INTAKE

This section analyzes the effect of a continuous discharge from Indian Point on water drawoff at Chelsea and is subdivided as follows:

1. A steady state of equilibrium analysis
2. A transient analysis or approach to steady state

1. ANALYTICAL DEVELOPMENT FOR STEADY STATE CONDITION

Figure 15 depicts the problem. The defining differential equation is given by Equation 4. Since this equation does not include discharge at Indian Point or drawoff at Chelsea, it will not define behavior across these two planes. For these reasons, the Hudson is divided into three regions, one above Chelsea, one between Chelsea and Indian Point and one below Indian Point. A solution for each region is obtained by application of proper boundary conditions to the general solution of Equation 4.

The steady state form of Equation 4 is:

$$\frac{E d^2 c}{d x^2} - \frac{U d c}{d x} - K c = 0 \quad \dots\dots (10)$$

The general solution of this second order, linear, ordinary differential equation is:

in which h

$$c = C_1 e^{jx} + C_2 e^{kx} \quad \dots\dots (11)$$

$$j = \frac{U + \sqrt{U^2 + 4KE}}{2E}$$

$$k = \frac{U - \sqrt{U^2 + 4KE}}{2E}$$

$C_1, C_2 =$ arbitrary constants

QUIRK, LAWLER & MATUSKY ENGINEERS

Equation 11 is the form of the general solution for each of the three regions. Designating River velocity above Chelsea as U_1 and below Chelsea as U_2 , the general solution in each of the three reaches is written:

$$c_I = C_1 e^{j_1 x} + C_2 e^{k_1 x} \dots\dots\dots (11a)$$

$$c_{II} = C_3 e^{j_2 x} + C_4 e^{k_2 x} \dots\dots\dots (11b)$$

$$c_{III} = C_5 e^{j_2 x} + C_6 e^{k_2 x} \dots\dots\dots (11c)$$

S-59 9

S-60 Figure 15

$$\text{In which } \left. \begin{array}{l} \frac{j_1}{k_1} \\ \frac{j_2}{k_2} \end{array} \right\} = \frac{U_1 \pm \sqrt{U_1^2 + 4KE}}{2E}$$

To evaluate the six arbitrary constants, six boundary conditions are necessary. These are developed as follows:

1. The contaminant can be expected to reach negligible concentrations before passing out of the estuary into the ocean. This is not due to any diluting effect of the ocean, but rather because the distance between Indian Point and New York Harbor is sufficiently long to permit virtually complete disappearance of contaminant originating at Indian Point by the time this contaminant reaches the Harbor. This means that the downstream end of the estuary has no influence on contaminant distribution in the estuary. The estuary may therefore be considered to be infinitely long and the first boundary condition may be written:

$$C_{III} \Big|_{x=\infty} = 0 \quad \text{BC \#1}$$

2. In the upstream region, convection opposes dispersion and the distance from Indian Point to the upper end of the estuary is even greater than the distance from Indian Point to the lower end. For these reasons, the statements concerning BC #1 are even more applicable here and

the second boundary condition is written:

$$C_I \Big|_{x=-\infty} = 0 \quad \text{BC \#2}$$

3. Although Equation 10 does not define behavior across sections at Indian Point and Chelsea, and discontinuity in some derivative will occur at these points, the contaminant concentration itself is continuous and therefore single-valued at all points. This fact gives rise to the third and fourth boundary conditions:

$$C_I \Big|_{x=a} = C_{II} \Big|_{x=a} \quad \text{BC \#3}$$

$$C_{II} \Big|_{x=0} = C_{III} \Big|_{x=0} \quad \text{BC \#4}$$

S-61

10

4. To describe the behavior at the boundary between regions II and III, a material balance about the plane of discharge is constructed as shown on Figure 15. The steady state material balance is written:

$$\left[Q_2 c_{II} - EA \frac{dc_{II}}{dx} \right]_{x=\frac{\Delta x}{2}} + q^r c_{II} + q^{IP} c^{IP} - q^r c_{II} - \left[Q_3 c_{III} - EA \frac{dc_{III}}{dx} \right]_{x=\frac{\Delta x}{2}} = K \bar{c} \Delta x \quad \dots\dots (12)$$

in which Q_2 = River flow above Indian Point

q^{IP} = volumetric discharge from plant

Q_3 = $Q_2 + q^{IP}$ = net River flow below Indian Point

c^{IP} = concentration of plant contaminants prior to introduction to recirculating flow

q^r = recirculating River flow through plant

Simplifying Equation 12 and taking the limit as $\Delta x \rightarrow 0$ yields:

$$q^{IP} [c^{IP} - c_{II}]_{x=0} - EA \left[\frac{dc_{II}}{dx} - \frac{dc_{III}}{dx} \right]_{x=0} \quad \dots\dots (13)$$

In reality, virtually all of the flow from Indian Point is recirculated from the River. Therefore $q^{IP} \ll Q_2$, and for all practical purposes $Q_2 = Q_3$. Call $(q^{IP} - c^{IP})$, W , the continuous load on the River, take the limit of Equation 12 and obtain for the fifth boundary condition:

$$W = EA \left[\frac{dc_{II}}{dx} - \frac{dc_{III}}{dx} \right] \quad \text{BC \#5}$$

Notice that the first derivatives of the contaminant concentration are discontinuous at the point of discharge. This behavior is shown clearly by the contaminant profile in Figure 1.

5. The behavior at the boundary between regions I and II is developed

similarly. A material balance about the plane of drawoff is constructed in Figure 15 and is written:

$$\left[Q_1 c_I - EA \frac{dc_I}{dx} \right]_{a-\frac{\Delta x}{2}} - q_c c_a - \left[Q_2 c_{II} - EA \frac{dc_{II}}{dx} \right]_{a+\frac{\Delta x}{2}} - K \bar{c} A \Delta x = 0 \quad \dots \dots (14)$$

in which Q_1 = River flow above Chelsea

q_c = drawoff at Chelsea

Q_2 = Q_1 - q_c River flow below Chelsea

c_a = contaminant concentration at Chelsea

S-62

11

As Δx approaches zero, $c_I = c_{II} = c_a$ and Equation 14 becomes:

$$\left. \frac{dc_I}{dx} \right|_{x=a} = \left. \frac{dc_{II}}{dx} \right|_{x=a} \quad \text{BC \#6}$$

Notice, in the case of drawoff from the River, the concentration of contaminant in the withdrawn flow is identical to the concentration of contaminant in the River at the point of drawoff. In the case of discharge to the River, the contaminant concentration in the discharged flow is much larger than in the River at this point. Thus, in the case of drawoff, the defining differential equation does not hold across the point of drawoff because the River flow is changed, while in the case of discharge, it does not hold because of the imposition of a net load on the River.

Substitution of Equations 11a, b, c into these six boundary conditions yields values for the six arbitrary constants. The explicit solutions for contaminant concentration becomes:

$$c_I = \frac{W e^{(j_2 - j_1)} a + j_1 x}{AE (j_1 - k_2)} \quad \dots \dots (15)$$

$$c_{II} = \frac{W}{AE} \left[\frac{e^{j_2 x}}{j_2 - k_2} + \frac{(j_2 - j_1) e^{(j_2 - k_2) a + k_2 x}}{(j_2 - k_2) (j_1 - k_2)} \right] \quad \dots \dots (16)$$

$$c_{III} = \frac{W}{AE} \left[\frac{(j_1 - k_2) + (j_2 - j_1) e^{(j_2 - k_2) a}}{(j_2 - k_2) (j_1 - k_2)} \right] e^{k_2 x} \quad \dots \dots (17)$$

For the case of no decay, $K = 0$, and:

$$\begin{aligned}j_1 &= \frac{U_1}{E} \\j_2 &= \frac{U_2}{E} \\k_2 &= 0\end{aligned}$$

For this case, the concentrations at $x = 0$ (Indian Point) and at $x = a$ (Chelsea) are, respectively:

$$C_o = \frac{W}{Q_1} \left[\frac{U_1}{U_2} \left(1 - e^{-\frac{U_2 a}{E}} \right) + e^{-\frac{U_2 a}{E}} \right] \quad \dots \dots \dots (18)$$

$$C_a = \frac{W}{Q_1} e^{-\frac{U_2 a}{E}} \quad \dots \dots \dots (19)$$

S-63 12

For no drawoff at Chelsea, Equation 18 and 19 reduce to the simple case of discharge of a conservative contaminant at $x = 0$; i.e., $U_1 = U_2$, $Q_1 = Q_2 = Q$ and:

$$C_o = \frac{W}{Q} \quad \dots \dots \dots (20)$$

$$C_a = \frac{W}{Q} e^{-\frac{U a}{E}} \quad \dots \dots \dots (21)$$

The ratio of concentration at Chelsea to concentration at Indian Point is:

$$\frac{C_{\text{Chelsea}}}{C_{\text{Indian Point}}} = \frac{C_a}{C_o} = \frac{1}{1 + \frac{U_1}{U_2} \left(e^{\frac{U_2 a}{E}} - 1 \right)} \quad \dots \dots \dots (22)$$

For the case of no drawoff at Chelsea, this reduces to $e^{-\frac{U a}{E}}$.

2. TRANSIENT CONDITION

Subsequent to commencement of a steady, continuous discharge, a time lag occurs before steady state profiles, described by Equation 15 through 21, are established. To determine concentration build-up as a function of time as well as of space, an unsteady state analysis of Equation 4 must be made. Such an analysis has been judged necessary in this study, not only to establish the rapidity of approach to steady state, but also to serve as a basis for a computer solution of the maximum permissible continuous release when radioactive decay

is taken into account (7).

Analysis shows that the 100 mgd Chelsea draw has only a slight effect on equilibrium concentration at Chelsea. The same can be expected during the approach to equilibrium so that transient analysis without consideration of draw-off was used. This has been developed previously in considerable detail (8). The final equation for the distribution of contaminant upstream of the point of waste discharge is:

$$^cI(x,t) = \frac{W}{2Q\sqrt{1+\frac{4KE}{U^2}}} \left[E x P \left[\frac{U}{2E} \left(1 + \sqrt{1 + \frac{4KE}{U^2}} \right) x \right] \cdot ERFC \left(\frac{-x}{\sqrt{4Et}} - \sqrt{\frac{U^2+4KE}{4E}} t \right) \right. \\ \left. - EXP \left[\frac{U}{2E} \left(1 - \sqrt{1 + \frac{4KE}{U^2}} \right) x \right] \cdot ERFC \left(\frac{-x}{\sqrt{4Et}} + \sqrt{\frac{U^2+4KE}{4E}} t \right) \right] \quad \dots \dots \dots (23)$$

S-64 13

The corresponding steady state solution, given by Equation 16 when $U_1 = U_2$ (no drawoff, $U_1 = U_2$), is:

$$^cI(x) = \frac{W}{Q\sqrt{1+\frac{4KE}{U^2}}} e^{-\frac{U}{2E} \left[1 + \sqrt{1 + \frac{4KE}{U^2}} \right] x} \quad \dots \dots \dots (24)$$

The ratio of the transient response to the equilibrium response is:

$$\frac{^cI(x,t)}{^cI(x,\infty)} = \frac{1}{2} \left[ERFC \left[\frac{-x}{\sqrt{4Et}} - \sqrt{\frac{U^2+4KE}{4E}} t \right] \right. \\ \left. - EXP \left[-\frac{U}{E} \sqrt{1 + \frac{4KE}{U^2}} x \right] \cdot ERFC \left[\frac{-x}{\sqrt{4Et}} + \sqrt{\frac{U^2+4KE}{4E}} t \right] \right] \quad \dots \dots \dots (25)$$

For the case of no decay, Equation 25 reduces to:

$$\frac{^cI(x,t)}{^cI(x,\infty)} = \frac{1}{2} \left[ERFC \left[\frac{-x}{\sqrt{4Et}} - \sqrt{\frac{U^2}{4E}} t \right] - EXP \left[-\frac{U}{E} x \right] \cdot ERFC \left[\frac{-x}{\sqrt{4Et}} + \sqrt{\frac{U^2}{4E}} t \right] \right] \quad \dots \dots \dots (26)$$

S-65 14

IV. INSTANTANEOUS RELEASE

This case represents the condition of an accidental spill of radioactive contaminant to the River. A slug of material is released over a short time interval, which for practical purposes can be assumed to be instantaneous. The object is to determine the time of appearance of and the value of maximum concentration at Chelsea.

1. PREVIOUS STUDIES

Studies of the effect of instantaneous release of conservative substances at Indian Point were conducted on the Hudson River Model at the Waterways Experiment Station, Vicksburg, Mississippi, circa 1962 (9). Figure 16 is a reproduction of Plate 30, reference 9, and shows the distribution of conservative dye, released over a single tidal cycle at Indian Point, for a River flow of 12,000 cfs. Notice that the spread is asymmetrical, favoring the downstream direction. This documents the variable nature of the dispersion coefficient and the fact that it increases in the downstream direction, as shown previously in Figure 12. A more detailed analysis of these data, in terms of the mechanisms which cause E to vary, may be found in references 5 and 6.

The occurrence of maximum upstream E values between mile points 45 and 50 is demonstrated by Figure 16. Within this reach a decreasing slope, particularly for tidal cycles 15 through 30, can be seen, indicative of greater spreading or longitudinal dispersion. For a flow of 12,000 cfs, salinity is well below mile point 55, the approximate location of the mouth of Newburgh Bay, and therefore not available to induce circulation, i.e., increase E . Below this point the channel narrows, the velocity is higher, and the downstream-directed

QUIRK, LAWLER & MATUSKY ENGINEERS

convection strong. However, the rate of tidal energy dissipation, besides salinity-induced circulation, the other major cause of dispersion, is relatively high and dispersion is enhanced and the dye moves up this far.

Tidal energy dissipation in the larger expanse of the bay is relatively low; without salinity-induced circulation present, dispersion becomes negligible and is overpowered by downstream-directed convection. Thus, at the flow of 12,000 cfs, dye does not appear above mile point 55.

At drought flows, of course, salinity is present for north of this point; significant dispersion, at these times, can be expected in the vicinity of Chelsea.

S-66

15

S-67

Figure 16

2. CONSTANT PARAMETER ANALYSIS

Draw off at Chelsea is not considered; the results of the continuous analysis indicate this is not a serious omission. Detailed analysis of the instantaneous release for constant River characteristics has been developed previously (8); a brief outline of the development is given here.

The defining differential equation is Equation 4. The initial and boundary conditions are developed as shown on Page 9 and are:

Initial Condition: $C|_{t=0} = 0, -\infty \leq x \leq \infty$

Boundary Conditions #1, #2: $C|_{x=\pm\infty} = 0, \text{ all } t$

Boundary Conditions #3 $C|_{x \rightarrow 0^-} = C|_{x \rightarrow 0^+} \text{ all } t$

Boundary Conditions #4 $AE \left[\frac{dc}{dx} \Big|_{x \rightarrow 0^-} - \frac{dc}{dx} \Big|_{x \rightarrow 0^+} \right] = f(t), t > 0$

$f(t)$ in B. C. #4 is the delta function and is written:

$$f(t) = \begin{cases} \frac{M}{\Delta t}, & 0 < t < \Delta t \\ 0, & \Delta t < t \leq \infty \end{cases}$$

in which M = Mass of contaminant released

The Laplace Transform Solution of Equation 4, subject to the above conditions, yields:

$$C(x,t) = \frac{M}{2A\sqrt{\pi Et}} e^{-\frac{(x-Ut)^2}{4Et}} - Kt \quad \dots\dots (27)$$

To compute the dilution effect only, set K = 0. Equation 27 becomes:

$$C(x,t) = \frac{M}{2A\sqrt{\pi Et}} e^{-\frac{(x-Ut)^2}{4Et}} \quad \dots\dots (28)$$

The maximum value of C(x,t) at a given x is desired. Differentiate Equation 28 with respect to t and equate the results to zero to determine the time at which the maximum concentration occurs. This procedure yields:

$$t_{critical} = \frac{E}{U^2} \left[-1 + \sqrt{1 + \frac{U^2 x^2}{E^2}} \right] \quad \dots\dots (29)$$

S-68

16

VIII. REFERENCES

1. Kent, R. "Diffusion in a Sectionally Homogeneous Estuary." Paper No. 3392, Transactions, American Society of Civil Engineers, Vol. 128, Part III (1963).
2. Holley, E. R., Jr. and Harleman, D. R. F. "Dispersion of Pollutants in Estuary Type Flows." Report No 74, Hydrodynamics Laboratory, Massachusetts Institute of Technology, Cambridge, Mass. (January 1965).
3. Lawler, J. P. "Mathematical Analysis of Estuarine Pollution," in "Engineering Aspects of Marine Waste Disposal." Environmental Health Sciences and Engineering Training Course Manual, R. A. Taft Sanitary Engineering Center, Cincinnati, Ohio (1965).
4. Bird, R. B., Stewart, W. E. and Lightfoot, E. N. "Transport Phenomena." John Wiley and Sons, New York, N. Y. (1960).
5. "Evaluation of Waste Diffusion in the Hudson River at Peekskill." Report to Standard Brands, Incorporated by Quirk, Lawler and Matusky, Water Resources Engineers, New York, N. Y. (December 1964).
6. "Hudson River Dispersion Characteristics." Progress Report to Consolidated Edison Company of New York, Incorporated by Quirk, Lawler and Matusky,

QUIRK, LAWLER & MATUSKY ENGINEERS

Water Resources Engineers, New York, N. Y. (October 1965)

7. "Indian Point Station – River Diffusion Study." Consolidated Edison Company of New York, Incorporated – Memorandum from C. A. Larson to W. J. Cahill, Jr. (April 26, 1966).
8. Lawler, J. P. "Differential Equations" in "Stream and Estuarine Analysis." Training Manual, Tenth Summer Institute in Water Pollution Control, Manhattan College, New York, N. Y. (June 1965).
9. "Joint Pollution Studies in the New York Harbor Model." Miscellaneous Paper No. 2-558, U. S. Army Engineer Waterways Experiment Station, Vicksburg, Miss. (February 1963).

S-69

17

QUIRK, LAWLER & MATUSKY ENGINEERS

[Historical Information]

Consolidated Edison Company of New York, Inc.

EVALUATION OF FLOODING CONDITIONS
AT INDIAN POINT
NUCLEAR GENERATING UNIT NO. 3

April, 1970

Revision of Report of February, 1969

Quirk, Lawler & Matusky Engineers
Environmental Science & Engineering Consultants
505 Fifth Avenue
New York, New York 10017

I-1

TABLE OF CONTENTS

	Page
Letter or Transmittal	
Acknowledgments	
Summary of Findings, Conclusions & Recommendations	S-1 – S-8
I Introduction	1
II Description of the Hudson River Basin	6
III Probable Maximum Flood for the Hudson River Basin	17
IV Hudson River Basin Reservoir Flood Routing and Dam Failure Analysis	56
V Maximum River Elevation for Flooding Conditions at Indian Point	96
<u>Appendix A</u>	
Maximum River Elevation at Indian Point Resulting from Probable Maximum Hurricane and Spring High Tide	
<u>Appendix B</u>	
Upper Hudson River Basin Flood Study – Stone & Webster Engineering Corporation	
<u>Appendix C</u>	
Notations & Symbols Used in the Report	
<u>Appendix D</u>	
References	

ACKNOWLEDGMENTS

Many persons have contributed either directly or indirectly to this report.

We are particularly grateful to Mr. Dwight E. Nunn, of the AEC and Mr. P. Carpenter of the FWPCA for their many helpful suggestions and contributions.

Acknowledgment is hereby given to Messrs. Robert Forrest of the Board of Hudson River-Black River Regulating District, Robert J. O'Conner, H. Siemer and Leslie W. Waters of N.Y.C. Board of Water Resources, and Mr. Vincent V. Terenzio of N.Y.C. Board of Water Supply for the use of data and valuable discussions concerning the Sacandaga and Ashokan Dams.

We are grateful also to Messrs. Kenneth I. Darmer and Chintu Lai of the U. S. Geological Survey for the supply of several publications and discussions concerning the Hudson River activities of the Water Resources Division.

We are indebted to Messrs. Andrew Matuskey and Frank L. Panuzio of the Corps of Engineers for advise, consultation and assistance in providing helpful data regarding the probable maximum flood and hurricane.

the investigation was conducted by Quirk, Lawler & Matusky Engineers under the direction of Dr. John P. Lawler. Mr. Karim A. Abood of Q.L & M served in the capacity of project engineer and wrote this report. Dr. Karel Konrad of Q.L. & M. contributed materially to this study and performed any of the calculations reported herein.

I-3

-S-1-

SUMMARY OF FINDINGS, CONCLUSIONS & RECOMMENDATIONS

1. Consolidated Edison Company of New York, Incorporated, (Con Ed) plans to build a third nuclear generating unit at its Indian Point site. The site is located in the town of Buchanan, Westchester County, New York and lies along the east bank of the Hudson River, some 43 river miles above New York City Harbor. The proposed facility will have a guaranteed output of 965 megawatts electric.

2. The Atomic Energy Commission (AEC), by virtue of the Atomic Energy Act, is empowered to review and issue licenses to construct and operate nuclear power plants. The AEC licensing regulations include submission of a Preliminary Safety Analysis Report (PSAR). The site safety criteria for this report requires an analysis of the area's hydrology.

3. Quirk, Lawler & Matislu Engineers (Q/L & M.), Environmental Science & Engineering Consultants were retained by Con Ed to study the hydrology of the Indian Point site and to determine the maximum water-surface elevations that can occur as a result of possible flooding conditions at the site. The establishment of such flood levels is necessary to provide adequate protective measures during flood conditions.

Three previous studies had been performed prior to this investigation. The results of those studies were submitted to the AEC. The first appears in Supplement 10, Docket 50-286; the second is Q. L. & M's report of February, 1969 and the third is Q.L. & M's Summary of March, 1970.

The present study was conducted along the lines of a number of specific guidelines developed during several meetings with AEC staff personnel. The study is of a comprehensive and detailed nature involving careful analysis and accepted methodology and follows closely the procedures utilized by the U.S. Corps of Engineers for estimating the hydraulic events under consideration.

4. Several flooding conditions governing the maximum water elevation at the site, were investigated including:
- a. Flood resulting from runoff generated by a Hudson River Probable maximum Precipitation (PMP).
 - b. Flooding caused by the occurrence of a dam failure concurrent with heavy runoff generated by a Hudson River

I-4

-S-2-

Standard Project Flood (SPF). This condition was considered because the previous condition did not result in a dam failure.

- c. Flooding due to the occurrence of a Probable maximum Hurricane (PMH) concurrent with spring high tide.

5. The determination of the most severe water surface elevations at the site was based upon the simultaneous occurrence of the above-delineated flooding conditions with several critical boundary conditions in the Hudson River including:

- a. Mean Water Elevation
- b. High tide Water Elevation
- c. Low tide water Elevation
- d. Standard Project Hurricane (SPH)
- e. Probable maximum Hurricane (PMH)

6. The work required to achieve these objective included:

- a. Determination of the Hudson River hydraulic and Hydrodynamic characteristics, which include channel Geometry, flow resistance, tidal dynamics and basin Hydrology.
- b. Derivation of the Maximum Probable Flood (PMF) and Standard Project Flood (SPF) for the Hudson River Basin upstream of the site.
- c. Structural and hydraulic analysis of the major dams in the basin to determine their stability and failure possibility under PMP conditions.
- d. Determination of the Probable Maximum Hurricane (PMH) and Standard Project Hurricane (SPH) for the New York Harbor area and resulting peak storm surge heights in the Hudson River.

The specific details of these items are given in Chapters II, III, IV and Appendix A respectively. The results of the determination of the maximum water-surface elevations resulting from the flooding conditions of Item 4 and boundary conditions of Item 5 above are presented in Chapter V.

The procedures employed and major findings are summarized below in the following six items (#7 through 12).

7. A PMP of 14 inches in 72 hours and a probable maximum storm (PMS) pattern similar to the one derived by the U.S. Weather Bureau for the adjacent Susquehanna Basin at Danville were used in this study. These were adopted on the basis of similarity in topography,

I-5
-S-3-

shape and size between the two neighboring basins.

The 6-hour incremental rainfall depths and related runoffs for the entire basin arranged in a critical time sequence documented in Figure S-1.

The Hudson Basin was divided into 28 subbasins and a flood hydrograph for each subbasin was established using the PMP values corresponding to the selected PMS together with the appropriate rainfall losses and unit hydrograph. To illustrate the procedures employed, a brief description of the development of a typical subbasin flood hydrograph is presented below.

Figure S-2 summarizes the basic flood data for the Catskill Creek Basin used in this study. An isohyetal map of the subbasin appears in the upper right hand corner. The isohyets, shown as broken lines, represent the subbasin portion of the total Hudson Basin PMS. This total PMS is shown in Figure III-8. The rainfall values are for the total storm duration of 72 hours. Twelve sets of such values corresponding to twelve 6-hour subdurations were established.

For each time increment, average rainfall depth over the subbasin was computed. These increments were then rearranged in accordance with a recommended critical time sequence. The appropriate initial and infiltration losses (1" and .05"/hr. respectively) were subtracted to obtain the subbasin rainfall excesses (runoff) for each subduration. The resulting rainfall and runoff distributions are shown in the upper left hand corner.

The generated runoff was applied to the 6-hour unit hydrograph to develop the subbasin flood hydrograph.

with base flows added the flood hydrographs of the 28 subbasins were combined in their proper time sequence and/or routed downstream to give the inflows into the Hudson River from its tributaries.

An example of the flood hydrograph combination and routing is depicted in Figure S-3. The example considers subbasins No. 15, 16 and 17 of the Mohawk River Basin. The flood hydrographs of subbasins No. 15 and 16 were combined to obtain the Mohawk River flood hydrograph at the mouth of Schoharie Creek. The resultant was routed through the river using the classical Muskingum coefficient method to Cohoes. This routed hydrograph was then combined with subbasin No. 17 flood

QUIRK, LAWLER & MATUSKY ENGINEERS

I-6	
Figure S-1	I-7
Figure S-2	I-8
Figure S-3	I-9

-S-4-

hydrograph to establish the total Mohawk River hydrograph at the confluence of the Mohawk River with the Hudson.

the main river inflows were then routed downstream in a similar manner until the flood hydrograph at Indian point was determined.

The routed hydrographs at several locations along the Hudson River are depicted in Figure S-4.

The above-listed steps were verified by predicting flows using actual rainfall-runoff records and then comparing the results with published values at Cohoes, Green Island and the Wallkill River.

The peak discharge thus obtained at Indian Point amounts to 1.1 million cubic feet per second and represents the Probable Maximum Flood (PMF) at the site. The corresponding Standard Project Flood was selected as equal to 50 per cent of this value.

In developing the PMF, every effort was made to make all the necessary assumptions as conservative as possible and the results were closely checked with the U.S. Army Corps of Engineers generalized curves.

The computed PMF agrees reasonably well with its Susquehanna, Delaware and Potomac Rivers counterparts. It is more than 60 per cent higher than the statistically evaluated 10,000 year flood at Indian Point.

8. To obtain the most severe flooding conditions, the heavy rainfall centers of the selected PMS were deliberately placed over the basins of the largest two reservoirs in the Hudson River Basin. These reservoirs are the largest regulating feature in the basin (Sacandaga) and New York City's reservoir at Ashokan. These reservoirs are located some 180 and 75 miles upstream of the site respectively

Inflows to Sacandaga and Ashokan Reservoirs resulting from placing the heavy rainfall centers of the PMS over their basins were routed through the reservoirs. The results clearly indicate that both dams have sufficient storage to pass this flood without danger of overtopping or piping, i.e. erosion of the surface of the downstream face. The specific details follow.

9. The Sacandaga Reservoir Dam, know as the Conklingville Dam, is extremely stable and has proven its ability to withstand sever

I-10

Figure S-4

I-11

-S-5-

earthquakes and floods. It has an ample cross-section with a very broad base and a substantial freeboard of 24 feet above the crest of spillway at elevation 771.0.

The dam is relatively impervious, made of excellent material consisting of glacial drift, has an impermeable earth core and is founded on rock. It has an unusually large toe, sizable cover of riprap and sufficient outlet works and spillway capacity.

when routing the probable maximum inflow through the reservoir, the maximum stage reached was elevation less than elevation 784.0, more than 11 feet below the crest of the dam.

Computation of the location of the free water surface within the dam showed that the seepage water caused by the maximum possible water elevation would collect in the rock toe and would be safely discharged without carrying soil grains with it. This was the case even when a highly conservative and hypothetical case consisting of the maximum possible stage upstream and a 20 foot water depth downstream of the dam.

These estimates are based upon several conservative assumptions including:

- a. Outlet works would start operation when the reservoir level reaches elevation 771.0, the crest of spillway elevation.
- b. High initial reservoir level at elevation 768.0 prior to the beginning of the PMS.
- c. Inoperative power house pumps.
- d. Homogeneous material, i.e. no advantage was taken of the deflection in seepage curve caused by the relatively impermeable core.
- e. Presence of water downstream of the dam.

10. The study of the effect of routing the Esopus Creek flood hydrograph (upstream of the Ashokan Dam) resulting from the Hudson River PMS through the Ashokan Reservoir indicates that the dam would not fail from overtopping or seepage. The maximum possible reservoir elevation would be below the crest of the masonry core in the dikes and more than 11 to 15 feet below the crest of the east and west basin reservoirs respectively. The dam has proven its ability to withstand such high elevation on March 31, 1951 when the elevation in the east basin reached a record high of 592.23 feet, about 1.5 feet higher than the elevation resulting from the Hudson River PMP.

-S-6-

11. Since the results of the previous item indicated that the Ashokan Dam would not fail, a more critical condition resulting in a dam failure was investigated. The reason behind consideration of a more severe Ashokan Dam condition stems from the fact that the Ashokan Reservoir contains the largest volume of stored water in the basin within less than 100 miles from the Indian Point site.

This flooding condition consists of the simultaneous occurrence of a probable maximum flood over the Esopus Creek Basin upstream of the Ashokan Dam and a Standard Project Flood over the rest of the Hudson River Basin.

this condition resulted in a peak reservoir inflow of 200,000 cfs causing a dam failure as a result of a reservoir elevation higher than the crest of the masonry wall in the west dike and earth part of the main dam.

However, the structural analysis of the masonry part of the main dam showed that this part would not fail from overturning and sliding with minimum factors of safety of about 1.1. and 1.9 respectively.

The failure of the Ashokan Dam would cause a maximum reservoir outflow of 2.6 million cfs and create a seven billion cubic feet lake extending from the dam to Glenerie Falls some 5 miles west of the Hudson River. The lake would have a total length of 14 miles and a surface width ranging from 4,000 to 1,800 feet. It would also have a control section at Glenerie Falls. The outflow of this lake would be about 620,000 cfs.

This outflow was combined with the flood hydrographs resulting from Esopus Creek PMP and Hudson River PMP and routed downstream to Indian Point. Much of the discussion on the determination of the PMF at Indian Point summarized in Item 7 above applies here, mutatis mutandis.

the maximum discharge at Indian Point resulting from this condition would be 705,000 cfs.

12. The maximum water-surface elevations at the site resulting from the flooding conditions summarized in item 4 concurrent with the initial conditions of Item 5 above were determined. These conditions were conservatively grouped in seven different ways on the basis of a simultaneous occurrence of an appropriate set of flooding, hurricane and tidal conditions.

I-13

-S-7-

As in the case of flooding from dam failure, the tidal variation in the Hudson Estuary was treated as an integral part of the system and its influence was simultaneously coupled with the other hydraulic occurrences. The results of this study suggest that the river above the Tappan Zee Bridge, some 27 miles above the Battery, would experience relatively small tidal variations under the PMP conditions. However, to examine the effect on Indian Point the upstream extent of tidal influence was extended to the site.

In the evaluation of the maximum water surface elevation at the site, the wind produced local oscillatory short period waves were also included. The computed stages were increased by one foot to account for this effect.

The standard Step Method was employed in this investigation to determine the flow profiles and stages at the site. The computations were initiated at the Battery, the mouth of the Hudson River. The results were checked with a more refined and newly developed method.

The seven groups of flooding, hurricane and tidal conditions and the corresponding stages at Indian Point are summarized in Table S-1

Cases No. 1 through 3 consider the Indian Point stage at peak discharge due to runoff generated by the PMP over the basin and mean, high and low tide stages at the Battery. The flow profiles corresponding to these cases are depicted in Figure S-5.

Case No. 4 considers the maximum river stage at the site resulting from the dam failure concurrent with the Hudson River SPF summarized in Item 11 above.

To carry the degree of severity a step further, a more critical boundary condition consisting of the peak storm surge at the Battery resulting from the SPH was imposed on the flooding condition of steps No. 5 and 6.

To maintain the selection of severe conditions and in accordance with the high degree of conservatism adopted in this report, the SPH based on the transposition of the September 1944 hurricane rather than the less critical SPH of the 1938 hurricane was used. The 1944 value is 75 per cent higher than the maximum storm surge during hurricane "Donna" which struck on September 1, 1960 and which is the storm having the greatest effect since 1821.

Case No. 6 considers an even more critical set of occurrences con-

Table S-1	I-15
-----------	------

Figure S-5

I-16

-S-8-

sisting of the simultaneous occurrence of the following three severe conditions:

- a. PMP over the Ashokan Reservoir resulting in a dam failure
- b. runoff generated by the SPP over the Hudson Basin
- c. Peak storm surge resulting from the SPH for the New York Harbor area

The simultaneous occurrence of these three conditions is extremely remote. Each one of these three conditions are in themselves unlikely events. The combination of all three decreases, therefore, the likelihood of occurrence significantly.

The flow profiles corresponding to cases No. 4 through 6 are depicted in Figures S-6.

For convenience, the results of routing the PMH through the Hudson River to the site presented in our report are also listed in Table S-1.

Conclusion – These analyses show clearly that the maximum elevation at Indian Point due to flooding and wave runup is 15 feet or less.

I-17

Figure S-6 I-18

I. INTRODUCTION

Consolidated Edison Company of New York, Incorporated, plans to build a third nuclear generating unit on the Hudson River at Indian Point. The new facility is called Indian Point No. 3 reactor since two other nuclear power units have been authorized for the same site.

The Indian Point site is located in the town of Buchanan, Westchester County, New York. The property lies along the east bank of the Hudson River, some 43 river miles above New York City Harbor.

The proposed facility will have a guaranteed output of 965 megawatts electric. On completion of Unit No 3, the total manufacturer's guaranteed rating of Unit Nos. 2 & 3 will be 2123 megawatts electric.

The Atomic Energy Commission (AEC), by virtue of the Atomic Energy Act, is empowered to review and issue licenses to construct and operate nuclear power plants. The AEC licensing regulations include submission of a Preliminary Safety Analysis Report (PSAR). Site safety criteria for this report requires an analysis of the area's hydrology.

I-19

-2-

Quirk, Lawler & Matusky Engineers (QL&M), Environmental Science and Engineering Consultants were retained by Consolidated Edison to study the hydrology of the Indian Point site and to determine the maximum water elevations that can occur as a result of possible flooding conditions at the site of the Indian Point Nuclear Generating Unit No. 3. The establishment of such a flood level at the site is necessary to provide the necessary protective measures during flood conditions.

Preliminary analysis based upon highly conservative estimates were conducted in 1968. The results of that study are delineated in Supplement 10, Indian Point Unit No. 3, AEC Docket 50-286.

The following two flooding conditions, which the AEC indicated would govern the maximum water elevation, were investigated:

1. Flooding from maximum rainfall concurrent with dam failure at Sacandaga and Ashokan Reservoirs and flow at ebb tide.
2. Flooding resulting from the probable maximum hurricane current with spring high tide.

In the 1968 report it was noted that a more refined flooding analysis would give more realistic results, and that the hurricane surge analysis was based upon a theory applicable to conditons of open

I-20

seas and neglected frictional resistance in the Hudson River Channel.

The 1968 preliminary values were then modified as a result of a new study which considered surrounding topography, land use, river geometry and frictional losses. A report documenting the results of the new study was submitted to the AEC in February, 1969.

Because the 1969 results indicated that the hurricane surge analysis proved to be controlling, specific attention was paid to determining the water elevation resulting from the occurrence of probable maximum hurricane.

After a review of the February, 1969 report, including conferences with AL & M and Con Ed by the AEC, the commission requested that the applicant restudy in depth the runoff resulting from heavy rainfall over the basin drainage area and revise the water elevation computation at Indian Point.

In particular, the AEC objected to the use of the so-called "rational formula" for the runoff computations and the Manning Open Channel Flow Equation for the determination of the water elevation

I-21

-4-

The AEC suggested a more refined approach including the use of the Corps of Engineers findings and procedures to determine the probable maximum flood and the backwater profile method to predict the water surface elevation resulting from flooding due to probable maximum precipitation over the basin.

A study along the lines of the suggested procedures was instituted in January of this year and involved a thorough evaluation of the maximum predictable stage of the Hudson River at the Indian Point site. Major emphasis was placed on the determination of the probable maximum flood, dam failure analysis, influence of the tidal flow and the maximum water elevations for several flooding conditions. Two meetings were held on March 26 and April 21, 1970 between the AEC staff personnel, Con Ed and Q & M to discuss the proposed program and to delineate requirements for further refinements. At these meetings, a number of specific guidelines for the analyses of all pertinent parameters and accepted methodology were developed. The procedures and methods adopted for this study follow closely the developed guidelines and those utilized by the U.S. Corps of Engineers.

The purpose of this report is to present the results of this study. For convenience, the results of the revised probable maximum hurricane study of the February, 1969 report are also included in this report.

I-22

-5-

the report is formulated as follows:

1. A general description of the Hudson River Basin and the channel characteristics is given in Chapter II.
2. The specific details and adopted methodology in computing the Hudson River probable maximum flood at Indian Point are presented in Chapter III. The results of the previous flood investigations are also documented in this chapter.
3. chapter IV presents the results of the flood routing and dam failure analysis of the Hudson River Basin Reservoirs.
4. A discussion of the procedures and results of the maximum water elevations for several flooding conditions resulting from a probable maximum flood, dam failure and tidal flow is given in Chapter V.
5. The results of the revised analysis of the water elevation at Indian Point resulting from the occurrence of a probable maximum hurricane concurrent with spring high tide are documented in Appendix A. The material included in this Appendix is essentially that of Chapter III of the February, 1969 report.

I-23

-6-

II. DESCRIPTION OF HUDSON RIVER BASIN *

A. Description of the Basin

The Hudson River Basin is located in the eastern part of New York State, draining an area of 12,650 square miles. Most of this area lies in the east central part of New York State, with small portions in Vermont, Massachusetts, Connecticut and New Jersey. A plan view of the Basin is shown in Figure II-1. Several locations of interest to this study are underlined in Figure II-2. The distance in river miles above the mouth of the river is also shown in Figure II-2.

The Hudson River Basin is bounded on the north by the St. Lawrence and the Lake Champlain Drainage basins; on the east by the Connecticut River, the Housatonic River Basins and the Connecticut Coastal Area; on the west by the Delaware, Susquehanna, Oswego and Black River Basins; and on the south by the basins of small streams tributary to the Hudson River in New York Harbor. The Hudson River watershed extends 128 miles east-to-west and 238 miles north-to-south.

The Hudson River has its source in Henderson Lake in the Adirondack

Mountains in northern New York State and flows generally south for 315 river miles to its mouth at the Battery where it discharges into New

* Some of the material covered in the first two sections of this chapter is based on several Federal and State publications on the Hudson River 8-14

II-1

II-2
II-3

FIGURE II-2

-7-

York Upper Bay. Upstream of Henderson lake, the stream is known as the Opalescent River and its headwaters are in Lake Tear-of-the-Clouds on the Southwest slop of Mount Marcy in Essex County.

The major tributaries entering the main stream are mohawk River, Hoosic River, Kinderhook Creek, Indian River, Sacandaga River, Esopus Creek and Rondout Creek. The drainage areas of these and other principle tributaries are listed in Table II-1. For convenience, the entire Hudson River Basin has been separated into three principal drainage areas; the Upper Hudson, the Mohawk River, and the Lower Hudson sub-basins.

The division between the Upper and Lower Hudson Basin is at the confluence of the Mohawk River with the Hudson at Green Island. The Federal Dam at Troy, some 154 river miles above the Battery, is the head of tidewater.

The Upper Hudson River flows generally south-southeast to the confluence with the Sacandaga River where it turns to the east. At Hudson Falls it turns again to the South. Its total length to Green Island is about 150 miles. The river drains an area of some 4627 square miles. From its source to Troy Dam, the Hudson River drops 1810 feet, resulting in an average bottom slope of about 12 feet per mile.

II-4

TABLE II-1

Drainage Areas Of

Hudson River Basin

<u>Stream</u>	<u>Drainage Area</u> (square miles)
Upper Hudson River	
Cedar River	164
Indian River	201
Boreas River	92
Schroon River	568
Sacandaga River	1,058
Batten Kill	441
Kayaderosseras – Fish Creek	252
Hoosic River	713
Minor streams and direct drainage	1,138
Sub-total	4,627
Mohawk River	
Oriskany Creek	146
West Canada Creek	562
East Canada Creek	291
Schoharie Creek	926
Minor streams and direct drainage	1,537
Sub-total	3,462
(Hudson River at Green Island)	8,090
Lower Hudson River	
Kinderhook Creek, including Stockport Creek	512
Catskill Creek	417
Roeliff-Jansen Kill	208
Esopus Creek	425
Rondout Creek, including Wallkill River	1,197
wappinger Creek	208
Minor streams and direct drainage	1,594
Sub-total	4,561
Total of Hudson River Basin at the Battery	12,650

-8-

The Mohawk River has its source in the hills near the boundary between Lewis and Oneida Counties, New York. It flows in a southerly direction to Rome, thence it follows a general east-southeast course to its junction with the Hudson River at Cohoes, New York. The total length of the river is about 155 miles and it drains some 3462 square miles. The Mohawk River falls irregularly from its source at elevation 1800 feet above mean sea level to elevation 14.3 feet where it joins the Hudson River at Cohoes.

The Lower Hudson River commences at the junction of the Mohawk and Upper Hudson Rivers at Troy and discharges into the Upper New York Bay. All of this section of the river is tidal. Because of its special nature, detailed description of the estuary portion of the Hudson River is presented in another section of this chapter.

The total length of the Lower Hudson River is about 154 miles and it drains an area of some 4561 square miles.

The average slope in the Lower Hudson, as represented by the half-tide level, is about 2 feet in 150 miles. The slope is greatest in the section of the river from Troy to Catskill and least between Catskill and Tarrytown.

II-6

-9-

The major physiographic features of the Hudson River Basin are a mountainous terrain covering 48 per cent of the basis; cultivated lands covering 42 per cent of the basin; lakes and water bodies covering 2 per cent of the basin; and urban developments covering 8 per cent of the basin.

B. Basin Hydrology

The general climate of the Hudson River Basin may be considered as moist continental. The Upper Hudson Basin has comparatively long, cold and snowy winters sand short mild summers. In the Lower Hudson Basin, the climate is much milder due to the modifying influence exerted by the valley. For these areas there are usually longer summer periods and milder winters. The Mohawk River Basin has variable weather conditions with characteristics of both areas.

The average annual temperature within the basin ranges from 50°F in the southern portion to 40°F in the Adirondack Mountains. The corresponding average July temperature varies form 75°F to 65°F and the average January temperature is 30°F and 15°F respectively. The maximum and minimum temperatures recorded in the basin are 106°F and -42°F respectively.

II-7

-10-

The average annual precipitation varies from 34 inches in the center of the basin to more than 50 inches in the Adirondacks. Most of the basin receives an average of about 40 inches. In general, the precipitation is distributed evenly through the year with a slight rise during the summer. Figure II-3 depicts the normal annual precipitation for the entire Hudson River Basin.

The average annual snowfall for the basin ranges from about 30 inches in New York City to over 130 inches in the Adirondack mountains.

A summary of major basin characteristics including rainfall and runoff data for the three subbasins i.e. the Upper Hudson, Mohawk and Lower Hudson Rivers, is given in Table II-2.

The U.S. Geological Survey (U.S.G.S.) maintains stream gages at some 62 locations in the basin; 21 in the Upper Hudson, 11 in the Mohawk and 30 in the Lower Hudson Basin. Because of tidal oscillation, it is not possible to measure the fresh water flow in the Lower Hudson River directly. Flow histograms in the tidal portion of the river are usually constructed from a knowledge of the Green Island time-discharge relation (the most downstream gaging station above tidewater). The ratio of the drainage areas tributary to Green Island and the Battery is 1.65. However, analysis of data developed by the U.S.G.S. indicates that a yield factor of 1.225

II-8

QUIRK, LAWLER & MATUSKY ENGINEERS

II-10

TABLE II-2

HUDSON RIVER BASIN CHARACTERISTICS

Storage Subbasin	Drainage Area (sq.mi.)	Channel Length (miles)	Mean Annual Temp °F	Mean An- nual pre- cipitation (inches)	Mean Annual Evaporation & Trans Precipitation	Mean Annual Runoff cfs	Mean Annual Usable cfs	Mean Annual ity in	Mean Annual sq.mi.
Capac- acre – ft.									
Upper Hudson River Basin	4627	150	40	40	16	7400	1.60	24	863,000
Mohawk River Basin	3462	155	45	46	24	5600	1.61	22	203,900
Lower Hudson River Basin	4561	154	48	42	20	8700*	1.90	22	551,000

* Estimated

QUIRK, LAWLER & MATUSKY ENGINEERS

-11-

represents the statistically probable value of the ratio of the Lower Hudson discharge to Green Island discharge.

A summary of runoff data at several stations representative of the three subbasins, i.e. the Upper Hudson, Mohawk and Lower Hudson Rivers, is given in Table II-3.

A comparison of long term Lower Hudson monthly average flows with the 1964 histogram is shown on Figure II-4. These histograms were prepared from the Upper Hudson flow measurements at the Mechanicville gage and the Mohawk River measurements at the Cohoes gage for the period from 1918 to 1947 and the Green Island gage for later years. The Lower Hudson River values referred to in this section were established using the yield factor of 1.225.

Flood records indicate that in the past several major floods in the Hudson River Basin have occurred during the spring as well as during the fall or early winter. General storms covering the entire watershed are usually of the transcontinental (cyclonic) or tropical types.

The greatest flood of record over most of the basin occurred in March, 1913 as the result of a period of rapid thaw followed by five days of heavy rainfall. The March, 1936 storm, which followed a sudden rise in temperature after a winter of heavy snowfall was the second greatest

II-11

QUIRK, LAWLER & MATUSKY ENGINEERS

TABLE II-3
STREAMGAGE SUMMARY AT REPRESENTATIVE
STATIONS IN THE HUDSON RIVER BASIN

Station	Area (sq.mi.)	Mean Flow (cfs)	Mean Runoff (csm) (inches)	Years of Record
<u>Mohawk River Basin</u>				
<u>Mohawk River</u>				
near Rome	150	379	2.53	47
near Little Falls	1,348	2,708	2.01	41
at Cohoes	3,453	5,537	1.61	43
<u>Upper Hudson River Basin</u>				
<u>Hudson River</u>				
near Newcomb	192	387	2.02	43
at Gooley	419	830	1.98	52
at North Creek	792	1,534	1.94	61
at Hadley	1,664	2,849	1.71	47
at Mechanicville	4,500	7,431	1.65	70
<u>Sacandaga River</u>				
near Hadley	1,055	2,106	2.00	61
<u>Hoosic River</u>				
near Eagle Bridge	510	903	1.77	56
<u>Schroon River</u>				
at Riverbank	527	795	1.51	61
<u>Lower Hudson River Basin</u>				
<u>Hudson River At</u>				
Green Island	8,090	13,060	1.62	22
<u>Kinderhook Creek</u>				
at Rossman	329	454	1.38	44

II-12

TABLE II-3 (Continued)

STREAMGAGE SUMMARY AT REPRESENTATIVE
STATIONS IN THE HUDSON RIVER BASIN

Station	Area (sq.mi.)	Mean Flow (cfs)	Mean (csm)	Runoff (inches)	Years of Record
Catskill Creek at Oak Hill	98	126	1.29	17.5	58
Walkill River at Gardiner	711	1,045	1.47	20.0	44

II-13

FIGURE II-4

A solid black horizontal bar redacting the content of Figure II-4.

QUIRK, LAWLER & MATUSKY ENGINEERS

-12

Several tropical type storms occurred in October, 1869; November, 1927; and September, 1938.

Table II-4 summarizes the peak discharges and stages of the Hudson River at Troy and Albany during the eight largest floods since 1846.

Several peak discharge frequency curves based upon a number of statistical evaluation methods are shown in Figure II-5. Further discussion of these curves is presented in the next chapter.

Most of the major floods occurred prior to construction of the Sacandaga Reservoir in 1930 which greatly moderated downstream flows. This reservoir and several other reservoirs control about 20 per cent of the entire Hudson River watershed, they have been built to control floods, augment the natural river flows, and for municipal and industrial supply. The major seven reservoirs in the Basin are listed in Table II-5. Detailed description of these reservoirs appear in Chapter IV of this report.

C. Hudson River Channel Characteristics

The major Hudson River Channel characteristics used in flood routing of the probable maximum flood and backwater computations are summarized below.

II-15

TABLE II-4

Flood Stages and Discharges, Hudson River

(Hudson River Basin)

Flood	Troy, N. Y. Drainage Area 8,090 sq.mi.		Albany, N. Y. Drainage Area 8,270 sq.mi.	
	Peak Stage (ft.m.s.1.)	Peak Discharge (c.f.s.)	Peak Stage (ft.m.s.1.)	Peak Discharge (c.f.s.)
October 5, 1869 <u>1/2</u>			18.98	
April 10, 1895 <u>1/2</u>			16.42	
March 28, 1913 <u>1/2</u>	29.4	223,000	21.45	228,000
April 12, 1922 <u>1</u>	25.7	154,000	15.98	158,000
November 4, 1927 <u>1</u>	24.8	150,000	15.96	153,000
March 19, 1936	19.17	215,000	17.5	220,000
September 22, 1938	27.1	183,000	16.5	187,000
December 31, 1948	26.74	181,000	17.46 <u>3</u>	185,000 <u>3</u>
Bank full stage	24.0		11.0	

1 Before completion of Sacandaga Reservoir and 27 ft. navigation channel to Albany

2 Before construction of Federal lock and dam at Troy.

3 January 1, 1949.

QUIRK, LAWLER & MATUSKY ENGINEERS

Figure II-5

II-17

TABLE II-5

MAJOR HUDSON RIVER BASIN RESERVOIR SUMMARY

No.	Reservoir	Year Placed in Distance Area	Stream Area	Usable Capacity Service	Drainage from Indian Point	Purposes (ac-ft)	(miles)
MOHAWK RIVER BASIN							
1	Delta Reservoir	1912	Mohawk River	64,500	140	Canal Regulation	225
2	Hinckley Reservoir	1914	West Canada Creek	78,000	374	Canal Regulation and Utica Water Supply	217
3	Schoharie Reservoir	1926	Schoharie Creek	61,400	314	New York City Water Supply	190
UPPER HUDSON RIVER BASIN							
4	Indian Lake	1898	Indian River	103,000	131	River Regulations, Power	250
5	Sacandaga Reservoir	1931	Sacandaga River	760,000	1,044	River Regulation, Flood Control, Power	180
LOWER HUDSON RIVER BASIN							
	Ashokan Reservoir	1915	Esophs Creek	383,000	257	New York City Water Supply	75
	Rondout Reservoir		Rondout Creek	158,000	95	New York City Water Supply	75

-13-

The Lower Hudson River Channel is a relatively deep and straight channel. The variation in the cross sectional area, at mean low water, between the ocean entrance and the head at the Federal Dam at Troy is shown in Figure II-6. The variation is significant and erratic and cannot be accurately described by a simple mathematical model. The total area in the Lower Hudson ranges between over 250,000 sq. ft. in Haverstraw Bay and less than 50,000 sq. ft. at Troy with an average of about 120,000 sq. ft.

The top width at mean low water is shown in Figure II-7. The variation in the surface width is even more erratic than the cross-sectional area. This is due to the presence of several bays and shoals in the Lower Hudson. Two major bays are located on Figure II-6. These are Haverstraw Bay and Newburgh Bay.

The mean depth of the river is shown in Figure II-8. The mean depth is defined as the cross-sectional area divided by the top width. From the Battery to the head of Haverstraw Bay, the mean depth generally decreases from some 38 feet to about 16 feet. Upstream of Haverstraw Bay the depth abruptly increases, in an erratic manner, reaching a maximum of approximately 100 feet in the vicinity of West Point. Point values approach some 200 feet. This abrupt increase in depth has a significant effect on salt water intrusion in the river.

II-19

QUIRK, LAWLER & MATUSKY ENGINEERS

FIGURE II-6		II-20
FIGURE II-7	II-21	
FIGURE II-8		II-22

-14-

As indicated before, the Lower Hudson River is a tidal estuary between the Federal Dam at Troy and the New York Harbor. It is also classified as a dampened, reflected tidal wave regimen.¹⁵ Dampening occurs by dissipation of tidal energy via channel friction as the oceanic tidal wave progresses upstream. Reflection includes secondary wave propagations caused by channel obstructions. Complete reflection occurs at the Federal Dam at Troy. Additional wave reflections occur due to significant changes in channel width. As widths increase, wave amplitudes tend to decrease, whereas a decrease in channel width causes an increase in wave amplitudes. Tidal behavior at any section is the composite effect of ocean tide, channel friction and wave reflection. The primary ocean tides are also variable with maximum amplitudes occurring during spring tide and minimum amplitude during neap tide. Variations in fresh water discharge and the barometric conditions also contribute to changes in amplitude.

Figure II-9 illustrates the principal tidal characteristics along the stretch of river between the ocean entrance and Poughkeepsie.

High and low water above mean low water at Sandy Hook, New Jersey are shown on the upper figure. The half-tide level indicates the average slope in the river. The total fall from Troy to the sea is about 2 feet.

II-23

FIGURE II-9

II-24

-15-

The variation in the tidal range along the river is shown in the middle figure. It will be noted that, in moving upstream, the range of tide diminishes from about 4.4 feet at the Battery to a minimum of about 2.6 feet at a point near Storm King (mile point 56). The tidal range then reaches a maximum of 4.1 feet at a point near Catskill and then increases to 4.8 feet at Troy.

The high water and low water lunar intervals, as referred to the transit of the moon over the meridian of Greenwich, are shown on the lower figure.

Figure II-10 shows the variation of mean sectional, tidal velocity along the river. The raw data for the ebb and flood strengths were obtained from the 1929 U.S.G.S. study. Ebb and flood strengths were each averaged across the river cross section. Mean absolute velocity over a tidal cycle was then obtained by averaging section averaged ebb and flood strengths.

The variation of the mean tidal "flow" along the river is also shown on Figure II-10. It will be noticed that the mean tidal flow decreases from a maximum of 425,000 cfs at the Battery to zero at the Federal Dam at Troy (about mile point 153).

II-25

FIGURE II-10

II-26

-16-

Hudson River salt intrusions at equilibrium, or near equilibrium conditions, for selected flows are shown on Figure II-11. Data are shown for both the Hudson River model and the prototype conditions. Prototype profiles were obtained by chemical and electrical measurements and are representative of equilibrium conditions. Model profiles represent steady state equilibrium conditions and were obtained by chemical measurement on the Hudson River model at the Waterways Experiment Station, U.S. Army Corps of Engineers, Vicksburg, Mississippi. Salinities shown are tidal average values over a tidal cycle and a full channel cross-section. The Vicksburg model is operated for the mean tide.

Figure II-12 shows the relationship between the length of salt water intrusion at equilibrium in miles and fresh water flow in the lower Hudson. This length is defined as the point on the intrusion curve at which the salinity is 100 ppm.

These results indicate that the salinity intrusion is influenced by the oceanic tidal action which causes the ocean-derived salt to advance landward and the up river inflow which tends to flush the estuary.

II-27



QUIRK, LAWLER & MATUSKY ENGINEERS

FIGURE II-11	II-28
FIGURE 11-12	II-29

-17-

III. HUDSON RIVER BASIN PROBABLE MAXIMUM FLOOD AT INDIAN POINT

A. Introduction

The probable maximum flood (PMF) has been defined as a hypothetical flood produced by the most severe, but reasonably possible, rainfall and related runoff, at a particular area. A rainfall producing a probable maximum flood is often called "Probable Maximum Precipitation" (PMP). The probable maximum flood has also been described as the boundary between possible floods and impossible floods, i.e. a flood having a probability of occurrence approaching zero or a return period of infinity.

No detailed investigation had been performed prior to this study to determine the maximum probable flood for the entire Hudson River Basin.

A semi-empirical approach was followed by Q L & M in early 1970 to estimate such a flood at Indian Point. This approach was based upon several Corps of Engineers studies of a number of neighboring river basins as well as a detailed study of the Upper Hudson River Basin. The probable maximum flood for the Upper Hudson River Basin was conducted by Stone & Webster Engineering Corporation in 1969. The shaded area in Figure III-1 represents the area studied by Stone & Webster.

III-1

Figure III-1

III-2

-18-

A more comprehensive study of a formal or detailed nature involving careful analyses and accepted methodology was conducted in 1970 by Q L & M. The details of that study are given in this chapter. However, the procedures followed are delineated below.

1. A pattern and a time distribution of a probable maximum precipitation were developed for the Hudson River Drainage Basin at Indian Point.
2. The Hudson River Drainage Basin was divided into twenty-eight subbasins and a unit hydrograph was developed for each subbasin. The twenty-eight subbasins are located on Figure II-1.
3. The probable maximum precipitation of Item 1 was applied to the developed unit hydrographs of Item 2 with the appropriate initial and infiltration losses to establish the subbasin flood hydrographs.
4. The subbasin flood hydrographs of Item 3 were combined in their proper time sequence to give a main river hydrograph. The main river hydrograph was then routed downstream. This process started at the uppermost subbasin and continued in the downstream direction until the resultant probable maximum flood hydrograph at Indian Point was obtained.

The results of the sem-empirical study are presented first followed by the delineation of the detailed study. A copy of the Stone & Webster Upper Hudson River study is appended to this report.

III-3

-19-

B. Previous Investigations

As indicated in Chapter I, three flood studies had been performed prior to this investigation to determine the maximum flow for the Hudson River at Indian Point. A brief description of these studies follows.

The first study was of a preliminary nature and was based upon highly conservative estimates. The results of that study which was conducted in 1968 are delineated in Supplement 10, Indian Point unit No. 3, AEC Docket 50-286.

The 1968 preliminary estimates were then modified as a result of a new study in the early part of 1969. This study considered surrounding topography, land use, river geometry and frictional losses. The so-called "rational formula" was used for the runoff computations. The results of the 1969 study are summarized in Table III-1.

Another investigation based upon several Corps of Engineers studies of a number of adjacent river basins and on a detailed study of the Upper Hudson River Basin was conducted in the early part of 1970. A brief discussion of this study is presented below.

Six different methods were used to determine the probable maximum

III-4

IP3
FSAR UPDATE

QUIRK, LAWLER & MATUSKY ENGINEERS

TABLE III-1

COMPONENT FLOW & WATER ELEVATION
AT INDIAN POINT
February 1969 Estimates

1. Maximum Ebb Flow	275,000 cfs
2. Flow Caused by Dam Failure	785,000 cfs
3. Flow Cuased by Maximum Rain	<u>397,000 cfs</u>
4. Total Flow at Indian Point	1,457,000 cfs
5. Elevation at Indian Point Resulting from the Total Flow	11.7 ft (MSL Datum)

-20-

food for the Hudson River at Indian Point. These methods and the corresponding results are listed in Table III-2.

The PMF values at Indian Point were predicted on the basis of a thorough comparison of the Hudson River Basin with the following basins:

1. Susquehanna River at Harrisburg
2. Potomac River at Washington D.C.
3. Delaware River at Montague
4. Hudson River at Stillwater

The following four basins parameters were used for this purpose:

1. Size of the drainage area (A)
2. Available storage capacity (S)
3. Maximum observed peak discharge (Q)
4. Probable maximum flood (PMF)

The values corresponding to the above listed basins are compared with their Hudson River at Indian Point counterparts in Table III-3. Several interesting conclusions may be drawn from this comparison. On the basis of drainage area size, the Hudson River has the highest available storage capacity and the lowest maximum observed peak. These results indicate that the Hudson River is a highly regulated

III-6

TABLE III-2
A SUMMARY OF THE METHODS USED TO
PREDICT PROBABLE MAXIMUM FLOOD AT INDIAN POINT

#	Method	Figure	PMF at I. P. (CFS)
1	PMF vs. other Basins Drainage Area	III-2	1,300,000
2	Stillwater PMF x Ratio of D.A.	III-2	1,010,000
3	PMF vs. Hudson River Basin D.A.	III-2	530,000
4	PMF vs. Max Observed Flood	III-3&4	850,000
5	1 : 10,000 Yr. Instant. Peak-NYSCD 1918-54	II-5	688,000
	1 : 10,000 Yr. Instant Peak –QL&M, log-Normal 1918-70)		(610,000)*
6	Dimensional Analysis	III-5	880,000
7	Average		880,000

*Not included in Average

III-7

TABLE III-3

COMPARISON OF DRAINAGE BASINS

Basin	(A) Drainage Area 10 ³ sq. miles	(S) Available Storage cu. miles	(Q) Max. Obs. Peak 10 ⁶ cfs	PMF 10 ⁶ cfs	PMF Q	Q A
Susquehanna @ Harrisburg	24.1	.065	.740	1.75	2.36	30.8
Potomac @ Washington D.C.	11.56	.0089	.484	1.34	2.77	42.0
Delware @ Montague	3.48	.246	.260	.785	3.02	74.5
Hudson River @ Indian Point	12.65	.515	.284	.88	3.10	22.4
Hudson River @ Stillwater	3.76	.29	.097	.30	3.10	25.8

III-8

-21-

basin. Therefore, prediction of its PMF on the basis of the drainage area size alone may be misleading.

The relationship between the drainage area and computed probable maximum flood for the adjacent basins is shown in Figure III-2. The Upper Hudson River value at Stillwater is also shown and is well below the majority of the points. For comparison purposes, the value corresponding to the present study is also shown.

The fact that the Hudson River Basin is regulated appreciably is clearly seen in Figure III-3 which correlates the maximum observed peak flow with the drainage area size for the basins of interest. The Hudson River maximum observed peak is 60 per cent lower than that of an adjacent river of equivalent size.

A prediction of the Hudson River PMF on the basis of the maximum observed peaks was also attempted. The results are depicted in Figure III-4. The result of the formal PMF study of this report is also shown on this Figure.

A more realistic approach taking into consideration the combined influence of drainage area size (A), available storage capacity (S), and maximum observed peak flow (Q) on the probable maximum flood (PMF) was then investigated. The classical dimensional analysis

III-9

QUIRK, LAWLER & MATUSKY ENGINEERS

FIGURE III-2 PROBABLE MAXIMUM FLOOD – DRAINAGE AREA RELATIONSHIP

Figure III-3 II-11

Figure III-4 III-12

-22-

method was employed for this purpose. This tool recognizes the fact that the physical factors influencing a physical phenomenon should be related in a mathematical model which is dimensionally homogeneous. The parameters A, S and Q were treated as the independent variables representing the physical factors and the PMF as the dependent variable defining the physical phenomenon. The results of this approach are shown in Figure III-5. The value corresponding to the present study is also shown.

Another simple estimate equating the probable maximum flood to a statistically evaluated 1:10,000 year peak flood is also shown in Table III-2. A discharge-frequency curve based on a statistical evaluation of the available 50 U.S.G.S. data points (1918-1969) were prepared as shown in Figure II-5 and extended to 10,000 years. The data points corresponding to discharges prior to the completion of the Sacandaga Reservoir in 1930 were not adjusted for discharges from the Sacandaga river which would have been impounded by the Conklingville Dam.

III-13

Figure III-5

III-14

-23-

C. Probable Maximum Precipitation

The Hudson River Flood records at Green Island show that in the past most major floods have occurred in the spring months as a result of an early spring storm combined with melting snow. The hydrologic history of the Hudson River at Green Island was discussed in Chapter II. The probable maximum precipitation for the spring months, however, is about 50 per cent of the all season probable maximum precipitation². Moreover, the adjacent Connecticut River Drainage Basin study³ indicated that the maximum storm would be at least equal to the maximum combination of rainfall and snow melt. Therefore, a summer or fall storm producing a runoff at least as great as a spring storm with melting snow was used in this study.

The probable maximum precipitation for this study was developed from the 72-hour precipitation and depth-duration-drainage area (DDA) curves prepared by the U.S. Weather Bureau for the adjacent Susquehanna River basin¹. A copy of the Susquehanna DDA Curves is reproduced in Figure III-6.

The PMP curves of Figure III-6 were obtained by transposing storms of record into the Susquehanna Basin and adjusting them for maximum moisture at the transposed location.

III-14a

Figure III-6

III-15

-24-

The general level of these curves has been found to be consistent with that of recent estimates for the Potomac & Delaware River Basins¹.

On the basis of these curves, a probable maximum precipitation depth of 14 inches associated with a duration of 72 hours was used for the entire 12,650 square miles of the Hudson River Basin above Indian Point.

1. Selection of Pattern & Areal Distribution of the Probable Maximum Precipitation Storm

The storm selected for application to the Hudson River Basin is similar in areal distribution to that of the Susquehanna River at Danville. The Danville pattern was developed by the U.S. Weather Bureau¹ and is reproduced in Figure III-7.

This pattern was considered in this study due to the similarity in shape and drainage area size between the Susquehanna River at Danville (11,220 Sq. Miles) and the Hudson River at Indian Point (12,650 Sq. Miles). The two rain centers of the Danville pattern were shifted and rotated so as to give best fit to the Hudson River Basin. The resulting pattern is shown in Figure III-8. The letters in Figure III-8 represent different values of the pattern storm Isohyets as will be shown later. One of the selected storm centers

III-16

QUIRK, LAWLER & MATUSKY ENGINEERS

Figure III-7	III-17
Figure III-8	III-18

-25-

was located on the Sacandaga River Basin (Subbasin 8) in the Upper Hudson River Basin and the other one on the Catskill Creek Basin (Subbasin 18.3) in the Lower Hudson River Basin. The direct distance between these two centers is about 80 miles.

Because of the comparatively small differences between the average elevation of the Hudson River Basin and the elevations of the terrain covered by the selected storm isohyets, no adjustment was made for difference in elevation.

2. Computation of the Isohyet Values for the Total Duration of the Probable Maximum Storm

The purpose of this step is to define rain concentration associated with the 72 hour total storm within the Hudson River Basin. The procedure employed in this step was also used to compute the isohyet values for incremental durations as discussed in subsequent sections of this chapter.

The computational procedure is described below. Due to the presence of two storm centers, the values of the lettered isohyets of Figure III-8 were determined as follows:

- a. The two centers were treated as separate storms and the areas within Isohyets A_1 , B_1 , C_1 , A_2 , B_2 , C_2 , were measured.

III-19

-26-

b. The average depth of rainfall corresponding to each one of the areas of Step a was obtained from the appropriate DDA curves of Figure III-6. The 72 hour curve was used for the computation of the isohyet values for the total duration of the probable maximum storm.

c. To insure that the precipitation averaged along the individual isohyets must equal the basin average PMP, an auxiliary isohyet C'_1 enveloping the A_1, B_1, C_1 , center, extending down to the A_2, B_2, C_2 , center, and forming a border line with the northern end of C_2 , isohyet was established.

d. The area enclosed by C'_1 isohyet was conveniently selected equal to that of C_2 isohyet. The average depth of rainfall corresponding to C'_1 isohyet is therefore equal to its C_2 counterpart.

e. The average rainfall depth over an area equivalent to $C'_1 + C_2$ was computed using the appropriate DDA curves of Figure III-6.

f. The average rainfall depths of "Step b," were then adjusted by multiplying them by the ratio of the average depth computed in "Step e" to that of "Step d." As mentioned earlier, this was done to insure that the precipitation averaged along the individual

III-20

-27-

isohyets must equal the basin average PMP.

g. The average depths of rainfall over the areas bounded by isohyets D and E which envelop both centers were computed in a manner similar to that outlined in Steps a and b.

h. The individual values for the selected isohyets were determined graphically as shown in Figure III-9 and summarized below:

i. compute the average value of any two adjacent isohyets using the following equation which assumes linear depth-area relationship.

$$\frac{V_n + V_{n+1}}{2} = \frac{P_{n+1}A_{n+1} - P_nA_n}{A_{n+1} - A_n}$$

in which

V_n, V_{n+1} = Values of isohyets number n and n+1. These numbers refer to the lettered isohyets shown in Figure III-8.

A_n, A_{n+1} = Area bounded by isohyets number n and n + 1. (Steps a and g above).

P_n, P_{n+1} = Average depth of rainfall over the areas bounded by

III-21

Figure III-9

III-22

-28-

isohyets 1 and 2 (steps f and

g above).

ii. Plot the computed average values of the

isohyets versus the corresponding average

areas, i.e. $\frac{V_n + V_{n+1}}{2}$ vs. $\frac{A_n + A_{n+1}}{2}$

iii. Locate the area enclosed by the individual isohyets on the plot of item ii above and draw straight lines between any two locations passing through the individual points and following the general shape of the curve of step ii above.

iv. Obtain the values of the isohyets corresponding to the straight lines of step iii.

v. Check the values obtained in step iv by computing the average values of any two isohyets (step iv) and comparing it against the values computed in step i.

vi. Repeat until the computed values of step iv are the same as those obtained using equation 1. This trial and error procedure was found to be very stable and its convergence was remarkable.

III-23

-29-

The results of the areas (step a), separate storm depths of rainfall (step b), adjusted depths (step f and g), and isohyet values (step h) for the total duration of the probable maximum storm are summarized in Table III-4.

3. Time Distribution of PMP

The purpose of this step is to distribute the volume of the rain associated with the total duration of the probable maximum storm in time. A procedure similar to that outlined in Hydrometeorological Report No. 40 was employed. The procedure consists of the following two steps:

a. Time concentration of PMP: This expresses how much of the total rainfall in 72 hours is concentrated in the maximum (1st) 6-hour increment, the next highest (2nd) 6-hour increment, 3rd, 4th, etc. The total basin rain volume was distributed proportional to the 6-hour incremental values from the PMP depth-duration curve of Figure III-6. Thus the maximum (1st) 6-hour increment is the 6-hour PMP at the area of the basin, the next highest (2nd) 6-hour increment is the difference between 12-hour and 6-hour PMP etc.

This procedure is conservative in that it combines PMP for all durations in one storm event.¹

III-24

TABLE III-4
ISOHYET VALUES FOR THE TOTAL DURATION
OF THE PROBABLE MAXIMUM STORM

Isohyet ¹ No.	Area Enclosed ² by Isohyet (sq.mi.)	Two Storm ³ Ave. Rainfall Depth (in.)	Adjusted ⁴ Ave. Rainfall Depth (in.)	Isohyet ⁵ Value (in.)
A ₁	56	28.6	25.8	22.6
B ₁	330	24.2	21.8	19.4
C ₁	1,060	21.2	19.1	16.8
C ₁	2,130	19.2	17.3	14.2
A ₂	140	26.2	23.6	20.8
B ₂	710	22.3	20.1	17.6
C ₂	2,130	19.2	17.3	14.2
D	11,020	14.7	14.7	12.0
E	17,210	13.3	13.3	9.6

1 See Figure III-8

2 Step a of the procedure

3 Step b and g of the procedure

4 Step f of the procedure

5 Step h of the procedure

III-25

-30-

b. Sequence of increments: The 6-hour incremental values of PMP over the entire Hudson Basin at Indian Point were rearranged in accordance with the following criteria recommended in Hydrometeorological Report No. 40:

i. Group the four highest 6-hour increments of the 72-hour PMP in a 24-hour period, the middle four increments in a 24-hour period, and the lowest four increments in a 24-hour period.

ii. Within each of these 24-hour periods, arrange the four increments in accordance with sequential requirements; that is, the second highest next to the highest, the third highest adjacent to these, and the fourth highest at either end.

iii. Arrange the three 24-hour periods in accordance with the sequential requirements; that is, the second highest 24-hour period next to the highest with the third at either end. Any possible sequence of three 24-hour periods is acceptable with the exception of placing the lowest 24-hour period in the middle.

III-26

-31-

4. Computation of 6-hour increments of PMP

The incremental average depth for the 12 6-hour subdurations were obtained using the DDA curves of Figure III-6 and within-basin depth-area curves. The within-basin curves were derived for several subdurations and sizes of areas in a manner similar to that recommended in Hydrometeorological Report No. 40. The within-basin curves gave results higher than those based upon the entire basin ratio.

The results of the incremental average depth for the first 4 6-hour increments and for the second and third days are summarized in Table III-5. For successive 6-hour values within the second and third days the recommended U.S. Weather Bureau¹ percentages shown in Table III-5 were used.

The incremental values of the isohyets for the 12 subdurations were computed using the procedure outlined in the preceding item. The results are given in Table III-6.

5. Computation of Subbasin Probable Maximum Precipitation & Runoff

The values of the probable maximum precipitation corresponding to the 12 subdurations for each one of the 28 subbasins shown in Figure II-1 were computed by planimetering the area between the isohyets within the subbasin boundaries.

III-27

TABLE III-5

VALUES OF AVERAGE DEPTH OVER AREAS
BOUNDED BY STATED ISOHYETS

A ₁	A ₂	B ₁	B ₂	C ₁	C ₂	D	E
----------------	----------------	----------------	----------------	----------------	----------------	---	---

AVERAGE DEPTH OVER AREAS IN INCHES

72 hours	25.8	23.6	21.8	20.1	19.1	17.3	14.7	13.3
1 st 6 hours	12.3	10.8	9.6	8.4	7.8	6.5	4.9	4.3
2 nd 6 hours	2.7	2.6	2.5	2.4	2.3	2.2	1.9	1.7
3 rd 6 hours	2.3	2.2	2.1	2.0	2.0	1.9	1.7	1.5
4 th 6 hours	1.8	1.7	1.6	1.5	1.5	1.4	1.3	1.2
2 nd day *	4.5	4.3	4.1	3.9	3.7	3.5	3.3	3.2
3 rd day ^V	2.2	2.0	1.9	1.9	1.8	1.8	1.6	1.4
Total area of Isohyet (sq. mi)	56	140	330	710	1060	2130	11020	17210

* For successive 6-hr. values use 34, 28, 21, and 17% of 2nd day values.

^V For successive 6-hr. values use 29, 26, 23, and 22% of 3rd day values.

III-28

TABLE III-6

VALUES OF PATTERN STORM ISOHYETS
FOR HUDSON RIVER AT INDIAN POINT
Basin Size 12,650 Sq. Mi.

Center 1	Center 2	A ₁	A ₂	B ₁	B ₂	C ₁	C ₂	D	E
-------------	-------------	----------------	----------------	----------------	----------------	----------------	----------------	---	---

Isohyet Values (inches)

72 hours	26.8	25.4	22.6	20.8	19.4	17.6	16.8	14.2	12.0	9.6
1 st 6 hours	12.9	12.1	10.3	8.8	7.9	6.8	6.1	4.4	3.4	3.0
2 nd 6 hours	2.75	2.7	2.6	2.5	2.3	2.2	2.2	2.0	1.4	1.2
3 rd 6 hours	2.35	2.3	2.1	2.0	2.0	1.9	1.8	1.8	1.3	1.0
4 th 6 hours	2.0	1.8	1.6	1.5	1.5	1.4	1.4	1.3	1.2	0.9
2 nd day *	4.5	4.5	4.3	3.9	3.7	3.4	3.4	3.2	3.1	3.0
3 rd day ^V	2.2	2.1	2.0	1.9	1.9	1.8	1.7	1.7	1.2	1.0
Total area of Isohyet (sq. mi)	30.0	30.0	56	140	330	710	1060	2136	11020	17210

* For successive 6-hr. values use 34, 28, 21, and 17% of 2nd day values.

^V For successive 6-hr. values use 29, 26, 23, and 22% of 3rd day values.

III-29

TABLE III-7

COMPUTATION OF 6 HR INCREMENTS OF PROBABLE MAXIMUM PRECIPITATION
ON CATSKILL CREEK BASIN (SUBBASIN 18.3)

ISOHYETS	AREA BETWEEN ISOHYETS (ONLY PLANIMETER READING)	1 ST 6 HR INCREMENT	2 ND 6 HR INCREMENT	3 RD 6 HR INCREMENT	4 TH 6 HR INCREMENT	2 ND DAY INCREMENT	3 RD DAY INCREMENT
		Average isohyet value (inches) 2x3	Average isohyet value (inches) 2x5	Average isohyet value (inches) 2x7	Average isohyet value (inches) 2x9	Average isohyet value (inches) 2x11	Average isohyet value (inches) 2x13
1	2	3 4	5 6	7 8	9 10	11 12	13 14
D – C ₂	0.35	3.90 1.365	1.70 0.595	1.55 0.543	1.25 0.438	3.15 1.102	1.45 0.508
C ₂ – B ₂	0.95	5.60 5.320	2.10 1.990	1.85 1.759	1.35 1.282	3.30 3.135	1.75 1.663
B ₂ – A ₂	0.75	7.80 5.850	2.35 1.762	1.95 1.462	1.45 1.088	3.65 2.740	1.85 1.388
A ₂	0.80	10.80 9.500	2.60 2.080	2.20 1.760	1.70 1.360	4.30 3.420	2.00 1.600
TOTAL AVERAGE DEPTH (IN.)	2.85	22.350 7.75	6.427 2.26	5.524 1.94	4.168 1.52	10.397 3.64	5.159 1.81

2 nd Day				3 rd Day			
	%	IN		%	IN		
5 th 6 HR's	34	1.24		29	0.53		9 th 6 HR's
6 th 6 HR's	28	1.02		26	0.47		10 th 6 HR's
7 th 6 HR's	21	0.77		23	0.42		11 th 6 HR's
8 th 6 HR's	17	0.61		22	0.39		12 th 6 HR's

III-30

IP3
FSAR UPDATE

QUIRK, LAWLER & MATUSKY ENGINEERS

TABLE III-8

UPPER HUDSON RIVER BASIN – PROBABLE MAXIMUM PRECIPITATION AND RUNOFF

DAY OF PMP		1 ST DAY				2 ND DAY				3 RD DAY			
6 – HR INCREMENT		7 TH	5 TH	6 TH	8 TH	3 RD	1 ST	2 ND	4 TH	12 TH	10 TH	9 TH	11 TH
Hours from beginning of PMP		6	12	18	24	30	36	42	48	54	60	66	72
Subbasin	Note	6 hour increments / inches				6 hour increments / inches				6 hour increments / inches			
1	PMP	0.65	1.00	0.86	0.53	1.12	3.14	1.28	1.02				
	Runoff	0	0.35	0.56	0.23	0.82	2.84	0.98	0.72				
2.1	PMP	0.69	1.11	0.92	0.56	1.74	5.04	2.02	1.33				
	Runoff	0	0.50	0.62	0.26	1.44	4.74	1.72	1.03				
2.2	PMP	0.65	1.06	0.87	0.53	1.57	4.15	1.75	1.26				
	Runoff	0	0.41	0.57	0.23	1.27	3.85	1.45	0.96				
3	PMP	0.66	1.00	0.89	0.54	1.55	4.10	1.73	1.25				
	Runoff	0	0.44	0.59	0.24	1.25	3.80	1.43	0.96				
4	PMP	0.64	1.00	0.86	0.52	1.16	3.22	1.31	1.06				
	Runoff	0	0.38	0.56	0.22	0.86	2.92	1.01	0.76				
5	PMP	0.65	1.00	0.86	0.53								
	Runoff	0	0.39	0.56	0.23								
6	PMP	0.71	1.00	0.95	0.57								
	Runoff	0	0.56	0.65	0.27								
7	PMP	0.72	1.00	0.96	0.58								
	Runoff	0	0.58	0.66	0.28								
8	PMP	0.77	1.00	1.03	0.61								
	Runoff	0	0.72	0.7356	0.31								

QUIRK, LAWLER & MATUSKY ENGINEERS

-32-

The results of one of the subbasins (Catskill Creek – Subbasin 18.3) are summarized in Table III-7.

These increments were rearranged in accordance with the recommended sequence. The following rainfall losses, as recommended by Mr. Nunn of the AEC,¹⁷ were then subtracted to obtain rainfall excesses for each subbasin and subduration:

Initial Losses = 1 in.

Infiltration Losses = .05 in./hour

The recommended rainfall losses agreed reasonably well with the October, 1955 storm and resulting stream flows at several U.S.G.S. gaging stations as will be discussed in the next section of this chapter.

The results of the probable maximum precipitation and runoff computations are given in Tables 8, 9, and 10 for the subbasins in the Upper Hudson, Mohawk and Lower Hudson Rivers respectively.

The incremental PMP values and related runoff for the entire Hudson River Basin above Indian Point are depicted in figure III-10. It is interesting to note that the runoff coefficient corresponding to these results is about 70 per cent more than twice the value used in the February, 1969 report.

III-35

Figure III-10

III-36

-33-

D. Unit Hydrograph Analysis

Six-hour unit hydrographs were established for each of the Hudson River subbasins shown in Figure II-1.

Unit hydrographs for 12 subbasins in the Upper Hudson were taken from the Stone & Webster Report⁴ on the Upper Hudson. A copy of that report is appended to this report. A discussion of these unit hydrographs is reproduced from reference below:⁴

"Unit hydrographs were determined from records of nine gaging stations located on the various streams and reservoirs within the basin having drainage areas varying in size from 90 to 1,044 square miles. In general, the unit hydrographs were developed from the hurricane storm of September 1938 and compared with the next largest storm for which data were available. The second storm used varied from area to area. The storm of September 1938 produced the largest floods without snow melt for which adequate records are available.

It was not possible to develop a unit hydrograph for the Indian Lake Reservoir and Batten Kill from the September 1938 storm because of inadequate rainfall data, and other storms were used. A computer program described by D. W. Newton and J. W. Vinyard, was used in developing the unit hydrographs for the gaged areas.

III-37

-34-

Unit hydrographs for approximately 70 percent of the total drainage area were developed from rainfall and runoff records. The unit hydrographs for the Sacandaga Reservoir and Indian Lake inflows and the Hudson River at the USGS gage at Gooley were used without modification. The unit hydrographs developed at the gaging stations on the Schroon River, Batten Kill and Kayaderosseras Creek were transposed to their respective mouths using Snyder's coefficients and the method outlined in Unit Hydrographs – Part I Principles and Determinations."

Synthetic unit hydrographs were derived for the three subbasins in the Mohawk Basin, Subbasins 9, 13, and 14 in the Upper Hudson and all the Lower Hudson Subbasins (excluding Subbasin 18.5). Taylor & Schwarz's method⁵ was used for this purpose. This method was developed for basins in the north and middle Atlantic states. The basic data used in the development includes the Hoosic River, one of the major tributary streams of the Hudson River.

No unit hydrograph was derived for subbasin 18.5. This subbasin has a small drainage area and the runoff from the precipitation over this area was assumed to be instantaneous.

III-38

QUIRK, LAWLER & MATUSKY ENGINEERS

TABLE III-11

III-39

III-40

III-41

III-45

Figure III-11

TABLE III-12

Figure III-15

-35-

The basic equations used in the derivation of the synthetic unit hydrographs are listed in Table III-11.

The construction of the shape of the synthetic unit hydrographs was guided by the empirical Corps of Engineers⁶ relationship between the peak discharge rate and the width of unit hydrographs at ordinates exceeding approximately 50 per cent of the maximum. This relationship corresponding to ordinates equal to 50 and 75 per cent of the peak ordinate is reproduced in Figure III-11.

The area under the synthetic unit hydrographs which should be equivalent to one inch of direct runoff provided another control.

The basic subbasin characteristics used in deriving the unit hydrographs are summarized in Table III-12. The computed unit hydrograph peak flows and lag time are also listed in Table III-12.

Three typical unit hydrographs for three subbasins in the Upper Hudson, Mohawk and Lower Hudson Basins are depicted in Figure III-12, III-13, and III-14 respectively.

Figure III-15 compares the unit hydrograph peaks used in this study with those prepared by the Corps of Engineers through September, 1961.

III-46

QUIRK, LAWLER & MATUSKY ENGINEERS

-36-

The Corps of Engineers results are represented by a mean, upper and lower limit lines which were drawn to envelop some 200 observed peak discharge values of 6-hour unit hydrographs.

The Hudson River Basin synthetic unit hydrograph values are represented by open circles. Notice that the synthetic peaks used in this study are higher than those represented by the Corps of Engineers mean line.

The Upper Hudson unit hydrograph peaks which were developed from the hurricane storm of September, 1938 are also shown in Figure III-15. These points fall within the upper and lower limit lines with the majority of them above the mean line. Only subbasin #5 (Schroon River) value is below the lower limit line. Since the Schroon River Subbasin has a very small slope (6×10^{-4}) and large natural storage capacity and since its unit hydrograph was developed from observed data, it was not found necessary to adjust its peak.

A more elaborate verification of the developed Hudson River Basin unit hydrographs based upon observed precipitation and runoff data was conducted. The flood of October 1955¹⁸ was used for this purpose because of availability of adequate rainfall data in the Hudson River Basin.

III-47

QUIRK, LAWLER & MATUSKY ENGINEERS

-37-

Storms swept the New York and southern New England area in three periods; October 6-8, 13-17, 30-31. The worst floods occurred in mid-October, 1 or 2 days before or after October 16. The areas most affected were western Massachusetts, western Connecticut, southeastern New York, and a separated area in south-central New York and north-central Pennsylvania.

Maximum 4-day rainfall (October 14-17) at Esopus Creek and Schoharie Creek Subbasins was 17.72 and 16.77 inches respectively. October rainfall at individual stations ranged from 3.14 inches at Plattsburgh, New York to 25.27 inches at West Shokan. This last figure is about 60 per cent of the mean annual rainfall in New York.

The Mohawk River discharge observed at Cohoes reached a peak of 100,000 cfs on October 17. The corresponding Hudson River peak at Green Island and Wallkill River peak at Gardiner in the Lower Hudson Basin were 113, 000 cfs on October 17 and 30,800 cfs on October 16 respectively.

The unit hydrographs developed for the above-mentioned basins (all of the Upper Hudson, Mohawk and Wallkill River unit hydrographs) and the rainfall losses used in this study were verified using the October 1955 storm rainfall and runoff data in the following manner:

III-48

-38-


1. Isohyetal maps corresponding to 12 6-hour increments of rainfall commencing at 24:00 on October 13, 1955 were constructed. Hourly precipitation data observed at 25 weather bureau station in the Hudson River Basin were used for this purpose. A sample of these isohyetal maps is depicted in Figure III-16.
 2. The average depth of rainfall for the 12 subdurations for each subbasin was obtained.
 3. The rainfall losses used previously were then subtracted to obtain the rainfall excesses for each subbasin; i.e. initial losses of 1 inch and infiltration losses of 0.05 inch/hour. The rainfall and runoff results for the Upper Hudson, Mohawk and Wallkill River Basins are listed in Tables III-13, III-14 and III-15 respectively.
 4. Using the beginning of the storm (24:00 October 13) as a common time base, the runoffs were applied to the developed 6-hour unit hydrographs to produce successive 6-hour flood hydrographs for each subbasin.
 5. The subbasin flood hydrographs were then combined and routed downstream to the gaging stations; i.e. Cohoes, Green Island and Gardiner. The routing procedure employed for this purpose will be presented in the next section of this chapter.
 6. The generated floods of "Step 5" above are compared to the observed Hudson, Mohawk and Wallkill River data in Figures III-17, III-18 and III-19 respectively. The observed data were obtained from the U.S.G.S. hourly records.
- The agreement between the
- III-49

QUIRK, LAWLER & MATUSKY ENGINEERS

Figure III-16

A large black rectangular redaction box covering the content of Figure III-16.

Figure III-17

A large black rectangular redaction box covering the content of Figure III-17.

III-55

A large black rectangular redaction box covering the content of III-55.

-39-

computed Mohawk and Upper Hudson River floods and their measured counterparts is remarkable. The computed values are somewhat higher than the observed data.

The agreement between the observed and computed results for the Wallkill River is reasonable. The generated peak is about 10 per cent higher than its measured counterpart. This and the other minor differences in the Upper Hudson and Mohawk River results may be due to the non-uniform aerial distribution over large subbasins, base flow and losses estimates. The non-uniform aerial distribution over the long and narrow Wallkill River Subbasin (100 miles x 15 miles) was significant and maybe the reason behind the 10 per cent disagreement.

The good agreement between the measured and computed results indicate that the use of the developed unit hydrographs and recommended rainfall losses is justified.

E. Development of the Hudson River Probable Maximum Flood at Indian Point

1 Description of Procedure: The procedure followed for determination of the probable maximum flood at Indian Point was delineated earlier and may be summarized as follows:

- a. Flood hydrographs for all of the Hudson River Subbasins were established using the probable maximum

III-58

QUIRK, LAWLER & MATUSKY ENGINEERS

-40-

precipitation (PMP) amounts from the selected probable maximum storm (PMS) together with rainfall losses (Section C above) and the derived unit hydrographs (Section D above).

b. With base flows added the flood hydrographs were combined and/or routed downstream to give the inflows into the Hudson River from its tributaries. Inflows to the Sacandaga and Ashokan reservoirs were routed through the reservoirs. The reservoirs' outflows were then combined with the appropriate subbasin flood hydrographs to define the inflows in the main channel.

c. The main river inflows were then combined with the Hudson River bank subbasin flood hydrographs and routed downstream to Indian Point using the beginning of the probable maximum precipitation as the time origin.

The specific details of this procedure, excluding reservoir flood routing, are presented in this section. When possible, the Mohawk River Basin computations will be used in a detailed manner to illustrate the adopted procedure.

The results of the reservoir outflows are used in this section. How-

III-59

QUIRK, LAWLER & MATUSKY ENGINEERS

-41-

ever, the details of the reservoir flood routing procedure, are discussed in the next chapter in connection with a thorough treatment of dam failure analysis.

2. Mohawk River Flood Development

a. Mohawk River Subbasins

As indicated earlier, the Mohawk River Basin was divided into three subbasins. These are designated as subbasins numbers 15, 16 and 17 in Figure II-1.

Subbasin No. 15 envelops an area of 2170 square miles and includes the Mohawk River drainage area above the mouth of Schoharie Creek.

Subbasin No. 16 includes Schoharie Creek basin which drains an area of 926 square miles.

Subbasin No. 17 includes the remaining 366 square miles of the Mohawk River Basin and extends from the mouth of Schoharie Creek to Cohoes at the junction of the Mohawk and Upper Hudson Rivers.

b. Subbasin Flood Hydrographs

III-60

-42-


To illustrate the procedures employed in this study, a detailed description of the basic flood data and results of a typical subbasin is presented below. The Schoharie Creek Subbasin was arbitrarily selected for this purpose.

Figure III-20 summarizes the necessary basic data for Schoharie Creek. An isohyetal map of the subbasin appears in the upper right hand corner. Isohyets D and C² of the selected PMS (Figure III-8) are shown in Figure III-20. Several values interpolated between the pattern isohyets are also shown. The values shown in the Figure correspond to the 72-hour duration. The values of the 12 6-hour subdurations are listed in Table III-6.

The subbasin precipitation, determined by planimetry of the area between the isohyets within the subduration is depicted in the upper left hand hyetograph. The rainfall losses (1" initial and .05"/hr. infiltration) as well as the rainfall excesses (shaded area) are also shown. The rainfall excesses were obtained by subtracting the rainfall losses from the incremental rainfall

III-61

FIGURE III-20
III-62

A large black rectangular redaction box covers the content of the figure, starting from the right side of the text 'FIGURE III-20' and extending across the width of the page.

-43-

values. This procedure is outlined in Tables III-9 through III-12.

The synthetic 6-hour unit hydrograph for this sub-basin is represented by the broken line in the lower left hand side of the figure. The method used to derive this as well as the other synthetic unit hydrographs is outlined in Table III-11. The results are summarized in Table III-12. The Schoharie basin characteristics required for the derivation of the unit hydrograph are listed in Figure III-20.

The Schoharie Creek flood hydrograph is also given in the figure. This hydrograph was obtained by applying the rainfall excesses to the 6-hour unit hydrograph.

c. Flood Hydrograph Combination and River Channel
Flood Routing

A base flow of 1 cfs/square mile was added to the product of the rainfall excesses and unit hydrograph values to obtain the subbasin outflow. This base flow value which represents the stream flow main-

III-63

QUIRK, LAWLER & MATUSKY ENGINEERS

-44-

tained by ground water return and subsurface storm flow represents a long term average for the Hudson River Basin. For the Upper Hudson River Subbasins, base flows obtained from observed flood hydrographs were used. These base flows are listed in Table 4 of the Stone & Webster Report⁴.


The generated flood curve in Figure III-20 includes the appropriate base flow value for the Schoharie Creek Subbasin, i.e. 926 cfs.

The generated flood hydrographs for the three Mohawk River Subbasins were combined and routed downstream to the Hudson River. The procedure used for this purpose is depicted in Figure III-21.

The individual flood hydrographs for the three subbasins are represented by the solid curves in Figure III-21. The Mohawk River Flood downstream of its conjunction with the Schoharie Creek was obtained by combining the flood hydrographs of subbasins 15 and 16. The resultant is represented by (15 + 16) curve in Figure III-21.

III-64

Figure III-21
III-65

A solid black rectangular box redacting the content of Figure III-21.

-45-

The resultant flood hydrograph was then routed through the Mohawk River to Cohoes. The output is represented by the broken curve in Figure III-21. The classical Muskingum coefficient method for routing⁷ was used for this purpose. This method will be described later.

The routed hydrograph was then combined with the flood hydrograph of subbasin #7 to obtain the total Mohawk River flood hydrograph at Cohoes. The resultant hydrograph is shown in Figure III-21

The foregoing procedure and the one outlined in the previous section of this chapter were programmed for solution of RAPIDATA time-sharing facilities. A listing of the Mohawk River Program is given in Plate III-1.

Plate III-2 is a listing of the input or data file for the Mohawk River Program which includes rainfall excess (Table III-9), unit hydrograph ordinates (Figure III-21) above flows for the three subbasins.

The solution printouts including the flood hydro-

III-66

-46-

graph for each subbasin and the results used to construct Figure III-20 are shown in Plate III-3. A more detailed description of the unit hydrographs for all subbasins is also included in Plate III-3.

A description of the flood routing procedure follows.

The Muskingum Method expresses the outflow as the summation of products of routing constants and inflows. The relationship is expressed in equation

III-2

$$o_2 - o_1 = \frac{2 \Delta t}{2k(1-x) + \Delta t} [I_1 - o_1] + \frac{\Delta t - 2kx}{2k(1-x) + \Delta t} [I_2 - I_1]$$

in which

o_1, o_2 = Outflow from reach 1 and 2

I_1, I_2 = Inflow at upstream end of reach 1 and 2

Δt = Length of the routing period having a maximum value of $2kx$ and may be taken as equal to k . The routed hydrograph is relatively insensitive to the value of Δt .

k = Time of travel of flood wave and also

III-70

-47-

the change of storage per unit change
of discharge.

x = A dimensionless constant representing an
index of the wedge storage in a routing
reach.

The routing coefficients x and k used in this study
are summarized in Table III-16. The Upper Hudson River
coefficients were determined by Stone & Webster⁴ from
available flood records.

The October, 1955 storm flood records described in the
previous section of this chapter were analyzed to deter-
mine the Mohawk River routing coefficients.

The Lower Hudson River routing coefficients were evaluated
using a step backwater calculation as will be shown in
the next section of this chapter.

Except for two subreaches in the Upper Hudson a value of
0.3 was used for the dimensionless constant x . This value
is conservative and is representative of wide rectangular
channels.⁷ The influence of variation in x on the Hudson

III-81

-48-

River routed hydrographs is discussed in the last section of this chapter.

3. Upper Hudson River Flood Development

A procedure similar to the one outlined in the preceding section was used to derive the Upper Hudson River flood hydrograph at Green Island.

Because of the presence of the Sacandaga Reservoir which controls nearly 30 per cent of the total Upper Hudson basin area, the basin was divided into two segments. The first portion extends from the source to the mouth of Sacandaga River and the second includes the remaining portion of the basin, i.e. from Sacandaga River to Mechanicville.

A computer program, data file, and printouts similar to their Mohawk River counterparts were developed for both segments and are presented in Plates III-4 through III-9. The results are presented graphically in Figure III-22.

The upper portion of this basin includes subbasins 1 through 8. the outflow from subbasin 8 (Sacandaga River Basin) was obtained by routing the flood hydrograph through Sacandaga Reservoir using

III-83

-49-

a detailed reservoir flood routing procedure. The procedure is described in the next chapter.

The flood hydrographs of subbasins 1 through 7 were combined and/or routed downstream to Sacandaga River. The Sacandaga Reservoir outflow was then combined with the resultant of the upstream subbasins. This new flood hydrograph was combined and/or routed with the hydrographs of subbasin 9 through 14 to obtain the resultant Upper Hudson River flood hydrograph at Mechanicville.

The Upper Hudson unit hydrographs at Mechanicville, upstream and downstream of Sacandaga River are shown in Figure III-22. The outflow from Sacandaga Reservoir is also depicted.

The routing coefficients used were obtained from the Stone & Webster Report. A description of the method used to determine these coefficients is reproduced from reference #4 below:

"The interrelated constants X and K, used to determine the coefficients for routing by the coefficient method, were evaluated on the section of the river above Thurman Station, because of lack of adequate flood data, evaluation of these constants was made from the stage-discharge-volume relationship for each reach. This

III-111

-50-

procedure required determination first of K, which is the travel time for an elemental discharge wave to traverse the reach. Then an x, which is a measure of the wedge storage in the reach, was assumed and the flood was routed.

Finally, to check the correctness of the assumed X, the actual wedge storage was calculated using a step backwater calculation with varying flow within the reach corresponding to the inflow and outflow hydrographs. Trials were continued until the assumed and calculated X's were substantially in agreement."

The Mechanicville flood hydrograph was then combined with the Cohoes hydrograph to obtain the flood hydrograph at Green Island. The Mechanicville hydrograph was not routed to Cohoes since Subbasin 14 of the Upper Hudson Basin extends all the way down to the junction of the Mohawk and Hudson Rivers near Troy. The results are shown in Figure III-23.

4. Lower Hudson River Flood Development

A procedure similar to the Mohawk and Upper Hudson River procedures was employed to route the river hydrographs to the Indian Point site. The Lower Hudson River computer program, input or data file and

III-112

-51-

printouts are listed in Plates III-10 through III-12.

The input or data file includes the resultant flood hydrograph at Green Island, Ashokan Reservoir outflow, rainfall excess and unit hydrograph data for the Lower Hudson Subbasins.

The specific details of the Ashokan Reservoir flood routing is presented in the next chapter.

The coefficients used in the Lower Hudson River Channel routing are described below.

A conservative value of 0.3 representative of a wide rectangular channel was used for the dimensionless coefficient x . A lower x value corresponding to wide parabolic channel results in a small reduction in the probable maximum flood at Indian Point. The Lower Hudson River Channel is somewhere in between these two shapes. To be on the conservative side, however, the value of 0.3 was adopted. The results of this study, as will be shown later, indicate that the probable maximum flood at Indian Point is relatively insensitive to the value of x .

The celerity method suggested by the Corps of Engineers^{7, 19} was

III-114

QUIRK, LAWLER & MATUSKY ENGINEERS

-52-

employed to determine the coefficient k . This method is based upon

Seddon's principle, which may be expressed by the following equation:

$$V_w = \left[\frac{1}{B} \right] \left[\frac{dq}{dy} \right] \quad \text{III-3}$$

in which

V_w = Rate of movement of flood wave

B = Breadth of channel at water surface

q = discharge

y = Height above bed

$\frac{dq}{dy}$ = Slope of discharge rating curve of a station whose cross-section is representative of the reach for steady flow

The value of k is then the ratio of reach length to wave celerity V_w .

The relationship of Equation III-3 was discovered experimentally by James A. Seddon in studies of flood movements on the Mississippi and Missouri Rivers in 1889. The same relationship was developed mathematically by Kleitz in 1877.¹⁹

Several Lower Hudson River water surface profiles corresponding to flows ranging from 20,000 cfs to 1,100,000 cfs were developed using an accepted backwater program. The results are shown in III-135

-53-

Figure III-24. The backwater program used is described in detail in Chapter V of this report.

The Lower Hudson River between Green Island and Indian Point was then divided into 11 reaches. A discharge rating curve was established for each reach using the surface profile curves of Figure III-24. The discharge rating curves are shown in Figure III-25.

As suggested by the Corps of Engineers,⁷ a single value of k corresponding to the average of the initial flow and anticipated peak outflow for each subreach was used. The anticipated peak outflow was determined by trial and error.

The results of this step indicate that the total time of travel of the flood wave between Green island and Indian Point (a distance of more than 150 river miles) is 16 hours. The values for the individual subreaches are listed in Table III-16.

Several other x and k values were used to examine the influence of the routing coefficients on the probable maximum flood at Indian Point. The results are depicted in Figure III-26. It can be clearly seen that the PMF is relatively insensitive to the value of x .

III-136

-54-

The dependence of the Indian Point PMF on k is due to the degree of synchronization of the Green Island peak and Esopus Creek peak. In other words, the shorter the time of travel between Green Island and Esopus Creek the smaller the lag time between the two peaks and vice versa.

The use of a weighted average k equivalent to the ratio of the area under k vs. time curve to the total time for each subreach resulted in a longer time of travel, i.e. lower PMF at Indian Point. However, as an added measure of conservatism, the averaging technique suggested in reference number 7 was adopted.

The routed hydrographs at several locations along the Hudson River are shown in Figure III-27.

5. Probable Maximum Flood at Indian Point

The peak discharge thus obtained at the Indian Point site amounts to 1,100,000 cfs and represents the probable maximum flood at Indian Point.

On the basis of drainage area size, this value agrees reasonably well with its Susquehanna, Delaware and Potomac Rivers counterparts shown in Figure III-2.

III-140

-55-

It is also about 25 per cent and 60 per cent higher than the dimensional analysis value of 880,000 cfs of Figure III-5 and the statistically evaluated 10,000 year flood at Indian Point of Figure II-5.

As a final verification step, the unit hydrographs corresponding to the Green Island flood hydrograph and the Indian Point probable maximum flood were derived and compared to the Corps of Engineers generalized curves of Figure III-15. The 72-hour unit hydrographs were developed by inverting the flood hydrograph procedure, i.e. deducting the base flow from the flood hydrograph and dividing the resultant by the appropriate rainfall excess. The 6-hour unit hydrographs were then developed using the standard S-hydrograph method.⁵

The Green Island and Indian Point unit hydrographs thus obtained are shown in Figures III-28 and III-29 respectively. As shown in Figure III-15 these unit hydrographs produced peak discharges in excess of the Corps of Engineers mean line values. It was then concluded that the Indian Point PMF of 1,100,000 cfs represents a conservative estimate.

III-142

-56-

IV. FLOOD ROUTING & DAM FAILURE ANALYSIS OF HUDSON RIVER BASIN RESERVOIRS

A. Introduction

The purpose of this chapter is to present the results of the dam failure analysis of the Hudson river Basin Reservoirs and to determine the effect on the maximum possible stage at Indian Point 3 point.

A conservative estimate of the combined failure effect is presented first. The combined effect was obtained by locating the major Upper Hudson and Mohawk Basin reservoirs at Sacandaga and the Lower Hudson Basin reservoirs at Ashokan.

Following this is a detailed evaluation of the probable maximum effect of the largest two reservoirs in the basin (Sacandaga and Ashokan).

Reservoir flood routing procedures used in this study and referred to in the previous chapter are also presented in this chapter.

B. Combined Failure Effect

The purpose of this section is to show that the effect of failure of dams other than Sacandaga and Ashokan is insignificant.

IV-1

QUIRK, LAWLER & MATUSKY ENGINEERS

-57-

The major reservoirs located upstream of the Indian Point site and their characteristics are summarized in Table II-5. The table values clearly indicate that the largest two reservoirs are the Sacandaga in the Upper Hudson and the Ashokan in the Lower Hudson Basin. The total capacity of both of these reservoirs is more than 250 per cent in excess of all other reservoirs combined. Moreover, most of these reservoirs are located in the Upper Hudson and Mohawk River basins and are all farther from Indian Point than is Sacandaga or Ashokan.

to obtain a conservative, but realistic, estimate of the failure effect of these dams, the Delta, Hinckley, Schoharie and Indian Lake were located at Sacandaga and Rondout at Ashokan.

A formula developed by Lishtwan²⁰ and a wave profile expression derived by Chow²¹ were then used to compute the flow resulting from dam failure of the hypothetical Sacandaga and Ashokan Reservoirs, i.e. including the relocated capacity of the other reservoirs.

Chow's²¹ equation of the wave profile, resulting from the failure of a dam is in the form of:

$$X = 2t \sqrt{gh} - 3t \sqrt{gy} \quad (IV-1)$$

in which

X = The distance measured from the dam site

IV-2

QUIRK, LAWLER & MATUSKY ENGINEERS

-58-

h = The depth of the impounding water

y = The depth of the wave profile

t = The time after dam failure

Equation IV-1 may also be written as follows:

$$y = \frac{1}{g} \left[\frac{2\sqrt{gh}}{3} - \frac{x}{t} \right]^2 \quad (IV-2)$$

Integrating this equation from the origin at the dam site to the

wave front $2t\sqrt{gh}$ and solving for the total volume of water $\int yBdx$,

$$\text{Volume} = \frac{8\sqrt{g}}{27} Bh^{3/2} t \quad (IV-3)$$

Where B = channel width the initial discharge after dam failure Q_0 may be computed by dividing the volume of equation IV-3 by a very conservative failure time of one second. Therefore,

$$Q_0 = \frac{8\sqrt{g}}{27} Bh^{3/2} \quad (IV-4)$$

Lishtwan's²⁰ equation of the flow downstream of the dam site may be expressed as follows: $Q' = \frac{W_0 Q_0}{W_0 + Q_0 L_a}$

$$(IV-5)$$

where

Q' = The flow resulting from dam failure at a distance L downstream

IV-3

-59-

QUIRK, LAWLER & MATUSKY ENGINEERS

of the dam site

Q_0 = The initial dam failure discharge.

W_0 = The volume of the stored water.

$$a = \frac{1}{2} \left(\frac{1}{v_2} - \frac{1}{v_1} \right) = 0.224 \text{ for basins having a drainage area of up to}$$

about 20,000 square miles and river slopes ranging from

$.1 \times 10^{-4}$ to 5×10^{-4}

v_1 = The wave front velocity.

v_2 = The wave tail velocity.

Equations IV-4 and IV-5 were used to determine the flow at Indian Point 3 Point resulting from failure of the hypothetical reservoirs at Sacandaga and Ashokan. The computations and results are summarized in plate IV-1.

Comparison of these results with those resulting from the failure of Sacandaga and Ashokan Dams alone indicated that the effect of the smaller dams represents a small percentage of the total effect. this, coupled with the fact that these dams are farther from Indian Point 3 Point then the two major reservoirs, concentrated the detailed analysis on the failure of Sacandaga and Ashokan Dams alone.

Furthermore, no advantage was taken of the storage available in the the smaller reservoirs, (Delta, Hinckley, Gilboa, Indian Lake and

IV-4

IP3
FSAR UPDATE

QUIRK, LAWLER & MATUSKY ENGINEERS

IV-5

QUIRK, LAWLER & MATUSKY ENGINEERS

IV-6 -60-

Rondout) from the standpoint of PMP flood routing. In other words, the runoff resulting from the probable maximum precipitation was routed through Sacandaga and Ashokan Reservoirs only. The flood storage capacity of these two reservoirs is 12 and 2.3 billion cubic feet respectively.

C, Sacandaga Reservoir Studies

1. Description of Reservoir and Dam

As indicated earlier, the Sacandaga reservoir is the largest regulating feature in the entire Hudson River Basin. It controls all of the Sacandaga River drainage area of 1044 square miles – Subbasin No.8 in Figure II-1. The reservoir is of a multiple use – stream regulation and flood control – type and was formed by construction of the Conklingville Dam in 1930. The Conklingville Dam is located on the Sacandaga River which discharges into the Upper Hudson River some 70 miles upstream of Troy. The Sacandaga Reservoir and Conklingville Dam are located in Figure IV-1.

At elevation 771.0 feet above mean sea level (Crest of Conklingville Dam Spillway), the reservoir has a surface area of 27,000 acres and a total capacity of 37.8 billion cubic feet. The total capacity consists of the following three components:

IV-7

IV-8

QUIRK, LAWLER & MATUSKY ENGINEERS

-61-

<u>Use</u>	<u>Elevation</u>	<u>Storage Capacity</u> <u>Billion Cubic Feet</u>
Dead Storage	700 – 735	4.60
Stream Regulation Storage	736 – 768	29.67
Flood Control Storage	768 – 771	3.45

Figure IV-2 shows the capacity curve of Sacandaga Reservoir.

Other interesting characteristics are summarized below:

Length = 27 miles

Width = 2,000 to 28,000 feet

Length of Shore Line = 125 miles

Flow Line Elevation = 771.0' above sea level

Storage Above Elevation 768.0 = 12 billion cubic feet (total

flood storage)

A typical cross-section of the Conklingville Dam is depicted in Figure IV-3.

The dam was built by the state of New York and is maintained and operated by the Hudson River-Black River Regulating District.

It is an earth dam with a relatively impermeable core founded on rock and earth, with a concrete gravity spillway built on rock.

The earth dam was built by the semi-hydraulic fill method. The

IV-9

QUIRK, LAWLER & MATUSKY ENGINEERS

IV-10

IV-11

QUIRK, LAWLER & MATUSKY ENGINEERS

-62-

earth fill was obtained from borrow pits located at the south abutment and consisted of glacial drift that proved to be ideal for the purpose.

Core samples, taken after completion of the dam construction, showed that the entire dam material is very well packed and the non-core material is an impermeable as the core material itself.¹⁶ The soil characteristics of the core material are listed in table IV-1A and documented in Figure IV-3A. Subsequent to award of the construction contract, the rock excavation for the spillway channel was increased. The extra rock material was added to the downstream toe of the dam, providing an unusually large rock toe section.

The dam is very stable and has proven its ability to withstand severe earthquakes⁴ and floods.¹⁶

A two-day inspection of the dam and reservoir, conducted after occurrence of the highest recorded earthquake on April 20, 1931 at Lake George, new York, showed no evidence of damage.⁴

The dam is relatively impervious and seepage is reduced by the use of a very broad base. The seepage water collects in the unusually large rock toe and moves to a point where it is safely discharged. the maximum measured seepage and leakage through the dam is about 20 cfs.¹⁶

IV-12

IV-14

QUIRK, LAWLER & MATUSKY ENGINEERS

-63-

The upstream slope of the dam is protected against wave action by a sizable cover of riprap. The riprap cover extends to above the crest of the core.

Major dam dimensions and information are summarized below.

Crest Width = 43 feet

Crest Elevation = 795.0 feet

Base Width = 650 feet

Maximum Height = 96 feet

Length of Dam = 1100 feet

Length of Spillway = 405 feet

Crest of Spillway Elevation = 771.0 feet

Crest of Core Elevation = 780.0 feet

Record High Reservoir Stage Elevation = 769.72 feet (on May 21, 1969)

The outlet works consist of three 8 foot diameter Dow Valves and two 18 foot by 8 foot siphons. The spillway and diversion canal are located in a rock section away from and to the left of the earth dam. The spillway is ungated free overflow section 405 feet long. In addition, a power house with a pumping capacity of some 5600 cfs at elevation 769.0 feet is also available.¹⁶

Figure IV-4 shows the combined discharge variation with the stage in the Sacandaga Reservoir. The curve values were based upon re-

QUIRK, LAWLER & MATUSKY ENGINEERS

IV-15

IV-16

QUIRK, LAWLER & MATUSKY ENGINEERS

-64-

sults of the January – February, 1931 test and information supplied by the Hudson River – Black River Regulating District. The curve values do not include the power house pumping capacity.

2. Flood Routing through Sacandaga Reservoir

The outflow pattern that is produced by the Sacandaga River Basin (Subbasin #8) inflow into the reservoir was determined by an analytical procedure based upon a stepwise analysis of the various hydraulic occurrences: varying inflow, changing water level and varying outflow. The equation used for this purpose may be expressed follows:

$$\left[\frac{I_n + I_{n+1}}{2} - \frac{O_n + O_{n+1}}{2} \right] (t_{n+1} - t_n) = S_{n+1} - S_n \quad (IV-6) \quad 2 \quad 2$$

in which,

I = Rate of inflow into the reservoir

O = Rate of outflow from the reservoir

S = Available storage above spillway level

n, n+1 = Subscripts denoting successive intervals of time of length $t_{n+1} - t_n$

Equation IV-6 was programmed as shown on Plate IV-2 and the input or data file included:

- a. Subbasin #8 unit hydrograph – see Table III-11.

IV-17

IV-18

IV-19

-65-

- b. Subbasin #8 inflow storm hydrograph computed using the procedure of Section E of Chapter III.
- c. Reservoir stage – discharge curve – see Figure IV-4. This curve does not take advantage of the available power house pumping capacity of 5600 cfs. This added discharge capacity was not considered to be on the safe side and to account for the possibility of inoperative pumps during probable maximum conditions.
- d. Reservoir storage curve – see Figure IV-2. A straight line extrapolation was used for elevations in excess of crest of spillway elevation. This was done in accordance with the data supplied by the HR-BRRD.¹⁶
- e. A time interval of six hours.

It was assumed that the outlet works would start operation when the reservoir level reaches elevation 771.0, the crest of Spillway elevation. It was also assumed that the initial reservoir level, prior to the storm, would be at elevation 768.0 (bottom of flood storage – Figure IV-2). These assumptions are very conservative since the PMP considered in this report is a late summer or fall storm and the reservoir would usually be below the flood storage elevation and the outlet work would probably be started before the

IV-20

QUIRK, LAWLER & MATUSKY ENGINEERS

-66-

level reaches elevation 771.0. The long term late summer-fall average reservoir elevation ranges between 758.37 in August and 752.71 in November.

The program output includes subbasin #8 flood hydrograph (inflow to the reservoir), reservoir outflow hydrograph, and reservoir water surface elevation.

The program, data file and printout are shown in plates IV-2 through IV-4 respectively.

The results are shown graphically in Figures IV-5 and IV-6. Figure IV-5 depicts the reservoir inflow and outflow hydrographs. The variation in water surface elevation is documented in Figure IV-6. The computed reservoir inflow reached a peak of 262,362 cfs some 42 hours subsequent to the beginning of the probable maximum precipitation. The corresponding maximum reservoir outflow is 69,500 cfs occurring 78 hours after the beginning of PMP.

The maximum reservoir stage resulting from routing subbasin #8 flood hydrograph is elevation 783.94. This elevation is about 11 feet below the crest of the Conklingville Dam and less than 4 feet above

IV-21

IV-22

IV-23

IV-24

IV-25

IV-26

QUIRK, LAWLER & MATUSKY ENGINEERS

-67-

the crest of the core. This value is almost the same as the maximum possible level, elevation 784.0, determined by Stone & Webster.⁴

These findings were discussed with Mr. Robert Forrest, Chief Engineer of the Board of Hudson River – Black River Regulating District, on April 27, 1970. Mr. Forrest stated that the Conklingville Dam is capable of “taking this load without damage.” to support this conclusion, he gave the following reasons:

- a. The dam was designed for large surcharge and has a sufficient freeboard (24 feet above the spillway crest).
- b. The dam has a substantial cross-section and has proven its ability to withstand severe earthquakes.
- c. The excellent material used and the settlement and consolidation during the past 40 years have resulted in an inherently stable dam. Core samples taken after completion of construction showed that the dam material is homogenous and relatively impermeable.
- d. The unusually large rock toe section downstream of the dam provided a safe disposal system.
- e. Percolation from the top will not occur because of the paved highway which has its crest at elevation 795.6

IV-27

-68-

These comments and the dam failure analysis of the next section of this chapter indicate that the Conklingville Dam will not fail.

3. Conklingville Dam Failure Analysis

The results of the previous section showed that the Conklingville Dam will not be overtopped. Another dam stability criterion involving the position of the free water surface within the dam was considered. This criterion was evaluated to determine the effect of the computed maximum reservoir elevation on the safety of the dam.

In general, earth dams will fail when seepage water escapes at the downstream face of the embankment in sufficient volume to erode the surface and carry soil grains with it. This phenomenon is usually called "piping." To avoid this, seepage is usually deflected from the face of a dam by the proper use of an earth core on a rock toe.

As indicated earlier, the Conklingville Dam is provided with an unusually large rock toe as well as an earth core. The position of the free water surface within the dam was estimated for the following two downstream conditions:

Condition 1 No water downstream of the dam

IV-28

QUIRK, LAWLER & MATUSKY ENGINEERS

-69-

Condition 2 A more conservative case involving a water depth of 20 feet downstream of the dam.

the assumptions and equations used to determine the location of the seepage curve are summarized in Plate IV-5.

For the purpose of computing the seepage curve, the dam cross-section was simplified by the sketch shown in Plate IV-5 and divided into three parts A, B and C. No advantage was taken of the deflection in curve caused by the presence of the core. In other words, the material was assumed to be homogenous. The foundations were assumed to be practically impervious. These assumptions are justifiable,¹⁶ conservative and realistic

The equations are based upon Darcy's equation:

$$q = ki y \quad \text{IV-7}$$

$$\text{or } q/k = i y \quad \text{IV-8}$$

in which

q = seepage per unit width

y = depth of seepage curve

i = hydraulic gradient and is equivalent to the slope of the seepage curve $\frac{dy}{dx}$

k = permeability coefficient

IV-29

IV-30

-70-

The product (iy) for parts A, B and C may be determined as follows:

Part A:

The flow lines in this portion may be approximated by

circles having a common origin at the location of maximum water elevation (Point A in Plate IV-5) using a head loss of (a), the maximum depth at Point A may be taken as the difference between the total depth (H) and the head loss (a). The hydraulic gradient is equivalent to (a) divided by the arc length $\pi (90 - \theta) h / 360$ where $\tan \theta$ is the slope of the upstream face of the dam. Substitution in equation IV-8 yields:

$$q/k = \frac{ah}{\frac{\pi (90 - \theta) h}{360}} \simeq \frac{115 (H-h)}{90 - \theta} \quad \text{IV-9}$$

Part B:

Integration of Darcy's equation and the use of the boundary conditions $y(x=0) = h$ and $y(x=s) = h_1$ yields

$$q/k = \frac{h^2 - h_1^2}{2s} \quad \text{IV-10}$$

and

$$x = \frac{k}{q} \left(\frac{h^2 - y^2}{2} \right) \quad \text{IV-11}$$

IV-31

-71-

Part C:

When the distance s_1 is small by comparison to s, the slope of the flow line at point B may be taken as 1, and Equation IV-8 becomes:

$$q/k = h_1 \quad \text{IV-12}$$

When a downstream water depth of h_o is considered, equation IV-12 becomes:

QUIRK, LAWLER & MATUSKY ENGINEERS

$$q/k = h_1 - h_o \quad \text{IV-13}$$

Since the dam is assumed to be homogeneous, the variable q/k for the three parts is the same under steady state conditions.

Equations IV-9, IV-10 and IV-12 can be solved simultaneously to obtain the three unknowns h_1 , h and q/k and equation IV-11 gives the profile within the middle part of the dam "B". The parameters used in solving these equations include:

$H = 80$ feet

$\theta = 18.43^\circ$

$h_o = 0$ and 20 feet for conditions 1 and 2 respectively

$s = 169$ feet and 189 feet for conditions 1 and 2 respectively

The results for both conditions are depicted in Figure IV-7. In both cases, the downstream ordinate of the seepage curve is well below the crest of the rock toe.

This indicates that the seepage water would collect in the rock toe

IV-32

IV-33

-72-

and would be safely discharged without carrying soil grains with it. In other words piping would not occur.

As a conclusion, therefore, the safety of the Conklingville Dam under the probable maximum precipitation conditions considered in this study would not fail from earthquake, overtopping or piping.

C. Ashokan Dam Studies

1. Introduction

This section presents the results of the Ashokan Reservoir studies. As in the previous section, the presentation begins with a general description of the reservoir and dam followed by delineation of the reservoir flood routing procedure used in connection with the Indian Point PMF determination. Evaluation of the Ashokan Dam

QUIRK, LAWLER & MATUSKY ENGINEERS

failure is given next.

The work required to achieve the dam failure analysis objective includes:

- a. Determination of the effect of routing the Esopus Creek flood hydrograph resulting from the selected probable maximum storm (Figure III-8) through the reservoir on the dam.
- b. Since the results of item (a) above showed that the dam will not fail, a more critical condition involving

IV-34

IV-35

-73-

the effect of a local probable maximum storm (over Esopus Creek Basin only) on the dam was investigated. This condition resulted in a partial failure of the dam.

The last item in this section documents the results of the combined effect at Indian Point resulting from simultaneous occurrence of the Ashokan Dam failure and a Hudson River Standard Project flood.

2. Description of Ashokan Reservoir and Dam

The Ashokan Reservoir is the second largest regulating feature in the Hudson River Basin. It controls some 257 square miles of the Esopus Creek Basin which drains the southerly slope of the Catskill Mountains. This area is designated as Subbasin No. 19 in Figure II-1.

The reservoir is an artificial lake about 12 miles long, located about six miles west of the city of Kingston, and is part of the New York City Water Supply System. It was formed by construction of the Ashokan Dam during 1907-11. The dam is located on Esopus

QUIRK, LAWLER & MATUSKY ENGINEERS

Creek which discharges into the Hudson River some 60 miles upstream of Indian Point. The layout of the reservoir is shown in Figure IV-8.

IV-36

-74-

The reservoir has a surface area of 8180 acres and consists of two basins connected by a dividing weir. The west basin controls about 90 per cent of the drainage area and has a storage capacity of 6.3 billion cubic feet at elevation 590.0. The east basin is 3 feet lower than the west basin and has a capacity of 10.8 billion cubic feet at elevation 587.0.

The reservoir has a maximum surface width of three miles with an average of about 1 mile. The reservoir depth averages about 50 feet and reaches a maximum of 190 feet.

the reservoir is provided with a 900 foot long spillway having a crest elevation of 587.0. The spillway is located at the eastern end of the east dike. The stored water flows through the east basin and is carried by the Catskill Aqueduct to the New York City Water Supply System. The aqueduct has a capacity of some 600 million gallons per day. Except for the dividing weir, the west basin is not provided with any kind of outlet works.

The capacity curves of the east and west basins are shown in Figure IV-9.

As shown in Figure IV-8 the Ashokan Dam consists of several parts. The length and elevation of each part are summarized in Table IV-1.

IV-37

IV-38

TABLE IV-1

QUIRK, LAWLER & MATUSKY ENGINEERS


LENGTH AND ELEVATION
OF ASHOKAN DAM PART

Part	Length (ft)	Elevation, MSL	
		Crest of Dam	Crest of Core
Main Dam			
Masonry Part	1000	610	
Earth Part	3650	610	596
West Dike	1700	610	596
Middle Dike	6700	606	593
East Dike	2600	602	593
Spillway	900	587	
IV-39			
			-75-

Typical cross-sections of the main dam (both the masonry and earth parts), west, middle and east dikes are shown in Figures IV-10 and IV-10a.

3. Flood Routing through Ashokan Reservoir

The outflow pattern that is produced by the Esopus Creek Basin (Subbasin No. 19) inflow into the Ashokan Reservoir was determined by an analytical procedure similar to the one used for Sacandaga Reservoir routing. Because the Ashokan Reservoir consists of two basins, Equation IV-6 was adjusted to account for the various occurrences as follows:

$$I_{wn} + I_{wn+1} - O_{wn} + O_{wn+1} +$$


QUIRK, LAWLER & MATUSKY ENGINEERS

$$\begin{aligned}
 & \frac{2}{2} \\
 & - \left(\frac{I_{en}}{2} + \frac{I_{en+1}}{2} + \frac{O_{wn}}{2} + \frac{O_{wn+1}}{2} - \frac{O_{en} + O_{en+1}}{2} \right) \\
 & (t_{n+1} - t_n) = S_{wn+1} - S_{wn} + S_{en+1} - S_{en} \quad \text{IV-14}
 \end{aligned}$$

in which

e and w = subscripts denoting east basin and west basin respectively.

Equation IV-14 was programmed as shown on Plate IV-6 and the input or data file included:

- Subbasin No.19 unit hydrograph – see Table III-11
- Subbasin No. 19 inflow storm hydrograph computed using

IV-40

IV-41

IV-42

IV-43

IV-44

-76-

the procedure of Section E of Chapter III. This flood hydrograph was divided between the east and west basin on the basis of their drainage areas.

c. Reservoir storage curves of Figure IV-9. A straight line extrapolation was used for elevations in excess of elevations 587.0 and 590.0 for the east and west basins respectively.

d. A time interval of 2 hours.

e. Reservoir state – discharge formulas. No advantage was taken of the 600 million gallons per day capacity of the Catskill Aqueduct.

The outflow from the east basin, O_e , (spillway discharge only) was determined using the following equation:

QUIRK, LAWLER & MATUSKY ENGINEERS

$$O_e = CLH^{3/2} \quad (IV-15)$$

in which

C = Constant equal to 4 feet^{1/2}/second determined from data supplied by new York City Department of Water Resources.

L = Length of Spillway (900 feet).

H = Water head above the spillway in feet.

The west basin outflow, O_w (over the dividing weir) was computed using the following equation:

IV-45 -77-

$$O_w = CLH_w^{3/2} \left[1 - \left(\frac{H_e}{H_w} \right)^{3/2} \right] \quad (IV-16)$$

in which

C = Constant equal to 4 feet^{1/2}/second

L = Length of weir in feet

H_w = Water head above the crest in the west basin in feet

H_e = Water head above the crest in the east basin in feet.

The Ashokan Reservoir outflow was then combined with subbasin No. 20 flood hydrograph (directly downstream of the dam) to obtain the total Esopus Creek flood hydrographs.

The program, data file and printout are shown in Plates IV-6 through IV-8 respectively.

Figure VI-11 depicts the reservoir inflow and outflow hydrographs. The computed inflow reached a peak of about 58,000 cfs some 44 hours after the beginning of the storm. The corresponding maximum reservoir outflow is about 26,000 cfs occurring 8 hours later.

QUIRK, LAWLER & MATUSKY ENGINEERS

The variation in the water surface elevation in the east, as well as in the west basin, is shown in Figure IV-11a. The maximum elevation in the east basin is less than 591. This is more than two feet below the crest of the east dike core and more than 11 feet below

IV-46

IV-47

IV-48

IV-49

IV-50

IV-51

IV-53

IV-54 -78-

the crest of the east dike. The maximum elevation in the west basin is about 595 feet above mean sea level. This value is about one foot below the crest of the concrete wall core and 15 feet below the crest of the dike.

4. Ashokan Dam Failure Analysis

a. Under Hudson River Probable Maximum Flood Conditions

The results of the previous section showed that under the Hudson River PMF conditions, the water level in the east and west basin would reach a maximum elevation of 590.74 and 595.14 respectively. These values are below the elevations of the crest of the concrete wall core and well below the dike crest elevations. Therefore, seepage or overtopping of the dam would not occur. This conclusion is supported by the events of the March, 1951 flood. The elevation of the water in the east basin reached a record high of 592.23 feet at 4:45 A.M. on March 31, 1951.²² This value is about 1.5 feet higher than the above presented value of 590.74. The March, 1951 flood was the highest of records extending back to 1904.

Moreover, structural analysis of the Ashokan Dam indicated

QUIRK, LAWLER & MATUSKY ENGINEERS

that the dam is stable under these conditions. Details of the structural analysis under a more critical condi-

IV-55

-79-

tion are presented in the subsequent section.

Therefore, there is no reason to believe that the Ashokan Dam would fail, under the Hudson River PMF conditions from overtopping or seepage.

b. Under Esopus Creek Probable Maximum Flood Conditions

As indicated earlier, a more critical condition suggested by the AEC personnel was investigated. It was considered because the lower center of the selected PMS (Figure II-8) covers an area to the east of the dam site. Another storm pattern would have resulted in a storm center over the Esopus Creek Basin. It was then decided to evaluate a probable maximum storm over Esopus Creek Basin, study its effect on Ashokan Dam and determine the water surface elevation at Indian Point as a result of this flood and a standard project flood over the rest of the Hudson River Basin.

The Esopus Creek PMF and its effect on the dam are presented in this section. The effect on the Indian Point site is considered in the next section of this chapter.

IV-56

-80-

Much of the discussion on the determination of the probable maximum flood at Indian Point presented in Chapter III applies here, mutatis mutandis.

The depth-duration values of PMP for a basin having a drainage area of 257 square miles were obtained from Figure III-6. The results are shown in

QUIRK, LAWLER & MATUSKY ENGINEERS

Figure IV-12. The total rainfall for such basin is about 25 inches in 72 hours. The 6-hours incremental values of PMP over this subbasin were then rearranged in accordance with the Hydrometeorological Report No. 40 criteria. The rainfall excesses were obtained by subtracting the rainfall losses of Chapter III from the PMP values. the incremental PMP values and related runoff for subbasin No.19 are depicted in Figure IV-13. The results are also summarized in Table IV-2. Subbasin No.19 unit hydrograph – see Table III-12 – was then applied to the rainfall excess to obtain the flood hydrograph.

IV-57

I-58

IV-59

IV-60

IV-61

-81-

this hydrograph was routed through the Ashokan Reservoir following the procedure described earlier. Computer outputs of the reservoir inflow and outflow hydrographs as well as the related water surface elevations in both basins are shown in Plate IV-9. The reservoir inflow hydrograph is shown in Figure IV-14. The computed inflow reached a peak of about 200,00 cfs some 44 hours after the beginning of the Esopus Creek probable maximum flood. This peak is about four times the peak resulting from the Hudson River probable maximum flood and resulted in a water surface elevation higher than the crest of the masonry wall in the west dike and earth part of the main dam.

The variation in water elevation caused by runoff generated by the Esopus Creek PMP in both basins is

QUIRK, LAWLER & MATUSKY ENGINEERS

shown in Figure IV-15.

It was assumed that failure of the dikes and earth part of the main dam would occur with the reservoir water level at a foot higher than the crest of the

IV-62

IV-63

IV-64

IV-65

-82-

masonry core wall. In other words, failure of the west dike and earth part of the main dam would occur when the west basin water level reaches elevation 597.0. The corresponding east basin failure elevation is 594.0.

The results of Figure IV-15 indicate that the failure elevation would be reached in the west basin 40 hours after the beginning of the storm. The corresponding maximum water elevation in the east basin is about 590.5 or 2.5 feet below the crest elevation of the east basin dikes.

Structural analysis of the main dam, presented in the next section of this chapter, showed that the masonry part would not fail under the Esopus Creek PMP conditions.

It was concluded, therefore, that only the west dike and the earth part of the main dam would fail 40 hours after the beginning of the Esopus Creek PMP.

The influence of this failure on the reservoir outflow

IV-66 -83-

and elevation is depicted in Figures IV-14 and IV-15 respectively. The specific details and effect of dam failure on the Indian Point site are presented in the last part of this chapter.

c. Structural analysis of the masonry Part of the Main Dam (Olive Bidge Dam)

The purpose of this section is to show that the masonry part of the main dam shown in Figure IV-10 would not fail under the Esopus Creek PMP conditions. the following two conditions were evaluated:

Condition i – An upstream water level at elevation 610.0 and no water downstream of the dam.

Condition ii – An upstream water level equivalent to the east basin failure elevation of 597.0 and a water depth of 20 feet downstream of the dam.

Condition i:
The major forces acting on the dam are indicated in Figure IV-16 and defined below:

IV-67

IV-68

-84-

F_H = Horizontal component of hydrostatic

pressure, acting along a line $H/3$

feet above the base

= $1/2 H^2$, where γ = specific weight of

water.

F_v = vertical component of hydrostatic
pressure

= weight of fluid mass vertically
above the upstream face, acting
through the centroid of that mass.

W = Weight of dam = (area of cross-
section of dam) (S_y) where S =
specific gravity of masonry,
approximately 2.4 or 2.5, acting
through centroid of cross-section

F_u = Uplift force on base of dam, as
determined by foundation seepage
analysis, and integration of point
pressure intensities over base area;
if foundation is homogeneous and
impermeable, pressure varies approxi-
mately linearly from full hydro-

static head at the heel to full

tailwater head, and F_u is approxi-

IV-69

-85-

mately $1/2yHB$, acting at $B/3$ from

the heel. This value is often

multiplied by some fraction less

than 1 if the foundation is rela-

tively impermeable, but it is on

the safe side to assume uplift

over the entire base area.

F_E = Vertical component of earth pressure

acting on downstream face, i. e.

weight of earth mass vertically

above the downstream face, acting

through the centroid of that mass.

R = Resultant of foundation shear and

bearing pressures: horizontal com-

ponent, $R_H = F_H + F_E$ acting along

the base; vertical component, $R_v =$
 $W + F_v - F_u$ acting at a distance
 x from the toe that can be deter-
mined by the requirement for rota-
tional equilibrium of the dam, by
equating to zero the sum of the
moments of all the foregoing forces
about the toe of the dam.

IV-70 -86-

$G =$ Resultant of all forces acting on the
dam, equal to R but in the opposite
direction.

For further explanation of these formulas,
the reader is referred to reference 23. The
equations used to determine these forces and
the results are listed in Table IV-3. The
horizontal and vertical components of the

QUIRK, LAWLER & MATUSKY ENGINEERS

resultant of all forces are $1,510 \times 10^3$
and 2542×10^3 pounds respectively. The
location of the resultant is in the middle
third of the base about 72.5 feet from the
toe.

The factor of safety against sliding and
overtuning for this condition are 1.09
and 1.87 respectively. The maximum
normal stress and shear stress are less
than the allowable limits.

These results indicate that the masonry
Part of the main dam would not fail.

IV-71

I-72

-87-

Condition ii

The equations used to compute the various

QUIRK, LAWLER & MATUSKY ENGINEERS

forces and the results for this condition
are listed in Table IV-4.

The horizontal and vertical components of
the resultant are 1088×10^3 and 2044×10^3
pounds respectively. The location of the
resultant is in the middle third of the
base about 91 feet from the toe.

The factors of safety against sliding
and overturning for this condition are
1.22 and 1.86 respectively. These results
indicate that condition i is more critical.

Therefore failure of the masonry part
of the Olive Bridge Dam from overturning
or sliding would not occur.

5. Combined Effect at Indian Point resulting from Simultaneous
Occurrence of Ashokan Dam Failure and Hudson River Standard

QUIRK, LAWLER & MATUSKY ENGINEERS

Project Flood

IV-73

IV-74

-88-

The following procedure was employed to determine the flood hydro-

Graph at Indian Point resulting from Ashokan Dam failure and Hudson

River standard project flood:

a. Computation of Reservoir Outflow Hydrograph after

Dam Failure

The work required to achieve this objective includes:

i. The use of Equation IV-4 to determine

the initial dam failure discharge. The affected

area of the west basin dike and main dam is

238,670 feet with an average depth of 47 feet.

This area was conservatively approximated by a

rectangular cross-section. The computed initial

dam failure flow is about 2.6 million cubic

feet per second.

QUIRK, LAWLER & MATUSKY ENGINEERS

ii. Determination of west basin emptying time.

The dam break hydrograph was conservatively assumed to have a triangular shape with the initial flow as the height and emptying time as the base. The emptying time is, therefore,

equivalent to $\frac{2v}{Q_0}$ where v is the total volume.

of water stored in the west basin (6.765

IV-75

-89-

billion cubic feet) and Q_0 is the initial flow

(2.6 million cfs). These values give an empty-

ing time of 5200 seconds or 1.45 hours.

iii. Combination of dam break hydrograph with

the east basin outflow over the main spillway

to obtain the reservoir outflow hydrograph.

the east basin was computed in a manner simi-

lar to that outlined in Section 3 of this

QUIRK, LAWLER & MATUSKY ENGINEERS

chapter.

The reservoir outflow hydrograph including dam break wave is shown in Figure IV-14. Subsequent to the emptying time the resultant hydrograph coincides with the reservoir inflow hydrograph. This is a conservative assumption since no advantage is taken of the “cushioning effect” of the east basin.

b. Routing of Esopus Creek Flood Hydrograph to the Hudson River.

This step requires the following:

i. Combination of Ashokan reservoir outflow Hydrograph (including dam break wave) of

IV-76

-90-

previous step with the flood hydrograph of the remaining part of the Esopus Creek Basin, i.e. Subbasin No. 20. Since the contribution of Subbasin No. 20 represents only a fraction of

QUIRK, LAWLER & MATUSKY ENGINEERS

the reservoir outflow hydrograph, the resultant
is essentially the same as the reservoir outflow
hydrograph shown in Figure IV-14.

ii. Computation of Valley storage in Sub-
basin No. 20 (between the dam and Hudson River).

It was assumed, as suggested by reference 21,
that the wave front moves in a steeply inclined
wall of water whose profile is unchanging as
long as the channel conditions remain fixed
and the source of supply is constant. Therefore,
this can be considered a special case of uniformly
progressive flow, known specifically as the roll
wave. The wave front discharge, Q_w , may be
obtained using Manning's Equation:

$$Q = \frac{1.49}{n} B Y^{5/3} S_o^{1/2} \quad \text{IV-17}$$

In which

QUIRK, LAWLER & MATUSKY ENGINEERS

S_o = Channel slope

N-77

-91-

Y' = Depth at the crest of the wave

B = Channel width

n = Manning's coefficient (.035 was used for
this purpose)

As a conservative estimate of the wave
profile, a constant flow equivalent to
the maximum initial failure flow of 2.6
million cfs and the valley characteristics
(B and S_o) obtained from the **U.S.G.S.** maps
were used.

A careful study of the topography of Esopus
Creek Valley indicated that the flood gener-
ated by the Esopus Creek PMP and Ashokan Dam

QUIRK, LAWLER & MATUSKY ENGINEERS

failure would create a lake extending from the dam to Glenerie Falls some 5 miles west of the Hudson River. The lake would have a total length of some 14 miles and a surface width ranging from 4000 to 1800 feet. The lake would have a control section at Glenerie Falls where width decreases

IV-78

-92-

suddenly from 6000 feet to 500 feet. A sketch showing the size, direction of flow through the lake and the location of the control section is presented in Figure IV-17.

The maximum water surface level at Glenerie Falls would be at elevation 180.0. This value was computed using Equation IV-17 and the standard step method of computing gradually varied steady flow profiles. Elevation 180, there-

QUIRK, LAWLER & MATUSKY ENGINEERS

fore, delineate the shore lines of the lake at this elevation is about 7 billion cubic feet. This value is almost the same as the storage capacity of the Ashokan west basin. This provides an added confirmation of the computed elevation of 180.0.

The storage capacity curve of this lake is shown in Figure IV-18.

The outflow from the lake at Glenerie Falls was computed using the standard critical depth formula:

IV-79
IV-80
IV-81

-93-

$$Q = \frac{q A^3}{\sqrt{B}}$$

IV-18

A stage-discharge curve was established for this lake and is shown in Figure IV-18.

ii. Routing of Esopus Creek Flood Hydrograph
through the lake was accomplished by using a
computer program similar to the one described
in Section 3. The program, data file and
printouts are given in Plates IV-10 through
IV-12. The input includes the initial
lake outflow of 620,000 cfs at elevation
180.0. Subbasin No. 19 flood hydrographs
generated by Esopus Creek PMP and Subbasin
No. 20 flow caused by runoff generated by
the Hudson River Standard Project Flood.

The 620,000 cfs represents the effect of
the dam failure at Glenerie Falls and is
equivalent to the lake outflow at elevation
180.0. This is a conservative, but realistic,
estimate of the failure effect since the
volume of the stored water in the lake is

IV-82
IV-83
IV-84
IV-85
IV-86
IV-87
IV-88
IV-89

-94-

essentially the same as the Ashokan west basin

capacity.

c. Routing of Esopus Creek Flood Hydrograph and Hudson

River Standard Project Flood to Indian Point

The Esopus Creek flood hydrograph resulting from Ashokan

dam failure, Subbasin No. 19 PMP and Subbasin No. 20 SPF

as computed above is represented by Curve I in Figure

IV-19.

The Hudson River Standard Project Flood upstream of

Esopus Creek was obtained by dividing the probable

maximum flood values of Figure III-27 by two. The

QUIRK, LAWLER & MATUSKY ENGINEERS

factor two is within the range of 40 per cent to 60

per cent developed by the Corps of Engineers for the

Susquehanna River Basin²⁴ and was suggested by Mr.

Nunn of the AEC.¹⁷ Curve II of Figure IV-19 shows

the SPF above Esopus Creek.

Curve III in Figure IV-19 represents the combined

effect (Curve I + Curve II) just downstream of the

mouth of Esopus Creek.

IV-90

IV-91

-95-

The combined hydrograph was then routed through the

Hudson River Channel to Indian Point using the pro-

cedures developed in Chapter III. The resultant

at Indian Point is shown as Curve IV in Figure IV-19.

The program, data file and printouts for this condition

are listed in Plates IV-13 through IV-15 respectively.

The maximum discharge at Indian Point resulting from

QUIRK, LAWLER & MATUSKY ENGINEERS

the conditions considered in this chapter is 705,000
cfs. The probable maximum flood at Indian Point is
about 50 per cent higher than this value.

IV-92
IV-93
IV-94
IV-95
IV-96
IV-97
IV-98
IV-99
IV-100
IV-101
IV-102
IV-103
IV-104

-96-

V. MAXIMUM RIVER ELEVATION FOR FLOODING CONDITIONS AT INDIAN POINT

A. Introduction and Summary of Procedures Employed

The purpose of this chapter is to determine the maximum water
surface elevation at the Indian Point site resulting from several
flooding conditions including:

1. Runoff generated by the Hudson River probable maximum precip-
itation presented in Chapter III.

QUIRK, LAWLER & MATUSKY ENGINEERS

2. Flooding caused by the occurrence of the Ashokan Dam failure concurrent with the standard project flood for the Hudson River Basin considered in Chapter IV.
3. Flooding resulting from the probable maximum hurricane for the New York Harbor area concurrent with spring high tide discussed in Appendix A.

To achieve this objective, backwater curves were calculated using the well known standard step method²¹ as well as a newly developed numerical method of computing gradually varied flow profiles,²⁵ starting with several assumed water-surface elevations at a control point on the river. The hydrodynamic and physical characteristics of the Hudson River dictated the use of the ocean entrance at the battery as the control section. Therefore, the backwater computa-

V-1

-97-

tions were initiated at this location and the following boundary conditions, at the Battery, were evaluated:

1. Mean sea level

QUIRK, LAWLER & MATUSKY ENGINEERS

2. High tide water elevation
3. Low tide water elevation
4. Standard project hurricane
5. Probable maximum hurricane

The tidal variation in the Hudson River Estuary discussed in Chapter II influenced the choice of the proper boundary conditions as well as the value of the discharge for which the flow profile is desired. As in the case of flooding from dam failure and unlike the previous attempts, the tidal variation was treated as an integral part of the system and its influence was simultaneously coupled with the other relevant hydraulic occurrences.

In the evaluation of the maximum water surface elevation at Indian Point resulting from the above delineated flooding and boundary conditions, the wind produced local oscillatory short period waves were also considered. The computed Indian Point stages corresponding to the various flooding conditions were conservatively increased by one foot to account for this effect. A detailed discussion of this effect appears in Appendix A.

V-2

-98-

A detailed description of the standard step method employed in this study as well as the newly developed flow profile numerical method is presented first. Following this is a discussion of the influence of the Hudson River tidal variation. The results of the various flooding and boundary conditions are discussed and presented last.

B. Methods of Backwater Computation

The so-called "Standard Step Method"²¹ was employed in this study to determine the water elevation at Indian Point as well as the time of travel of the flood hydrograph between Troy and Indian Point.

However, a new numerical method of computing gradually varied steady flow profiles developed by Prasad²⁵ was used to verify the Standard Step Method results.

A discussion of both methods follows.

1. Standard Step Method

This method is characterized by dividing the channel into

QUIRK, LAWLER & MATUSKY ENGINEERS

several short reaches and carrying the computation step by step from one end of the reach to the other. The basic equation that defines the procedure may be expressed as

V-3 -99-

follows:

$$H_{i+1} = H_i + h_f + h_e \quad (V-1)$$

in which

H = Total head (elevation of the energy line) above

a horizontal datum. The mean sea level was

selected in this study as the datum.

h_f = Friction loss between two end sections i and

$i + 1$

h_e = Eddy loss. For convenience of computation,

this loss was considered part of the friction

loss h_f

The friction loss h_f may be computed as follows:

$$h_f = \bar{S}_f D x = \frac{1}{2} (S_i + S_{i+1}) D x \quad (V-2)$$

QUIRK, LAWLER & MATUSKY ENGINEERS

where

\bar{S}_f = Friction slope taken as the average of the slopes

at the two end stations, i.e. $\bar{S}_f = \frac{1}{2}(S_i + S_{i+1})$

Δx = Longitudinal distance between the two end sec-

tions.

Manning's formula was used to compute the friction slope

$$S_f = \frac{n^2 v^2}{1.49^2 R_h^{4/3}} \quad (V-3)$$

where

n = Manning's roughness coefficient

V-4 -100-

v = River velocity and is equal to $\frac{Q}{A}$

R_h = Hydraulic radius

Q = River discharge

A = Cross-sectional area

The total head or elevation of the energy line above

mean sea level may be expressed as follows:

QUIRK, LAWLER & MATUSKY ENGINEERS

$$H_i = Y_i + \ell \frac{v_i^2}{2g} \quad (V-4)$$

in which

Y = Water surface elevation above mean sea level

ℓ = Energy coefficient. This coefficient was assumed to be unity because of the fairly straight alignment and regular cross-section of the river between the Battery and Indian Point.

The river channel was conservatively approximated by a rectangular cross-section defined by the mean water surface width B and the mean depth D . Thus

$$A_i = B_i D_i = B_i (Y_i + Z_i) \quad (V-5)$$

in which

Z_i = Water depth below mean sea level

No advantage was taken of the increase in surface width

V-5 -101-

above mean sea level. Since the channel is of a wide

QUIRK, LAWLER & MATUSKY ENGINEERS

rectangular shape, the hydraulic radius R_h was approx-

imated by the mean depth $Y_i + Z_i$.

The foregoing equations were programmed for solution on

RAPIDATA time-sharing facilities. The program is listed

in Plate V-1.

The Lower Hudson River Channel was divided into 136

reaches ranging in length from 0.3 to 2 miles. The

wide variation in channel geometry influenced the

selection of these subreaches. The surface width at

mean water B and mean depth below mean sea level Z

corresponding to the 136 sections are listed in

Plate V-2. The locations of these stations expressed

in miles above the ocean entrance at the Battery are

also shown in Plate V-2.

An estimated average value 0.025 was used for Manning's

roughness coefficient n in the Lower Hudson. Limited

information is available for an accurate determination

QUIRK, LAWLER & MATUSKY ENGINEERS

of this coefficient. The 0.025 value was selected on the basis of several U.S.G.S. estimates of the Lower

V-6

-102-

Hudson River flow resistance coefficient. These estimates were derived from velocity measurements made by the U. S. Geological Survey at the Poughkeepsie gaging site. Values ranging from .019 to .024²⁶ were computed using available, but inconclusive, data and several computer programs developed by the U.S.G.S.²⁷⁻³²

Moreover, the selected n value falls within the range recommended by Dronkers³³ for tidal rivers. (Chezy coefficients of 50 to 70 meter ¹/₂/sec for shallow waters and deep inlets respectively. The corresponding Manning n values, for a channel having an average hydraulic radius of 30 feet are 0.029 and .021 respectively.)

The procedure used to compute the backwater profiles

QUIRK, LAWLER & MATUSKY ENGINEERS

may be summarized below:

- a. Select a boundary condition, i.e. water surface elevation above MSL at the control section (the Battery).
- b. Select a flooding condition in the Lower Hudson River such as flooding resulting from PMP, dam failure etc. Use a constant flow

V-11

-103-

value Q equivalent to the peak of the flood hydrograph. This is a conservative assumption since the flow, prior and subsequent to the peak time, is substantially less than this value.

- c. Compute the control section velocity corresponding to the selected water surface elevation – Step a – and flooding condition - Step b – using the continuity equation

$$V_i = Q / B_i (Y_i + Z_i)$$

QUIRK, LAWLER & MATUSKY ENGINEERS

d. Compute the friction slope S_f^i using

Equation V-3.

e. Determine the energy line elevation

H_i above MSL using Equation V-4.

f. Estimate the water surface elevation at

the upstream section of the first reach i.e.

section $i + 1$. As a first approximation use

$$Y_{i+1} = Y_i = S_f^{(i)} \Delta x$$

g. Using the estimated Y_{i+1} - Step f – repeat

steps c, d and e to determine V_{i+1} , $S_f(i + 1)$

and H_{i+1} .

h. Compute the difference between the elevation

of the energy line at sections i and $i + 1$, i.e.

V-12 -104-

$$\Delta H = H_{i+1} - H_i$$

i. Compute the friction loss h_f between the

QUIRK, LAWLER & MATUSKY ENGINEERS

two sections using Equation V-2.

j. If the difference between ΔH and h_f is

greater than .05 feet, assume a new value

of Y_{i+1} and repeat steps g through i until

agreement with the control $|\Delta H - h_f| \leq .05$

feet is obtained.

k. Proceed to the next reach using the final

Y_{i+1} value of the first reach as the

downstream control for the second reach.

l. Repeat until the water surface elevation

at the last section is determined.

2. Numerical Method of Computing Gradually Varied

Flow Profiles

This method was developed by Prasad in 1968.²⁵ Prasad

describes his method as “simple, fast, efficient, and

does away with most of the approximations and limita-

tions of other methods of computing gradually varied flow

QUIRK, LAWLER & MATUSKY ENGINEERS

profiles."

The method is based on the following two equations:

V-13

-105-

$$D \phi = \left(\frac{Q^2}{g A^3} - \frac{n^2 Q^2}{2.22 A^2 R_h^{4/3}} \right) / \left(\frac{Q^2 B}{g A^3} \right) \quad (V-6)$$

and

$$D_{i+1} = D_i + \frac{D \phi_{i+1} + D \phi_i}{2} \Delta x \quad (V-7)$$

in which

D = River Depth

$$D \phi = \frac{dD}{dx}$$

S_o = Slope of river bed

Equation V-6 is the well-known differential equation

of gradually varied flow expressed in terms of channel

geometry and hydraulic characteristics. Equation V-7

utilizes the classical trapezoidal method of integra-

tion to express the depth in terms of its derivative

QUIRK, LAWLER & MATUSKY ENGINEERS

with respect to the longitudinal distance x . This

equation requires a very small reach length Δx .

These two equations can be solved numerically to

determine the two unknowns D and $D\phi$. The procedure

suggested by Prasad is reproduced below.

a. Compute $D\phi$ from equation V-6 in which

D_i is given as an initial condition or from

V-14

-106-

a previous calculation.

b. Assume $D_{i+1} = D\phi$ as a first approximation

c. Calculate an approximate value of D_{i+1}

from equation V-7 using the value of $D\phi_{i+1}$ obtained from step b or d.

d. Compute a new value of D_{i+1} ob-

tained in step c.

e. If this new value of $D\phi_{i+1}$ is not very

close to the previously assumed value in

step b, repeat steps c through e. Other-

QUIRK, LAWLER & MATUSKY ENGINEERS

wise repeat the whole procedure for another
i, or, advance the solution by one integra-
tion step.

The foregoing procedure was programmed for solution on
RAPIDATA time-sharing facilities. A listing of the
program appears on Plate V-3. The input data are identical
to those used in the Standard step method. However, because
of the use of the trapezoidal integration method in this
program, the reach size Δx was reduced by 400 per cent.

V-15 -107-

C. Influence of Hudson River Tidal Variation on Water Surface Level at Indian Point

As indicated earlier, the influence of tidal variation in the
Hudson River during probable maximum flood conditions was treated
as an integral part of the problem and simultaneously coupled
with the other hydraulic occurrences. In the past studies, a
somewhat piecemeal method consisting of adding a constant com-
ponent flow equivalent to the maximum observed ebb flow to the

QUIRK, LAWLER & MATUSKY ENGINEERS

the flood hydrograph at Indian Point was employed. A careful evaluation of this effect during high runoff conditions revealed the following findings:

1. The tides and currents in the river are subject to large seasonal variations due primarily to fluctuations in the fresh-water discharge.
2. Near the mouth of the river this variation is relatively small, but in advancing up the river the variations become more important and reach their maximum at the head.
3. At the time of high runoff from the Upper Hudson and Mohawk Basins, the tide may be completely masked in the upper portion of the river, the water continuing to rise or fall for a period of several days without any tidal oscillation.
4. The ocean derived salinity intrusion length is influenced, to a great extent, by the upland runoff. The relationship between

V-18

-108-

the intrusion length and the fresh water flow in the Lower

Hudson River is shown in Figure II-12. Extrapolation based

QUIRK, LAWLER & MATUSKY ENGINEERS

upon the equations of Figure II-12 shows that under the PMP conditions the salinity concentration in the Lower Hudson would be less than 250 ppm. This indicates that only a small reach of negligible length would be influenced by the ocean derived salt.

On the basis of these observations, a more realistic approach was adopted. The new approach may be illustrated by the following steps:

1. Assume that the tidal variation at the ocean entrance is not influenced by the probable maximum precipitation. This assumption is supported by the USC and GS tidal measurements over a very long period (1899-1932).³⁴ A comparison between the tidal characteristics at the mouth (the Battery) and head (Albany) for the year 1922 is shown in Table V-1. This year was selected for this purpose because of the high runoff that occurred in April (154,000 cfs at Troy). The table values clearly indicate the influence of land runoff at the Battery is relatively small. The April values are

QUIRK, LAWLER & MATUSKY ENGINEERS

within 1 to 2 per cent of their annual average counterparts.

V-19 -109-

In the vicinity of Albany, on the other hand, the April values are 60 to 150 per cent higher than the annual average.

2. For a given flooding condition, such as the probable maximum flood at Indian Point (1,100,000 cfs) and a known boundary condition, such as mean water level at elevation 0.0, compute the Lower Hudson River flow profile. The standard step method may be used for this purpose. Designate time (t) to this profile.

3. At the beginning of the flood cycle, the state at the Battery starts to increase until it reaches a maximum elevation of +2.2 some three hours later. This increase in elevation causes a decrease in the slope of the Lower Hudson River water surface profile. This change results in a stage increase along the river ranging from a maximum of 2.2 feet at the Battery to zero at some upstream location. The amount of water stored within the reach of influence (ΔV) is equivalent

QUIRK, LAWLER & MATUSKY ENGINEERS

to the product of the time interval (Δt) and decrease in river flow caused by channel storage (ΔQ).

The process is then reversed during the second half of the flood cycle, i.e. the water stored during the first half of

V-21 -110-

of the flood cycle is released causing an increase in the flow and a decrease in water surface elevation within the same influenced reach. About three hours later the flow profile approaches its initial condition (before the beginning of the flood cycle)

4. During the first half of the ebb cycle (from mean water to low water), the stage at the Battery starts to decrease until it reaches a minimum elevation of -2.2 during maximum ebb. This control section stage variation causes an increase in the water surface gradient resulting in a stage decrease along the influenced reach. The water volume released during this interval is again equivalent to the product of the time interval and the difference between the initial and final flows.

QUIRK, LAWLER & MATUSKY ENGINEERS

The process then continues until the flow profile returns to its original shape.

The tidal cycle at the Battery was divided into 16 intervals having a duration of about 45 minutes. The boundary conditions corresponding to these intervals were obtained from the USC and GS tidal measurements at the Battery. A trial and error procedure was then employed to determine the length of influenced reach, amount of

V-22 -111-

water stored or released during each interval and related channel flow values. The standard step method was then employed using the computed flows and given boundary conditions to obtain the flow profiles in the Lower Hudson. The final results are presented in the next part of this chapter.

D. Water Surface Level at Indian Point

Several severe Hudson River flooding conditions and water-surface elevations at the Battery were presented in the previous chapters. These conditions were conservatively grouped in seven different ways on the basis of a simultaneous occurrence of an appropriate

QUIRK, LAWLER & MATUSKY ENGINEERS

set of flooding, hurricane and tidal conditions.

The seven groups are outlined in the following tabulation:

Case No.	Flooding Condition at Indian Point	Water-surface Elevation at the Ocean Entrance
1	Probable Maximum Flood	Mean Tide, i.e. M.S.L.
2	Probable Maximum Flood concurrent with tidal flow	High Tide
3	Probable Maximum Flood concurrent with tidal flow	Low Tide
4.	Dam failure concurrent with standard project flood	Mean Tide
5.	Standard Project Flood	Standard Project Hurricane
V-23		-112
6.	Dam Failure concurrent with standard project flood	Standard Project Hurricane
7.	Probable Maximum Hurricane concurrent with Spring high tide	Probable Maximum Hurricane

A detailed description of these cases and their significance

QUIRK, LAWLER & MATUSKY ENGINEERS

follows:

Case 1

This case considers the Indian Point stage at peak discharge due to runoff generated by the probable maximum precipitation over the Hudson River drainage area upstream of the site. The mean tide at the ocean entrance which corresponds to the mean sea level was selected as a boundary condition for this case.

The probable maximum flood of 1.1 million cubic feet per second, discussed in Chapter III, was considered to prevail in the Lower Hudson River for a long period. In other words, a steady state flow condition of 1.1 million cfs in the reach between the ocean entrance and the site was assumed. This assumption is conservative since the flood hydrograph under PMP conditons (Figure III-27) indicates that the duration of the peak discharge (PMF) is only several hours.

V-24

-113-

The mean sea level at the ocean entrance (the Battery) was selected as the boundary condition for this case since the tidal variations

QUIRK, LAWLER & MATUSKY ENGINEERS

under PMP conditions would be relatively small. Examination of the USC & GS measurements³⁵ indicate that under such conditions the tide would be completely masked in a significant portion of the river. The results of cases No. 2 and 3 suggest that only the lower 27 miles of the river would be subjected to significant tidal oscillation.

The standard step method for water surface profiles presented earlier was employed to determine the stage at the Indian Point site for the above-delineated conditions, i.e. flow of 1.1. million cfs and mean sea level at the Battery. The results are listed in Plate V-4 and shown in Figure V-1. The results of Cases No. 2 and 3 are also shown in Figure V-1.

The flow profile corresponding to Case No. 1 conditions was verified using the newly developed Prasad's method discussed in Section B of this chapter. These results are shown in Plate V-5 and compared to their Standard Step Method counterparts in Table V-2. The agreement between the two methods is remarkable. In general the new method gives slightly lower stage values with a maximum difference of -0.5

QUIRK, LAWLER & MATUSKY ENGINEERS

feet.

V-25 -114-

The probable maximum flood would result in a river stage of ele-

vation 12.7 feet above the mean sea level at Indian Point.

The account for the influence of the local oscillatory wave at

Indian Point referred to in Section A of this Chapter, the computed

stage must be increased by one foot. This estimate is conservative

and discussed in detail in Appendix A.

Therefore, the Indian Point river stage corresponding to Case No.

1 conditions and including the influence of the local oscillatory

wave would be 13.7 feet above mean sea level.

Cases No. 2 and 3

These cases were considered to evaluate the influence of the tidal

variation on the Indian Point stage during the probable maximum

conditions. The procedure outlined in the previous section of

QUIRK, LAWLER & MATUSKY ENGINEERS

this chapter was used for this purpose. The tidal variation at the ocean entrance, its influence on the probable maximum flood and river stage at Indian Point are depicted in Figure V-2. The specific details of the procedure are listed in Table V-3.

Figure V-1 documents the flow profiles corresponding to cases No. 2 and 3 conditions, probable maximum flood concurrent with

V-39 -115-

tidal flow at Indian Point and high water and low water elevations at the Battery respectively.

As indicated earlier, these results suggest that the river above the Tappan Zee Bridge, some 27 river miles above the Battery, would experience relatively small tidal variations under the PMP conditions. The upstream extent of the reach influenced by tidal variations was located using the material balance procedure described earlier.

The conclusion seems to be in good agreement with the lack of tidal oscillation observed in the upper portion of the river during the

QUIRK, LAWLER & MATUSKY ENGINEERS

floods of March 28, 1913 and March 19, 1936. The maximum discharge measured at the head of the estuary during the 1913 and 1936 floods were 223,000 and 215,000 cfs respectively. These floods pushed the tide back downstream resulting in a flattening of the slope of the measured flood profiles some 30 miles downstream of Troy.³⁵ Thus, a peak discharge of more than one million cfs would be expected to mask the tide in a significantly longer reach. Figure V-1 estimates the length of this reach to be some 120 miles (between Troy and the Tappan Zee Bridge). Theoretically speaking, therefore, the ocean-derived tidal influence would not be experienced at Indian Point under the probable maximum precipitation conditions.

V-42

-116-

However, to be on the conservative side, the reach of tidal influence was extended upstream to the site at Indian Point. The tidal effect resulted in the following changes:

Case No.	Stage at the	Peak Flow at	Water-surface ele-
----------	--------------	--------------	--------------------

QUIRK, LAWLER & MATUSKY ENGINEERS

	Battery (M.S.L.)	Indian Point	vation at Indian
		(cfs)	Point
1	Mean Water	1,100,000	12.70
2	High Water	1,013,500	12.37
3	Low Water	1,164,800	13.05

As a conclusion, the water-surface elevation at the site would range between 12.37 and 13.05 depending upon the tidal phase at the Battery.

As before, these values must be increased by one foot to account for the local oscillatory wave at Indian Point.

Case No. 4

This case considers the maximum river stage resulting from a failure of the Ashokan Dam concurrent with the Hudson River Standard Project Flood at Indian Point. This flooding condition was discussed in detail in Chapter IV.

It should be also recalled that one of the centers of the probable maximum storm was placed over the largest reservoir in the basin.

Due to the cross-shaped watershed of the basin, the reshaping of

V-43

-117-

the isohyets recommended by the Weather Bureau placed the lower center several miles upstream of the second largest reservoir.

As indicated in Chapter IV, the runoff generated by the probable maximum precipitation over the entire basin as described above would not result in failure of the basin dams.

However, because the Ashokan Dam contains the second largest volume of stored water in the basin and is closer to Indian Point than any other dam in the basin, a flooding condition resulting in a failure of this dam was considered. As suggested by the AEC, the flooding condition consisted of the simultaneous occurrence of a probable maximum flood over the Esopus Creek Basin upstream of Ashokan and a standard project flood over the rest of the Hudson River Basin.

As far as the Ashokan Dam failure is concerned, the suggested condition proved to be more critical than a hypothetical condition placing the lower center of the selected PMS directly over the Ashokan Reservoir.

QUIRK, LAWLER & MATUSKY ENGINEERS

The suggested condition resulted in a failure of the Ashokan Dam and a peak flow of 705,000 cfs at Indian Point. This flow would

V-44 -118-

result in a river stage of Elevation 7.2 above mean sea level at the Indian Point site. This value corresponds to a mean sea level elevation at the ocean entrance. Because this condition is less critical than the probable maximum flood conditions (Cases No. 1 through 3), additional evaluation concerning the influence of the tidal variation was not undertaken.

Case 4 results, as well as Cases 5 and 6, are depicted in Figure V-3.

Cases No. 5 and 6

To carry the degree of severity a step further, a more critical boundary condition was imposed on two flooding conditions. The peak storm surge at the Battery resulting from the Standard Project Hurricane for the New York Harbor area was used as the boundary condition for these two cases. The flooding condition of Case No. 4, as well as a similar flooding condition, in which the effect of Ashokan Dam failure was excluded, were used for these two cases.

QUIRK, LAWLER & MATUSKY ENGINEERS

The New York Harbor hurricane studies^{36, 37} undertaken by the New York District Corps of Engineers showed that the peak storm surge height at the Battery resulting from the Standard Project Hurricane is 11.0 feet. This value was based on the transposition of the September, 1944 hurricane to a path critical to the New York Harbor

V-45 -119-

area, using parameters given in U.S. Weather Bureau Memoranda HUR 7-60 and HUR 7-60a dated 27 March 1959 and 7 April 1959 respectively. The parameters finally selected for this storm were a maximum wind speed of 116 miles per hour, a central pressure range from 27.55 to 27.95 inches of mercury with a normal pressure of 30.12 inches, a radius to maximum winds of 30 nautical miles, and a forward speed of 40 knots. The corresponding peak storm surge height at Sandy Hook, some 17 miles downstream of the Battery, is approximately 12 feet.

Similar computations were made by the Corps of Engineers for a 1938 hurricane transposed to a path critical to New York Harbor. The computations, which were based on parameters given in the U.S. Weather

QUIRK, LAWLER & MATUSKY ENGINEERS

Bureau Memorandum HUR 7-25, dated 25 February 1957, and a forward storm speed of 35 knots, yielded surges of 8.9 feet at Sandy Hook and 8.8 feet at Fort Hamilton. The maximum surge of record at Fort Hamilton, which is 8.2 feet, was experienced during the extratropical storm of 25 November 1950.

To maintain the selection of severe conditions and in accordance with the high degree of conservatism adopted in this study, the value based upon the transposed September 1944 hurricane was selected. This value is 75 per cent higher than the maximum storm surge during

V-47 -120-

hurricane "Donna" that struck on September 12, 1960. Hurricane "Donna" was the latest storm to have the greatest effect in the New York Harbor area since the September 1821 hurricane.

Simultaneous occurrence of the standard project hurricane with a flooding condition resulting from runoff generated by a standard project precipitation over the entire basin would result in a river stage of elevation 13.0 at the site.

Case No. 6 considers an even more critical set of occurrences con-

QUIRK, LAWLER & MATUSKY ENGINEERS

sisting of the simultaneous occurrence of the following three severe conditions:

1. Probable Maximum Precipitation over the Ashokan Reservoir drainage basin resulting in a failure of the Ashokan Dam.
2. Runoff generated by the standard project precipitation over the rest of the basin.
3. Peak storm surge at the Battery resulting from the Standard Project Hurricane for the New York Harbor area.

This case would result in a river stage of elevation 14.0 at Indian Point. This value is higher than any of the previous five estimates. The simultaneous occurrence of the above-delineated three severe conditions is extremely remote. Moreover, each one

V-48

-121-

of these three individual conditions was based upon several conservative assumptions discussed in previous chapters. Combination of these conditions, therefore, increases the degree of conservatism substantially.

The resulting flow profiles corresponding to this case as well as

QUIRK, LAWLER & MATUSKY ENGINEERS

Case No. 5 are shown in Figure V-3.

For convenience, the results of the six cases are summarized and compared in Table V-4. The computer printouts for the individual cases are presented in Plates V-2 and V-6 through V-10 respectively.

Case No. 7 considers the water surface elevation at the site resulting from the occurrence of a PMH concurrent with spring high tide.

This case was the main subject of Q.L. & M's report of February, 1969 which is appended to the main body of this report. The results are included in Table S-1 for convenience and comparison purposes.

A summary of the determination of the results follow.

Using the general equations for surge in an estuary, presented in a paper by J. Proudman, an internationally respected oceanographer, a procedure to route the hurricane surge through the Hudson Estuary was developed. This procedure considered channel frictional resis-

V-49 -122-

tance, geometric changes in cross-section, and estuary storage of the surge flow. The large storage capacity of Haverstraw Bay acts as an on-line reservoir to attenuate the hurricane surge as it flows

QUIRK, LAWLER & MATUSKY ENGINEERS

toward Indian Point.

A conservative estimate of the routed hurricane surge height at Indian Point is 8.8 feet above mean tidal level, with an additional surge due to wind setup of 1.0 feet, and combined with a spring high tide of 3.0 feet. The total calculated elevation is 13.5 feet above mean sea level.

In addition, estimated local oscillatory waves will reach a height of 1.0 feet above the calculated level in the river. Provision should be made for protecting any structures and appurtenances from this 1.0 foot wave action above the 13.5 foot mean sea level calculated elevation. This value was added to all of the computed stages corresponding to the seven cases and the results are listed in the last column of Table S-1.

V-56

-A-1-

APPENDIX A

MAXIMUM RIVER ELEVATION AT INDIAN POINT

RESULTING FROM PROBABLE MAXIMUM HURRICANE
AND SPRING HIGH TIDE *

QUIRK, LAWLER & MATUSKY ENGINEERS

A. Hurricane Parameters

The probable maximum hurricane (pmh) for zone 4, latitude 41°N, as defined by the United States Weather Bureau, has the following meteorological characteristics.

Central Pressure	27.26 inches of Hg
------------------	--------------------

Radius of Maximum Winds	24 nautical miles (weighted mean)
-------------------------	-----------------------------------

	8 nautical miles (min. limit)
--	-------------------------------

	48 nautical miles (max. limit)
--	--------------------------------

Forward Speed of Hurricane	34 knots (weighted mean)
----------------------------	--------------------------

	15 knots (min. limit)
--	-----------------------

	51 knots (max. limit)
--	-----------------------

Maximum Wind Speed	124 mph to 136 mph
--------------------	--------------------

	127 mph (at mean forward speed)
--	---------------------------------

Inspection of published data showed that the vast majority of the hurricane parameters cluster around the mean values reported above.

The minimum and maximum ranges represent the limits of the frequency distribution of the parameters as defined by isolated storms.

Parameters used in the analysis included a forward speed of 34

QUIRK, LAWLER & MATUSKY ENGINEERS

knots, a radius of maximum wind of 24 nautical miles, and a maximum wind speed of 127 mph. These values represent a probable maximum

* The material included in Appendix A is essentially that of Chapter III of the February, 1969 report.

A-1 -A-2-

hurricane with a recurrence interval estimated within the range of 1,000 to 10,000 years.

I should be noted that the very low probability of occurrence of the pmh must be multiplied by the probability of occurrence of spring tides, which occur twice in a lunar cycle of approximately one month, in order to determine the probability of occurrence of the hurricane surge concurrent with maximum high tides. The resulting flooding condition is, therefore, very conservative.

For this hurricane, procedures published by the U.S. Army Coastal Engineering Research Center were used to determine the surge height at the Battery.

B. Summary of Procedures Employed

The initial step involved the construction of the isovel field for

QUIRK, LAWLER & MATUSKY ENGINEERS

the meteorological characteristics of the pmh. The field was constructed using standard procedures developed by the U.S. Weather Bureau in the aforementioned report.

Following the construction of this field, the wind stresses for several lines passing through the hurricane and parallel to the direction of its movement were computed. The stress coefficient for a hurricane moving over a sloping bottom was used. The maximum

A-2

-A-3-

wind stresses occur on a line which passes through the radius of maximum winds.

the maximum wind stresses were routed along several tracks along the Atlantic Coast, to determine which tract would produce the highest surge at Sandy Hook. After selecting this critical hurricane track, the maximum hurricane stress was then routed through New York Harbor to the Battery.

The greatest surge height resulting from the probable maximum hurricane was computed to be approximately 15.6 feet in New York Bay. This calculation agrees with a published estimate of a maximum surge of

QUIRK, LAWLER & MATUSKY ENGINEERS

15.3 feet by B. Wilson.

Using an additional stage increase of 1.9 feet due to a condition of atmospheric pressure reduction, the estimated surge in New York Bay is 17.5 feet above mean sea level. A stage-time hydrograph was estimated according to the variation predicted by Wilson.

J. Proudman solved the general equations of motion and continuity for a long progressive wave in an estuary. He developed an equation to compute stage at any point in the estuary as a function of an input stage variable at the estuary's mouth.

A-3 -A-4-

Using Proudman's equation for the case of an estuary where the product of base width multiplied by celerity at various cross-sections are similar, a routing of a critical hurricane stage hydrograph was made from the Battery to Dobbs Ferry. This reach is essentially uniform. However, the reach from Dobbs Ferry through Haverstraw Bay, to Indian Point is approximately double the width of the former reach. This allows considerable attenuation of the hurricane surge as a result of the increased channel storage. In this latter reach, a more complex

QUIRK, LAWLER & MATUSKY ENGINEERS

procedure was used to route the Dobbs Ferry stage-time hydrograph upstream to Indian Point.

The surge routing procedure employed considers the effect of friction in the channel, and the large storage capacity of Haverstraw Bay. Haverstraw Bay acts as an on-line reservoir to attenuate any surge condition.

The attenuated surge stage at Indian Point is approximately 8.8 ft. above mean tidal level. The calculated subsidence is affected somewhat by variations in the channel cross-section and the assumed resistance formula. Values of depth and width were computed at channel sections where the river's geometry changed. Linear variations were assumed at intermediate sections. The channel was divided into eleven reaches between the Battery and Indian Point.

A-4

-A-5-

Prior calculations show that the additional increase in surge height due to the forward advance of the hurricane from the Battery to Indian Point was about 1.0 feet. These calculations assumed that the hurricane would essentially follow a direction parallel to the

QUIRK, LAWLER & MATUSKY ENGINEERS

Hudson, but that winds would be reduced somewhat by the sheltering topography surrounding the river.

The basic theory used was the Corps of Engineers procedure for surge routing in open seas.

In the evaluation of the maximum surge height, it should be remembered that the wind which produces the storm surge, also produces oscillatory short period waves. Calculations for the area downstream from Indian Point show that the maximum fetch length for wave development is 6.85 miles. In order to transfer energy fully from wind to water, a high speed wind must exist for a minimum duration of many hours or days. The short duration of high speed winds as the hurricane passes the critical Indian Point fetch reduces the height of waves. Increased stage is conservatively estimated at 1 foot.

It is possible for the hurricane surge to occur at high tide conditions. The spring high tide at Indian Point is estimated to increase the stage by 3.0 feet above M.T.L. (very conservative),

QUIRK, LAWLER & MATUSKY ENGINEERS

A-5 -A-6-

The routed surge and water elevations for the probable maximum hurricane moving along a critical track to Indian Point are summarized below:

	Elevation
Routed Hurricane Stage	8.8 feet
Additional surge due to wind set up from the Battery to Indian Point	1.0 feet
Spring high tide	3.0 feet 12.8 feet above M.T.L. or 13.5 feet above M.S.L.
Estimated maximum local oscillatory wave height above M.S.L.	1.0 feet

The routed hurricane surge elevation of 13.5 feet exceeds the 11.7 feet elevation computed for the flood runoff condition and is therefore considered to be the controlling elevation for flood protection. Historical records of flooding at Indian Point show that the extreme high water mark of 7.4 feet above M.S.L. occurred during the November 25, 1950 hurricane. Unfortunately, data concerning water

QUIRK, LAWLER & MATUSKY ENGINEERS

elevations at both the Battery and Indian Point are meager.

A general idea of the magnitude of surge reduction in the Hudson

Estuary can be obtained from the depth increases between mean tidal

level to mean high water. At the Battery, the depth increases by

A-6

-A-7

2.3 feet, and at Indian Point, by 1.5 feet. This is a ratio of

about 1.5. The corresponding ratio of the 17.5 foot hurricane

surge at the Battery to the attenuated 9.8 surge at Indian Point

is about 1.8. The 1.8 ratio is reasonable, since a higher surge

travels at a faster velocity, with greater friction losses than

a lower surge. The necessary calculations, figures and tables

for the hurricane surge routing are presented below.

A-7

APPENDIX A

Selected Calculations and Figures from the Preliminary Report

A-43

QUIRK, LAWLER & MATUSKY ENGINEERS

IP3
FSAR UPDATE

APPENDIX B

FLOOD STUDY

OF

UPPER HUDSON RIVER BASIN

MARCH 21, 1969

STONE & WEBSTER ENGINEERING CORPORATION

BOSTON, MASS.

B-1

IP3
FSAR UPDATE

QUIRK, LAWLER & MATUSKY ENGINEERS

**REPORT ON
FLOOD STUDY
UPPER HUDSON RIVER BASIN**

Contents	Page
INTRODUCTION	1
Purpose and Scope	1
Summary of Results	1
Description of the Basin	1
Stream Flow Data	2
Stream Flow Regulation	2
Record Floods	3
PROBABLE MAXIMUM FLOOD	5
Definition	5
Probable Maximum Precipitation	6
Unit Hydrographs	7
Storm Hydrographs	9
Reservoir flood Routing	9
Channel Routing Methods	11
River Channel Characteristics	12
Hydraulic Characteristics	12
Mannings "n"	13
Stage-Discharge-Volume	13
X and K	14
Routing Procedure	15
Stage-Discharge Relation	16
DAM BREAK WAVE	17
Upstream Reservoirs	17
Conklingville Dam	17
Mode of Failure	18
Dam-Break Hydrograph	19

QUIRK, LAWLER & MATUSKY ENGINEERS

Routing of Dam Break Wave	21
DISCUSSION OF RESULTS	23
Probable Maximum Flood	23
Dam Break Wave	24
REFERENCE LIST	
OTHER SOURCES	

B-2

LIST OF TABLES

Table No. 1 – Representative Stream Gaging Stations
Table No. 2 – Pertinent Flood Data for Key Gaging Stations
Table No. 3 – Observed Unit Hydrograph Data
Table No. 4 – Subbasin Unit Hydrograph Data
Table No. 5 – Six Hour Unit Hydrographs
Table No. 6 – Major Dams in Upper Hudson River Basin

LIST OF FIGURES

Fig. No. 1 – Plan-Upper Hudson River Basin
Fig. No. 1A – Plan-Upper Hudson River Basin (with 72 hr P.M.P. isohyets)

QUIRK, LAWLER & MATUSKY ENGINEERS

Fig. No. 2 - Profile – Hudson River Above Troy
Fig. No. 3 - Probable Maximum Flood Hydrograph
Fig. No. 4 - Stage Discharge Curve
Fig. No. 5 - Discharge Frequency Curves

B-3

INTRODUCTION

PURPOSE AND SCOPE

In order to develop hydrological data for the Upper Hudson River Basin during flood conditions, an investigation was made to determine the maximum predictable stage of the Hudson River at Stillwater less than five miles upstream of Mechanicville and immediately above the mouth of the Hoosic River.

A determination of stage was made for the following two conditions:

1. Probable Maximum Flood – Stage at peak discharge due to runoff from the probable maximum precipitation over the drainage area upstream of Stillwater.
2. Dam Failure – Stage due to an assumed failure of the Conklingville Dam at the time the Sacandaga Reservoir is at its highest stage from the probable maximum flood.

SUMMARY OF RESULTS

The results of the investigation for the two conditions is as follows:

1. The probable maximum flood would have a peak flow of 300,000 cfs and result in a river stage of El. 110.0 (USGS Datum) at the Stillwater.
2. The maximum river stage resulting from a failure of the Conklingville Dam would be El. 124.0 (USGS Datum) at the Stillwater.

DESCRIPTION OF THE BASIN

The basin covered by this study is that portion of the Upper Hudson River Basin north of Stillwater, New York and is located in the central part of the great trough that extends northward from New York harbor to the St. Lawrence River. Its drainage area, lying principally in east central New York, is about 3,760 square miles. (See Figure 1.)

The major topographical feature of the Watershed is the rugged eastern portion of the Adirondack Mountains which has peaks rising up to about 5,000 ft. The northern part of the basin is wilderness country which has dense forests and contains many lakes and small streams. The valleys of the basin are covered by extensive deposits of glacial material produced by the ice sheets which formerly covered the area.

The Hudson River has its source in the Adirondack Mountains at Lake Henderson at an elevation of 1,808 ft above sea level and flows southerly for a distance of about 315 river miles to enter New York Bay. From its source to Stillwater Dam the river drops about 1,725 ft in a distance of about 140 river miles. Abrupt drops of 80, 45 and 60 ft occur at Palmer Falls, Glens Falls and Bakers Falls, respectively.

B-4

2.

The tributaries of the Upper Hudson are numerous, the more important in order of size being the Sacandaga River uniting with the main stream at Hadley, the Schroom River at Thurman, Batten Kill and Fish Creeks at Schuylerville, and the Indian River near Gooley. The flow into the Hudson from these tributaries is controlled by dams which form reservoirs that are maintained at

QUIRK, LAWLER & MATUSKY ENGINEERS

relatively fixed levels.

The climate of the Upper Hudson River Basin is characterized by long, cold and snowy winters and short, mild summers. The average annual rainfall varies from about 40 in. in the central portion to over 50 in. in the headwaters of the Sacandaga River. The precipitation is normally fairly evenly distributed throughout the year, with only a slight rise during the summer. The average annual runoff from the basin is about 55 percent of the average rainfall, with the runoff from the easterly half being a lower percentage than the westerly portion.

STREAMFLOW DATA

Stream gaging stations have been maintained by the U.S. Geological Survey and others for various periods of time at over 30 locations within the upper Hudson River watershed above Stillwater.

The main river gaging station with the longest period of published record is located at Mechanicville, New York, four and one-half miles downstream of Stillwater. The drainage area above the gage is 4,500 square miles, of which approximately 650 square miles is in the Hoosic River watershed which enters the Hudson River one and one-half miles above the gage. Continuous stream flow data at Mechanicville have been published for the period October 1887 to September 1956. The USGS have maintained a gaging station on the Hoosic River at Eagle Bridge with a drainage area of 510 square miles from 1910 to date. Using the records of both these gages, an estimate of past stream flow at Stillwater can be made with reasonable confidence.

A summary of runoff data at 10 stations representative of the basin in general is shown in Table 1.

STREAMFLOW REGULATION

The Upper Hudson River is well regulated from the standpoint of flood control. The most important regulating feature is the Sacandaga Reservoir, operated by the Hudson River – Black River Regulating District. This reservoir, controlling the Sacandaga River drainage area of 1,044 square miles or nearly 30 percent of the total upper basin area, has a storage capacity of 866,000 acre-ft at spillway crest level. The high crest and relatively

B-5

3.

small spillway at Conklingville Dam also provide the reservoir with a large amount of flood detention capacity above the rated storage. Additional tributary regulation is provided by Indian Lake Reservoir, operated by the Indian River Company. This reservoir has a capacity of 114,000 acre-ft and controls 131 square miles of Indian River drainage.

Natural storage for reducing flood flows is also provided by widespread lake areas such as Schroon Lake, Chain Lakes and Saratoga Lake. Small dams at the outlet of Schroon Lake and on Fish Creek downstream of Saratoga Lake effectively increase the natural lake storage and reduce the flood potential of drainages of about 560 and 250 square miles on the Schroon River and Fish Creek, respectively.

On the main stem of the Upper Hudson there are a number of man-made controls, principally in the form of power dams. The river profile is shown on Figure 2. From Corinth to Fort Edward, a distance of about 23 river miles, there is a series of eight privately owned power dams. In this distance, the river drops about 420 ft. Although the storage capacity of none of these

QUIRK, LAWLER & MATUSKY ENGINEERS

dams is very large, their combined effect is to retard flood flows and reduce flood stage downstream.

Proceeding downstream, the Champlain Canal, part of the New York State Barge Canal System, makes use of the Hudson between Port Edward and Troy. The river is channeled and controlled for navigation by a series of dams and locks. The river drops about 60 ft between Fort Edward and the Upper Mechanicville Dam. This section of the river channel, generally larger in cross sectional area than upstream, provides additional flood control regulation through natural valley storage.

RECORD FLOODS

The highest flood on record on the Hudson River at Mechanicville occurred in March 1913, prior to construction of the Sacandaga Reservoir. The flow reached a peak of 120,000 cfs on March 28. The rainfall causing this flood was general over the entire north-central and northeastern United States. The storm was preceded by a thaw with temperatures rising to 70 F, followed by over 5 in. of rain in five days. The estimated maximum mean daily flow at Stillwater was 107,000 cfs during this storm.

The second greatest flood at Mechanicville was the New Year flood of 1949, which had a peak flow of 118,000 cfs on January 1, 1949. The runoff was the result of over 6 inc. of precipitation which fell as a combination of rain, snow and sleet. The estimated maximum mean daily flow at Stillwater was 61,5000 cfs. The significantly lower flood flow at the Stillwater in comparison

B-6

4

with the 1913 storm is due to large measure to the flood storage

QUIRK, LAWLER & MATUSKY ENGINEERS

provided by the Sacandaga Reservoir. The flood flows in the Hudson River above the Sacandaga River and in the Sacandaga above Conklingville for both storms were approximately equal. However, the discharge of the Sacandaga during March 1913 reached a peak of 35,500 cfs, while during the 1949 flood the two-day average discharge was less than 500 cfs.

Following is a list of the major floods and maximum mean daily flows recorded at Mechanicville and estimated at Stillwater:

<u>Date</u>	<u>Recorded Flow at Mechanicville, cfs</u>	<u>Estimated Flow at Stillwater cfs</u>
March 1913	113,500	107,000
April 1914	64,800	59,000
April 1922	72,900	67,000
March 1936	72,700	54,500
September 1938	65,600	38,000
January 1949	94,400	61,500

Maximum stages and discharge for key gaging stations within the watershed are shown on Table 2.

B-7

5.

DEFINITION

The probable maximum flood has been defined as an estimate of the hypothetical flood characteristics that are considered to be the most severe "reasonably possible" at a particular location, based on comprehensive hydrometeorological analyses of critical runoff producing precipitation and hydrologic factors favorable for

QUIRK, LAWLER & MATUSKY ENGINEERS

maximum flood runoff. ⁽¹⁾ It has been further described as the estimate of the boundary between possible floods and impossible floods. The objective, therefore, is to obtain a flood that has a chance of occurrence approaching zero or a return period of infinity.

Using the above definition as a guide the probable maximum flood for the Hudson River at Stillwater was developed as follows:

1. The basin was divided into subbasins or hydrologic units on the basis of tributary drainage area and location of hydraulic controls and unit hydrographs developed for each subbasin.
2. The probable maximum precipitation was applied to the unit hydrographs with the appropriate infiltration losses to develop the flood hydrograph for each subbasin.
3. Starting at the uppermost reach in the Hudson River, the subbasin flood hydrographs were combined in their proper time sequence and routed downstream. The process of combining inflows and routing continued in the downstream direction until the flow at Stillwater was determined.

A detailed description of the development of the hydrometeorological characteristics of the basin and synthesis of the probable maximum flood are given in the following sections.

B-8

6.

PROBABLE MAXIMUM PRECIPITATION

QUIRK, LAWLER & MATUSKY ENGINEERS

The records show that a number of large floods on the Hudson river are the results of an early spring storm combined with melting snow. However, the data contained in Hydrometeorology Report No. 33⁽²⁾ indicate that the probable maximum precipitation for the spring months would be about 50 percent of the all season probable maximum precipitation. In addition a study made by the U. S. Army Corps of Engineers for the adjacent Connecticut River Basin concluded that the maximum storm rainfall would be at least equal to the maximum combination of rain and melting snow⁽³⁾. It was therefore concluded that use of a summer or fall storm would produce a runoff of at least as great as a spring storm with snow melt.

The probable maximum precipitation used in this study was developed from the 72-hour precipitation and depth-duration-drainage area curves prepared by the Hydrometeorological Section, U.S. Weather Bureau, for the Delaware River at the U.S. Army Corps of Engineers dam site at Tocks Island.⁽⁴⁾

Tocks Island rainfall data include two subtropical storm patterns A and B, which have been given transposition limits. However, since there is a general similarity in orientation, size, shape and topography of the Delaware River Basin above Tocks Island and the Upper Hudson River Basin, both storms were transposed over the Upper Hudson River Basin within the orientation limits prescribed by the Weather Bureau so as to produce the maximum rainfall on critical areas. It was found that transposed storm pattern B produced the greater rainfall and it was used in this study. This storm pattern is of the extra-tropical type where rainfall centers are associated with convergence in the vicinity of waves on frontal boundaries. In its early stages, it was of tropical character.

The 72-hour isohyets for storm pattern B in the transposed location used in this study are shown in red on Fig. 1A. The

QUIRK, LAWLER & MATUSKY ENGINEERS

pattern produces a 72-hour total precipitation equivalent to an average of 14.3 in. over the entire drainage area above Stillwater. Using applicable rainfall data contained in Hydrometeorological Report No. 28, ⁽⁵⁾ and Hydrometeorological Report No. 40, ⁽⁶⁾ it was determined that the probable maximum 72-hour precipitation for the area under study would be 13.0 and 14.4 in., respectively.

Incremental average depths for subdurations were obtained by applying the time ratio from the Tocks Island DDA curves to the 72-hour basin probable maximum precipitation. The precipitation for each subbasin was determined by planimetering the area between isohyets within the subbasin boundaries. The incremental

B-9

average depth for the subduration for each subbasin was obtained by applying the same ratio as found for the entire basin. The six-hour incremental probable maximum values were rearranged in accordance with the following criteria recommended in Hydrometeorological Report No. 40:

- a. Group the four highest six-hour increments of the 72-hour PMP in a 24-hour period, the middle four increments in a 24-hour period, and the lowest four increments in a 24-hour period.
- b. Within each of these 24-hour periods, arrange the four increments in accordance with sequential requirements; that is, the second highest next to the highest, the third highest adjacent to these, and the fourth highest at the either end.
- c. Arrange the three 24-hour periods in accordance with the sequential requirements: that is, the second highest 24-

QUIRK, LAWLER & MATUSKY ENGINEERS

hour period next to the highest, with the third at either end. Any possible sequence of three 24-hour periods is acceptable with the exception of placing the lowest 24-hour period in the middle.

The 6-hour incremental precipitation depths for the entire area under study arranged in order according to the above criteria are as follows:

Hour	Incremental Depth-in	Accumulative Depth-in
6	0.2	0.2
12	0.4	0.6
18	0.6	1.2
24	0.2	1.4
30	1.3	2.7
36	7.8	10.5
42	2.3	12.8
48	1.1	13.9
54	0.1	14.0
60	0.1	14.1
66	0.1	14.2
72	0.1	14.3

UNIT HYDROGRAPHS

Unit hydrographs were derived for 19 subbasins in the basin by the methods described in "Unit Hydrographs – Part – Principles and Determination,"⁽⁷⁾ and "Hydrology Guide for Use in Watershed Planning".⁽⁸⁾

B-10

8.

Unit hydrographs were determined from records of nine gaging

QUIRK, LAWLER & MATUSKY ENGINEERS

stations located on the various streams and reservoirs within the basin having drainage areas varying in size from 90 to 1,044 square miles. In general, the unit hydrographs were developed from the hurricane storm of September 1938 and compared with the next largest storm for which data were available. The second storm used varied from area to area. The storm of September 1938 produced the largest floods without snow melt for which adequate records are available. It was not possible to develop a unit hydrograph for the Indian Lake Reservoir and Batten Kill from the September 1938 storm because of inadequate rainfall data, and other storms were used. A computer program described by D. W. Newton and J. W. Vinyard,⁽⁹⁾ was used in developing the unit hydrographs for the gaged areas. Data for the observed unit hydrographs are shown on Table 3.

Unit hydrographs for approximately 70 percent of the total drainage area were developed from rainfall and runoff records. The unit hydrographs for the Sacandaga Reservoir and Indian Lake inflows and the Hudson River at the USGS gage at Gooley were used without modification. The unit hydrographs developed at the gaging stations on the Schroon River, Batten Kill and Kayaderosseras Creek were transposed to their respective mouths using Snyder's coefficients and the method outlined in "Unit Hydrographs – Part I Principles and Determination."

Synthetic unit hydrographs were developed for the large ungaged subbasins using Snyder's relations and coefficients developed from the gaged area unit hydrographs and data developed by Taylor and Schwarz,⁽¹⁰⁾ for basins in the north and middle Atlantic states.

The remaining unit hydrographs were developed by the method contained in "HYdrology Guide for Use in Watershed Planning." These unit hydrographs are for the short, very steep streams immediately adjacent to the Hudson River. In general, the

QUIRK, LAWLER & MATUSKY ENGINEERS

drainage areas for the individual streams are small, and they have been combined into large subbasins extending between routing points on the Hudson River.

No unit hydrographs have been developed for a few small, mostly water surface subbasins adjacent to the Hudson River. It was assumed that runoff from the precipitation is instantaneous for these areas.

The data for the 19 subbasin unit hydrographs are shown on Table No. 4 and the 6-hour unit hydrographs are listed on Table No. 5.

B-11

9

STORM HYDROGRAPHS

In order to define the time discharge relationship for inflows to the major reservoirs and to the Hudson from its tributaries and the drainage areas along its banks, storm hydrographs were developed using the unit hydrographs previously described. The time distribution of the rainfall in each subbasin was the same as was used for the entire basin. For a subbasin, the amount of direct runoff resulting from the rainfall during each time increment was then determined using the method described in Chapter II, Section 53, "Design of Small Dams."⁽¹¹⁾ the curve numbers used in the above method were selected after analysis of precipitation and runoff data in the basin. Where these data were available for more than one storm, the curve number was used which corresponded to the largest runoff-to-precipitation ratio.

The direct runoff increments were applied to the unit hydrograph to produce the flood hydrograph for each subbasin. With base flows added where applicable, these storm hydrographs defined the

QUIRK, LAWLER & MATUSKY ENGINEERS

inflows into the Hudson River from its tributaries and bank drainage areas.

RESERVOIR FLOOD ROUTING

Inflows to Indian Lake, Sacandaga Reservoir, Stewarts Bridge Reservoir and Saratoga Lake resulting from the probable maximum storm were routed through these reservoirs using a graphical solution of the step method of flood routing. The data used for routing were: (1) inflow storm hydrographs, except for Stewarts Bridge; (2) reservoir storage curves, and (3) spillway rating curves. At Stewarts Bridge, the inflow used for routing was the discharge from Conklingville Dam with a small adjustment for inflow from the intervening drainage area.

Reservoir conditions assumed prior to the storm and predictions of reservoir operation during routing of the probable maximum flood are shown in the following tabulation:

B-12

10.

Reservoir	Water Surface Elevation Before Storm	Conditions During Routing		
		Max W.S. El.	Max Discharge Cfs	Time Hours
Indian Lake	1651.35 (spillway crest)	1660.5	10,950	72
Sacandaga	768.0 (bottom of flood storage)	784.0	44,000	90
Stewarts Bridge	705.0 (normal H.W.)	710.5	43,000	90

QUIRK, LAWLER & MATUSKY ENGINEERS

Saratoga Lake	202.4 (top of flash-boards at Winnies Reef)	215.4	14,200	84
---------------	---	-------	--------	----

*Time from beginning of P.M.P.

B-13

11.

The Sacandaga Reservoir flood control storage pool between Elev. 768 and 771 is rarely used except during the spring months when an effort is made to store the maximum volume of snow melt and spring precipitation. In over 45 years of operation the maximum reservoir state was Elev. 769.43 on April 19, 1954, and at that elevation less than half of the flood control storage pool was used. The probable maximum precipitation for this study is a late summer or fall storm and the Sacandaga Reservoir would normally be below the flood pool. However it is possible that a prior storm could result in an abnormally high level and it is judged that an initial reservoir level of Elev. 768.0 for this study is conservative and reasonable. The other reservoirs have no specified volume allocated for flood storage and the initial water surfaces were chosen as being the maximum that could exist at the time.

Discharges were calculated at Indian River Dam with the sluice gates closed, at Conklingville Dam with the Dow Valves open and no flow through the E. J. West hydroelectric Station, and at Stewarts Bridge with the five Tainter gates open and no flow through the turbines.

At Indian Lake, the maximum water surface elevation predicted is approximately at the crest of the earth dike section of the dam. it was assumed that for a flood of this magnitude and duration,

QUIRK, LAWLER & MATUSKY ENGINEERS

precautionary measures would be taken at the dam to prevent overtopping of the earth sections and overflow discharge would be confined to the masonry sections. Minimum freeboards at Conklingville and Stewarts Bridge are 10.5 ft and 3.5 ft, respectively. Winnies Reef, the control for Saratoga Lake, would be submerged at the flow predicted, but overtopping this low concrete structure presents no serious structural hazard.

Outflows derived from the preceding reservoir routings were then routed down their respective channels to the Hudson River using the stream flood routing techniques described in the following sections.

CHANNEL ROUTING METHODS

Two general methods were used in routing the probable maximum flood down the main stem of the Hudson River. The first method, used for the upper portion of the river between North Creek and Hadley and for the lower portion between Fort Edward and Stillwater, was based on what is commonly called the coefficient method of routing. The procedures used generally followed the methods outlined in Corps of Engineers Engineering and Design Manual on Flood Routing.⁽¹²⁾ The second method used was the step method of reservoir routing. This method was used for the B-14

12.

portion of the river between Hadley and Fort Edward because of the many dams within the reach which control the river flow.

RIVER CHANNEL CHARACTERISTICS

Most of the effort required to perform the flood routing was connected with the collection and evaluation of physical data necessary to define the river flow and valley storage

QUIRK, LAWLER & MATUSKY ENGINEERS

characteristics. The task of determining these characteristics at the stages anticipated was greatly complicated by the fact that there are no floods of record approaching the maximum discharges being studied.

In order to route the flood using the two methods mentioned above, several river parameters had to be defined. Reduced to simplest form, these were:

- a. Hydraulic characteristics of the river, which include area, top width and hydraulic radius at enough river cross sections to adequately define the channel.
- b. Manning's "n"
- c. State-discharge-volume relationships for the various reaches of the river
- c. X and K, which are constants used to determine routing coefficients

The methods used to determine the above parameters will be described briefly.

Hydraulic Characteristics

The hydraulic characteristics of the river were determined mainly from river cross section data. Approximately 120 river cross sections were used between Mechanicville and Thurman Station, a distance just under 75 river miles. The majority of the above water portions of these sections were taken from large scale topographic maps furnished by Niagara Mohawk Power Corporation. Large scale topographic maps were not available for a section of the river below Fort Edward and another section between Palmer and Hadley, and field cross sections were made in the fall of

QUIRK, LAWLER & MATUSKY ENGINEERS

1968. Underwater soundings, by fathometer, for most cross sections were obtained from the Albany office of the U.S. Geological Survey, which were combined with the above data to obtain a complete cross section of the river channel and banks. Additional valuable information on the section of the river below Fort Edward was obtained from the New York State Barge Canal charts of the Chamblain Canal. Use was made of all available

B-15

13.

U.S. Geological Survey maps of the area for general river channel topography and to fill in any gaps in the above-mentioned information.

In the fall of 1968, prior to making field surveys, a field reconnaissance of the river and its major tributaries was made by two engineers from Stone & Webster Engineering Corporation. Accompanied by engineers from Niagara Mohawk Power Corporation, they visited all the major hydraulic structures in the drainage basin and collected hydraulic data and pertinent drawings of the structures wherever available from state and federal agencies and private industry. In addition, a determination was made of where field survey data were required and a photographic record made of these areas and at the locations of available cross sections.

Mannings's "n"

Limited data were available for a determination of Manning's "n" from velocity measurements made by the U.S. Geological Survey. These data were used to determine an "n" value at three locations using the velocity distribution method. (reference 13, p.207). An additional value for "n" was calculated from flood stage discharge data. Based on these calculations and the visual observations recommended by Barnes⁽¹⁴⁾ made during the field

QUIRK, LAWLER & MATUSKY ENGINEERS

reconnaissance, an estimated average value of 0.025 was used in the final calculations. However, because of uncertainty in the determination of average "n" values at flood stages, trial calculations were made assuming $n=0.035$. The higher value, while tending to increase river stage for a particular discharge, also increased the valley storage which resulted in a somewhat lower maximum discharge at the site. Therefore, from these calculations it was judged that the stage variation which would result from varying "n" within reasonable limits would be less than the tolerances of the other physical data upon which the calculations were based.

Stage-Discharge-Volume

Both of the methods used for flood routing required determination of the state-discharge-volume relationships for certain reaches of the river. To facilitate this, the river from Mechanicville to Thurman Station was divided into 13 reaches, each reach starting at a control point on the river. Backwater curves were calculated using the standard step method (reference 13, p.265) for each reach, starting with assumed discharges at the downstream control. A digital computer program was used to make these calculations. Input required included the hydraulic characteristics, Manning's "n," a discharge rating curve for the downstream control and an estimate of eddy and form losses from bends and contractions in the river channel. The output

B-16

14.

consisted of a water surface profile and volume of water stored in the reach at a particular steady state discharge.

At high flows, the river stage would in many cases overflow the banks. A precise determination of the amount of flow in the

QUIRK, LAWLER & MATUSKY ENGINEERS

overbank under these conditions in the absence of records is impossible. A solution to this problem was effected by the use of two different cross sections at each river station where hydraulic characteristics were determined. One section was made for the complete river valley including overbank. The second section, which was in most cases less than the first, included only that portion of the river valley in which appreciable flow was judged to take place. The determination of this second or flow section was based largely on judgement after careful consideration of topography, vegetation and all physical features, including those which were man-made, in the river valley. All storage values were based on the overbank sections, while backwater profiles for steady state flow were determined using the flow sections.

Rating curves for most of the dams in this section of the river were furnished by the owners. Theoretical rating curves were calculated at several points and all rating curves were extended theoretically when the discharge exceeded the design capacity of the spillways. The rating curves were developed using the fixed crest of the structures, assuming no flash boards in place, all spillway gates open, and no flow through turbines or supplementary outlets.

In computing the valley storage for the reach between Stillwater and Hadley, it was assumed that all dams could pass the probable maximum flood without failure. It was further assumed that the volume below the fixed dam crest under consideration could be ignored and that only the volume above the crest was usable.

X and K

The interrelated constants S and K, used to determine the coefficients for routing by the coefficient method, were evaluated on the section of the river above Thurman Station by

QUIRK, LAWLER & MATUSKY ENGINEERS

the inverse flood routing process. Below Thurman Station, because of lack of adequate flood data, evaluation of these constants was made from the stage-discharge-volume relationship for each reach. This procedure required determination first of K, which is the travel time for an elemental discharge wave to traverse the reach. Then an X, which is a measure of the wedge storage in the reach, was assumed and the flood was routed.

Finally, to check the correctness of the assumed X, the actual wedge storage was calculated using a step backwater calculation

B-17

15.

with varying flow within the reach corresponding to the inflow and outflow hydrographs. Trials were continued until the assumed and calculated X's were substantially in agreement.

Values used for X and K were as follows:

<u>River Reach</u>	<u>X</u>	<u>K(Hr)</u>
Gooley to North Creek	0.4	3
North Creek to Thurman Station	0.3	3
Thurman Station to Hadley	0.1	6
Fort Edward to Thomson	0.3	3
Thomson to Stillwater	0.3	6

The routing coefficients used were those tabulated in reference 12 for the above values of X and K when t=3 hrs.

QUIRK, LAWLER & MATUSKY ENGINEERS

ROUTING PROCEDURE

Routing the maximum probable flood from the headwaters to Hadley was accomplished using the coefficient method and the procedure described in Reference 12. The routing started with the inflow flood hydrograph at Gooley and proceeded to Hadley in two steps. Tributary inflow and riverbank runoff were combined with main stream flow at the appropriate times. Discharge from Indian Lake was routed to the Hudson River using the coefficient method also.

From Hadley to Fort Edward the river was divided into reaches varying from about two to seven miles long, each reach terminating at one of the eight dams shown on Figure 2 for that stretch of the river. Inflow from the Sacandaga River was combined with flow in the Hudson at Hadley and routed from dam to dam using the step method of reservoir routing. Using the storage curves developed from backwater computations, routing was accomplished in three-hour time steps with addition at appropriate locations of the flood hydrographs of the inflows along the riverbanks from the subareas of subbasin 9 shown on Figure 1. Checks of wave travel times for the various reaches were made by calculating the change in storage with discharge for the various discharges considered. These travel times were found to vary from a few minutes to about one and a half hours, considerably less than the time step used.

Flow characteristics and water surface profiles for the reaches below Fort Edward were determined starting at the Upper Mechanicville Dam, because it was not known initially where river

B-18

16.

control might be for establishing stage at Stillwater. It was found that critical depth occurred at Stillwater Dam for flow

QUIRK, LAWLER & MATUSKY ENGINEERS

up to at least 300,000 cfs. It was also determined that critical depth did not occur at Crockers Reef except at flows below 50,000 cfs. Therefore, this section of the river was divided into three reaches terminating at the dams at Fort Miller, Thomson and Stillwater. Calculations of change in storage with discharge were made for these reaches and the travel times were determined as being about three hours from Fort Edward to Thomson and about six hours from Thomson to Stillwater. The discharge at Fort Edward was accordingly routed to Thomson and then to Stillwater using the coefficient method, again adding tributary and riverbank inflow at appropriate times and locations.

STAGE-DISCHARGE RELATION

the stage-discharge relation shown on Figure 4 is for the river section at the northern end of the Easton Site, approximately 4 ½ miles upstream of Stillwater Dam.

The rating curve was developed from backwater curves calculated from Stillwater or Upper Mechanicville Dams. Because Stillwater Dam is a relatively low structure, the backwater computations were initiated at Upper Mechanicville and flow conditions checked for control at Stillwater Dam. It was found that at flows greater than 500,000 cfs Stillwater Dam became submerged and control shifted downstream to Upper Mechanicville Dam. The backwater curves were computed as described in the section under flood routing and verified, where possible, with Champlain Barge Canal gage records.

B-19

17.

DAM BREAK WAVE

UPSTREAM RESERVOIRS

The major existing dams with significant storage located above Stillwater are listed in Table No. 6. In addition, there are a number of smaller dams with minor storage capacities located on the various tributaries above Stillwater. It is obvious that the largest single block of storage is contained in the Sacandaga Reservoir behind the Conklingville Dam, with a volume greatly in excess of all other reservoirs combine. Failure of the Conklingville Dam would release the largest confined volume of water in the basin and would result in the highest conceivable stage at Stillwater if it should occur coincident with flood conditions.

CONKLINGVILLE DAM

The Conklingville Dam, completed in 1930, is located on the Sacandaga River, as shown on Figures 1 and 2. It is an earth dam founded on rock and earth, with a concrete gravity spillway built on rock. The earth dam was built by the semi-hydraulic fill method. It has a crest width of 43 ft. at El. 794.5 and a base width of 650 ft. at its maximum height of 96 ft., the width-to-height ratio being 6.75 to 1. At spillway crest El. 771.0, the reservoir has a total capacity of 37.8 billion cubic feet. The reservoir volume above El. 768.0 is reserved for flood control purposes. The diversion canal and spillway are located in a rock section away from and to the left of the earth dam. The outlet works consists of three 8 ft. diam. Dow Valves and two 18 ft. by 8 ft. siphons. The spillway is an ungated free overflow section 405 ft. long.

The dam was designed for large surcharge, having a freeboard height of 23.5 above the spillway crest. The maximum level attained by the reservoir during the 38 years of operation was

QUIRK, LAWLER & MATUSKY ENGINEERS

El. 769.43, 1.57 ft below the spillway crest. When routing the probable maximum flood through the reservoir, the maximum stage reached was El. 784.0, 10.5 ft below the crest of the earth dam.

The dam was built by the State of New York and is maintained and operated by the Hudson River – Black River Regulating District. Subsequent to award of the construction contract, the rock excavation for the spillway channel was increased. This rock material was spoiled at the downstream toe of the dam, providing an unusually large rock toe section. The dam has an ample cross section, is inherently stable, and has proven its ability to withstand severe earthquakes, as mentioned below.

B-20

18.

A series of significant earthquakes have occurred in the area since completion of the dam. The highest recorded earthquake occurred on April 20, 1931, at Lake George, New York. This earthquake was recorded at Intensity VII (Modified Mercalli Scale) and was perceptible over an area of 60,000 square miles. The Sacandaga Reservoir level was at E. 752.2 at the time. Following the earthquake, a two-day inspection of the dam and reservoir was conducted and no damage was found.

there is no reason to believe that the Conklingville Dam would fail from earthquake, overtopping, or any other natural cause. However, because it does contain the largest volume of stored water in the entire basin, it was used in determining the stage at Stillwater from an assumed dam failure.

It was assumed that failure would occur with the reservoir at its maximum possible level, El. 784.0, which is caused by runoff generated by the probable maximum precipitation. At this

QUIRK, LAWLER & MATUSKY ENGINEERS

surcharged elevation, the reservoir contains approximately 54 billion cubic feet of water.

It was further assumed that Stewarts Bridge Dam would fail prior to Conklingville Dam. This assumption is based on the fact that, in routing the maximum flood through the tow reservoirs, it is found that the freeboard at the Conklingville Dam would be 10.5 ft as compared to 3.5 ft at the Stewart Bridge Dam. While this shows that neither of the dams would be overtopped during the maximum probable flood, in the event of a catastrophe, the smaller freeboard at the Stewart Bridge Dam would make it more likely to fail first.

MODE OF FAILURE

In a hypothetical study of this type, the first assumption to be made concerns the mode in which the structure fails, for this will greatly effect the resulting hydrograph. Earth fill structures such as Conklingviell Dam generally fail progressively, failure starting from an initial breach which increases in size by erosion of material under influence of the current. This mode of failure produces a hydrograph with an initially low discharge, increasing with time to a maximum, then decreasing as the reservoir elevation drops. The quantitative determination of this type hydrograph depends on the assumption of size and location of the initial breach, and rate of erosion, both of which are subject to question.

The maximum discharge rate would be obtained if failure were assumed to be instantaneous and complete and, for a discrete
B-21

19.

volume of water, produces a hydrograph of shortest duration,

QUIRK, LAWLER & MATUSKY ENGINEERS

maximizing the flow concentration. This is the most conservative mode of failure that can be assumed, and was used for this study.

DAM BREAK HYDROGRAPH

The physical laws governing unsteady flow in natural channels caused by a dam failure are among the most complex in the field of hydraulics. The first attempt to solve the problem was carried out by Saint-Venant who gave two differential equations bearing his name. These are based on a series of hypotheses which render them applicable only to gradually unsteady flow. While no integration of the equations is possible in the general case, certain simplifications and additional hypotheses have been used which have allowed integration and furnished solutions of limited applicability. Contributions based on theory and experiments have been made by many researchers including Ritter⁽¹⁵⁾, Schocklitsch⁽¹⁶⁾, Re⁽¹⁷⁾, Pohle⁽¹⁸⁾, Levin⁽¹⁹⁾, Dressler⁽²⁰⁻²¹⁾, Stoker⁽²²⁾, Snyder⁽²⁴⁾, and U.S. Army Engineers⁽²⁵⁾.

Essentially, the sudden destruction of a dam results in a positive wave, advancing in downstream direction in the river channel, and a negative wave propagating in upstream direction into the storage reservoir. The wave velocity and profile depend on many factors including height of dam, channel and reservoir cross-section, channel resistance initial stream flow conditions, and length of storage reservoir. The simplifications commonly adopted by most researchers with a view to reducing the mathematical complexity of the problem included consideration of a prismatic, rectangular channel, horizontal channel bottom, and negligible flow resistance. The analytical methods which have been developed based on these simplifications have been confirmed by model studies, and as such can now be used as an engineering tool for determining flow conditions generated a sudden dam failure.

QUIRK, LAWLER & MATUSKY ENGINEERS

The objective of the Conklingville Dam failure study, as related to determination of the maximum possible stage at Stillwater, was to calculate a dam-break hydrograph to be used in flood routing. The hydrograph was determined by two independent approaches.

The first approach is essentially based on Stoker's method⁽²²⁾ which is the outgrowth of most of the theoretical and analytical work carried out to date. According to this method, the water depth in a rectangular channel at the dam site is $4/9$ of the head in the reservoir until the negative wave reaches the end of the reservoir. To apply this method to the hypothetical failure of Conklingville Dam, the channel cross section at the Dam was approximated by three rectangles with a total area equaling that

B-22

20.

of the actual section. The downstream depth of flow was taken equal to that determined for the total flow at any time. The total releases were determined by the summation of the flows from each rectangle under a given head in the reservoir. The water surface in the reservoir was considered horizontal at any time and the drops in water level ranged between 0.5 ft and 5 ft, depending on stage. By plotting the calculated releases versus time, the Dam-break hydrograph was obtained. The results have been closely checked by the more recent work of the U.S. Army Corps of Engineers⁽²⁴⁾.

The second approach was developed as an independent check of the previously discussed method and was aimed at determining a conservative upper limit for the releases after hypothetical dam failure. It is assumed that flows are controlled only by the reservoir stage and channel characteristics and no energy is expended for negative wave motion. Critical depth is assumed to

QUIRK, LAWLER & MATUSKY ENGINEERS

prevail at the dam section throughout the period under consideration and for all the flows after dam break. Essentially, this would mean that the channel bottom at the control section forms a broad-crested weir over which the water from the reservoir must flow. This would not be inconsistent with the relative steepness and geometry of the Sacandaga River channel below the dam. This assumption is the most conservative, since for a given head, the maximum flow is always released at critical depth. In determining the releases, a minor adjustment was made for head losses due to a change in channel cross section upstream of the dam. The results were again based on the assumption that the water surface in the reservoir is horizontal at any time. By plotting the calculated releases versus time, the dam-break hydrograph was obtained.

The hydrographs obtained with the two independent approaches described above are as follows:

Time, Hr	Stoker's Method		Critical Depth Method	
	Discharge, Cfs x 10 ³	Total Outflow, Cu ft x 10 ⁹	Discharge, Cfs x 10 ³	Total Outflow, Cu ft x 10 ⁹
0	990	0	1,410	0
5	780	14.5	980	20.0
10	616	25.9	690	33.3
15	482	34.3	479	42.1
20	380	40.8	336	48.2
25	300	46.0	215	52.0

B-23

21.

As anticipated, the critical depth method, which was used as an

QUIRK, LAWLER & MATUSKY ENGINEERS

upper limit verification for Stoker's method, leads to higher flows, with the peak discharge 42 percent greater, and the volume released in the first 25 hours 11 percent greater.

ROUTING OF DAM BREAK WAVE

The downstream movement of the dam break wave is described as unsteady flow governed by the principles of conservation of energy and conservation of matter. Continuity and dynamic equations which mathematically describe the phenomenon of unsteady flow were first presented in the 19th century by Saint-Venant and are found in most texts dealing with unsteady flow. The equations have been verified by observations and experiments. However, owing to their mathematical complexity, an exact integration of the equations is almost impossible. Solutions therefore must be made by methods based on simplifying assumptions and approximate step methods.

The stream channels of the Sacandaga River and Hudson River between Conklingville Dam and Stillwater are of widely varying characteristics. The river has many sharp bends, man-made and natural constrictions and abrupt drops, all of which made the use of wave theory impracticable. The method used was the same as described in the section on routing the maximum probable flood. This method neglects the energy relationship and is based on the conservation of matter and, in effect, is a storage routing procedure. Because the energy relationship is neglected, the results obtained by using this method are very approximate for locations a short distance downstream of a breached dam. However as the reach length increases, the storage relationship becomes the more predominate factor in wave attenuation and results are of greater accuracy. Stillwater is approximately 60 miles downstream of the Conklingville Dam and it is believed that the storage routing procedure produces results within the accuracy of available physical data.

QUIRK, LAWLER & MATUSKY ENGINEERS

In routing, no advantage was taken of the storage available in the Sacandaga River. This reach is about six miles long, with a relatively narrow channel, without flood plains, containing a very small amount of valley storage, and it was conservatively assumed that the dam outflow hydrograph would be transposed to the confluence of the Sacandaga and Hudson Rivers undiminished.

The stage-storage-discharge relationships for the reaches downstream of the confluence were determined as described under the probable maximum flood routing section with the exception of the reach above Palmer Falls, which includes the mouth of the Sacandaga. It was recognized that a large flow from the Sacandaga would divide when it reached the Hudson River and flow

B-24

22.

would be in the upstream as well as the downstream direction. This storage upstream of the confluence was calculated from the stage at the confluence determined by steady state backwater calculations from Palmer Falls, assuming a horizontal water surface upstream of the confluence. An adjustment in this volume was made by subtracting the volume occupied by the flow in the Hudson River at the time the dam break wave arrives.

It was assumed that all the dams downstream of the mouth of the Sacandaga River would pass the Conklingville Dam break wave without failure. It is realized that for some of the dams this assumption is not valid. However the combined volume impounded by all the dams on the Hudson River above Stillwater is about 1 billion cubic feet. This is about 2 percent of the total volume in the Sacandaga Reservoir at the time of the hypothetical failure and considerably less than the difference in the two dam

QUIRK, LAWLER & MATUSKY ENGINEERS

break hydrographs discussed in the previous section. To include this volume in the computations would greatly increase the complexity of the solution without increasing the validity of the results.

The dam break hydrographs determined by both methods were routed to Stillwater using a time increment of 20 minutes. Tributary inflow and river bank runoff from the probable maximum precipitation were combined with the dam break wave in the proper time sequence as the wave was routed.

B-25

23.

DISCUSSION OF RESULTS

PROBABLE MAXIMUM FLOOD

The probable maximum flood at Stillwater reaches a peak discharge of 300,000 cfs and a river stage elevation of 110 ft approximately 64 hours after the start of the precipitation. The maximum 24 hour mean discharge is 260,000 cfs. Figure 3 shows the hydrograph of the flood at the site.

At the existing Bakers Falls Dam the probable maximum flood has a peak discharge of 230,000 cfs and a maximum headwater elevation of 221 ft.

It has been said that no method has been devised which can accurately indicate the frequency of large floods in the absence of stream flow records over long periods⁽²⁵⁾. If the large flood being considered is several times larger than any observed event, as is the case for the predicted probable maximum flood of this study, the above statement can hardly be questioned. In

QUIRK, LAWLER & MATUSKY ENGINEERS

fact, the probable maximum flood by definition has a frequency which is extremely large. However, in an attempt to bring some degree of perspective to the question of flood probability on the Hudson River at Stillwater, discharge-frequency curves based on a statistical evaluation of the available data were prepared, as shown on Figure 5, and extended to 10,000 years.

The data used for plotting the curves were based on USGS flow records at the Mechanicville gage from 1911 to 1956. Maximum daily discharge at Stillwater was obtained by correcting the Mechanicville flow for discharge from the Hoosic River and, prior to 1930, for discharge from the Sacandaga River which would have been impounded by the Conklingville Dam.

the two curves, plotted on extreme value paper, are based on two of the numerous methods which have been suggested for estimating discharge-frequency relationships. These curves are thought to define the extremes of these relationships for the Hudson River at Stillwater. Curve A, based on a Type I extreme value distribution as suggested by Gumbel, represents an unsymmetrical data distribution with a fixed skew. When the data are plotted, the flood of record falls considerably above the curve. Curve B is based on a graphical fit of the data distributed according to a method used by the U.S. Geological Survey⁽²⁶⁾. The points plotted are for the latter distribution, but they are located approximately in the same position for both methods. The graphical fit shown by Curve B assumes a difference in the distribution parameters for the four floods with return periods exceeding 10 years. It has been suggested that outstanding

B-26

24.

floods may in fact follow some law of their own which comes into

QUIRK, LAWLER & MATUSKY ENGINEERS

operation at very long interval.,⁽²⁵⁾.

From Figure 5, the estimated discharge for a flood with a frequency of 10,000 years is as follows:

	Discharge – Cfs	
	Mean Daily	Peak=Mean Daily x 1.15
Curve A	121,000	139,000
Curve B	232,000	267,000

The factor of 1.15 used to determine the peak discharge from the mean daily, is the ratio of these discharges found for the probable maximum flood.

Based on the above analysis, the peak discharge for a flood with a return period of 10,000 years would fall between 139,000 and 267,000 cu. ft. per second. These results indicate that the maximum flood predicted has a return period well in excess of 10,000 years and meets the requirements of obtaining a flood that has a change of occurrence approaching zero.

It should be noted that the predicted maximum flood produces stages along the river which would inundate large areas, including many existing communities. However, it is recognized by most experts that all work can not be economically protected against such remote occurrence and lesser floods are normally used for most design purposes.

Often the U.S. Army Corps of Engineers use a lesser flood designated as the Standard Project Flood for design. This flood represents critical concentration of runoff from the most severe combination of precipitation that is considered "reasonably characteristic" of the drainage basin involved. The Standard Project Flood Peak discharge and volume is usually equal to 40 percent to 60 percent of the probable maximum flood for the same

QUIRK, LAWLER & MATUSKY ENGINEERS

drainage basin⁽¹⁾. There are some other design floods criteria used, which consider the degree of risk, hazards involved and consequences of failure. The use of probable maximum flood as a design flood is not always justified or warranted for all projects and the design flood should be selected only after a complete study of all the factors involved.

DAM BREAK WAVE

The decision to assume that Conklingville Dam would fail in determining the effect of a dam break wave at Stillwater was based only on determining a hypothetical stage Stillwater. We believe that the probability of a

B-27

25.

failure of Conklingville Dam is extremely remote. The probable maximum flood study clearly indicates the reservoir has sufficient storage and the dam ample freeboard to pass this flood safely without danger of overtopping. The dam has successfully withstood a significant earthquake without damage. However, because a hypothetical failure of Conklingville Dam would cause the highest possible stage at Stillwater this possibility was included in the study.

The determination of the maximum river stage at a point almost 60 miles downstream from a hypothetical dam failure is, at best, a rough estimate, greatly dependent on a large number of assumptions for solution. A conscientious effort was made to make all assumptions as reasonably conservative as possible. Two different approaches were used in determining the initial dam break hydrograph. Stoker's method is the most reasonable based on the present state of knowledge. The critical depth approach was used only as an upper limit verification, since it is admittedly ultraconservative. By routing the dam-break

QUIRK, LAWLER & MATUSKY ENGINEERS

hydrographs obtained with the two approaches to Stillwater the following results were obtained:

	<u>Stoker's Method</u>	<u>Critical-Depth Method</u>
Max Discharge at Conklingville	990,000 cfs	1,410,000 cfs
Max Discharge at Stillwater	670,000 cfs	810,000 cfs
Max Stage at Stillwater	El. 124	El. 128

From the above tabulation it is apparent that in terms of maximum state at Stillwater the results obtained with the two independent approaches are reasonably close. In our opinion, this confirms the validity of Stoker's method which is itself based on many conservative assumptions. As pointed out before, the results obtained with this method were closely checked with a more recent work of the U.S. Army Corps of Engineers. Therefore, the maximum possible river stage at Stillwater resulting from the failure of Conklingville Dam coincident with the maximum flood is El. 124.

B-28

REFERENCE LIST

1. Definition of Terms, "Survey Conducted by the Committee on Failure and Accidents to Large Dams Other Than in Connection with the Foundations," United States Committee on Large Dams, Feb. 1968
2. Hydrometeorological Report No. 33 "Seasonal Variation of the Probable Maximum Precipitation East of the 105th Meridian for Areas from 10 to 1,000 Square Miles and Durations of 6,

QUIRK, LAWLER & MATUSKY ENGINEERS

- 12, 24 and 48 Hours” U.S. Department of Commerce, Weather Bureau, U.S. Government Printing Office, 1956
3. “Report on Project Flood for Review of Reports on Flood Controls for the Connecticut River Basin” Unpublished Report, U.S. Army Corps of Engineers, Providence District, August 1946
 4. Gilman, C. S., Chief Hydrometeorological Section, U.S. Weather Bureau, Memorandum to Mr. A. L. Cochran, Civil Works, Office of Chief of Engineers, “Preliminary Estimate of Probable Maximum Precipitation for the Delaware River at Tocks Island Dam Site,” July 3, 1956
 5. Hydrometeorological Report No. 28, “Generalized Estimate of Maximum Possible Precipitation Over New England and New York,” U.S. Department of Commerce, Weather Bureau, U.S. Government Printing Office, 1952
 6. Hydrometeorological Report No. 40, “Probable Maximum Precipitation – Susquehanna River Drainage Above Harrisburg, Pa.”, U.S. Department of Commerce, Weather Bureau, U.S. Government Printing Office, 1965
 7. “Unit Hydrographs, Part I – Principles and Determinations,” Civil Works Investigation, Project 152, U.S. Army Engineer District, Baltimore: Corps of Engineers, Baltimore, Md., 1963
 8. “Hydrology Guide for Use in Watershed Planning,” National Engineering Handbook, Sec. 4, Supplement A, U.S. Department of Agriculture, Soil Conservation Service Central Technical Unit, Beltsville, Md., 1957
 9. Newton, D. W., and Vinyard, J. W., “Computer-Determined Unit Hydrograph from Floods,” Proceeding ASCE, Journal of the Hydraulic Division, Vol. 93, Hy-5, September 1967

QUIRK, LAWLER & MATUSKY ENGINEERS

10. Taylor, A. B., and Schwartz, H. E. , "Unit-Hydrograph Lag and Peak Flow Related to Basin Characteristics," Trans. Amer. Geophysical Union, Vol. 33, No. 2, April 1952

11. "Design of Small Dams," U.S. Department of Interior, Bureau of Reclamation, U.S. Government Printing Office, Washington, D.C., 1965

B-29

2

12. "Routing of Floods Through River Channels" U.S. Army Corps of Engineers, Engineering and Design Manuals EM 1110-2-1408, U.S. Government Printing Office, Washington, D.C., March 1960

13. Chow, V. T., "Open Channel Hydraulics," McGraw-Hill Book Company, New York 1959

14. Barnes, H. H., Jr., "Roughness Characteristics of Natural Channels," Geological Survey Water Supply Paper 1849, U.S. Government Printing Office, Washington, D.C., 1967

15. Ritter, A., "Die Fortpflanzung der Wasserwellen," (Propagation of Waves) , Zeitschrift des Vereines deutscher Ingenieure, Vol. 36, No. 33, pp. 947-954, Aug. 13, 1892

16. Shocklitsch, A., "Über Dambruchwellen," (On Waves Produced by Broken Dams), Stützungsberichte, Mathematisch-naturwissenschaftliche Klasse, Akademie der Wissenschaften in Wien, Vol. 126, Part IIa, pp. 1489-1514, Vienna, 1917

17. Re., R., "Etude de Lacher Instantane d'une Retenue d'eau Dans un Canal par La methods Graphique," (Study of the Instantaneous Release of Water in a Reservoir to a Canal by the Graphic method), La Houille Blanche, 1st year, No. 3,

QUIRK, LAWLER & MATUSKY ENGINEERS

pp. 181-187, Grenoble, May 1946

18. Pohle, F. V., "Motion of Wave Due to Breaking of a Dam and Related Problems," Paper No. 8, in Symposium on Gravity Waves, U.S. National Bureau of Standards, Circular 521, pp. 47-53, 1952
19. Levin, L., "Mouvement Non Permanent Sur Le Cors d'eau a la Suite de Rupture de Barrage' (Unsteady Flow in Channels Following the Rupture of Dam), Revue Generale de l'Hydraulique, Vol. 18, No. 72 pp. 293-315, Paris, Dec. 1952
20. Dressler, R. F., "Hydraulic Resistance Effect Upon the Dam-Break Functions," Paper 2356, Journal of Research, U.S. National Bureau of Standards, Vol. 49, No. 3, pp. 217-225, Sept. 1952
21. Dressler, R. F., "Comparison of Theories and Experiments for the Hydraulic Dam-break Wave," Assemblee Generale de Rome, 1954, International Association of Scientific Hydrology, Publication No. 38, Vol. 3, pp. 319-328, 1954
22. Stoker, J. J., "Water Waves," Vol. IV of "Pure and Applied Mathematics," Interscience Publishers, Inc. New York, 1957
23. Snyder, F. F. "Hydrology of Spillway Design; Large Structures Adequate Data" Proceedings of ASCE, Journal of the Hydraulics Division, Vol. 90, HY-3, May 1964

B-30

3

24. "Floods Resulting from Suddenly Breached Dams" Miscellaneous Paper 2-374, Conditions of Minimum Resistance Report No. 1, February 1960, Condition of High Resistance Report No. 2, November 1961, U.S. Army Engineers Waterways Experiment Station, Vicksburg, Mississippi

QUIRK, LAWLER & MATUSKY ENGINEERS

25. "Review of Flood Frequency Methods," Final Report of the Subcommittee of the Joint Division Committee on Floods, Transactions, ASCE vol. 118, pp. 1220-1230, 1953
26. Riggs, H. C., Frequency Curves, Chap. A2, "Techniques of Water Resources Investigations of the United States Geological Survey," U.S. Department of the Interior, U.S. Government Printing Office, Washington, D.C. 1968

B-31

OTHER SOURCES

Chow, V. T., "Handbook of Applied Hydrology," McGraw-Hill Book Company, New York, 1964

Lensley, R. K., Jr., Kohler, M.A., and Paulkus, J.C. H. "Applied Hydrology," McGraw-Hill Book Company, New York, 1949

Davis, C.V., "Handbook of Applied Hydraulics," McGraw-Hill Book Company, New York, 1952

"Backwater Curves in River Channels," U.S. Army Corps of Engineers, Engineering and Design Manual EM 1110-2-1409, U.S. Government Printing Office, Washington, D.C., December 1952, Change 1, September 1960

Topographic Maps – Entire Basin, 7.5 Min and 15 Min Quadrangles and 1:250,000 Scale, U.S. Department of Interior Geological Survey, Topographic Division, Washington, D.C.

Topographic Maps – Hudson River, Fort Edward Dam to Palmer Falls Dam, Scale 1 In. = 200 ft, Niagara Mohawk Power Corporation

Topographic Maps – Hudson River, Palmer Falls Dam to Curtis

QUIRK, LAWLER & MATUSKY ENGINEERS

Falls Dam, Scale 1 In. – 100 Ft, International Paper Company,
1966

Topographic Maps – Hudson River, Hadley to Mouth of the Schroon
River, Scale 1 In. = 400 Ft, Niagara Mohawk Power Corporation,
1922

U. S. Lake Survey Chart No. 180, New York State Barge Canal
System, U. S. Army Corps of Engineers, Detroit, Michigan,
1964

River Soundings, Fathometer Readings, Hudson River, Troy Locks
to Corinth Bridge, U.S. Geological Survey, Albany, New York,
1967

Field Cross Sections and River Soundings, Clarkeson and Clough
Associates, Albany, New York, 1968

Precipitation Records of Stations Within and Adjacent to Basin,
National Weather Records Center, Asheville, North Carolina

Water Supply Papers, U.S. Department of Interior Geological
Survey, Water Resources Division, U. S. Government Printing
Office, Washington, D.C.

Unpublished Stage Recordings and Rating Tables, U.S. Department
of Interior, Geological Survey, Water Resources Division,
Albany, New York

B-32

2

Unpublished Gage Readings, Champlain Barge Canal, Lock 3c to
Lock 7C, New York State Barge Canal, Canal Engineer, Waterford,
New York

"Report on the Water Power and Storage Possibilities of the
Hudson River" New York Water Power Commission, State of

QUIRK, LAWLER & MATUSKY ENGINEERS

New York, 1922

U. S. Army Corps of Engineer "308 Report," Hudson River Basin,
House Document No. 149, 72nd Congress, 1st Session,
December 1931

Plans and data on the following dams were obtained from the
listed owners:

<u>Dam</u>	<u>Owner</u>
Indian Lake Dam	Indian River Company
Conklingville Dam	Board of Hudson River- Black River Regulating District
Stewarts Bridge Dam	Niagara Mohawk Power Corporation
Curtis Falls Dam	International Paper Company
Palmer Falls Dam	International Paper Company
Spiers Falls Dam	Niagara Mohawk Power Corporation
Sherman Island Dam	Niagara Mohawk Power Corporation
Feeder Dam	State of New York, Moreau Manufacturing Corporation

QUIRK, LAWLER & MATUSKY ENGINEERS

Glens Falls Dam	Finch, Pruyn & Company, Inc., Niagara Mohawk Power Corporation
-----------------	--

Bakers Falls Dam	Niagara Mohawk Power Corporation
------------------	-------------------------------------

Crockers Reef	State of New York
---------------	-------------------

B-33

3

<u>Dam</u>	<u>Owner</u>
------------	--------------

Fort Miller Dam	Fort Miller Pulp & Paper Company
-----------------	-------------------------------------

Thomson Dam	United paperboard Corporation, Thomson Paper Company
-------------	--

Stillwater Dam	Niagara Mohawk Power Corporaiton
----------------	-------------------------------------

Upper Mechanicville Dam	State of New York, West Virginia Pulp and Paper Company
----------------------------	---

Winnies Reef	Niagara Mohawk Power Corporation
--------------	-------------------------------------

B-34

APPENDIX C

NOTATIONS & SYMBOLS USED IN THE REPORT

A = Cross-sectional area

a = $0.5(1/v_2 - 1/v_1)$

$A_n A_{n+1}$ = Area bounded by isohyets number n and n+1

B = Channel width

C = Constant equal to 4 feet ^{1/2}/second determined from data supplied

D = River depth

D' = $\frac{dy}{dx}$

dg/dy = Slope of discharge rating curve at a station whose cross-section is representative of the reach for steady flow

F
E = Vertical component of earth pressure acting on downstream face, i.e. weight of earth mass vertically above the downstream face, acting through the centroid of that mass.

F
H = Horizontal component of hydrostatic pressure, acting along a line H/3 feet above the base. $\frac{1}{2}yH^2$, where y = specific weight of water

F
u = Uplift force on base of dam, as determined by foundation seepage analysis, and integration of point pressure intensities over base area; if foundation is homogeneously

permeable, pressure varies approximately linearly from full hydrostatic head at the heel to full tailwater head, and F_u is approximately $1/2yHB$, acting at $B/3$ from the heel. This value is often multiplied by some fraction less than 1 if the foundation is relatively impermeable, but it is on the safe side to assume uplift over the entire base area.

F_v = Vertical component of hydrostatic pressure. Weight of fluid mass vertically above the upstream face, acting through the centroid of that mass.

C-1

NOTATIONS & SYMBOLS USED IN THE REPORT (Continued)

H = Resultant of all forces acting on the dam, equal to R but in the opposite direction.

H = Total head (elevation of the energy line) above a horizontal datum. The mean sea level was selected in this study as the datum.

H' = Water head above the spillway crest in feet

h = Depth of impounding water

h_e = Eddy loss. For convenience of computation, this loss was considered part of the friction loss h_f .

h_f = Friction loss between two end sections i and $i+1$

h = Depth of water below the dam

QUIRK, LAWLER & MATUSKY ENGINEERS

o

I = Rate of inflow into reservoir

i = Hydraulic gradient. It is equivalent to the slope of the seepage curve dy/dx .

I_1, I_2 = Inflow at upstream end of reach 1 and 2

K = Permeability coefficient (ft/sec)

k = Time of travel of flood wave and also the change of storage per unit change of discharge

L = Distance from dam

L' = Length of Spillway or weir

n = Manning's roughness coefficient

$n, n+1$ = subscripts denoting successive intervals of time of length $t_{n+1} - t_n$

O = Rate of outflow from the reservoir

C-2

NOTATIONS & SYMBOLS USED IN THE REPORT (Continued)

O_1, O_2 = Outflow from reach 1 and 2

P_1, P_{n+1} = Average depth of rainfall over the areas bounded by Isohytes 1 and 2

QUIRK, LAWLER & MATUSKY ENGINEERS

Q = River discharge

Q' = Flow resulting from dam failure at a distance L
Downstream of the dam site

Q_o = Initial discharge after dam failure

\mathcal{L} = Seepage (cfs/ft)

R = Resultant of foundation shear and bearing pressures;
Horizontal component, $R_H = F_H + F_E$ acting along the base;
Vertical component, $R_V = W + F_V - F_U$ acting at a distance
 X from the toe that can be determined by the requirement
For rotational equilibrium of the dam, by equating to zero the
sum of the moments of all the foregoing forces about the toe of the dam.

R_h = Hydraulic radius

S = Available storage above spillway level

S_f = Friction slope taken as the average of the slopes at the two
end stations, i.e. $p_f = \frac{1}{2} (S_i + S_{i+1})$

S_o = Slope of river bed

T = Time after dam failure

V = River velocity and is equal to Q/A

V_1 = Velocity of wave front

V_2 = Velocity of wave tail

V_n, V_{n+1} = Values of isohyets number n and $n+1$. These numbers
refer to the lettered isohyets shown in Figure III-8

V_w = Rate of movement of flood wave.

W = Weight of dam – (area of cross-section of dam) (S_y)
where S = specific gravity of masonry, approximately
2.4 or 2.5, acting through centroid of cross-section

C-3

NOTATIONS & SYMBOLS USED IN THE REPORT (Continued)

W_o = Amount of water stored in reservoir

X = A dimensionless constant representing an index of
the wedge storage in a routing reach

x = Distance measured from dam site

Y = Water surface elevation above mean sea level

Y' = Depth at the crest of the wave

y = Depth of seepage curve

Z_1 = Water surface elevation above mean sea level

θ° = Angle between horizontal line and upstream face of the dam.

Δt = Length of the routing period having a maximum value of $2K_x$ and may be taken as equal to k . The routed hydrograph is relatively insensitive to the value of Δt

e = Energy coefficient. This coefficient was assumed to be unity because of the fairly straight alignment and regular cross-section of the river between the Battery and Indian Point

C-4

APPENDIX D

REFERENCES

1. U. S. Department of Commerce, Weather Bureau, Hydrometeorological Report No. 40, PROBABLE MAXIMUM PRECIPITATION, SUSQUEHANNA RIVER DRAINAGE BASIN ABOVE HARRISBURGH, PA., Washington, May 1965
2. U. S. Department of Commerce, Weather Bureau, Hydrometeorological Report No. 33, SEASONAL VARIATION OF THE PROBABLE MAXIMUM PRECIPITATION EAST OF THE 105TH MERIDIAN FOR AREAS FROM 10 TO 1,000 SQUARE MILES AND DURATION OF 6, 12, 24, AND 48 HOURS, U. S. Government Printing Office, 1956.
3. U. S. Army Corps of Engineers, Unpublished Report, REPORT ON PROJECT FLOOD FOR REVIEW OF REPORTS ON FLOOD CONTROLS FOR THE CONNECTICUT RIVER BASIN, Providence District, August, 1946.
4. Stone & Webster Engineering Corporation, FLOOD STUDY OF UPPER HUDSON RIVER BASIN, Boston, Mass., March 21, 1969.
5. U. S. Army Engineer District, Baltimore Corps of Engineers, Civil Works Investigations, Project 152, UNIT HYDROGRAPHS, PART I, PRINCIPLES AND DETERMINATIONS, Baltimore, Maryland, 1963.
6. U. S. Army Corps of Engineers, Engineering and Design Manuals EM 1110-2-1405, FLOOD HYDROGRAPH ANALYSIS AND COMPUTATIONS, U. S. Government Printing Office, Washington, D. C., August 31, 1959.
7. U. S. Army Corps of Engineers, Engineering and Design Manuals EM 1110-2-1408, ROUTING OF FLOODS THROUGH RIVER CHANNELS, U. S. Government Printing Office, Washington, D. C., March 1, 1960.
8. State of New York Hudson River Valley Commission, THE HUDSON WATER RESOURCES, New York, 1966
9. New England, New York Inter-Agency Committee, THE RESOURCES OF THE NEW ENGLAND-NEW YORK REGION, Part Two, Chapter XXXVII Subregion E (Hudson River Basin), New York, Vermont, Mass., 1955

QUIRK, LAWLER & MATUSKY ENGINEERS

10. Water Pollution Control Board, New York State Department of Health, LOWER HUDSON RIVER DRAINAGE BASIN SURVEY SERIES REPORT NO. 5, New York, 1953
D-1
11. Water Pollution Control Board, New York State Department of Health, LOWER HUDSON RIVER DRAINAGE BASIN SURVEY SERIES REPORT NO. 8, New York, 1960.
12. Summary Report of the Hudson River Valley Commission, THE HUDSON, New York, February 1, 1966.
13. Hudson River Valley Commission of New York, HUDSON RIVER ECOLOGY, New York, October, 1966.
14. Water Resources Commission, State of New York Conservation Department, Bulletin 61, THE HUDSON RIVER ESTUARY, A Preliminary Investigation of Flow and Water-Quality Characteristics, New York, 1967.
15. Quirk, Lawler & Matusky, HUDSON RIVER DISPERSION CHARACTERISTICS; Memo Report to Con Ed, October, 1965.
16. Several telephone conversations with Mr. Robert Forrest, Chief Engineer, Board of Hudson River-Black River Regulating District, March-April, 1970.
17. Several meetings and telephone conversations with Mr. Dwight E. Nunn, the Atomic Energy Commission, and Mr. P. Carpenter, FWPCA, March-April, 1970.
18. United States Geological Survey, FLOODS OF AUGUST-OCTOBER 1955, NEW ENGLAND TO NORTH CAROLINA, Water Supply Paper No. 1420.
19. Gilcrest, B. R., FLOOD ROUTING, Chapter X in Engineering Hydraulics, John Wiley & Sons Inc., New York, 1950.
20. Listvan, L.L., RASCOT MAKSIMALNOGO RASCHODA VODY OT PRORYVA NEKAPITALNYCH PLOTIN PRI PROJEKTIROVANII MOSTOVYCH PERECHODOR in Russian, or Computation of Flow after Dam Break for Design of Bridges, STPMS, Moscow, 1948.
21. Chow, Ven Te, OPEN-CHANNEL HYDRAULICS, McGraw-Hill Book Company, Inc., New York, 1959.

QUIRK, LAWLER & MATUSKY ENGINEERS

22. Data and Correspondence supplied by New York City Department of Water Resources concerning Ashokan Dam and Reservoir.
23. Morris, Henry M., APPLIED HYDRAULICS IN ENGINEERING, the Ronald Press Company, New York, 1963.
- D-2
24. A meeting with Mr. Andrew Matusky of the U. S. Army Engineers District, Baltimore, February, 1970.
25. Prasad, Ramanand, A NUMERICAL METHOD OF COMPUTING GRADUALLY VARIED FLOW PROFILES, Presented to the Specialty Conference of the Hydraulics Division ASCE, at the Massachusetts Institute of Technology, Cambridge, Massachusetts, August 21, 1968.
26. Several telephone conversations between the author, Karim A. Abood of Q. L. & M. and Mr. Kenneth I. Darmer, Supervisory Hydrologist, Water Resources, Division, U.S.G.S., Albany, N.Y., March-April, 1970.
27. Baltzer, R. A. and Shen, J., FLOWS OF HOMOGENEOUS DENSITY IN TIDAL REACHES, U.S.G.S., Washington, September, 1961, Reprinted July, 1966.
28. Lai, Chintu, FLOWS OF HOMOGENEOUS DENSITY IN THE REACHES, SOLUTION BY THE METHOD OF CHARACTERISTICS, U.S.G.S., open file report, Washington, D.C., 1965.
29. Lai, Chintu, , FLOWS OF HOMOGENEOUS DENSITY IN TIDAL THE REACHES, SOLUTION BY THE IMPLICIT METHOD, U.S.G.S., open file report, Washington, D.C., 1965.
30. Lai, Chintu, , NUMERICAL SIMULATION OF WAVE-CREST MOVEMENT IN RIVERS AND ESTUARIES, Extract of "The Use of Analog and Digital Computers in Hydrologic," Symposium of Tucson, December, 1968.
31. Lai, Chintu, COMPUTATION OF TRANSIENT FLOWS IN RIVERS AND ESTUARIES BY THE MULTIPLE-REACH IMPLICIT METHOD, U.S.G.S. Prof. paper 575-B, 1967.
32. Lai, Chintu, COMPUTATION OF TRANSIENT FLOWS IN RIVERS AND ESTUARIES BY THE MULTIPLE-REACH METHOD OF CHARACTERISTICS, U.S.G.S. Prof. paper 575-D, 1967.

QUIRK, LAWLER & MATUSKY ENGINEERS

33. J. J. Dronkers, TIDAL COMPUTATIONS IN RIVERS AND COASTAL WATERS, Interscience publishers, Division of John Wiley and Sons, N. Y., 1964.
34. U.S.C. & G.S., TIDAL AND CURRENTS IN HUDSON RIVER, Special publication No. 180 by Paul Schureman, Washington, 1934.

D-3

35. Darmer, Kenneth I., HYDROLOGIC CHARACTERISTICS OF THE HUDSON RIVER ESTUARY, presented at the 2nd HRVC Hudson River Symposium, 1969.
36. Gofseyeff, S. and Panuzio, Frank L., HURRICANE STUDIES OF NEW YORK HARBOR, Journal of the Waterways and Harbors Division, proceedings of the ASCE, February 1962.
37. Wilson, B., THE PREDICTION OF HURRICANE STORM-TIDES IN NEW YORK BAY, Technical Memorandum No. 120, Beach Erosion Board Corps of Engineers, 1960.

D-4

2.6 Meteorology

The description of site meteorology is given in Section 2.6.1 while a brief discussion of specific site meteorological and atmospheric diffusion studies are given in section 2.6.2. The technical reports pertaining to these site specific studies are also include. The safety analysis presented in section 2.6.3 and 2.6.4 is based on the site specific studies discussed in section 2.6.2. Section 2.6.5 provides a brief description of the onsite meteorological monitoring program.

The discussion of site meteorology given in section 2.6.1 is based on selected individual years in which analysis of meteorological data was performed. It should be pointed out that although the years selected are representative of the site meteorology, at least some year to year variability in the meteorological parameters will occur.

2.6.1 Site Meteorology

Winds

An important meteorological characteristic of the Indian Point Environment is that both northerly and southerly winds occur at maximum frequency. This is evident in all meteorological data collected at Indian Point from 1955 to the present.

Figures 2.6-1 a, b, and c present some constructed wind roses prepared using meteorological data collected during 1984 from the onsite 122 meter meteorological tower ^(1,2,3,4). These wind roses provide an example of typical wind direction and frequency distributions that occur at Indian Point, on a quarterly basis for the 10 meter, 60 meter, and 122 meter levels of the tower. These wind roses show clearly the bidirectional frequencies in the wind directions, with frequency maximas in the north and south direction.

A comparison of the 10 meter level wind roses between each of the four quarterly periods during 1984 (Figure 2.6-1a) shows that north winds had the highest frequency during the period January-March, while northeast winds dominated during the remaining three quarterly periods. The period July-September had the highest frequency of northeast and south winds. South winds occurred with the lowest frequency during the period January-March.

At both the 60 meter and 122 meter levels (Figures 2.6-1b, 2.6-1c), a distinct peak in frequency of north winds occurred for all four quarterly periods. The 60 meter level, like the 10 meter level also displayed a peak in frequency of northeast winds particularly during the July-September period. This peak in northeast winds was not nearly as pronounced at the 122 meter level. The frequency of south and southeast winds was lowest during the period January-March and more pronounced during the remaining three quarterly periods. These figures also indicate a smaller third peak in the frequency of northwest winds which was most pronounced during the January-March period at all three tower levels. The relatively low frequency of south winds and the third peak in the frequency of northwest winds is likely to be the result of the stronger large scale (gradient) winds during the January-March period.

These wind characteristics for 1984 are generally consistent with wind observations collected during other years, with the most significant feature being the tendency for air flow along the axis of the valley. Differences in wind distributions that do occur between years can be attributed to year to year variability in the strength and movement of synoptic scale weather systems (cyclones and anticyclones).

IP3 FSAR UPDATE

The 1984 data, as well as analysis of meteorological data from other years (see section 2.6.2), suggests that winds in the region are controlled primarily by topography. It appears that both terrain channeling and a thermally driven valley wind is contributing to the observed wind direction frequency distribution.

Terrain channeling occurs when surface air flow at some angle to the valley, is deflected by the elevated valley walls and forced to flow along the valley axis. Terrain channeling is dependent only on the orientation of the valley, and the strength and direction of large scale winds. The thermally driven valley winds are induced by differential heating between one region of the valley and an adjacent region with different topography. The differential heating induces an along valley pressure gradient which drives the up or down-valley wind. Up-valley winds are confined during the daytime when surface heating is occurring while down-valley winds are primarily nocturnal, when there is significant surface radiative cooling. Consequently, up-valley winds will occur during hours with unstable stability classes while down-valley winds are characteristic of hours when low level inversions are occurring and stability classes are stable. These up and down-valley winds are most prevalent during the summer and fall season when the large scale (gradient) winds are weakest. Under these conditions it is common to observe north or northeast winds during the night and early morning at Indian Point, with a shift to southerly winds occurring within a few hours of sunrise, when surface heating commences. Thus, diurnal variations in winds at Indian Point will have the highest frequency of occurrence during the summer and fall season.

The diurnal variation of the vector mean wind as measured 70-feet above river during September-October 1955 is shown in Figure 2.6-2 for conditions in which the large scale flow was virtually zero (12 days) and in Figure 2.6-3 for conditions in which the large scale flow (gradient wind) was less than 16 MPH (35 days). It may be seen that for these virtually stagnant prevailing wind conditions, there is a regular diurnal shift in wind direction and that the mean vector wind associated with the down-valley flow is on the order of 6 MPH.

A measure of the reliability of the diurnal shift in wind direction is shown in figure 2.6-4 where the steadiness of the wind (vector) mean speed over the mean scalar speed is shown as a function of time and the strength of the prevailing flow. Where the steadiness is close to one (an extraordinarily high value for meteorological wind systems in this latitude), the reliability of a given wind direction is very high. It may be seen that the down-valley nocturnal flow is extremely reliable from 20-08 hours while the up-valley flow is as reliable from about 14-16 hours under zero pressure gradient conditions. For weak pressure gradient conditions the nocturnal flow direction is very probable from 24 to 08 hours and thereafter becomes quite unreliable. In short, these data indicate that a consecutive 24 hours down-valley flow with light wind speeds and inversion conditions is extremely improbable.

Atmosphere Stability

Tables 2.6-1, 2.6-2 and 2.6-3 provide the wind direction percent frequency distribution as a function of stability at the 10 meter level of the 122 meter meteorological tower.(5) The Pasquill stability classes are based on vertical temperature gradients (0C/100 meters) and are the same as the NRC classification of atmospheric stability (6). Table 2.6-1 shows the joint frequency distribution for a one year period while Table 2.6-2 and 2.6-3 give distributions for the summer season (May – October) and winter season (November – April), respectively.

IP3 FSAR UPDATE

Inspection of tables 2.6-1, 2.6-2 and 2.6-3 show that stability Class E occurred with the highest frequency for all wind directions (total) both for the one year period and for the summer and winter seasons. For the one year period it occurred 37.17% of the time. Similar percent frequencies are shown for the summer and winter seasons. This stability class occurred most frequently during south southwest winds with a second peak in frequency occurring for northeast winds. The total percent frequencies show stability Class D occurs with the second highest frequency while Class G had the lowest frequency occurring only 1.69% of the time for the one year period. Again similar percent frequencies are indicated for the summer and winter seasons.

Joint Frequency Distributions

Tables 2.6-4 (sheets 1 through 28) provides recent joint frequencies of wind direction, wind speed and atmospheric stability for the quarterly periods in 1986. Sixteen wind directions, seven wind speed categories including calm winds and seven Pasquill stability classes (A-G) are used. The stability classes are determined from 61-10 meter vertical temperature difference (delta-T). Data recovery during 1986 was 99 percent (13 missing hours) during the April-June period and 100 percent for the remaining quarterly periods.

Thunderstorms

Thunderstorms, although not unique to the Indian Point Site, are important since they can produce wind and precipitation patterns in the Indian Point environment that have considerable spatial and temporal variability. An important characteristic of thunderstorms is a downdraft of relatively cold air which spreads radially outward at the earth's surface. This cold air outflow, commonly called a gust front, can at times travel significant distances from the immediate storm environment. A typical gust front will appear as a sharp change in wind speed and direction and a drop in ambient air temperature.

Figure 2.6-5 shows the mean annual distribution of days with thunderstorms for the northeast United States. (7) This map is based on data from the period 1952-1962. Figure 2.6-5 shows that in the vicinity of Indian Point an average of between 20 and 30 days per year will have thunderstorms. Most of these thunderstorm days will occur during the summer season.

2.6.2 Meteorological and Atmospheric Diffusion Studies at Indian Point

New York University under a contract with Consolidated Edison Company made extensive tests on the meteorological conditions at the Indian Pont site. The testing program started in 1955 and was completed in 1957. Site meteorology (wind direction, wind speed and vertical temperature gradient) and atmospheric diffusion characteristics as determined from this testing program are described in three technical reports prepared by the New York University staff under the immediate direction of Professor Benjamin Davidson. The original New York University reports, or applicable excerpts there from, which were reviewed by Professor Davidson and the Consolidated Edison staff, are provided on pages Q1-Q44 and R1-11. In addition, information on precipitation, the prevalent wind directions associated with precipitation, a table of wind directions during thunderstorms and associated wind roses are given on pages R12-R20.

Due to questions concerning the relevancy of certain meteorological data obtained in the 1956-1957 period a new meteorological monitoring program in the Hudson River Valley was initiated to try to verify the results of the old study. The locations of the meteorological towers erected

IP3
FSAR UPDATE

for the new program did not correspond to the locations of the towers used in the earlier program, and the data were not reliable, due to instrumentation difficulties. The two sets of data were, therefore, difficult to compare although it was evident that no substantial change occurred in the valley meteorology from 1956-1969.

The experimental program was reorganized in the fall of 1969, and a new meteorological tower site was selected as close to the original 1956 one as was possible under current conditions. Wind observations were made at this 100-foot tower at Indian Point and at a ship anchored in the Hudson River northwest of Indian Point. The results of the program for the period 26 November 1969 to 1 October 1970 are presented in Dr. Halitsky's report NYU-TR-71-3 (see pages Y-1 to Y-32).

The conclusions, as stated in the report, are:

- 1) Annual average statistics of wind speed direction and vertical temperature differences were substantially the same for 1956 and 1970.
- 2) Average wind hodographs, as the ships exhibited the same diurnal reversal pattern and the same 2.5 m/sec nighttime down-valley speed in both years. The average wind hodograph at the tower showed a similar pattern of reversal, but the nighttime down-valley speed was about 2 m/sec.
- 3) All sixteen daily wind hodographs used for calculating the average hodograph at the tower showed the diurnal reversal and exhibited considerable variability in speed and direction from day to day through a complete cycle.
- 4) Maximum persistencies of low-speed inversion winds in the critical 005-020 sector were 2 hours, 4 hours and 3 hours for 1, 1.5 and 2 m/sec speeds, respectively, during the entire ten-month data record.

Additional data acquired from 1 January 1970 to 31 December 1971 is presented in NYU-TR-73-1 (see pages Z-1 to Z-82).

In addition to these meteorological studies, several diffusion studies pertaining to atmospheric diffusion modeling applied to the Indian Point Site were conducted. The final reports pertaining to these diffusion studies are given on pages 2.6.K-1 to 2.6.K-15, 2.6.L-1 to 2.6.L-67 and 2.6.M1 to 2.6.M-11.

2.6.3 Application of the Site Meteorology to the Safety Analysis of the Loss-of Coolant Accident

The atmospheric dispersion factors required for the safety analysis of Chapter 14 have been computed for the worst possible meteorological conditions which could prevail at the Indian Point site.

A search of the records indicates that the most protracted consecutive period during which the wind direction was substantially from the same directions was five days. The winds in this case were from the northwest and speeds ranged from 15 to 30 MPH. In view of the large wind speeds and slightly unstable to adiabatic range of thermal stability associated with this period of maximum wind direction duration, this case does not represent the most conservative meteorology associated with the Loss-of-Coolant Accident.

IP3
FSAR UPDATE

The most frequent wind flow at low heights under inversion conditions is down the axis of the valley. This direction, roughly 010-030o, is also the direction of maximum wind frequency at the 100 ft. tower level. Because of the relatively high frequency of inversion conditions associated with this wind direction, the safety analysis assumed that the distribution of wind speed and thermal stability during the hypothetical accident is exactly that measured at the 100 ft. tower level for the 005-020o wind direction. The valley wind is diurnal in nature, i.e., up-valley during unstable hours and down-valley during stable hours.

The safety analysis of the Loss-of-Coolant Accident assumed that the accident occurs during down-valley inversion flow conditions and that these conditions persisted for 24 hours with average wind speeds slightly less than 2 m/sec. Figures 2.6-2 and 2.6-3 indicate that the duration of the down-valley flow is about 12 hours rather than 24 hours, and that the vector mean wind speeds are on the order of 2.5 m/sec.

In view of the discussion above, it must be concluded that the safety analysis for the first 24 hours was conservative to within a factor of about two.

The remainder of the safety analysis assumed that for the next 30 days, 35% of the winds are in the 20o sector corresponding to the nocturnal down-valley flow and that wind speed and thermal stability were as observed over the period of one year as measured at the 100 ft. tower location. If the observations were distributed uniformly throughout the year, slightly over 100 hours per month of 005-020o winds could be expected to occur. The analysis assumes 276 hours of 005-020o winds occur in the first 31 days after the accident, and that about 130 of these hours are characterized by inversion conditions. Approximately 35 weak pressure gradient days were observed in September-October 1955 or about 430 hours per month. From Figure 2.6-4, the hours during which the down-valley flow is quite reliable under weak pressure gradient conditions are from 00-08 hours. Assuming that the reliability is 1.0 during these hours (it is fact about 0.9 or less), the number of down-valley inversion winds per month during September and October is on the order of 140 hours per month. This indicates that the meteorology assumed in the safety analysis beyond the first 24 hours is about right for the worst months (September and October) and is undoubtedly conservative, with varying degrees of conservatism, for about ten months of the year.

The inversion frequency assumed for the 30-day accident case is conservative because the evaluation was made from joint assumptions concerning the postulated meteorological conditions viz.,

- 1) Inversion conditions prevail for 42.4% of the time
- 2) The wind direction is within a narrow 20o sector, for 35% of the time

This is equivalent to assuming that in the model 20o sector, the inversion frequency is 14.8 percent for the 30-day period. The observed annual maximum inversion frequency for a 20o sector is 6.2% (p.29, Table 3-3, NYU Tech. Report 372.3, Section 1.6). If we assume that the inversion frequency is spread uniformly throughout the year, almost three months worth of inversion in the model 20o sector are considered to occur in the first 31-day month after the accident. The assumptions of uniform spread of inversion frequency over the year are examined above, where an attempt was made to isolate those local meteorological conditions at Indian Point which might yield the highest 30-day dose. It is concluded that the "worst" meteorological conditions are associated with the nocturnal down-valley flow which is most frequent during September and October.

2.6.4 Conservatism of Indian Point Site Meteorology with Respect to Calculation of Off-Site Doses

The conservatism of the site meteorology was evaluated with respect to wake dilution factors, Pasquill categories for stability classification and site shaping characteristics.

Building wake dilution factors, documented in reports by Dr. Halitsky titled “An Analysis of the Con Edison and AEC-DRL Wake Diffusion Models as Applied to the Indian Point Site”, (see pages 2.6.K-1 to 2.6.K-15) and “An Analysis of the Con Edison and AEC-DRL Accident meteorology models as Applied to the Indian Point Site”, (see pages 2.6.L-1 to 2.6.L-67) demonstrate that limiting the building wake dispersion correction factor to a value of 3, as required by AEC Safety Guide No. 4, is overly conservative. Both the Con Edison wake model and the Safety Guide model, without limiting the building wake dispersion correction factor, are realistically conservative when compared to actual field and wind tunnel measurements. The reports also evaluate the overall conservatism of the Con Edison accident diffusion model. Specific investigations of the turbulence characteristics and wind persistence for the site are presented.

In addition, these two reports show that the classification of atmospheric stability using the criteria documented in Safety Guide No. 23 is not appropriate for the Indian Point site. The significance of the valley influence in generating lateral dispersion, and meandering of the wind, create horizontal standard deviations of greater magnitude than those determined by using vertical temperature gradients. The data indicate Pasquill categories measured under inversion conditions with horizontal wind fluctuations similar to a Pasquill D category while, vertically, Pasquill categories are E, F, or G.

Pickard, Lowe and Garrick of Washington D.C., in the report, “A Study of Atmospheric Diffusion Condition Probabilities using the Composite Year of Indian Point Site Weather Data” (see pages 2.6.M-1 to 2.6.M-11), illustrate the effects of the site shaping technique for estimating the 95% confidence level of the annual average dispersion coefficient at the exclusion area envelope. In addition, the report shows the effect of using the “split sigma” model to account for the lateral wind meander observed in the valley.

The composite year of measured meteorological data was compiled in a form compatible with AEC Safety Guide No 23 in sheets 8 to 14 of Table 2.6-5. In order to conform with the sensor heights specified in Safety Guide No. 23 the measured ΔT was multiplied by a ΔT correction factor. The method used to determine this factor assumes an exponential relationship between temperature and height, such that measured temperature difference between any two heights can be represented as a temperature difference between two other heights, according to the following relationship:

$$\Delta T \text{ correction factor} = 1n(h_{ue}/h_{le}) / 1n(h_{um}/h_{lm})$$

where:

h_{ue} =	height of upper extrapolated temperature (ft)
h_{le} =	height of lower extrapolated temperature (ft)
h_{um} =	height of upper measured temperature (ft)

IP3
FSAR UPDATE

$h_{lm} =$ height of lower measured temperature (ft)

Sheets 1 to 7 of Table 2.6-5 show data normalized to the sensor heights specified in Safety Guide No. 23.

The composite year reflects those periods in which data recovery was the greatest. The composite year consists of January through July of 1970, August 1971, September and October 1972 and November and December of 1970.

Incorporation of the aforementioned characteristics unique to the Indian Point valley site into diffusion calculations, insure that off-site doses following a loss-of-coolant accident are within the limitations outlined in 10 CFR 100.

2.6.5 Onsite Meteorological Measurements Program

The meteorological measurement program consists of three instrumented towers, redundant power and ventilation systems, redundant communication systems, and a mini-computer processor/recorder. The meteorological measurement program complies with the acceptance criteria stated in Section 2.3.3. and in Section 17.2 of NUREG-75/087 Revision 1 (superseded by NUREG-0800, Rev. 2, July 1981) with the former section dealing with meteorological sensors and recorders, and the latter dealing with the Quality Assurance Program. The meteorological measurements program consists of primary and backup systems. The accuracy of the meteorological sensor and recording systems meet the system specifications given in the Section C.4 of proposed Revision 1 to Regulatory Guide 1.23.

Primary System

A 122-meter, instrumented tower is located on the site and provides:

1. Wind direction and speed measurement at a minimum of two levels, one of which is representative of the 10-meter level;
2. Standard deviations of wind direction fluctuations as calculated at all measured levels;
3. Vertical temperature difference for two layers (122-10 meters and 60-10 meters);
4. Ambient temperature measurements at the 10-meter level;
5. Precipitation measurements near ground level;
6. Pasquill stability classes as calculated from temperature difference.

To assure acceptable data recovery, the meteorological measurements system and associated controlled environmental housing is connected to a power supply system which has a redundant power source. A diesel generator has been installed to provide immediate power to the meteorological tower system in the event of a power outage. The generator becomes fully powered within 15 seconds after an automatic transfer switch is tripped. Various support systems include an uninterruptible power supply, dedicated ventilation systems, halon fire protection, and dedicated communications.

IP3 FSAR UPDATE

The meteorological data is transmitted simultaneously to two data loggers located at the Primary Tower site. One data logger transmits 15-minute average meteorological data to a computer to determine joint frequency distributions, and the second data logger transmits 15-minute average meteorological data to a computer located in the Buchanan Service Center, which provides the capability for accessing the meteorological data remotely.

Meteorological data can be transmitted simultaneously to the IP3 / IP2 emergency response organization and the NRC in a format designated by NUREG-0654/FEMA-REP-1.

Fifteen minute averages of meteorological parameters covering the 12-hour period previous to a recall command is available upon interrogation of the system.

Backup Systems

In the event of a failure of the primary meteorological measurement system, a backup meteorological system is used at the Indian Point site. This system is independent of the primary system and consists of an instrumented meteorological tower (a backup tower located approximately 2700 feet north of the primary tower). The associated data acquisition system for the backup tower is located in the Emergency Operations Facility. The backup system provides measurements of the 10-meter level of wind direction and speed, and an estimate of atmospheric stability (Pasquill category using sigma theta which is a standard deviation of wind fluctuation). The backup system provides information in the real-time mode. Changeover from the primary system to the backup system occurs automatically. In the event of a failure of the backup meteorological measurement system, a standby backup system exists at the 10-meter level of the Buchanan Service Center building roof. It also provides measurements of the 10-meter level of wind direction and speed, and an estimate of atmospheric stability (Pasquill category using sigma theta which is a standard deviation of wind fluctuations). The changeover from the backup system to the standby system also occurs automatically.

As in the case of the primary system, the backup meteorological measurements system and associated controlled environmental housing system is connected to a power system which is supplied from redundant power sources.

In addition to the backup meteorological measurements system, a backup communications line to the meteorological system is operational. During an interim period, the backup communications is provided via telephone lines routed through a telephone company central office separate from the primary circuits.

Atmospheric Dispersion Factors for Routine Releases

Extensive analyses and calculations were carried out in 1991⁽⁸⁾ to reevaluate the atmospheric dispersion factors for routine releases at Indian Point. The primary objective was to ensure the applicability of the dispersion factors in the Offsite Dose Calculation Manual (ODCM) in view of potential changes in the meteorological conditions at the site.

In the analyses, consideration was given to an extended meteorological database and up-to-date analytical models. Briefly, use was made of the following:

1. 10 years' worth of hourly meteorological data collected on site for the period 1981 through 1990.

IP3
FSAR UPDATE

2. Mixed-mode releases, whereby released plumes can be totally elevated, totally at ground level, or in between,
3. Valley-flow considerations for the assessment of channeling and recirculation effects (based on a site specific study⁽⁹⁾), and
4. Analytical models which permit the computation of radiation exposures due to inhalation and due to immersion in finite clouds of radioactive material.

The locations of interest were the site boundary, the nearest residences in each sector, and milking animals at 5 miles. See Ref. 8 for complete details and results.

References

1. Kaplan, Edward J. and B. Wuebber 1984(a), Quarterly Summary of Meteorological Data from Indian Point Meteorological Systems, First Quarter, January 1 – March 31, 1984, Prepared for the New York Power Authority, May 1984, Project No. 01-4251-02-1.
2. Kaplan, Edward J. and B. Wuebber, 1984(b), Quarterly Summary of Meteorological Data from Indian Point Meteorological Systems, Second Quarter, April 1 – June 30, 1984. Prepared for the New York Power Authority, September 1984, Project No. 01-4251-02-1.
3. Kaplan, Edward J. and B. Wuebber, 1984(c), Quarterly Summary of Meteorological Data from Indian Point Meteorological Systems, Third Quarter, July 1 – September 30, 1984. Prepared for the New York Power Authority, December 1984, Project No. 01-4251-02-1.
4. Kaplan, Edward J. and B. Wuebber, 1985, Quarterly Summary of Meteorological Data from Indian Point Meteorological Systems, Fourth Quarter, October 1 – December 31, 1984, prepared for the New York Power Authority, June 1985, Project No. 01-4251-05-1.
5. Kaplan, Edward J., B. Wuebber (1981) Facility Safety Analysis Report (FSAR), consolidated Edison Company of New York, Inc., Indian Point Nuclear Generating Unit No. 2, Meteorological update, September 1981, YSC Project No. 01-4122.
6. Nuclear Regulatory Commission, 1980, Proposed Revision 1 to Regulatory Guide 1.23, Meteorological Programs in Support of Nuclear Power Plants. U.S. Nuclear Regulatory Commission, Washington D.C.
7. Bryson Reid A. and F. K. Hare, 1974, World Survey of Climatology, volume 11, Climatology, volume 11, Climate of North America, Helmut Landsbert, Editor in Chief.
8. NYPA Corporate Radiological Engineering Calculation IP3-CALC-RAD-00001, "IP3 – Revised ODCM Atmospheric Dispersion Parameters (Multi-Year Hourly Data, Mixed-Mode Releases and Valley Effects" (10/1191)
9. Kaplan, Edward J., "Wind Field Analysis at Indian Point," York Services Corporation, Stamford, CT, Technical Report No. 4873-02 (3/19/91)

IP3
FSAR UPDATE

Table 2.6-1

ANNUAL SUMMARY OF WIND DIRECTION PERCENT FREQUENCY DISTRIBUTION
AS A FUNCTION OF STABILITY - 10M LEVEL
(JANUARY 1, 1979 - DECEMBER 31, 1980)

Wind Direction	Stability Class						
	<u>A</u>	<u>B</u>	<u>C</u>	<u>D</u>	<u>E</u>	<u>F</u>	<u>G</u>
N	1.28	0.36	0.48	3.39	2.67	0.50	0.09
NNE	1.76	0.40	0.46	3.15	3.33	0.80	0.17
NE	0.63	0.35	0.58	4.22	4.66	2.12	0.40
ENE	0.06	0.07	0.17	1.59	2.61	1.84	0.43
E	0.01	0.03	0.03	0.64	1.49	0.59	0.11
ESE	0.01	0.01	0.01	0.27	0.73	0.21	0.04
SE	0.03	0.01	0.02	0.23	0.67	0.26	0.02
SSE	0.09	0.03	0.04	0.45	1.04	0.31	0.05
S	2.04	0.25	0.29	1.74	3.39	0.76	0.11
SSW	2.58	0.51	0.38	2.14	5.04	0.72	0.05
SW	1.16	0.33	0.35	1.89	3.03	0.51	0.03
WSW	0.49	0.17	0.16	0.96	1.44	0.39	0.02
W	0.56	0.22	0.17	1.40	1.64	0.43	0.06
WNW	0.47	0.15	0.26	1.64	1.49	0.21	0.03
NW	0.70	0.31	0.32	2.36	1.85	0.10	0.01
NNW	0.80	0.40	0.49	3.26	1.60	0.17	0.04
CALM	0.00	0.00	0.00	0.00	0.00	0.00	0.00
MISSING	0.12	0.05	0.03	0.21	0.51	0.15	0.02
TOTAL %	12.80	3.66	4.23	29.56	37.17	10.08	1.69
NO. OF HOURS	2244	641	742	5183	6519	1768	297

IP3
FSAR UPDATE

Table 2.6-2
[Historical Information]

SUMMARY OF WIND DIRECTION PERCENT FREQUENCY
DISTRIBUTION AS A FUNCTION OF STABILITY
SUMMER SEASON - 10M LEVEL
(MAY 1, 1979, 80 - OCTOBER 31, 1979, 80)

Wind Direction	Stability Class						
	A	B	C	D	E	F	G
N	1.68	0.26	0.37	1.25	2.06	0.57	0.07
NNE	2.65	0.42	0.43	2.90	2.41	1.01	0.18
NE	0.58	0.31	0.46	3.46	4.44	3.17	0.35
ENE	0.11	0.10	0.24	1.38	2.66	2.62	0.39
E	0.02	0.07	0.01	0.57	1.57	0.61	0.05
ESE	0.01	0.01	0.00	0.31	1.01	0.36	0.06
SE	0.05	0.02	0.01	0.17	0.84	0.40	0.02
SSE	0.15	0.06	0.05	0.50	1.07	0.40	0.08
S	3.32	0.36	0.43	2.47	3.58	0.85	0.05
SSW	4.10	0.75	0.59	2.93	5.70	0.85	0.01
SW	1.84	0.49	0.48	2.23	3.03	0.51	0.05
WSW	0.87	0.20	0.18	0.94	1.05	0.34	0.00
W	0.88	0.28	0.19	1.38	1.42	0.34	0.07
WNW	0.80	0.09	0.25	0.94	1.03	0.15	0.05
NW	1.05	0.19	0.17	0.84	0.63	0.10	0.02
NNW	0.78	0.19	0.24	0.97	0.74	0.20	0.02
CALM	0.00	0.00	0.00	0.00	0.00	0.00	0.00
MISSING	0.22	0.06	0.01	0.31	0.68	0.22	0.03
TOTAL %	19.11	3.86	4.11	23.54	33.92	12.69	1.48
NO. OF HOURS	1687	341	363	2078	2994	1120	131

IP3
FSAR UPDATE

Table 2.6-3

SUMMARY OF WIND DIRECTION PERCENT FREQUENCY DISTRIBUTION AS A
FUNCTION OF STABILITY WINTER SEASON - 10M LEVEL (NOVEMBER 1, 1979,80 - APRIL
30, 1979,80) [Historical Information]

Table 2.6-4
(Sheet 1 of 28)

JOINT FREQUENCY DISTRIBUTION
INDIAN POINT JAN-MAR 1986
10 METER WIND SPEED & DIR. WITH 61-10 METER DELTA T
PASQUILL CLASS A

WIND DIRECTION	WIND SPEED (MPH)						
	01-03	04-07	08-12	13-18	19-24	>24	TOTAL
N	7.	49.	20.	0.	0.	0.	76.
NNE	3.	7.	0.	0.	0.	0.	10.
NE	7.	2.	0.	0.	0.	0.	9.
ENE	1.	0.	0.	0.	0.	0.	1.
E	2.	0.	0.	0.	0.	0.	2.
ESE	2.	1.	0.	0.	0.	0.	3.
SE	6.	4.	0.	0.	0.	0.	10.
SSE	12.	21.	0.	0.	0.	0.	33.
S	8.	18.	6.	0.	0.	0.	32.
SSW	7.	11.	7.	0.	0.	0.	25.
SW	2.	2.	1.	0.	0.	0.	5.
WSW	0.	0.	0.	0.	0.	0.	0.
W	4.	6.	5.	1.	0	0.	16.
WNW	0.	29.	13.	0.	0.	0.	42.
NW	4.	35.	16.	0.	0.	0.	55.
NNW	12.	33.	7.	0.	0.	0.	52.
TOTAL	77.	218.	75.	1.	0.	0.	371.
CALM	0.						

Table 2.6-4
(Sheet 2 of 28)

JOINT FREQUENCY DISTRIBUTION
INDIAN POINT JAN-MAR 1986
10 METER WIND SPEED & DIR. WITH 61-10 METER DELTA T
PASQUILL CLASS B

WIND DIRECTION	WIND SPEED (MPH)					
-------------------	------------------	--	--	--	--	--

IP3
FSAR UPDATE

	01-03	04-07	08-12	13-18	19-24	>24	TOTAL
N	5.	14.	8.	0.	0.	0.	27.
NNE	2.	1.	0.	0.	0.	0.	3.
NE	3.	0.	0.	0.	0.	0.	3.
ENE	3.	0.	0.	0.	0.	0.	3.
E	3.	0.	0.	0.	0.	0.	3.
ESE	1.	0.	0.	0.	0.	0.	1.
SE	0.	0.	0.	0.	0.	0.	0.
SSE	2.	1.	0.	0.	0.	0.	3.
S	4.	5.	2.	0.	0.	0.	11.
SSW	3.	5.	0.	0.	0.	0.	8.
SW	1.	0.	0.	0.	0.	0.	1.
WSW	1.	0.	0.	0.	0.	0.	1.
W	0.	0.	1.	0.	0.	0.	1.
WNW	3.	6.	6.	0.	0.	0.	15.
NW	2.	9.	8.	0.	0.	0.	19.
NNW	5.	8.	1.	0.	0.	0.	14.
TOTAL	38.	52.	26.	0.	0.	0.	113.
CALM	0.						

Table 2.6-4
(Sheet 3 of 28)

JOINT FREQUENCY DISTRIBUTION
INDIAN POINT JAN-MAR 1986
10 METER WIND SPEED & DIR. WITH 61-10 METER DELTA T
PASQUILL CLASS C

WIND DIRECTION	01-03	04-07	08-12	13-18	19-24	>24	TOTAL
N	4.	7.	3.	0.	0.	0.	14.
NNE	7.	6.	0.	0.	0.	0.	13.
NE	3.	0.	0.	0.	0.	0.	3.
ENE	3.	0.	0.	0.	0.	0.	3.
E	1.	0.	0.	0.	0.	0.	1.
ESE	3.	0.	0.	0.	0.	0.	3.
SE	3.	2.	0.	0.	0.	0.	5.
SSE	1.	4.	0.	0.	0.	0.	5.
S	2.	2.	0.	0.	0.	0.	4.
SSW	0.	3.	0.	0.	0.	0.	3.
SW	1.	0.	0.	0.	0.	0.	1.
WSW	2.	0.	0.	0.	0.	0.	2.
W	1.	0.	1.	0.	0.	0.	2.

IP3
FSAR UPDATE

WNW	3.	8.	3.	0.	0.	0.	14.
NW	2.	10.	13.	0.	0.	0.	25.
NNW	4.	10.	3.	0.	0.	0.	17.
TOTAL	40.	52.	23.	0.	0.	0.	115.
CALM	0.						

Table 2.6-4
(Sheet 4 of 28)

JOINT FREQUENCY DISTRIBUTION
INDIAN POINT JAN-MAR 1986
10 METER WIND SPEED & DIR. WITH 61-10 METER DELTA T
PASQUILL CLASS D

WIND DIRECTION	WIND SPEED (MPH)						
	01-03	04-07	08-12	13-18	19-24	>24	TOTAL
N	128.	109.	40.	0.	0.	0.	277.
NNE	62.	23.	2.	0.	0.	0.	87.
NE	29.	1.	0.	0.	0.	0.	30.
ENE	17.	0.	0.	0.	0.	0.	17.
E	11.	0.	0.	0.	0.	0.	11.
ESE	7.	0.	0.	0.	0.	0.	7.
SE	11.	0.	0.	0.	0.	0.	11.
SSE	13.	12.	0.	0.	0.	0.	25.
S	17.	23.	2.	0.	0.	0.	42.
SSW	5.	3.	5.	0.	0.	0.	13.
SW	0.	0.	0.	0.	0.	0.	0.
WSW	9.	0.	0.	0.	0.	0.	9.
W	6.	9.	2.	0.	0.	0.	17.
WNW	11.	31.	18.	1.	0.	0.	61.
NW	22.	81.	45.	1.	0.	0.	149.
NNW	54.	64.	30.	0.	0.	0.	148.
TOTAL	402.	356.	144.	2.	0.	0.	904.
CALM	6.						

Table 2.6-4
(Sheet 5 of 28)

JOINT FREQUENCY DISTRIBUTION
INDIAN POINT JAN-MAR 1986
10 METER WIND SPEED & DIR. WITH 61-10 METER DELTA T
PASQUILL CLASS E

IP3
FSAR UPDATE

WIND DIRECTION	WIND SPEED (MPH)						
	01-03	04-07	08-12	13-18	19-24	>24	TOTAL
N	71.	13.	0.	0.	0.	0.	84.
NNE	67.	8.	0.	0.	0.	0.	75.
NE	49.	3.	0.	0.	0.	0.	52.
ENE	14.	0.	0.	0.	0.	0.	14.
E	20.	0.	0.	0.	0.	0.	20.
ESE	7.	0.	0.	0.	0.	0.	7.
SE	14.	2.	0.	0.	0.	0.	16.
SSE	12.	12.	0.	0.	0.	0.	24.
S	19.	14.	1.	0.	0.	0.	34.
SSW	7.	6.	1.	0.	0.	0.	14.
SW	5.	2.	0.	0.	0.	0.	7.
WSW	0.	0.	0.	0.	0.	0.	0.
W	9.	1.	0.	0.	0.	0.	10.
WNW	16.	4.	0.	0.	0.	0.	20.
NW	13.	6.	1.	0.	0.	0.	20.
NNW	37.	5.	0.	0.	0.	0.	42.
TOTAL	360.	76.	3.	0.	0.	0.	439.
CALM	8.						

Table 2.6-4
(Sheet 6 of 28)

JOINT FREQUENCY DISTRIBUTION
INDIAN POINT JAN-MAR 1986
10 METER WIND SPEED & DIR. WITH 61-10 METER DELTA T
PASQUILL CLASS F

WIND DIRECTION	WIND SPEED (MPH)						
	01-03	04-07	08-12	13-18	19-24	>24	TOTAL
N	28.	1.	0.	0.	0.	0.	29.
NNE	61.	3.	0.	0.	0.	0.	64.
NE	19.	2.	0.	0.	0.	0.	21.
ENE	3.	0.	0.	0.	0.	0.	3.
E	10.	0.	0.	0.	0.	0.	10.
ESE	4.	0.	0.	0.	0.	0.	4.
SE	3.	0.	0.	0.	0.	0.	3.
SSE	9.	0.	0.	0.	0.	0.	9.
S	4.	3.	6.	0.	0.	0.	7.
SSW	1.	0.	0.	0.	0.	0.	1.

IP3
FSAR UPDATE

SW	1.	0.	0.	0.	0.	0.	1.
WSW	4.	0.	0.	0.	0.	0.	4.
W	1.	0.	0.	0.	0.	0.	1.
WNW	2.	1.	0.	0.	0.	0.	3.
NW	0.	0.	0.	0.	0.	0.	0.
NNW	8.	0.	0.	0.	0.	0.	8.
TOTAL	158.	10.	0.	0.	0.	0.	168.
CALM	1.						

Table 2.6-4
(Sheet 7 of 28)

JOINT FREQUENCY DISTRIBUTION
INDIAN POINT JAN-MAR 1986
10 METER WIND SPEED & DIR. WITH 61-10 METER DELTA T
PASQUILL CLASS G

WIND DIRECTION	WIND SPEED (MPH)						
	01-03	04-07	08-12	13-18	19-24	>24	TOTAL
N	5.	0.	0.	0.	0.	0.	5.
NNE	10.	1.	0.	0.	0.	0.	11.
NE	3.	2.	0.	0.	0.	0.	5.
ENE	1.	0.	0.	0.	0.	0.	1.
E	2.	0.	0.	0.	0.	0.	2.
ESE	2.	0.	0.	0.	0.	0.	2.
SE	0.	0.	0.	0.	0.	0.	0.
SSE	1.	0.	0.	0.	0.	0.	1.
S	0.	0.	0.	0.	0.	0.	0.
SSW	1.	0.	0.	0.	0.	0.	1.
SW	2.	0.	0.	0.	0.	0.	2.
WSW	1.	0.	0.	0.	0.	0.	1.
W	3.	0.	0.	1.	0.	0.	3.
WNW	0.	0.	0.	0.	0.	0.	0.
NW	1.	0.	0.	0.	0.	0.	1.
NNW	0.	0.	0.	0.	0.	0.	0.
TOTAL	32.	3.	0.	0.	0.	0.	35.
CALM	0.						

Table 2.6-4
(Sheet 8 of 28)

JOINT FREQUENCY DISTRIBUTION

IP3
FSAR UPDATE

INDIAN POINT APR-JUNE 1986
10 METER WIND SPEED & DIR. WITH 61-10 METER DELTA T
PASQUILL CLASS A

WIND DIRECTION	WIND SPEED (MPH)						
	01-03	04-07	08-12	13-18	19-24	>24	TOTAL
N	7.	69.	31.	2.	0.	0.	109.
NNE	2.	4.	10.	0.	0.	0.	16.
NE	0.	2.	1.	0.	0.	0.	3.
ENE	0.	2.	1.	0.	0.	0.	3.
E	0.	0.	0.	0.	0.	0.	0.
ESE	1.	0.	0.	0.	0.	0.	1.
SE	2.	4.	0.	0.	0.	0.	6.
SSE	7.	30.	2.	0.	0.	0.	39.
S	7.	43.	12.	0.	0.	0.	62.
SSW	0.	10.	6.	0.	0.	0.	16.
SW	1.	15.	1.	0.	0.	0.	17.
WSW	1.	5.	0.	0.	0.	0.	6.
W	3.	13.	0.	0.	0.	0.	16.
WNW	1.	9.	2.	0.	0.	0.	12.
NW	2.	20.	16.	0.	0.	0.	38.
NNW	4.	39.	11.	0.	0.	0.	54.
TOTAL	38.	265.	93.	2.	0.	0.	398.
CALM	0.						

Table 2.6-4
(Sheet 9 of 28)

JOINT FREQUENCY DISTRIBUTION
INDIAN POINT APR-JUNE 1986
10 METER WIND SPEED & DIR. WITH 61-10 METER DELTA T
PASQUILL CLASS B

WIND DIRECTION	WIND SPEED (MPH)						
	01-03	04-07	08-12	13-18	19-24	>24	TOTAL
N	1.	24.	4.	2.	0.	0.	31.
NNE	1.	6.	5.	0.	0.	0.	12.
NE	1.	1.	2.	0.	0.	0.	4.
ENE	0.	2.	0.	0.	0.	0.	2.
E	1.	0.	0.	0.	0.	0.	1.
ESE	0.	0.	0.	0.	0.	0.	0.
SE	2.	1.	0.	0.	0.	0.	3.

IP3
FSAR UPDATE

SSE	2.	6.	0.	0.	0.	0.	8.
S	2.	11.	1.	0.	0.	0.	14.
SSW	1.	2.	1.	0.	0.	0.	4.
SW	3.	1.	0.	0.	0.	0.	4.
WSW	0.	1.	0.	0.	0.	0.	1.
W	3.	1.	0.	0.	0.	0.	4.
WNW	1.	2.	2.	0.	0.	0.	5.
NW	1.	6.	2.	0.	0.	0.	9.
NNW	1.	6.	0.	0.	0.	0.	7.

TOTAL	20.	70.	17.	2.	0.	0.	109.
-------	-----	-----	-----	----	----	----	------

CALM	0.
------	----

Table 2.6-4
(Sheet 10 of 28)

JOINT FREQUENCY DISTRIBUTION
INDIAN POINT APR-JUNE 1986
10 METER WIND SPEED & DIR. WITH 61-10 METER DELTA T
PASQUILL CLASS C

WIND DIRECTION	WIND SPEED (MPH)						
	01-03	04-07	08-12	13-18	19-24	>24	TOTAL
N	6.	10.	4.	0.	0.	0.	20.
NNE	4.	7.	4.	0.	0.	0.	15.
NE	0.	2.	0.	0.	0.	0.	2.
ENE	1.	0.	0.	0.	0.	0.	1.
E	1.	0.	0.	0.	0.	0.	1.
ESE	0.	0.	0.	0.	0.	0.	0.
SE	2.	0.	0.	0.	0.	0.	2.
SSE	6.	3.	0.	0.	0.	0.	9.
S	7.	11.	0.	0.	0.	0.	18.
SSW	1.	4.	3.	0.	0.	0.	8.
SW	2.	1.	1.	0.	0.	0.	4.
WSW	0.	1.	0.	0.	0.	0.	1.
W	3.	4.	0.	0.	0.	0.	7.
WNW	0.	3.	0.	0.	0.	0.	3.
NW	0.	1.	1.	0.	0.	0.	2.
NNW	3.	5.	1.	0.	0.	0.	9.
TOTAL	36.	52.	14.	0.	0.	0.	102.

CALM	0.
------	----

Table 2.6-4
(Sheet 11 of 28)

IP3
FSAR UPDATE

JOINT FREQUENCY DISTRIBUTION
INDIAN POINT APR-JUNE 1986
10 METER WIND SPEED & DIR. WITH 61-10 METER DELTA T
PASQUILL CLASS D

WIND DIRECTION	WIND SPEED (MPH)						
	01-03	04-07	08-12	13-18	19-24	>24	TOTAL
N	28.	67.	20.	13.	5.	0.	133.
NNE	34.	44.	22.	0.	0.	0.	100.
NE	45.	24.	2.	0.	0.	0.	71.
ENE	32.	8.	0.	0.	0.	0.	40.
E	18.	0.	0.	0.	0.	0.	18.
ESE	14.	2.	0.	0.	0.	0.	16.
SE	23.	5.	0.	0.	0.	0.	28.
SSE	20.	41.	0.	0.	0.	0.	61.
S	24.	37.	3.	0.	0.	0.	64.
SSW	16.	11.	1.	0.	0.	0.	28.
SW	6.	3.	0.	0.	0.	0.	9.
WSW	7.	6.	0.	0.	0.	0.	13.
W	3.	4.	0.	0.	0.	0.	7.
WNW	2.	18.	2.	0.	0.	0.	22.
NW	1.	15.	3.	0.	0.	0.	19.
NNW	4.	21.	10.	0.	0.	0.	35.
TOTAL	277.	306.	63.	13.	5.	0.	664.
CALM	0.						

Table 2.6-4
(Sheet 12 of 28)

JOINT FREQUENCY DISTRIBUTION
INDIAN POINT APR-JUNE 1986
10 METER WIND SPEED & DIR. WITH 61-10 METER DELTA T
PASQUILL CLASS E

WIND DIRECTION	WIND SPEED (MPH)						
	01-03	04-07	08-12	13-18	19-24	>24	TOTAL
N	37.	41.	7.	0.	0.	0.	85.
NNE	44.	32.	7.	0.	0.	0.	83.
NE	72.	15.	0.	0.	0.	0.	87.
ENE	47.	3.	1.	0.	0.	0.	51.

IP3
FSAR UPDATE

E	15.	0.	0.	0.	0.	0.	15.
ESE	12.	0.	0.	0.	0.	0.	12.
SE	26.	2.	0.	0.	0.	0.	28.
SSE	37.	28.	0.	0.	0.	0.	65.
S	35.	39.	0.	0.	0.	0.	74.
SSW	15.	19.	1.	0.	0.	0.	35.
SW	6.	3.	0.	0.	0.	0.	9.
WSW	4.	2.	0.	0.	0.	0.	6.
W	7.	7.	1.	1.	0	0.	15.
WNW	5.	7.	0.	0.	0.	0.	12.
NW	1.	10.	0.	0.	0.	0.	11.
NNW	9.	13.	3.	0.	0.	0.	25.
TOTAL	372.	221.	20.	0.	0.	0.	613.
CALM	1.						

Table 2.6-4
(Sheet 13 of 28)

JOINT FREQUENCY DISTRIBUTION
INDIAN POINT APR-JUNE 1986
10 METER WIND SPEED & DIR. WITH 61-10 METER DELTA T
PASQUILL CLASS F

WIND							
DIRECTION	WIND SPEED (MPH)						
	01-03	04-07	08-12	13-18	19-24	>24	TOTAL
N	13.	1.	0.	0.	0.	0.	14.
NNE	48.	7.	0.	0.	0.	0.	55.
NE	59.	16.	0.	0.	0.	0.	75.
ENE	25.	0.	0.	0.	0.	0.	25.
E	18.	0.	0.	0.	0.	0.	18.
ESE	5.	0.	0.	0.	0.	0.	5.
SE	5.	1.	0.	0.	0.	0.	6.
SSE	8.	0.	0.	0.	0.	0.	8.
S	12.	3.	6.	0.	0.	0.	15.
SSW	6.	0.	0.	0.	0.	0.	6.
SW	1.	0.	0.	0.	0.	0.	1.
WSW	0.	0.	0.	0.	0.	0.	0.
W	1.	0.	0.	0.	0	0.	1.
WNW	1.	0.	0.	0.	0.	0.	1.
NW	3.	0.	0.	0.	0.	0.	3.
NNW	1.	0.	0.	0.	0.	0.	1.
TOTAL	206.	28.	0.	0.	0.	0.	234.
CALM	0.						

IP3
FSAR UPDATE

Table 2.6-4
(Sheet 14 of 28)

JOINT FREQUENCY DISTRIBUTION
INDIAN POINT APR-JUNE 1986
10 METER WIND SPEED & DIR. WITH 61-10 METER DELTA T
PASQUILL CLASS G

WIND DIRECTION	WIND SPEED (MPH)						
	01-03	04-07	08-12	13-18	19-24	>24	TOTAL
N	3.	1.	0.	0.	0.	0.	4.
NNE	13.	0.	0.	0.	0.	0.	13.
NE	12.	4.	0.	0.	0.	0.	16.
ENE	1.	0.	0.	0.	0.	0.	1.
E	3.	0.	0.	0.	0.	0.	3.
ESE	1.	0.	0.	0.	0.	0.	1.
SE	0.	0.	0.	0.	0.	0.	0.
SSE	0.	0.	0.	0.	0.	0.	0.
S	2.	0.	0.	0.	0.	0.	2.
SSW	1.	0.	0.	0.	0.	0.	1.
SW	0.	0.	0.	0.	0.	0.	0.
WSW	0.	0.	0.	0.	0.	0.	0.
W	0.	0.	0.	0.	0.	0.	0.
WNW	0.	0.	0.	0.	0.	0.	0.
NW	0.	0.	0.	0.	0.	0.	0.
NNW	2.	0.	0.	0.	0.	0.	2.
TOTAL	38.	5.	0.	0.	0.	0.	43.
CALM	0.						

Table 2.6-4
(Sheet 15 of 28)

JOINT FREQUENCY DISTRIBUTION
INDIAN POINT JULY-SEPT 1986
10 METER WIND SPEED & DIR. WITH 61-10 METER DELTA T
PASQUILL CLASS A

WIND DIRECTION	WIND SPEED (MPH)						
	01-03	04-07	08-12	13-18	19-24	>24	TOTAL
N	4.	67.	6.	0.	0.	0.	77.

IP3
FSAR UPDATE

NNE	1.	9.	1.	0.	0.	0.	11.
NE	1.	4.	2.	0.	0.	0.	7.
ENE	2.	1.	0.	0.	0.	0.	3.
E	0.	0.	0.	0.	0.	0.	0.
ESE	1.	0.	0.	0.	0.	0.	1.
SE	5.	2.	0.	0.	0.	0.	7.
SSE	11.	14.	0.	0.	0.	0.	25.
S	19.	72.	3.	0.	0.	0.	94.
SSW	7.	25.	8.	0.	0.	0.	40.
SW	3.	13.	0.	0.	0.	0.	16.
WSW	1.	7.	0.	0.	0.	0.	8.
W	6.	16.	0.	0.	0.	0.	22.
WNW	2.	5.	0.	0.	0.	0.	7.
NW	2.	16.	4.	0.	0.	0.	22.
NNW	5.	26.	6.	0.	0.	0.	37.
TOTAL	70.	277.	30.	0.	0.	0.	377.
CALM	0.						

Table 2.6-4
(Sheet 16 of 28)

JOINT FREQUENCY DISTRIBUTION
INDIAN POINT JULY-SEPT 1986
10 METER WIND SPEED & DIR. WITH 61-10 METER DELTA T
PASQUILL CLASS B

WIND DIRECTION	WIND SPEED (MPH)						
	01-03	04-07	08-12	13-18	19-24	>24	TOTAL
N	4.	18.	1.	0.	0.	0.	23.
NNE	3.	9.	1.	0.	0.	0.	13.
NE	0.	1.	0.	0.	0.	0.	1.
ENE	1.	0.	0.	0.	0.	0.	1.
E	1.	0.	0.	0.	0.	0.	1.
ESE	1.	0.	0.	0.	0.	0.	1.
SE	1.	0.	0.	0.	0.	0.	1.
SSE	1.	1.	0.	0.	0.	0.	2.
S	8.	18.	1.	0.	0.	0.	27.
SSW	2.	4.	0.	0.	0.	0.	6.
SW	1.	5.	0.	0.	0.	0.	6.
WSW	1.	1.	0.	0.	0.	0.	2.
W	3.	2.	0.	0.	0.	0.	5.
WNW	1.	2.	0.	0.	0.	0.	3.
NW	2.	0.	0.	0.	0.	0.	2.
NNW	1.	0.	0.	0.	0.	0.	1.

IP3
FSAR UPDATE

TOTAL	31.	61.	3.	0.	0.	0.	95.
CALM	0.						

Table 2.6-4
(Sheet 17 of 28)

JOINT FREQUENCY DISTRIBUTION
INDIAN POINT JULY-SEPT 1986
10 METER WIND SPEED & DIR. WITH 61-10 METER DELTA T
PASQUILL CLASS C

WIND DIRECTION	WIND SPEED (MPH)						
	01-03	04-07	08-12	13-18	19-24	>24	TOTAL
N	3.	21.	0.	0.	0.	0.	24.
NNE	2.	2.	0.	0.	0.	0.	4.
NE	4.	4.	1.	0.	0.	0.	9.
ENE	1.	0.	0.	0.	0.	0.	1.
E	1.	1.	0.	0.	0.	0.	2.
ESE	2.	0.	0.	0.	0.	0.	2.
SE	2.	0.	0.	0.	0.	0.	2.
SSE	3.	3.	0.	0.	0.	0.	6.
S	9.	15.	0.	0.	0.	0.	24.
SSW	3.	4.	1.	0.	0.	0.	8.
SW	1.	1.	0.	0.	0.	0.	2.
WSW	0.	1.	0.	0.	0.	0.	1.
W	3.	4.	0.	0.	0.	0.	7.
WNW	0.	0.	0.	0.	0.	0.	0.
NW	0.	2.	0.	0.	0.	0.	2.
NNW	4.	3.	0.	0.	0.	0.	7.
TOTAL	38.	61.	2.	0.	0.	0.	101.
CALM	0.						

Table 2.6-4
(Sheet 18 of 28)

JOINT FREQUENCY DISTRIBUTION
INDIAN POINT JULY-SEPT 1986
10 METER WIND SPEED & DIR. WITH 61-10 METER DELTA T
PASQUILL CLASS D

WIND DIRECTION	WIND SPEED (MPH)						
-------------------	------------------	--	--	--	--	--	--

IP3
FSAR UPDATE

	01-03	04-07	08-12	13-18	19-24	>24	TOTAL
N	11.	77.	7.	0.	0.	0.	95.
NNE	21.	36.	2.	0.	0.	0.	59.
NE	34.	22.	0.	0.	0.	0.	56.
ENE	34.	5.	0.	0.	0.	0.	39.
E	20.	6.	0.	0.	0.	0.	26.
ESE	5.	2.	0.	0.	0.	0.	7.
SE	22.	0.	0.	0.	0.	0.	22.
SSE	13.	4.	0.	0.	0.	0.	17.
S	43.	86.	5.	0.	0.	0.	134.
SSW	15.	39.	4.	0.	0.	0.	58.
SW	11.	3.	0.	0.	0.	0.	14.
WSW	12.	2.	0.	0.	0.	0.	14.
W	6.	8.	0.	0.	0.	0.	14.
WNW	2.	3.	1.	0.	0.	0.	6.
NW	2.	8.	1.	0.	0.	0.	11.
NNW	5.	13.	1.	0.	0.	0.	19.
TOTAL	256.	314.	21.	0.	0.	0.	591.
CALM	0.						

Table 2.6-4
(Sheet 19 of 28)

JOINT FREQUENCY DISTRIBUTION
INDIAN POINT JULY-SEPT 1986
10 METER WIND SPEED & DIR. WITH 61-10 METER DELTA T
PASQUILL CLASS E

WIND DIRECTION		WIND SPEED (MPH)					
	01-03	04-07	08-12	13-18	19-24	>24	TOTAL
N	31.	41.	0.	0.	0.	0.	72.
NNE	52.	49.	0.	0.	0.	0.	101.
NE	56.	38.	0.	0.	0.	0.	94.
ENE	26.	3.	0.	0.	0.	0.	29.
E	23.	2.	0.	0.	0.	0.	25.
ESE	19.	0.	0.	0.	0.	0.	19.
SE	36.	0.	0.	0.	0.	0.	36.
SSE	31.	2.	0.	0.	0.	0.	33.
S	76.	95.	2.	0.	0.	0.	173.
SSW	55.	42.	2.	0.	0.	0.	99.
SW	18.	3.	1.	0.	0.	0.	22.
WSW	9.	3.	0.	0.	0.	0.	12.
W	11.	4.	0.	0.	0.	0.	15.
WNW	10.	4.	0.	0.	0.	0.	14.

IP3
FSAR UPDATE

NW	19.	6.	0.	0.	0.	0.	25.
NNW	14.	18.	0.	0.	0.	0.	32.
TOTAL	486.	310.	5.	0.	0.	0.	801.
CALM	14.						

Table 2.6-4
(Sheet 20 of 28)

JOINT FREQUENCY DISTRIBUTION
INDIAN POINT JULY-SEPT 1986
10 METER WIND SPEED & DIR. WITH 61-10 METER DELTA T
PASQUILL CLASS F

WIND DIRECTION	WIND SPEED (MPH)						
	01-03	04-07	08-12	13-18	19-24	>24	TOTAL
N	21.	2.	0.	0.	0.	0.	23.
NNE	32.	6.	0.	0.	0.	0.	38.
NE	43.	24.	1.	0.	0.	0.	68.
ENE	15.	0.	0.	0.	0.	0.	15.
E	17.	0.	0.	0.	0.	0.	17.
ESE	6.	0.	0.	0.	0.	0.	6.
SE	8.	0.	0.	0.	0.	0.	8.
SSE	12.	0.	0.	0.	0.	0.	12.
S	6.	1.	0.	0.	0.	0.	7.
SSW	4.	0.	0.	0.	0.	0.	4.
SW	2.	0.	0.	0.	0.	0.	2.
WSW	1.	0.	0.	0.	0.	0.	1.
W	2.	0.	0.	0.	0.	0.	2.
WNW	2.	0.	0.	0.	0.	0.	2.
NW	5.	0.	0.	0.	0.	0.	5.
NNW	2.	0.	0.	0.	0.	0.	2.
TOTAL	178.	33.	1.	0.	0.	0.	212.
CALM	4.						

Table 2.6-4
(Sheet 21 of 28)

JOINT FREQUENCY DISTRIBUTION
INDIAN POINT JULY-SEPT 1986
10 METER WIND SPEED & DIR. WITH 61-10 METER DELTA T
PASQUILL CLASS G

IP3
FSAR UPDATE

WIND DIRECTION	WIND SPEED (MPH)						
	01-03	04-07	08-12	13-18	19-24	>24	TOTAL
N	2.	0.	0.	0.	0.	0.	2.
NNE	1.	0.	0.	0.	0.	0.	1.
NE	3.	3.	0.	0.	0.	0.	6.
ENE	1.	0.	0.	0.	0.	0.	1.
E	0.	0.	0.	0.	0.	0.	0.
ESE	1.	0.	0.	0.	0.	0.	1.
SE	0.	0.	0.	0.	0.	0.	0.
SSE	0.	0.	0.	0.	0.	0.	0.
S	2.	0.	0.	0.	0.	0.	2.
SSW	0.	0.	0.	0.	0.	0.	0.
SW	0.	0.	0.	0.	0.	0.	0.
WSW	0.	0.	0.	0.	0.	0.	0.
W	0.	0.	0.	0.	0.	0.	0.
WNW	0.	0.	0.	0.	0.	0.	0.
NW	0.	0.	0.	0.	0.	0.	0.
NNW	0.	0.	0.	0.	0.	0.	0.
TOTAL	10.	3.	0.	0.	0.	0.	13.
CALM	0.						

Table 2.6-4
(Sheet 22 of 28)

JOINT FREQUENCY DISTRIBUTION
INDIAN POINT OCT-DEC 1986
10 METER WIND SPEED & DIR. WITH 61-10 METER DELTA T
PASQUILL CLASS A

WIND DIRECTION	WIND SPEED (MPH)						
	01-03	04-07	08-12	13-18	19-24	>24	TOTAL
N	1.	22.	6.	0.	0.	0.	29.
NNE	0.	0.	0.	0.	0.	0.	0.
NE	0.	0.	0.	0.	0.	0.	0.
ENE	0.	0.	0.	0.	0.	0.	0.
E	0.	0.	0.	0.	0.	0.	0.
ESE	0.	1.	0.	0.	0.	0.	1.
SE	0.	0.	0.	0.	0.	0.	0.
SSE	3.	9.	0.	0.	0.	0.	12.
S	6.	16.	4.	0.	0.	0.	26.
SSW	1.	4.	5.	0.	0.	0.	10.
SW	0.	8.	0.	0.	0.	0.	8.

IP3
FSAR UPDATE

WSW	0.	1.	0.	0.	0.	0.	1.
W	1.	6.	1.	0.	0.	0.	8.
WNW	0.	11.	1.	0.	0.	0.	12.
NW	0.	16.	6.	0.	0.	0.	22.
NNW	1.	12.	2.	0.	0.	0.	15.
TOTAL	13.	106.	25.	0.	0.	0.	144.
CALM	0.						

Table 2.6-4
(Sheet 23 of 28)

JOINT FREQUENCY DISTRIBUTION
INDIAN POINT OCT-DEC 1986
10 METER WIND SPEED & DIR. WITH 61-10 METER DELTA T
PASQUILL CLASS B

WIND DIRECTION	WIND SPEED (MPH)						
	01-03	04-07	08-12	13-18	19-24	>24	TOTAL
N	0.	16.	6.	0.	0.	0.	22.
NNE	0.	1.	1.	0.	0.	0.	2.
NE	0.	0.	0.	0.	0.	0.	0.
ENE	0.	1.	0.	0.	0.	0.	1.
E	0.	0.	0.	0.	0.	0.	0.
ESE	0.	2.	0.	0.	0.	0.	2.
SE	1.	0.	0.	0.	0.	0.	1.
SSE	1.	2.	0.	0.	0.	0.	3.
S	4.	10.	1.	0.	0.	0.	15.
SSW	2.	2.	1.	0.	0.	0.	5.
SW	0.	1.	0.	0.	0.	0.	1.
WSW	2.	0.	0.	0.	0.	0.	2.
W	0.	0.	0.	0.	0.	0.	0.
WNW	1.	3.	0.	0.	0.	0.	4.
NW	1.	4.	5.	1.	0.	0.	11.
NNW	2.	8.	5.	0.	0.	0.	15.
TOTAL	14.	50.	19.	1.	0.	0.	84.
CALM	0.						

Table 2.6-4
(Sheet 24 of 28)

JOINT FREQUENCY DISTRIBUTION
INDIAN POINT OCT-DEC 1986
10 METER WIND SPEED & DIR. WITH 61-10 METER DELTA T

IP3
FSAR UPDATE

PASQUILL CLASS C

WIND DIRECTION	WIND SPEED (MPH)						
	01-03	04-07	08-12	13-18	19-24	>24	TOTAL
N	3.	14.	6.	1.	0.	0.	24.
NNE	1.	4.	0.	0.	0.	0.	5.
NE	0.	1.	0.	0.	0.	0.	1.
ENE	1.	1.	0.	0.	0.	0.	2.
E	0.	1.	0.	0.	0.	0.	1.
ESE	0.	0.	0.	0.	0.	0.	0.
SE	0.	0.	0.	0.	0.	0.	0.
SSE	2.	1.	0.	0.	0.	0.	3.
S	5.	3.	0.	0.	0.	0.	8.
SSW	7.	3.	1.	0.	0.	0.	11.
SW	1.	0.	0.	0.	0.	0.	1.
WSW	0.	0.	0.	0.	0.	0.	0.
W	1.	1.	1.	0.	0.	0.	3.
WNW	1.	2.	3.	0.	0.	0.	6.
NW	2.	2.	3.	0.	0.	0.	7.
NNW	4.	7.	5.	0.	0.	0.	16.
TOTAL	28.	40.	19.	1.	0.	0.	88.
CALM	0.						

Table 2.6-4
(Sheet 25 of 28)

JOINT FREQUENCY DISTRIBUTION
INDIAN POINT OCT-DEC1986
10 METER WIND SPEED & DIR. WITH 61-10 METER DELTA T
PASQUILL CLASS D

WIND DIRECTION	WIND SPEED (MPH)						
	01-03	04-07	08-12	13-18	19-24	>24	TOTAL
N	45.	127.	41.	8.	0.	0.	221.
NNE	29.	91.	26.	1.	0.	0.	147.
NE	19.	32.	2.	0.	0.	0.	53.
ENE	16.	13.	0.	0.	0.	0.	29.
E	8.	2.	0.	0.	0.	0.	10.
ESE	9.	0.	0.	0.	0.	0.	9.
SE	10.	3.	0.	0.	0.	0.	13.
SSE	14.	2.	0.	0.	0.	0.	16.

IP3
FSAR UPDATE

S	33.	48.	0.	0.	0.	0.	81.
SSW	28.	13.	1.	0.	0.	0.	42.
SW	13.	1.	0.	0.	0.	0.	14.
WSW	8.	4.	1.	0.	0.	0.	13.
W	10.	15.	5.	0.	0.	0.	30.
WNW	4.	21.	7.	2.	0.	0.	34.
NW	7.	46.	28.	2.	0.	0.	83.
NNW	14.	47.	28.	4.	0.	0.	93.
TOTAL	267.	465.	139.	17.	0.	0.	888.
CALM	0.						

Table 2.6-4
(Sheet 26 of 28)

JOINT FREQUENCY DISTRIBUTION
INDIAN POINT OCT-DEC1986
10 METER WIND SPEED & DIR. WITH 61-10 METER DELTA T
PASQUILL CLASS E

WIND DIRECTION	WIND SPEED (MPH)						
	01-03	04-07	08-12	13-18	19-24	>24	TOTAL
N	41.	26.	0.	0.	0.	0.	67.
NNE	59.	37.	2.	0.	0.	0.	98.
NE	58.	28.	0.	0.	0.	0.	86.
ENE	17.	4.	1.	0.	0.	0.	22.
E	17.	1.	0.	0.	0.	0.	18.
ESE	13.	1.	0.	0.	0.	0.	14.
SE	22.	0.	0.	0.	0.	0.	22.
SSE	33.	2.	0.	0.	0.	0.	35.
S	60.	55.	2.	0.	0.	0.	117.
SSW	30.	17.	0.	0.	0.	0.	47.
SW	23.	10.	0.	0.	0.	0.	33.
WSW	22.	4.	1.	0.	0.	0.	27.
W	18.	32.	1.	0.	0.	0.	51.
WNW	16.	19.	0.	0.	0.	0.	35.
NW	14.	19.	4.	0.	0.	0.	37.
NNW	20.	10.	4.	0.	0.	0.	34.
TOTAL	463.	265.	15.	0.	0.	0.	743.
CALM	0.						

Table 2.6-4
(Sheet 27 of 28)

IP3
FSAR UPDATE

JOINT FREQUENCY DISTRIBUTION
INDIAN POINT OCT-DEC 1986
10 METER WIND SPEED & DIR. WITH 61-10 METER DELTA T
PASQUILL CLASS F

WIND DIRECTION	WIND SPEED (MPH)						
	01-03	04-07	08-12	13-18	19-24	>24	TOTAL
N	25.	2.	0.	0.	0.	0.	27.
NNE	47.	4.	0.	0.	0.	0.	51.
NE	46.	30.	0.	0.	0.	0.	76.
ENE	13.	2.	0.	0.	0.	0.	15.
E	9.	0.	0.	0.	0.	0.	9.
ESE	0.	0.	0.	0.	0.	0.	0.
SE	5.	0.	0.	0.	0.	0.	5.
SSE	6.	0.	0.	0.	0.	0.	6.
S	10.	2.	0.	0.	0.	0.	12.
SSW	6.	0.	0.	0.	0.	0.	6.
SW	3.	0.	0.	0.	0.	0.	3.
WSW	6.	0.	0.	0.	0.	0.	6.
W	3.	0.	0.	0.	0.	0.	3.
WNW	2.	0.	0.	0.	0.	0.	2.
NW	4.	0.	0.	0.	0.	0.	4.
NNW	11.	0.	0.	0.	0.	0.	11.
TOTAL	196.	40.	0.	0.	0.	0.	236.
CALM	0.						

Table 2.6-4
(Sheet 28 of 28)

JOINT FREQUENCY DISTRIBUTION
INDIAN POINT OCT-DEC 1986
10 METER WIND SPEED & DIR. WITH 61-10 METER DELTA T
PASQUILL CLASS G

WIND DIRECTION	WIND SPEED (MPH)						
	01-03	04-07	08-12	13-18	19-24	>24	TOTAL
N	6.	0.	0.	0.	0.	0.	6.
NNE	3.	1.	0.	0.	0.	0.	4.
NE	4.	5.	0.	0.	0.	0.	9.
ENE	1.	0.	0.	0.	0.	0.	1.
E	0.	0.	0.	0.	0.	0.	0.

IP3
FSAR UPDATE

ESE	0.	0.	0.	0.	0.	0.	0.
SE	0.	0.	0.	0.	0.	0.	0.
SSE	1.	0.	0.	0.	0.	0.	1.
S	0.	0.	0.	0.	0.	0.	0.
SSW	1.	0.	0.	0.	0.	0.	1.
SW	0.	0.	0.	0.	0.	0.	0.
WSW	0.	0.	0.	0.	0.	0.	0.
W	0.	0.	0.	0.	0.	0.	0.
WNW	1.	0.	0.	0.	0.	0.	1.
NW	0.	0.	0.	0.	0.	0.	0.
NNW	2.	0.	0.	0.	0.	0.	2.
TOTAL	19.	6.	0.	0.	0.	0.	25.
CALM	0.						

IP3
FSAR UPDATE

Table 2.6-5

(Sheet 1 of 14)

[Historical Information]

**JOINT FREQUENCY DISTRIBUTION OF WIND SPEED AND
DIRECTION FOR PASQUILL STABILITY CATEGORY A**

Indian Point B(3) Using a delta t correction factor
of 0.605

Jan 1 1970 to Dec 31 1972 (Jan-July), Nov-Dec. 1970, Aug 1971, Sept-Oct 1972)

WIND

DIRECTION

WIND SPEED (MPH)

		01-03	04-07	08-12	13-18	19-24	Greater than 24	MISS	TOTAL
349-11	N	.0001	.0031	.0039	.0008	.0001	.0000	.0000	.0080
12-33	NNE	.0000	.0011	.0007	.0002	.0000	.0000	.0000	.0021
34-56	NE	.0000	.0003	.0003	.0000	.0000	.0000	.0000	.0007
57-78	ENE	.0000	.0005	.0000	.0001	.0001	.0000	.0000	.0007
79-101	E	.0000	.0000	.0000	.0001	.0000	.0000	.0000	.0001
102-123	ESE	.0000	.0000	.0000	.0000	.0000	.0000	.0000	.0000
124-146	SE	.0000	.0002	.0002	.0010	.0002	.0000	.0000	.0017
147-168	SSE	.0001	.0011	.0056	.0037	.0002	.0000	.0000	.0107
169-191	S	.0000	.0026	.0026	.0010	.0000	.0000	.0000	.0063
192-213	SSW	.0001	.0019	.0015	.0001	.0000	.0000	.0000	.0037
214-236	SW	.0000	.0015	.0009	.0001	.0000	.0000	.0000	.0025
237-258	WSW	.0002	.0008	.0008	.0000	.0000	.0000	.0000	.0018
259-281	W	.0002	.0014	.0016	.0001	.0001	.0000	.0001	.0035
282-303	WNW	.0001	.0002	.0015	.0023	.0009	.0000	.0008	.0058
304-326	NW	.0000	.0009	.0022	.0026	.0019	.0001	.0003	.0081
327-348	NNW	.0000	.0018	.0027	.0021	.0006	.0000	.0000	.0072
CALM		.0000							.0000
MISS		.0000	.0000	.0000	.0000	.0000	.0000		.0016

TOTAL .0009 .0176 .0246 .0143 .0042 .0001 .0029 .0646

Percentage of hours of temperature difference present in this stability category = 6.5 Numbers of
hours in this stability category = 565

Table 2.6-5 (Sheet 2 of 14)

**JOINT FREQUENCY DISTRIBUTION OF WIND SPEED AND
DIRECTION FOR PASQUILL STABILITY CATEGORY B**

Indian Point B(3) Using a delta t correction factor
of 0.605

JAN. 1 1970 1 DEC. 31 1972

WIND

DIRECTION

WIND SPEED (MPH)

IP3
FSAR UPDATE

		01-03	04-07	08-12	13-18	19-24	Greater than 24	MISS	TOTAL
349-11	N	.0002	.0010	.0014	.0005	.0001	.0000	.0000	.0032
12-33	NNE	.0001	.0006	.0006	.0003	.0000	.0000	.0000	.0016
34-56	NE	.0000	.0005	.0001	.0000	.0000	.0000	.0000	.0006
57-78	ENE	.0000	.0000	.0000	.0000	.0000	.0000	.0000	.0000
79-101	E	.0000	.0003	.0001	.0001	.0000	.0000	.0000	.0006
102-123	ESE	.0000	.0000	.0001	.0000	.0000	.0000	.0000	.0001
124-146	SE	.0000	.0002	.0002	.0001	.0000	.0000	.0000	.0006
147-168	SSE	.0000	.0008	.0017	.0014	.0000	.0000	.0000	.0039
169-191	S	.0002	.0017	.0014	.0002	.0000	.0000	.0000	.0035
192-213	SSW	.0001	.0010	.0006	.0000	.0000	.0000	.0000	.0017
214-236	SW	.0002	.0003	.0005	.0001	.0000	.0000	.0000	.0011
237-258	WSW	.0002	.0000	.0003	.0000	.0000	.0000	.0001	.0007
259-281	W	.0001	.0003	.0005	.0005	.0000	.0000	.0001	.0015
282-303	WNW	.0001	.0003	.0003	.0002	.0000	.0000	.0002	.0015
304-326	NW	.0001	.0002	.0003	.0008	.0002	.0001	.0001	.0018
327-348	NNW	.0000	.0006	.0014	.0005	.0003	.0001	.0000	.0029
CALM		.0000							.0000
MISS		.0000	.0000	.0000	.0000	.0000	.0000		.0002

TOTAL .0015 .0080 .0095 .0047 .0009 .0002 .0007 .0255

Percentage of hours of temperature difference present in this stability category = 2.5 Numbers of hours in this stability category

Table 2.6-5 (Sheet 3 of 14)

**JOINT FREQUENCY DISTRIBUTION OF WIND SPEED AND
DIRECTION FOR PASQUILL STABILITY CATEGORY C**

Indian Point B(3) Using a delta t correction factor
of 0.605

JAN. 1 1970 1 DEC. 31 1972

WIND

DIRECTION WIND SPEED (MPH)

		01-03	04-07	08-12	13-18	19-24	Greater than 24	MISS	TOTAL
349-11	N	.0005	.0008	.0010	.0005	.0000	.0000	.0001	.0025
12-33	NNE	.0001	.0003	.0008	.0002	.0000	.0000	.0000	.0015
34-56	NE	.0002	.0003	.0001	.0000	.0000	.0000	.0000	.0007
57-78	ENE	.0001	.0000	.0000	.0000	.0001	.0000	.0000	.0002
79-101	E	.0000	.0000	.0001	.0000	.0000	.0000	.0000	.0001
102-123	ESE	.0000	.0002	.0000	.0001	.0000	.0000	.0000	.0003
124-146	SE	.0000	.0000	.0002	.0001	.0000	.0000	.0000	.0003
147-168	SSE	.0000	.0014	.0013	.0007	.0001	.0000	.0000	.0034
169-191	S	.0000	.0013	.0010	.0001	.0000	.0000	.0000	.0024
192-213	SSW	.0000	.0008	.0003	.0000	.0000	.0000	.0000	.0011
214-236	SW	.0001	.0002	.0001	.0000	.0000	.0000	.0000	.0005

IP3
FSAR UPDATE

237-258	WSW	.0001	.0002	.0003	.0000	.0000	.0000	.0000	.0007
259-281	W	.0002	.0000	.0010	.0002	.0001	.0000	.0000	.0016
282-303	WNW	.0001	.0000	.0005	.0005	.0002	.0002	.0000	.0015
304-326	NW	.0003	.0002	.0005	.0007	.0006	.0003	.0000	.0026
327-348	NNW	.0001	.0006	.0007	.0007	.0002	.0000	.0000	.0023
CALM		.0000							.0000
MISS		.0000	.0000	.0000	.0000	.0000	.0000		.0001
TOTAL		.0019	.0064	.0080	.0038	.0014	.0006	.0002	.0223

Percentage of hours of temperature difference present in this stability category = 2.2 Numbers of hours in this stability

IP3
FSAR UPDATE

Table 2.6-5 (Sheet 4 of 14)

JOINT FREQUENCY DISTRIBUTION OF WIND SPEED AND
DIRECTION FOR PASQUILL STABILITY CATEGORY D

Indian Point B(3) Using a delta t correction factor
of 0.605

JAN. 1 1970 1 DEC. 31 1972

WIND

DIRECTION

WIND SPEED (MPH)

		01-03	04-07	08-12	13-18	19-24	Greater than 24	MISS	TOTAL
349-11	N	.0022	.0152	.0159	.0068	.0005	.0001	.0009	.0414
12-33	NNE	.0033	.0163	.0110	.0029	.0007	.0001	.0007	.0350
34-56	NE	.0027	.0072	.0019	.0006	.0002	.0000	.0006	.0133
57-78	ENE	.0023	.0018	.0005	.0002	.0000	.0000	.0005	.0053
79-101	E	.0026	.0013	.0009	.0001	.0000	.0000	.0001	.0056
102-123	ESE	.0022	.0021	.0014	.0005	.0000	.0000	.0002	.0063
124-146	SE	.0027	.0056	.0061	.0009	.0000	.0000	.0001	.0154
147-168	SSE	.0025	.0130	.0138	.0054	.0001	.0000	.0002	.0351
169-191	S	.0037	.0136	.0072	.0021	.0000	.0000	.0003	.0269
192-213	SSW	.0024	.0055	.0039	.0013	.0000	.0000	.0001	.0131
214-236	SW	.0026	.0025	.0009	.0010	.0001	.0000	.0003	.0075
237-258	WSW	.0018	.0019	.0009	.0015	.0000	.0000	.0001	.0063
259-281	W	.0011	.0021	.0037	.0030	.0009	.0002	.0007	.0117
282-303	WNW	.0018	.0014	.0053	.0119	.0071	.0019	.0003	.0297
304-326	NW	.0015	.0017	.0056	.0103	.0087	.0033	.0002	.0313
327-348	NNW	.0022	.0054	.0077	.0087	.0024	.0003	.0001	.0267
CALM		.0000							.0000
MISS		.0000	.0000	.0000	.0000	.0005	.0001		.0015

TOTAL .0377 .0971 .0865 .0568 .0211 .0062 .0065 .3119
Percentage of hours of temperature difference present in this stability category = 31.2 Numbers of hours in this
stability category = 2730

IP3
FSAR UPDATE

Table 2.6-5 (Sheet 5 of 14)

**JOINT FREQUENCY DISTRIBUTION OF WIND SPEED AND
DIRECTION FOR PASQUILL STABILITY CATEGORY E**

Indian Point B(3) Using a delta t correction factor
of 0.605

JAN. 1 1970 1 DEC. 31 1972

WIND

DIRECTION

WIND SPEED (MPH)

		01-03	04-07	08-12	13-18	19-24	Greater than 24	MISS	TOTAL
349-11	N	.0065	.0143	.0149	.0046	.0009	.0000	.0007	.0418
12-33	NNE	.0063	.0281	.0183	.0035	.0011	.0001	.0014	.0594
34-56	NE	.0059	.0123	.0043	.0006	.0005	.0000	.0014	.0250
57-78	ENE	.0031	.0032	.0008	.0000	.0000	.0000	.0002	.0073
79-101	E	.0025	.0041	.0018	.0001	.0001	.0000	.0001	.0088
102-123	ESE	.0029	.0041	.0021	.0001	.0000	.0000	.0002	.0094
124-146	SE	.0043	.0062	.0027	.0003	.0006	.0000	.0001	.0143
147-168	SSE	.0038	.0114	.0089	.0023	.0007	.0002	.0001	.0274
169-191	S	.0041	.0162	.0102	.0014	.0003	.0003	.0001	.0327
192-213	SSW	.0049	.0101	.0077	.0008	.0000	.0000	.0000	.0234
214-236	SW	.0042	.0078	.0038	.0007	.0001	.0001	.0001	.0168
237-258	WSW	.0030	.0038	.0029	.0013	.0007	.0002	.0001	.0119
259-281	W	.0023	.0025	.0055	.0019	.0015	.0005	.0007	.0149
282-303	WNW	.0022	.0017	.0072	.0079	.0059	.0016	.0007	.0272
304-326	NW	.0013	.0030	.0098	.0120	.0043	.0010	.0009	.0323
327-348	NNW	.0024	.0071	.0089	.0070	.0010	.0000	.0022	.0286
CALM		.0000							.0001
MISS		.0009	.0009	.0010	.0008	.0013	.0000		.0062
TOTAL		.0606	.1375	.1107	.0452	.0191	.0041	.0103	.3875

Percentage of hours of temperature difference present in this stability category = 38.7 Numbers of
hours in this stability category = 3391

IP3
FSAR UPDATE

Table 2.6-5 (Sheet 6 of 14)

**JOINT FREQUENCY DISTRIBUTION OF WIND SPEED AND
DIRECTION FOR PASQUILL STABILITY CATEGORY F**

Indian Point B(3) Using a delta t correction factor
of 0.605

JAN. 1 1970 1 DEC. 31 1972

WIND

DIRECTION

WIND SPEED (MPH)

		01-03	04-07	08-12	13-18	19-24	Greater than 24	MISS	TOTAL
349-11	N	.0043	.0033	.0007	.0000	.0000	.0000	.0000	.0083
12-33	NNE	.0053	.0143	.0051	.0005	.0000	.0000	.0001	.0253
34-56	NE	.0050	.0094	.0008	.0000	.0000	.0000	.0001	.0153
57-78	ENE	.0031	.0014	.0000	.0000	.0000	.0000	.0000	.0045
79-101	E	.0011	.0006	.0000	.0000	.0000	.0000	.0000	.0017
102-123	ESE	.0009	.0008	.0000	.0000	.0000	.0000	.0000	.0017
124-146	SE	.0016	.0016	.0001	.0000	.0000	.0000	.0000	.0033
147-168	SSE	.0029	.0041	.0005	.0001	.0000	.0000	.0000	.0075
169-191	S	.0022	.0043	.0007	.0000	.0000	.0000	.0000	.0072
192-213	SSW	.0031	.0058	.0006	.0000	.0000	.0000	.0001	.0096
214-236	SW	.0033	.0041	.0007	.0000	.0000	.0000	.0001	.0082
237-258	WSW	.0019	.0013	.0003	.0000	.0000	.0000	.0005	.0040
259-281	W	.0021	.0009	.0007	.0000	.0001	.0000	.0001	.0039
282-303	WNW	.0016	.0005	.0008	.0001	.0000	.0000	.0001	.0031
304-326	NW	.0017	.0006	.0007	.0002	.0000	.0000	.0000	.0032
327-348	NNW	.0024	.0015	.0006	.0001	.0000	.0000	.0000	.0046
CALM		.0000							.0000
MISS		.0002	.0000	.0000	.0000	.0000	.0000		.0011

TOTAL .0427 .00544 .0122 .0010 .0001 .0000 .0021 .1125
Percentage of hours of temperature difference present in this stability category = 11.3 Numbers of hours in this
stability category = 985

IP3
FSAR UPDATE

Table 2.6-5 (Sheet 7 of 14)

**JOINT FREQUENCY DISTRIBUTION OF WIND SPEED AND
DIRECTION FOR PASQUILL STABILITY CATEGORY G**

Indian Point B(3) Using a delta t correction factor
of 0.605

JAN. 1 1970 1 DEC. 31 1972

WIND

DIRECTION

WIND SPEED (MPH)

		01-03	04-07	08-12	13-18	19-24	Greater than 24	MISS	TOTAL
349-11	N	.0010	.0005	.0001	.0000	.0000	.0000	.0000	.0016
12-33	NNE	.0015	.0042	.0001	.0000	.0000	.0000	.0000	.0058
34-56	NE	.0018	.0034	.0000	.0000	.0000	.0000	.0000	.0053
57-78	ENE	.0008	.0001	.0000	.0000	.0000	.0000	.0000	.0009
79-101	E	.0010	.0002	.0000	.0000	.0000	.0000	.0000	.0013
102-123	ESE	.0005	.0002	.0000	.0000	.0000	.0000	.0000	.0007
124-146	SE	.0014	.0001	.0000	.0000	.0000	.0000	.0000	.0015
147-168	SSE	.0007	.0005	.0000	.0000	.0000	.0000	.0000	.0011
169-191	S	.0009	.0008	.0000	.0000	.0000	.0000	.0000	.0017
192-213	SSW	.0013	.0016	.0001	.0000	.0000	.0000	.0001	.0031
214-236	SW	.0016	.0005	.0000	.0000	.0000	.0000	.0000	.0021
237-258	WSW	.0009	.0002	.0001	.0000	.0000	.0000	.0000	.0013
259-281	W	.0008	.0003	.0000	.0000	.0000	.0000	.0000	.0011
282-303	WNW	.0010	.0002	.0000	.0000	.0000	.0000	.0000	.0013
304-326	NW	.0011	.0002	.0000	.0000	.0000	.0000	.0000	.0014
327-348	NNW	.0010	.0003	.0000	.0001	.0000	.0000	.0000	.0015
CALM		.0000							.0000
MISS		.0000	.0000	.0000	.0000	.0000	.0000		.0001

TOTAL .0174 .0135 .0005 .0001 .0000 .0000 .0002 .0316
Percentage of hours of temperature difference present in this stability category = 3.2 Numbers of hours in this
stability category = 277

IP3
FSAR UPDATE

Table 2.6-5 (Sheet 8 of 14)

JOINT FREQUENCY DISTRIBUTION OF WIND SPEED AND
DIRECTION FOR PASQUILL STABILITY CATEGORY A

Indian Point B(3) Using a delta t correction factor
of 0.605

JAN. 1 1970 1 DEC. 31 1972

WIND

DIRECTION

WIND SPEED (MPH)

		01-03	04-07	08-12	13-18	19-24	Greater than 24	MISS	TOTAL
349-11	N	.0010	.0070	.0080	.0025	.0002	.0000	.0001	.0189
12-33	NNE	.0005	.0042	.0027	.0010	.0000	.0000	.0001	.0086
34-56	NE	.0003	.0019	.0006	.0001	.0001	.0000	.0001	.0032
57-78	ENE	.0002	.0005	.0001	.0002	.0002	.0000	.0000	.0013
79-101	E	.0002	.0005	.0002	.0002	.0000	.0000	.0000	.0011
102-123	ESE	.0001	.0002	.0005	.0002	.0000	.0000	.0000	.0010
124-146	SE	.0005	.0006	.0014	.0016	.0002	.0000	.0000	.0042
147-168	SSE	.0002	.0050	.0103	.0071	.0003	.0000	.0000	.0230
169-191	S	.0010	.0090	.0066	.0017	.0000	.0000	.0000	.0184
192-213	SSW	.0003	.0054	.0029	.0002	.0000	.0000	.0001	.0089
214-236	SW	.0007	.0024	.0017	.0003	.0000	.0000	.0000	.0051
237-258	WSW	.0007	.0013	.0016	.0002	.0000	.0000	.0002	.0040
259-281	W	.0007	.0021	.0038	.0016	.0007	.0001	.0003	.0093
282-303	WNW	.0006	.0010	.0032	.0047	.0024	.0007	.0011	.0137
304-326	NW	.0008	.0015	.0037	.0055	.0038	.0007	.0005	.0163
327-348	NNW	.0007	.0041	.0056	.0042	.0013	.0001	.0000	.0160
CALM		.0000							.0000
MISS		.0000	.0000	.0000	.0000	.0000	.0000		.0022
TOTAL		.0086	.0466	.0528	.0315	.0093	.0016	.0048	.1552
Percentage of hours of temperature difference present in this stability category = 15.5 Numbers of hours in this stability category = 1358									

IP3
FSAR UPDATE

Table 2.6-5 (Sheet 9 of 14)

**JOINT FREQUENCY DISTRIBUTION OF WIND SPEED AND
DIRECTION FOR PASQUILL STABILITY CATEGORY B**

Indian Point B(3) Using a delta t correction factor
of 0.605

JAN. 1 1970 1 DEC. 31 1972

WIND

DIRECTION

WIND SPEED (MPH)

		01-03	04-07	08-12	13-18	19-24	Greater than 24	MISS	TOTAL
349-11	N	.0002	.0007	.0005	.0001	.0000	.0000	.0000	.0015
12-33	NNE	.0001	.0005	.0005	.0000	.0000	.0000	.0000	.0010
34-56	NE	.0005	.0003	.0000	.0000	.0000	.0000	.0000	.0008
57-78	ENE	.0001	.0002	.0000	.0000	.0000	.0000	.0001	.0005
79-101	E	.0002	.0000	.0000	.0000	.0000	.0000	.0000	.0002
102-123	ESE	.0003	.0005	.0000	.0001	.0000	.0000	.0000	.0009
124-146	SE	.0000	.0003	.0006	.0000	.0000	.0000	.0000	.0009
147-168	SSE	.0002	.0005	.0010	.0007	.0001	.0000	.0000	.0025
169-191	S	.0005	.0008	.0006	.0005	.0000	.0000	.0000	.0023
192-213	SSW	.0000	.0002	.0006	.0000	.0000	.0000	.0000	.0008
214-236	SW	.0003	.0001	.0000	.0000	.0000	.0000	.0000	.0005
237-258	WSW	.0006	.0002	.0000	.0001	.0000	.0000	.0000	.0009
259-281	W	.0000	.0000	.0007	.0001	.0000	.0000	.0000	.0008
282-303	WNW	.0002	.0000	.0000	.0005	.0003	.0000	.0000	.0010
304-326	NW	.0001	.0002	.0003	.0002	.0003	.0003	.0000	.0016
327-348	NNW	.0001	.0001	.0006	.0002	.0000	.0001	.0000	.0011
CALM		.0000							.0000
MISS		.0000	.0000	.0000	.0000	.0000	.0000		.0000

TOTAL .0035 .0047 .0053 .0025 .0008 .0005 .0001 .0174

Percentage of hours of temperature difference present in this stability category = 1.7 Numbers of hours in this stability category = 152

IP3
FSAR UPDATE

Table 2.6-5 (Sheet 10 of 14)

JOINT FREQUENCY DISTRIBUTION OF WIND SPEED AND
DIRECTION FOR PASQUILL STABILITY CATEGORY C

Indian Point B(3) Using a delta t correction factor
of 0.605

JAN. 1 1970 1 DEC. 31 1972

WIND

DIRECTION

WIND SPEED (MPH)

		01-03	04-07	08-12	13-18	19-24	Greater than 24	MISS	TOTAL
349-11	N	.0000	.0009	.0009	.0008	.0000	.0000	.0000	.0026
12-33	NNE	.0001	.0007	.0008	.0003	.0001	.0000	.0000	.0021
34-56	NE	.0002	.0005	.0001	.0001	.0000	.0000	.0000	.0009
57-78	ENE	.0001	.0000	.0002	.0000	.0000	.0000	.0000	.0003
79-101	E	.0000	.0001	.0000	.0001	.0000	.0000	.0000	.0002
102-123	ESE	.0000	.0001	.0000	.0000	.0000	.0000	.0000	.0001
124-146	SE	.0002	.0005	.0007	.0001	.0000	.0000	.0000	.0015
147-168	SSE	.0003	.0013	.0018	.0008	.0000	.0000	.0000	.0042
169-191	S	.0001	.0016	.0006	.0001	.0000	.0000	.0000	.0024
192-213	SSW	.0001	.0006	.0003	.0001	.0000	.0000	.0000	.0011
214-236	SW	.0003	.0005	.0002	.0003	.0000	.0000	.0000	.0014
237-258	WSW	.0001	.0000	.0002	.0003	.0000	.0000	.0000	.0007
259-281	W	.0000	.0002	.0005	.0008	.0001	.0000	.0000	.0016
282-303	WNW	.0005	.0002	.0002	.0013	.0011	.0005	.0000	.0038
304-326	NW	.0000	.0001	.0001	.0001	.0009	.0006	.0000	.0018
327-348	NNW	.0003	.0007	.0005	.0008	.0006	.0000	.0000	.0029
CALM		.0000							.0000
MISS		.0000	.0000	.0000	.0000	.0002	.0001		.0006
TOTAL		.0025	.0079	.0072	.0062	.0031	.0011	.0002	.0282
Percentage of hours of temperature difference present in this stability category = 2.8 Numbers of hours in this stability category = 247									

IP3
FSAR UPDATE

Table 2.6-5 (Sheet 11 of 14)

JOINT FREQUENCY DISTRIBUTION OF WIND SPEED AND
DIRECTION FOR PASQUILL STABILITY CATEGORY D

Indian Point B(3) Using a delta t correction factor
of 0.605

JAN. 1 1970 1 DEC. 31 1972

WIND

DIRECTION

WIND SPEED (MPH)

		01-03	04-07	08-12	13-18	19-24	Greater than 24	MISS	TOTAL
349-11	N	.0023	.0149	.0182	.0066	.0008	.0001	.0014	.0442
12-33	NNE	.0037	.0166	.0120	.0035	.0006	.0001	.0014	.0378
34-56	NE	.0030	.0066	.0026	.0003	.0003	.0000	.0006	.0135
57-78	ENE	.0022	.0016	.0001	.0001	.0000	.0000	.0006	.0046
79-101	E	.0024	.0019	.0010	.0000	.0000	.0000	.0002	.0056
102-123	ESE	.0023	.0016	.0013	.0002	.0000	.0000	.0003	.0057
124-146	SE	.0025	.0055	.0047	.0006	.0002	.0000	.0001	.0136
147-168	SSE	.0022	.0114	.0103	.0032	.0000	.0000	.0003	.0274
169-191	S	.0026	.0101	.0056	.0013	.0000	.0000	.0003	.0199
192-213	SSW	.0030	.0035	.0029	.0011	.0000	.0000	.0000	.0105
214-236	SW	.0021	.0019	.0009	.0006	.0001	.0000	.0003	.0059
237-258	WSW	.0011	.0018	.0008	.0011	.0000	.0000	.0000	.0049
259-281	W	.0013	.0018	.0022	.0017	.0008	.0001	.0006	.0085
282-303	WNW	.0015	.0010	.0050	.0097	.0063	.0011	.0002	.0249
304-326	NW	.0011	.0019	.0059	.0117	.0078	.0026	.0001	.0312
327-348	NNW	.0011	.0057	.0071	.0079	.0022	.0002	.0002	.0245
CALM		.0000							.0000
MISS		.0000	.0001	.0000	.0001	.0005	.0000		.0011

TOTAL .0343 .0881 .0806 .0498 .0195 .0043 .0072 .2838

Percentage of hours of temperature difference present in this stability category = 28.4 Numbers of
hours in this stability category = 2484

IP3
FSAR UPDATE

Table 2.6-5 (Sheet 12 of 14)

**JOINT FREQUENCY DISTRIBUTION OF WIND SPEED AND
DIRECTION FOR PASQUILL STABILITY CATEGORY E**

Indian Point B(3) Using a delta t correction factor
of 0.605

JAN. 1 1970 1 DEC. 31 1972

WIND

DIRECTION

WIND SPEED (MPH)

		01-03	04-07	08-12	13-18	19-24	Greater than 24	MISS	TOTAL
349-11	N	.0046	.0096	.0073	.0022	.0006	.0000	.0002	.0243
12-33	NNE	.0035	.0178	.0117	.0019	.0009	.0001	.0006	.0366
34-56	NE	.0034	.0070	.0026	.0006	.0002	.0000	.0009	.0147
57-78	ENE	.0023	.0026	.0006	.0000	.0000	.0000	.0000	.0055
79-101	E	.0014	.0035	.0016	.0001	.0001	.0000	.0000	.0067
102-123	ESE	.0015	.0034	.0018	.0001	.0000	.0000	.0001	.0070
124-146	SE	.0035	.0043	.0021	.0002	.0003	.0000	.0001	.0106
147-168	SSE	.0025	.0078	.0066	.0016	.0005	.0002	.0000	.0192
169-191	S	.0026	.0093	.0064	.0010	.0003	.0003	.0001	.0201
192-213	SSW	.0031	.0074	.0063	.0007	.0000	.0000	.0000	.0175
214-236	SW	.0025	.0045	.0029	.0007	.0001	.0001	.0000	.0107
237-258	WSW	.0019	.0029	.0018	.0009	.0007	.0002	.0000	.0085
259-281	W	.0014	.0018	.0046	.0014	.0008	.0005	.0001	.0105
282-303	WNW	.0010	.0009	.0048	.0058	.0041	.0014	.0002	.0183
304-326	NW	.0008	.0019	.0069	.0085	.0021	.0006	.0005	.0211
327-348	NNW	.0019	.0042	.0057	.0042	.0005	.0000	.0013	.0178
CALM		.0000							.0000
MISS		.0005	.0007	.0010	.0007	.0010	.0000		.0049
TOTAL		.0385	.0897	.0746	.0306	.0122	.0034	.0051	.2542
Percentage of hours of temperature difference present in this stability category = 25.4 Numbers of hours in this stability category = 2225									

IP3
FSAR UPDATE

Table 2.6-5
(Sheet 13 of 14)

JOINT FREQUENCY DISTRIBUTION OF WIND SPEED AND
DIRECTION FOR PASQUILL STABILITY CATEGORY F

Indian Point B(3) Using a delta t correction factor
of 0.605

JAN. 1 1970 1 DEC. 31 1972

WIND

DIRECTION		WIND SPEED (MPH)						MISS	TOTAL
		01-03	04-07	08-12	13-18	19-24	Greater than 24		
349-11	N	.0040	.0026	.0026	.0007	.0000	.0000	.0000	.0099
12-33	NNE	.0040	.0134	.0075	.0008	.0002	.0000	.0000	.0259
34-56	NE	.0031	.0082	.0017	.0000	.0000	.0000	.0005	.0135
57-78	ENE	.0016	.0013	.0002	.0000	.0000	.0000	.0000	.0031
79-101	E	.0013	.0003	.0001	.0000	.0000	.0000	.0000	.0017
102-123	ESE	.0013	.0007	.0000	.0000	.0000	.0000	.0000	.0019
124-146	SE	.0009	.0014	.0002	.0000	.0000	.0000	.0000	.0025
147-168	SSE	.0022	.0041	.0015	.0001	.0002	.0000	.0000	.0081
169-191	S	.0022	.0071	.0029	.0002	.0000	.0000	.0000	.0123
192-213	SSW	.0021	.0056	.0014	.0000	.0000	.0000	.0000	.0090
214-236	SW	.0027	.0049	.0009	.0000	.0000	.0000	.0001	.0087
237-258	WSW	.0021	.0013	.0009	.0000	.0000	.0000	.0005	.0047
259-281	W	.0011	.0010	.0011	.0001	.0003	.0000	.0007	.0045
282-303	WNW	.0010	.0008	.0022	.0009	.0001	.0001	.0006	.0057
304-326	NW	.0011	.0007	.0022	.0006	.0009	.0001	.0005	.0061
327-348	NNW	.0013	.0016	.0024	.0016	.0001	.0000	.0008	.0078
CALM		.0000							.0001
MISS		.0007	.0001	.0000	.0000	.0000	.0000		.0013
TOTAL		.0326	.0552	.0279	.0050	.0019	.0002	.0040	.1268
Percentage of hours of temperature difference present in this stability category = 12.7 Numbers of hours in this stability category = 1110									

IP3
FSAR UPDATE

Table 2.6-5 (Sheet 14 of 14)

JOINT FREQUENCY DISTRIBUTION OF WIND SPEED AND
DIRECTION FOR PASQUILL STABILITY CATEGORY G

Indian Point B(3) Using a delta t correction factor
of 0.605

JAN. 1 1970 1 DEC. 31 1972

WIND

DIRECTION

WIND SPEED (MPH)

		01-03	04-07	08-12	13-18	19-24	Greater than 24	MISS	TOTAL
349-11	N	.0027	.0025	.0003	.0000	.0000	.0000	.0000	.0056
12-33	NNE	.0047	.0125	.0014	.0000	.0000	.0000	.0001	.0186
34-56	NE	.0053	.0089	.0000	.0000	.0000	.0000	.0000	.0142
57-78	ENE	.0029	.0008	.0000	.0000	.0000	.0000	.0000	.0037
79-101	E	.0018	.0007	.0000	.0000	.0000	.0000	.0000	.0025
102-123	ESE	.0009	.0009	.0000	.0000	.0000	.0000	.0000	.0018
124-146	SE	.0024	.0014	.0000	.0000	.0000	.0000	.0000	.0038
147-168	SSE	.0023	.0023	.0002	.0000	.0000	.0000	.0000	.0048
169-191	S	.0021	.0027	.0005	.0000	.0000	.0000	.0000	.0053
192-213	SSW	.0033	.0040	.0003	.0000	.0000	.0000	.0002	.0079
214-236	SW	.0034	.0026	.0002	.0000	.0000	.0000	.0001	.0064
237-258	WSW	.0017	.0008	.0003	.0000	.0000	.0000	.0001	.0030
259-281	W	.0024	.0006	.0001	.0000	.0000	.0000	.0000	.0031
282-303	WNW	.0022	.0003	.0001	.0000	.0000	.0000	.0000	.0026
304-326	NW	.0021	.0005	.0000	.0001	.0000	.0000	.0000	.0026
327-348	NNW	.0026	.0008	.0001	.0001	.0000	.0000	.0000	.0037
CALM		.0000							.0000
MISS		.0000	.0000	.0000	.0000	.0000	.0000		.0008

TOTAL .0427 .0423 .0037 .0002 .0000 .0000 .0014 .0903

Percentage of hours of temperature difference present in this stability category = 9.0 Numbers of hours in this stability category = 790

2.7 GEOLOGY

Between 2005 and 2007, GZA GeoEnvironmental (GZA), performed a comprehensive hydrogeologic investigation of the site. This investigation was initiated to understand groundwater flow and contaminant transport. During this investigation numerous borings were advanced to study the site geology, hydrology and aquifer properties. Details of the geology, hydrology and aquifer properties can be found in the GZA report (Reference 7).

[Historical Information]

Indian Point 3 is located approximately two miles southwest of the city of Peekskill, Westchester County New York, on the east bank of the Hudson River. Geologically, it is located in the central part of the Peekskill Quadrangle. The complete geologic description is divided into two broad sections: regional geology, physiography and tectonics; and geology of the area surrounding the site.

2.7.1 Regional Geology, Physiography and Tectonics

The general landscape of the region (see Figure 2.7-1 – figure is not available) consists of bedrock-supported ridges following generally northeasterly structural trends and rather steep and broad swampy valleys. The highest elevation in the region is 1,000 ft, and elevations range from 50 to 300 ft above mean sea level in low-lying areas. At the plant site the ground is level, about 15 feet above sea level and is covered with fill. The surface is artificially leveled and bedrock lies very close to the surface.

The eastern part of the United States has gone through tectonism since the Precambrian age (Figure 2.7-2 – figure is not available) and is known as the Appalachian Orogen. The plant is situated within the Manhattan Prong of the Appalachian Mountains. It is estimated that the earliest tectonic activity in the Appalachian Orogen was in Precambrian age and was a result of continental rifting and associated intrusive activity. A striking characteristic of the region is the high degree of metamorphism exhibited by the rocks. This has resulted from their long and complex history (Precambrian through the mid- Ordovician time) which included extensive thrust faulting, folding, intrusion, etc. The Taconic Orogeny was intense in the Manhattan Prong region and produced most of the structures evident in the map today. Essentially, the rocks in the plant site area belong to three tectonic provinces, e.g., the Hudson Highlands, the Manhattan Prong and the Newark Basin. The geology of these provinces follows:

The Hudson Highlands

The Hudson Highlands are a part of the much larger Blue Ridge - New Jersey Highlands Province. Here the northeast trending ridges are underlain by complexly folded granitoid gneisses and schists. These also involve granodioritic intrusives. Prevailing dips in the entire region are steep towards the southeast. The bulk of the Highland rocks represent a sequence of Precambrian aged miogeosynclinal and eugeosynclinal deposits, however those in the areas of concern are in faulted and in-folded strata of Cambro - Ordovician age.

Helenock and Mose⁽²⁾ recognized a mappable sequence of five rock units in the Lake Carmel, New York, area of the Highlands. These rocks were metamorphosed to granulite facies, and were multiply deformed in the Greenville Orogeny. There was recrystallization to amphibolite facies accompanied by folding during the Taconic Orogeny (mid-Ordovician).

The Ramapo Fault Zone (Section 2.8) separates the Highlands from the Manhattan Prong and the Newark Basin.

The Manhattan Prong

The Manhattan Prong is bounded on the east by Cameron's line, on the west by the Newark Basin border fault and the Hudson River. It covers the geographic areas of New York City (Manhattan), Westchester County, New York and parts of Fairfield County, Connecticut.

The uppermost formation of sedimentary origin is called a Phyllite or Schist known as the Manhattan Schist. This is the most recent geologic formation. In order of increasing age and depth are the Inwood Marble, the Lowerre Quartzite, the Yonkers-Pound Ridge Granite and the Fordham Gneiss. Due to the extremely complicated nature of the region's geology this stratigraphy varies with location.

The Manhattan Formation was deposited in a miogeosyncline. It was metamorphosed, deformed and intruded during the Taconic and the Acadian episodes(3).

The Inwood Marble, consisting of dolomite and calcite marbles with interlayered calc - silicate schists, were deposited during the Cambrian - Ordovician period. It is widespread in the Appalachian Orogen.

The Lowerre Quartzite underlies the Inwood Marble. It is a relatively thin, discontinuous unit representing an arkosic sandstone. The Lowerre consists mainly of quartz with potassium feldspar and biotite. It is always found underlying the Cambro-Ordovician aged rocks.

The Yonkers and Fordham formations are Precambrian in age and are separated from the Lowerre. Inwood and Manhattan formations are joined by an angular unconformity. The Fordham formation was deformed and metamorphosed to granulite facies during the Greenville Orogeny. The Yonkers - Pound Ridge Granite, emplaced during the opening of the Proto-Atlantic in late Precambrian age, is mostly a metamorphosed rhyolite.

The Newark Basin

The Newark Basin formation, west of the Hudson River, extends from York County, Pennsylvania to Rockland County, New York. The northern tip of this basin very closely approaches the Indian Point Site on the opposite side of the Hudson River near Stony Point. This is an assemblage of conglomerates, sandstones and shales with their intercalated beds of basaltic lava and the well known intrusive sill of the "Palisades". Deposition was continuous from the late Triassic through the upper Jurassic ages(4). The boundary fault between this basin and older crystalline rocks is the well known Ramapo Fault.

2.7.2 Geology of the Area Surrounding the Site

The geology of the area surrounding the site is shown in Figure 2.7-3 (figure is not available). The Ramapo Fault System passes through the area surrounding the site. The Ramapo is a series of N - NE trending faults, with minimum age for movement being Greenville (5). The faults surrounding the plant site have been studied utilizing radiometric age determination, cross-cutting lithologic relationships and textural evidences, by Ratcliff (5); Dames & Moore(4) studied age based on geothermometry of fluid inclusions in calcite.

The most prominent faults that separate the Manhattan Prong from Hudson Highlands are the Thiells fault, the Annsville fault, the Peekskill fault and the Croton Falls fault. These are all believed to be of Paleozoic age. The N-S faults at Tomkins Cove across the Hudson River from Indian Point are the youngest in the area, presumably of Mesozoic age. Dames & Moore (4) mapped a group of faults at the Indian Point site with displacements no more than a few feet. They are filled with undeformed euhedral calcite crystals (Figure 2.7-4 – figure is not available)

Radiometric age determination of these, and the lack of fault related deformation of Pleistocene deposits and surface features, prove that the faults surrounding the site have not moved in the last 2 million years, although predominant movements took place in Precambrian time. Examination of recent core drills in the area indicate that the dip is consistently to the S-E and that the dominant latest motion in the fault was right oblique normal faulting.

References

- 1) Van Eysing, F. W. B, 1978 Geologic Time Scale
- 2) Heleneck, H. L. & Mose, D. G. 1978, Geology and Geochronology of Precambrian Rocks in the Lake Carmel Region Hudson Highlands, N. Y., Geological Society of America, V. 10. No. 2.
- 3) a) Brock, P.W.G and Mose, D. G., 1979, Taconic and Younger Deformations in the Croton Falls Area, S-Eastern N.Y., Bulletin of Geo. Soc of Am. Pt II V. 90.
b) Mose, D G. and Hall, L. M., 1979, Rb - Sr Whole-Rock Age Determination of Member C of the Manhattan Schist and its Bearing on Allochthony in the Manhattan Prong, SE New York Geo. Soc. of Am, Abstracts with Programs, V. II No. 1.
- 4) Dames & Moore, 1977, Geotechnical Investigation of the Ramapo Fault System in the Region of the Indian Point Generating Station.
- 5) Ratcliffe, N. M., 1976, Final Report on Major Fault Systems in the Vicinity of Tomkins Cove - Buchanan, N. Y. Report for Consolidated Edison Company, Inc. of N. Y.
- 6) Dames & Moore, Nov. 1975. Supplemental Geological Investigation of the Indian Point Generating Station for Consolidated Edison Co. of N. Y. Inc.
- 7) GZA, Hydrogeologic Site Information Report for the Indian Point Energy Center, January 7, 2008.

2.8 SEISMOLOGY [Historical Information]

2.8.1 Background and Seismic Design Bases

Geographic areas of the continental United States have been subdivided into regions of known or assigned seismic probability or risk and this has served as a useful basis for generating code provisions for earthquake - resistant structures. The Seismic Risk Map adopted by the International Conference of Building Officials for inclusion in the 1970 edition of Uniform Building Code, divides the United States into four (4) major zones of seismic risk or probability. The Indian Point Site is located in Zone I of this map with intensities limited to V and VI on the Modified Mercalli Intensity Scale of 1931 (Figure 2.8-1) and only slight earthquake activity can be expected.

However, the Indian Point 3 facility was actually built per requirements of Zone 2 of the Uniform Building Code i.e., corresponding to an intensity VII of the Modified Mercalli Scale. The range of expected horizontal acceleration of ground motion for earthquakes of this intensity is 70-150 cm/sec² near the epicenter or about 0.15 g max. At a distance of 100 miles from the epicenter, the acceleration drops to 50%. The nearest event larger than intensity VII occurred near Cape Ann, Massachusetts, a distance of more than 200 miles from the site, in 1755. This event was classified as intensity VIII on the Modified Mercalli Scale. It was believed, therefore, that the plant's structural design, allowing for safe shutdown in the event of an earthquake of intensity VII on the Modified Mercalli Scale, was adequate. A list of known earthquakes which have occurred in the vicinity of the plant having intensities of V through VII on the modified Mercalli Scale is provided by Table 2.8-1.

The Reverend Joseph Lynch, S. J., while Director of the Fordham University Seismic Observatory stated:

".... that the probability of a serious shock occurring in this area for the next several hundred years is practically nil. The area therefore would certainly seem to be as safe as any area at present known."

Captain Elliott B. Roberts, while Chief of the Geophysics Division of the Department of Commerce, substantially agreed with the conclusions of Rev. Lynch.

Rev. Lynch also stated that the "estimated maximum ground acceleration of 0.03 g is reasonably conservative for the area." This has been established as the basis for design of the plant. Rev. Lynch stated further that the "safety factor for a horizontal stress of 0.1 g is therefore.... more than adequate." For earthquakes having a horizontal acceleration of 0.1 g and a vertical acceleration of 0.05 g acting simultaneously at zero period, the plant is designed to have no loss of function of systems important to safety, although in some cases, the stresses may reach or slightly exceed yield points.

2.8.2 Public Concerns and Resolutions

Subsequent to the plant's construction, public concerns were raised on the following issues:

- 1) A series of N-NE trending faults pass through the area surrounding the site - collectively known as the Ramapo Fault System (Section 2.7). The concern raised was whether the Ramapo Fault is "capable" of causing an earthquake at the site.(1)
- 2) Because of the lack of historical records of earthquakes (Table 2.8-1) in the plant area - older than the Cape Ann earthquake, concerns were raised whether the safe shutdown earthquake (SSE) for the plant's design should be greater than intensity VII on the Modified Mercalli Scale.
- 3) As stated earlier, the plant was designed for 0.15 g max base shear for safe shutdown. Concern was that, if the SSE ground acceleration be raised from intensity VII to VIII on the Modified Mercalli Scale, would the 0.15 g base shear still be adequate?
- 4) An extended micro-monitoring system for measuring magnitude, accurately determining the location and even focal mechanism behavior of small magnitude earthquake near the plant and Ramapo Fault Zone was required by condition 2.C.4(c) of Amendment No. 2 to the Operating License of the plant. Concern was raised whether this extended micro-seismic-measuring instrumentation was considered as a licensing requirement.

An 18 month proceeding was held on the above concerns before a U.S. Nuclear Regulatory Commission (NRC) Atomic Safety and Licensing Board. Also, there have been numerous

extensive studies on these concerns. The findings by the board and these studies may be summarized as follows:

- 1) In testimony before the board, Charles F. Richter, who developed the Richter Scale, stated that the earthquakes in the Ramapo region are "of minor magnitude and relatively trivial". Radiometric age determination of undeformed minerals that have grown within fault zones was studied by Ratcliffe(2) and fault related deformation of Pleistocene deposits and surface features by Dames & Moore(3) and Ratcliffe(5). Both prove that the faults in the Indian Point area have not moved in at least the last 2 million years. The Ramapo Fault, therefore, is considered to be old, inactive and not a "capable" fault under Appendix A to 10 CFR 100.
- 2) The unanimous ruling by the board was - "In accordance with Appendix A to 10 CFR 100, neither the Cape Ann earthquake nor any other historic event requires the assumption of a safe shutdown earthquake for the Indian Point Site of greater than a Modified Mercalli intensity of VII(6)". Hearings were also held before the Advisory Committee on Reactor Safeguards. Despite some controversy over appropriate tectonic divisions, the Committee, scientists in the TERA Corp.(8)(9) and Dames & Moore(4) concluded that an event of intensity VII on the Modified Mercalli Scale is adequate as the design earthquake for the Indian Point Site.
- 3) Consistent with the above ruling, the board also ruled - "The ground acceleration value used for the design of Indian Point Units 2 and 3 should remain at 0.15 g".(6)
- 4) Amendment 2 to the Technical Specifications stated in Section 2(c)(4)(c) that an extended microseismic instrumentation network must be operated for at least two years following complete installation of all stations. The Atomic Safety and Licensing Appeal Board repealed this decision in hearings held on October 12, 1977(6) and the NRC issued Technical Specification Amendment 9 to reflect this. However, a network was operated from 1975-1990 and a final report(10) was published.

2.8.3 Conclusions

Microseismic activity recorded by the seismic monitoring network is evidence of minor crustal adjustments due to regional stresses. However, neither the readings from the network nor the bore-hole experiment(11) at Kent Cliffs show the evidence of any contemporary (geologic) movement along faults exposed at the surface as was suggested by Aggarwal and Sykes.(1) On the contrary, the last movement of the region (Mesozoic Period) was in a direction normal to the proposed direction.

It is therefore concluded that the seismic design criteria for structural analysis at the Indian Point site is satisfactory and that the plant is set on solid bedrock. No public hazard can be expected from the plant due to a probable earthquake in the region.

References

- 1) Aggarwal, Y. P. and Sykes, L. R., 1978, Earthquakes, Faults and Nuclear Power Plants in Southern New York and Northern New Jersey in "Science," V. 200.
- 2) Ratcliffe, N. M. 1976, Final Report on Major Fault Systems in the Vicinity of Tomkins Cove - Buchanan, New York: Report for Consolidated Edison Company of New York, Inc.

IP3
FSAR UPDATE

- 3) Dames & Moore, 1977, Geotechnical Investigation of Ramapo Fault System in the Region of the Indian Point Generating Station.
- 4) Dames & Moore, 1980, Seismic Ground Motion Hazard at Indian Point Nuclear Power Plant Site - A report prepared for Pickard, Lowe & Garrick, Inc.
- 5) Ratcliffe, N. M. 1981, Brittle Faults (Ramapo Fault) and Phyllonitic Ductile Shear Zones in the Basement Rocks of the Ramapo Seismic Zone, New York and New Jersey, and their Relationship to Current Seismicity published in: Manspeizer, W., editor, Field Studies of New Jersey Geology and Guide to Field Trips, 52nd Annual Meeting of the New York State Geological Association, Newark, New Jersey, Rutgers University.
- 6) United States Nuclear Regulatory Commission/Atomic Safety and Licensing Appeal Board, Farrar, M. C. - Chairman, Buck, J. H. and Quarles L. R. - Members at a Hearing cited as 6 NRC 547 (1977), ALAB -436.
- 7) Gutenberg, B. and Richter C. F. Earthquake Magnitude, Intensity, Energy and Acceleration, BSSA, 32,(3) July 1942.
- 8) TERA Corporation, Seismic Hazard Analysis - A Methodology for the Eastern United States, NUREG/CR-1582, 2, 1980.
- 9) TERA Corporation, Seismic Hazard Analysis Solicitation of Expert Opinion, NUREG/CR-1582, 3, 1980.
- 10) Woodward-Clyde; Scientific Results of Seismic Monitoring Network near the Indian Point Nuclear Generating Facilities, Final Report (10/27/92); R&D Project 92284
- 11) Woodward-Clyde, 1986: Kent Cliffs Bore-hole Research Project: A Determination of the Magnitude and Orientation of Tectonic Stress in Southeastern New York; Research Report EP 84-27, Empire State Electric Energy Research Corporation, New York, New York.

IP3
FSAR UPDATE

TABLE 2.8-1

LIST OF EARTHQUAKES OF INTENSITIES GREATER THAN OR EQUAL TO V ON MODIFIED MERCALLI SCALE
(SOURCE: EPRI)

DATE	TIME (HOUR)	GEOGRAPHIC COORDINATES		DEPTH (KM)	INTENSITY MODIFIED MERCALI SCALE	REMARKS
		LATITUDE (DEG. N)	Longitude (Deg. W)			
12-19-1737	04:00:00	40.80	74.00	0	VII	Felt Over 2,000 Sq. Miles
11-30-1783	03:50:00	41.00	74.50	0	VI	
09-29-1847	00:00:00	40.50	74:00	0	V	
12-11-1874	03:25:00	40.90	73.80	0	V	
10-04-1878	07:30:00	41.50	74.00	0	V	
08-10-1884	19:07:00	40.60	74.00	0	VII	
09-01-1895	11:09:00	40:70	74.80	0	VI	
06-01-1927	12:23:00	40.30	74.00	0	Between VI and VII	
10-08-1952	21:40:00	41.70	74.00	0	V	Felt Over 31,000 Sq. Miles
03-23-1957	19:02:00	40.60	74.80	0	VI	
11-17-1964	17:08:00	41.20	73:70	0	V	
11-21-1967	22:10:00	41.20	73.80	0	V	
03-11-1976	21:07:00	41.00	74.40	0	V	
04-13-1976	15:39:00	40.80	74.00	0	VI	
01-30-1979	16:30:52	40.32	74.26	5	VI	
03-10-1979	04:49:40	40.72	74.72	3	V	
12-30-1979	14:15:12	41.14	73.69	5	V	

(For location Map see Figure No. 2.7-3 – this figure is not available)

2.9 ENVIRONMENTAL MONITORING PROGRAM

2.9.1 General

A program to determine the environmental radioactivity in the vicinity of Indian Point Station was instituted in 1958, four years prior to the initial operation of Consolidated Edison's Indian Point Unit No. 1. The purpose of this survey was to determine the natural background radioactivity and to show the variations in the activities that may be expected from natural sources, fallout from bomb tests and other sources in the vicinity. This program has been continued to the present so that changes in the environment, resulting from station operations, could be accounted for. The results of these surveys are reported annually to the Nuclear Regulatory Commission.

In addition, the New York State Department of Health has conducted surveys throughout the State of New York since 1955, including extensive surveys in the vicinity of the Indian Point Station since 1958. In 1965 and 1966, they reported the findings in the vicinity of the Indian Point Station in two special reports. Since that time, their reporting has been on a statewide basis in quarterly bulletins and in annual reports.

In 1964, the New York University Medical Center began a research program on the ecology of the Hudson River. The New York University studies include the biology of the Hudson River, the distribution and abundance of fish in the river, pesticides and radio-ecological studies. The results of this program, supported by the United States Public Health Service, the New York State Department of Health, and the Consolidated Edison Company have been submitted in several program reports.

The various studies mentioned above included measurements of radioactivity in fresh water, river water, river bottom sediments, fish, aquatic vegetation, soil, vegetation and air in the vicinity of the Indian Point Station. The results of these monitoring programs have shown that the operation of the Indian Point Units 1, 2, and 3 have had no deleterious effects on the environment.

2.9.2 Survey Programs

The survey of environmental radioactivity in the vicinity of Indian Point Station provides an indication of the integrity of the in-plant radiation monitoring instrumentation and can reveal any buildup of long lived radionuclides.

By determining the activity of filterable air particulate, vegetation, drinking water and above ground gamma fields, an indirect monitoring of discharges to the atmosphere is provided by the environmental survey program.

The effect of liquid effluents on the Hudson River is monitored by measuring the activity of the cooling water inlet to and discharge from the station, discharges from the plant, activity analysis of river shoreline soils and river fish and invertebrates.

A detailed description of the media sampled in accordance with plant Environmental Monitoring Program and the ODCM is given below:

IP3 FSAR UPDATE

Air Particulate and Organic Iodide

Concentration of radioactive particles in the air is measured weekly from 5 stations.

Membrane filters precede charcoal impregnated filters. The particulate filters are assayed for gross beta activity and are composited for quarterly gamma spectral analysis. Charcoal filters have gamma spectral analysis for I-131 performed weekly.

Reservoir Water

Drinking water is sampled monthly from an area reservoir. The water sampled is analyzed for gross beta activity, and for other nuclides via gamma spectral analysis. A quarterly composite sample is analyzed for tritium.

Hudson River Water

Continuous flow samples of the condenser inlet cooling water and discharge water are collected and composited. Samples are taken, at a frequency specified in the ODCM, from continuous samples and composited for a monthly gamma spectroscopy analysis, and for a quarterly tritium analysis.

Hudson River Shoreline Soil

Twice a year, at least 90 days apart, samples of river shoreline soil are taken at two locations. Gamma spectral analysis is performed on each sample.

Hudson River Fish and Shellfish

Fish and invertebrates are caught seasonally (semi-annually if not seasonal) where available near the site and analyzed by gamma spectral analysis.

Vegetation

Samples of broad leaf vegetation are collected monthly, if available, in the critical wind sections within several miles of the plant. Gamma spectral and Iodine-131 analyses are performed on these samples.

Milk

Milk samples are obtained, when available, on a monthly basis (semi-monthly when animals are on pasture) from dairy farms, located within 5 miles of the site. The samples are analyzed for Iodine-131 content, and for other nuclides by gamma spectral analysis.

Direct Gamma (Continuous)

At 40 locations near the site and out to about 5 miles, the background gross gamma radiation is continuously monitored. The measuring devices consist of two sets of thermoluminescent dosimeters (TLDs). The TLDs are removed at quarterly intervals and the amount of absorbed background radioactivity is recorded.

2.9.3 Summary

The environmental monitoring program conducted by Entergy supplies sufficient data to determine the compliance of Indian Point Unit Nos. 1, 2 and 3 with the requirements of 10 CFR 20. The environmental survey program which monitors air, water, river shoreline sediments, terrestrial vegetation, milk and selected aquatic biota provides an indication of the cumulative amounts of radioactivity in the environment.

Results of the environmental monitoring program are reported on an annual basis to the nuclear Regulatory Commission, who are thereby advised of the short and long-term trends in the environment. In addition, discharges of radioactive liquids and gases are reported to the Nuclear Regulatory Commission.

In the event that the Indian Point Station Environmental Monitoring Program detects increases in the background radiation levels above the reporting levels specified in the Offsite Dose Calculation Manual (ODCM), Entergy will notify the Nuclear Regulatory Commission.

Although the design of Indian Point 3 and administrative controls are such that liquid and gaseous effluents are released in accordance with the requirements of 10 CFR 20, the environmental monitoring program conducted by IP3 and IP2 provides a redundant means of insuring that the operation of this facility does not pose any undue risk to the health and safety of the public.

IP3
FSAR UPDATE

An Analysis
of the Con Edison and AEC-DRL
Accident Meteorology Models
as Applied to the Indian Point Site

Prepared by

James Halitsky, Ph.D.
Associate Professor of Civil Engineering
University of Massachusetts
Amherst, Massachusetts 01002

for

Consolidated Edison Company of New York, Incorporated
4 Irving Place
New York, New York 10003

January 14, 1973

2.6.L-1

IP3
FSAR UPDATE

TABLE OF CONTENTS

	Page
List of Tables	iv
List of Figures	v
Summary	1
1. Introduction	3
2. Conservatism of the Con Edison and AEC-DRL Accident Meteorology Models as Applied to Indian Point	4
2.1 General Comments on Quantification of Conservatism.....	4
2.2 Data Analysis.....	5
2.21 The Con Edison Accident Diffusion Model.....	6
2.22 The AEC-DRL Accident Diffusion Model	6
2.23 Values of Hourly Average χ/Q from Observed Data	7
2.24 Cumulative Probability of Observed $\Sigma\chi/Q$	11
2.3 Accident Diffusion Model Conservatism Estimates	15
3. Building Wake Effects on Diffusion	17
3.1 Physical Appearance of Diffusion Model Wake Plumes	17
3.2 Wind Tunnel Test of Diffusion in the Indian Point Complex.....	20
4. Turbulence Characteristics Under Low Wind Speed Inversion Condition	23
4.1 Observations at the IP 2 Tower in 1969	23
4.2 Observations at the IP 3 Tower in 1970	25
4.3 Interpretation of Bivane Observations	27
5. Wind Persistence	29
5.1 Persistence Data Taken in 1955	29
5.2 Persistence Data Taken in 1970	31
5.21 Hodographs	31
5.22 Enumeration of Occurrences of Persistence	32

2.6.L-2

TABLE OF CONTENTS, Cont.

	Page
6. Recurrence of Annual Wind Statistics.....	33
7. Plume Behavior Beyond the Site Boundary	34
7.1 Steady Wind	34
7.2 Wind Reversal	35
References.....	37
Tables	39
Figures.....	47
Appendix A. Chronological Review of Events Relating to the Accident Meteorology Models	52

2.6.L-3

LIST OF TABLES

	Page
1. The Con Edison Meteorological Model	39
2. The AEC-DRL Meteorological Model for Pressurized Water Reactors	40
3. Values of $10^4 \sum \chi/Q$ (sec/m ³) According to the Con Edison and AEC-DRL Models for Various Time Periods and Distances	41
4. Values of Hourly Average $10^4 \chi/Q$ at 350 m from the Source During 15 Selected Light Wind Days, July 15 – September 15, 1970	42
5. Values of Hourly Average $10^4 \chi/Q$ at 520 m from the Source During 15 Selected Light Wind Days, July 15 – September 15, 1970	43
6. Values of Hourly Average $10^4 \chi/Q$ at 1100 m from the Source During 15 Selected Light Wind Days, July 15 – September 15, 1970	44
7. Probabilities and Safety Factors in the Con Edison and AEC-DRL Accident Meteorology Models	45
8. Wind Persistence at IP 3 under Inversion Conditions in Combined Sectors 002° and 022° - 040°*	46

* See note on Pg 32 regarding sector notation.

2.6.L-4

LIST OF FIGURES

	Page
1. Cumulative Probability of $\bar{a} c / Q$ for the 0-2 hr Period	47
2. Cumulative Probability of $\bar{a} c / Q$ at 1100 m from the Source	48
3. Annual Wind Direction Distribution	49
4. Wind Direction Distribution According to Temperature Gradient Class	50
5. Wind Direction Distribution According to Speed Class	51

2.6.L-5

Summary

The conservatism of the Con Edison and AEC-DRL accident meteorology models has been investigated for the initial 0-2 hr, 0-8 hr and 0-24 hr periods following the inception of a postulated leak through the containment structure.

Values of σ_c/Q for each model were compared to values calculated for 15 observed wind sequences which represented the longest persistences of lightest winds under inversion conditions in a two-month period. In computing the σ_c/Q for each observed hour, the Con Edison system of assigning stability classifications and selecting diffusion model equations, as described in the Unit 2 FSAR, was employed.

A tabulation of the results may be found in table 7. Roughly speaking, both models gave the same results. The 0-2hr σ_c/Q could be expected to be exceeded about 1% of the time, the 0-24 hr σ_c/Q would never be exceeded. Stated another way, the factor of safety at the 1% probability level was about 1 for the 0-2 hr period and 2 for the 0-24 hr period. At the 5% probability level the factors of safety were about 10 for the 0-2hr period and 3 for the 0-24 hr period. These values varied by about $\pm 25\%$, depending upon distance from the source.

Additional conservatism, apart from the ratios of σ_c/Q cited above, was found to exist in the models, but did not show up in the ratios because the same assumption was used for both the accident models and the observed sequences. This had to do with enhanced lateral diffusion within the Indian Point building complex. Wind tunnel tests were cited to show that lateral diffusion corresponding to about Pasquill C stability, coupled with restricted vertical diffusion,

2.6.L-6

would accurately predict measured concentrations in the wind tunnel. Also, bivane measurements at Indian Point under low speed inversion conditions showed that lateral turbulence increased as vertical temperature gradients increased from 0 to about $6^\circ\text{C}/100\text{ m}$ ($3^\circ\text{F}/88\text{ ft}$), while vertical turbulence was largely unaffected. A diffusion calculation based on the bivane measurements showed that the maximum value of σ_u/Q would occur at a vertical temperature gradient of about $1^\circ\text{C}/100\text{ m}$ ($0.5^\circ\text{F}/88\text{ ft}$), and the corresponding Pasquill stability class at that gradient would be C-D.

Therefore, it appears that the Pasquill F or Con Edison Inversion categories in the accident models should be replaced by Pasquill D or Con Edison Neutral, if the indications of the wind tunnel and field bivane measurements are to be taken as representing the true diffusion condition. Retaining the Inversion category rather than changing to the Neutral in the Con Edison model introduces a factor of safety of about 7 at the 520 m distance.

A detailed analysis of meteorological experiments conducted in 1969 and 1970 at Indian Point to assess the long term variability of annual wind statistics and the details of wind persistence and diurnal reversal of direction confirmed that the 1956 data, used as the basis for the Con Edison accident meteorology model, are still valid today.

2.6.L-7

Introduction

The report reviews and analyzes the meteorological model used in dose calculations for a postulated loss of coolant accident at the Indian Point site, with respect to questions raised by AEC staff meteorologists and consultants and by the AEC Atomic Safety and Licensing Board. Some of these questions have been answered in writing, some were answered orally during the Indian Point Unit 3 Construction permit hearings, and some could not be answered then owing to the lack of on-site experimental data, but can be answered now with data from meteorological experiments performed at Indian Point subsequent to the Unit 3 hearings.

In this report, the questions which appear to require further response are extracted from the record, and the answers are clarified or supplemented as indicated.

Because the documents in this record were filed over a 17 year period in a number of proceedings, a chronological review has been provided in Appendix A for the convenience of the reader.

Frequent reference will be made to the ConEdison and AEC-DRL accident meteorology models. These are presented in Tables 1 and 2.

2.6.L-8

1. Conservatism of the ConEdison and AEC-DRL Accident Meteorology Models As Applied to Indian Point

1.1 General Comments on Quantification of Conservatism

The application of conservatism in the choice of an accident meteorology model involves two concepts; one is probability, the other is factor of safety.

If one anticipates that a series of events of varying severity will occur, and can estimate the probabilities of their occurrences, then one can develop a functional inverse relationship between severity and probability, select an acceptably low probability, and design for the indicated severity.

There may, however, be uncertainty about the magnitudes of various quantities which enter into the specification of the indicated severity, and it may be desirable to design for an arbitrarily greater severity to provide a reserve against this uncertainty. The ratio of the arbitrarily greater severity to the severity dictated by the specified probability may be termed the factor of safety, or often, the factor of ignorance.

The selection of this arbitrarily greater severity may be based on the selection of a lower specified probability to yield a higher indicated severity, but, as frequently happens, sufficient data may not be available to allow extrapolation in this direction. One may then postulate a series of increasingly severe events, each having an intuitively or demonstrably zero probability of occurrence, and base the estimate of degree of conservatism on the magnitude of the factor of safety. This approach carries the implication that an event with the indicated severity will occur at some time, and that the arbitrarily chosen factor of safety will harden the design specifications to compensate for the inherent uncertainties in the design parameters.

2.6.L-9

2.2 Data Analysis

IP3 FSAR UPDATE

In the use of Con Edison and AEC-DRL accident meteorology models, it will be shown that according to past records, neither model has ever occurred in its 30-day entirety. Also, by considering the physics of fluid motions over irregular, non-isothermal terrain, it seems likely that the probability of their ever occurring is virtually zero. However, there is a finite probability that the initial stages of the models will occur. Much of the questioning on meteorology during the IP 3 Construction License hearings was directed toward ascertaining the probabilities and factors of safety during these initial stages, but the answers were inconclusive.

In the following sections, attention will be focused on the 0-2 hr, 0-8 hr, and 0-24 meteorological sequences. The contribution of the 1-30 day sequence to the total dose is so small as not to warrant a detailed investigation.

The general procedure will be to calculate from observed data a curve of the total dilution factor $\Sigma X/Q$ vs cumulative probability of occurrence for 0-2 hr, 0-8 hr and 0-24 hr meteorological sequences, and to calculate the values of $\Sigma X/Q$ according to the Con Edison and AEC-DRL models for the same time periods. From these computations, two estimates of conservatism will be presented:

- a) the probability of occurrence of each of the model predictions,
 - and
 - b) the factor of safety of each of the model predictions, using as a reference the $\Sigma X/Q$ value corresponding to arbitrary indicated low probability levels of 1% and 5%.
- The techniques used in the calculations, and important results, are presented in the following sections.

2.6.L-10

2.21 The Con Edison Accident Diffusion Model

For each hour of the first 24 hours, the dilution factor χ/Q is given by Eq 8, Pg 14.3.5-9

of the Unit 2FSAR⁽¹⁾, with $y = 0$:

$$\frac{\chi}{Q} = \frac{2}{\pi C_y C_z (X+X_0)^{2-n} \bar{u}} \quad (\text{steady wind model}) \quad (1)$$

where

$$\left. \begin{aligned} C_y &= 0.40 \text{ m}^{n/2} \\ C_z &= 0.07 \text{ m}^{n/2} \\ n &= 0.5 \end{aligned} \right\} \text{inversion stability}$$

$$\bar{u} = 1 \text{ m/s for first 2 hours}$$

$$= 2 \text{ m/s for next 22 hours}$$

$$X = 350 \text{ m for Unit 3 site boundary}$$

$$= 520 \text{ m for Unit 2 site boundary}$$

$$= 1100 \text{ m for Units 2 and 3 low population zone}$$

$$X_0 = (A/8C_y C_z)^{1/(2-n)} = 430 \text{ m when } A = 2000 \text{ m}^2$$

For each sequence in the model, the values of χ/Q for each hour calculated by Eq (1), may be summed to yield a χ/Q for the sequence. Sequence values of a χ/Q are given in Table 3.

2.22 The AEC-DRL Accident Diffusion Model

For each hour of the first 8 hours, the dilution factor χ/Q is given in AEC-DRS Safety

Guide 4⁽²⁾ as

$$\frac{\chi}{Q} = \frac{1}{(\pi \sigma_y \sigma_z + cA) \bar{u}} \quad (\text{steady wind model}) \quad (2)$$

With the restriction that $\pi \sigma_y \sigma_z + cA$ must not exceed $3 \pi \sigma_y \sigma_z$. Under conditions of F stability and $cA = 1000 \text{ m}^2$, this restriction becomes effective at distances between 0 and 500 meters from the source.

2.6.L-11

In Eq (2),

$$(\sigma_y \sigma_z) = 83 \text{ m}^2 \text{ at } X = 350 \text{ m}$$

$$165 \text{ m}^2 \text{ at } X = 520 \text{ m}$$

$$570 \text{ m}^2 \text{ at } X = 1100 \text{ m}$$

in F stability

$$\bar{u} = 1 \text{ m/s}$$

$$c = 0.5$$

$$A = 2000 \text{ m}^2$$

For the 9th through the 24th hours, the dilution factor is given by

$$\frac{\chi}{Q} = \frac{\sqrt{2/p}}{S_z X^b} \quad (\text{meandering wind model}) \quad (3)$$

where $\sigma_z = 6.4 \text{ m at } X = 350 \text{ m}$

IP3
FSAR UPDATE

8.8 m at X = 520 m

15.0 m at X = 1100 m

$$\beta = 22.5/57.3 = 0.393$$

Values of \bar{c}/Q are given in Table 3.

2.23 Values of Hourly Average \bar{c}/Q from Observed Data

The data used for this calculation are contained in Figs 10-11 of N.Y.U. Report TR 71-3⁽³⁾.

The meteorological parameters cited therein are as follows:

\bar{u} = wind speed (m/s)

θ = wind direction (deg from N)

$\Delta T = T_{95} - T_7$ (°F), temperature difference between the 95 and 7 ft elevations above

the base of the meteorology tower IP3 whose location is shown in Fig 1 of the above report.

2.6.L-12

The calculation of \bar{c}/Q for each hour was performed using Sutton Diffusion models with diffusion parameters given on Pg 14.3.5-9 of the Unit 2 FSAR. Two diffusion models are involved; one is the steady wind model described by Eq (1). The other is a meandering wind model similar to Eq (3) but written in the Sutton form and including a wide-plume factor. This wide-plume factor has not appeared in the various Con Edison submittals to the AEC-DRL. Its omission leads to illogical concentration predictions for meandering plumes, noted in the ESSA-AREL Comment on Pg 95 in Appendix C to the AEC-DRL Safety Evaluation of Unit 2⁽⁴⁾.

The meandering wind model used in this report is that shown on Pg Q11.10-1 of the Unit 2 FSAR multiplied by the wide-plume factor. Under conditions such that the plume centerline meanders uniformly within the sector boundaries during one entire hour, the equation for the hourly average \bar{c}/Q (using present notation) may be written as

$$\frac{\bar{c}}{Q} = \frac{2}{b\sqrt{p}} \frac{W}{\bar{u} C_y X (X + X_o)^{(1-n/2)}} \quad (4)$$

where

$$W = \frac{1}{\sqrt{2p}} \int_{-P}^{+P} \exp(-p^2/2) dp$$

and $P = Xb/2s_y = xb/\sqrt{2} C_y (X + X_o)^{1-n/2}$

Values of W may be found in Fig A-4 of "Workbook of Atmospheric Dispersion Estimates" by D. B. Turner⁽⁵⁾ for corresponding values of P .

The factor W has a value of unity when the plume width is less than the sector width. For example, assuming that the plume width is equal to $5s_y$,

2.6.L-13

and the sector width is equal to $X\beta$ then P is greater than 2.5 when $5s_y$ is less than $X\beta$. From Turner's Workbook, W is seen to have a value of .987 at $P = 2.5$ and to approach unity as P increases (corresponding to a narrowing plume).

When the plume is wider than the sector, P becomes less than 2.5 and W becomes increasingly smaller as the plume width increases.

The omission of W from published versions of the sector-averaged diffusion equation carries with it the implication that the plume width is smaller than the sector width. This is often true for inversions, particularly at large distances from the source, but it is generally not true for volume sources with wakes in neutral and lapse conditions.

Values of P and W for various stability and distances are given below:

	350			520			1100		
X(m)									
Stability	I	N	L ₁	I	N	L ₁	I	N	L ₁
X ₀ (m)	430	92	43	430	92	43	430	92	43
X + X ₀ (m)	780	449	393	950	612	563	1530	1192	1143
n	.5	.4	.2	.5	.4	.2	.5	.4	.2
C _y	.40	.47	.60	.40	.47	.60	.40	.47	.60
P	1.48	1.41	.67	1.76	1.62	.67	2.08	2.03	.81
W	.87	.85	.50	.92	.90	.50	.99	.95	.59

Inclusion of the wide plume factor in the meandering plume equation eliminates the anomaly of yielding a sector-average concentration that is greater than the steady concentration for all stabilities and wake corrections.

In applying the diffusion models to the observed data, it is necessary to translate ΔT into stability, and to specify whether the plume is steady or meandering during a given hour.

2.6.L-14

The Con Edison system for defining stability in terms of temperature gradients was defined by B. Davidson in N. Y. U. Tech. Rep. 372.3, which is included as Pgs. Q26-Q43 of Sec. 2.6 of the Unit 2 FSAR⁽¹⁾. Davidson divided the temperature gradient spectrum into three parts using the isothermal (0°F/1000 ft) and adiabatic (-5.5°F/1000 ft) temperature gradients as dividers. This yielded three stability categories lapse (L), neutral (N) and inversion (I). The L category was further subdivided into a light wind lapse (L₁) for wind speeds of 1-3 m/s and a strong wind lapse (L₂) for wind speeds > 4 m/s.

For the data from the IP3 tower, reported in N.Y.U. Rep. TR71-3⁽³⁾, the ΔT corresponding to an adiabatic lapse rate over a height interval of $95-7=88$ ft was -0.48°F . Accordingly, observations were assigned stability categories as follows:

inversion I	$0 < \Delta T$
neutral N	$-0.5^\circ\text{F} < \Delta T < 0$
lapse L ₁	$\Delta T < -0.5^\circ\text{F}$

The L₁ lapse was assumed since most of the wind speeds of interest were less than 4 m/s.

Meander was estimated from the progression of wind directions in Fig 11 of N.Y.U. Rep. TR-71-3⁽³⁾. Each data point represents an average wind direction for an even-numbered hour. The average wind directions during the odd-numbered hours were estimated by arithmetical averaging of adjacent even-hour values. If the difference between the two odd-hour wind directions straddling a given even hour was greater than 20° , the wind was presumed to have meandered during the even hour, and the dilution factor was calculated according to Eq (4).

2.6.L-15

If the odd-hour difference was less than 20° , the wind was assumed to have been steady, and Eq (1) was used. Steady plumes occurred 75% of the time.

On several occasions, ΔT data were missing. These hours were assigned I stability if the wind speed was less than 2 m/s and the wind meandered. N stability was used for all other cases. (See Section 4 for a discussion of stability under low speed inversion conditions.)

2.24 Cumulative Probability of Observed $\hat{\sigma}X/Q$.

Cumulative probability is derived by summing the frequency distribution from the tail end, representing zero or small probability, toward the center. The small probabilities are associated with very high values of hourly $\hat{\sigma}X/Q$, and these in turn are associated with light winds and inversion stability.

Inasmuch as we are interested in obtaining information regarding $\hat{\sigma}X/Q$ values at very low probabilities, it is not necessary to obtain the complete frequency distribution under all wind conditions. It is sufficient to make sure that all the high $\hat{\sigma}X/Q$ hours appear in the data base.

Figs 10a-d of N.Y.U. Rep TR 71-3⁽³⁾ show the wind behavior at IP 3 on all of the days in a two-month period when the geostrophic wind was virtually zero. This means that the wind-driven circulation in the valley was absent, and the resulting wind motions were due primarily to density currents originating along the valley slopes. These are the lightest winds possible in a valley system. Therefore, a cumulative frequency distribution in the low probability range, based on wind behavior during these days, should be essentially the same as a distribution which includes the days on which the wind-driven circulation is strong.

2.6.L-16

Fig 11 shows only those hours of Figs 10a-d when the wind fell into the 000° - 045° sector. The joint values of speed \bar{u} , direction θ , and temperature difference ΔT are given in the Figure at each data point.

The data base in Fig 11 includes 15 days of light winds during the two month period of July 15-Sept 15, 1970. This period was chosen because the tests were designed to duplicate, as closely as possible, similar experiments conducted at Indian Point during Sept.-Oct. 1955 and included in Sec 2.62 of the Unit 2 FSAR⁽¹⁾.

An analysis which surveys only two months out of a year may be criticized as being unrepresentative. However, to quote from Pg 2.6-3 of the Unit 2 FSAR⁽¹⁾: "In general, these local winds are most frequent under clear sky and relatively light prevailing wind conditions such as occur mostly in the fall of the year." Again, on Pg 2.6-6: "It is concluded that the "worst

meteorological conditions are associated with the nocturnal down-valley flow which is most frequent during September and October.”

The 1955 data include 12 days in which the large scale flow was virtually zero and 35 days in which the large scale flow was less than 16 mph. It is not known whether these are overlapping statements, but it seems likely that at least 50 days were included in the sample. Thus, the frequency of occurrence for the virtually zero flow was $12/50 = 25\%$ in 1955.

The 1970 data also show a frequency of $15/60 = 25\%$. Therefore, it seems likely that the 1970 tests were made in a period of high frequency of light winds, and that a sample taken throughout the year would show a lower average frequency. Consequently, use of the 1970 2-month data base is a conservative procedure.

2.6.L-17

The first step in the calculation was determine the individual values of χ/Q for each of the data points in Fig 11 of N.Y.U. Rep TR71-3⁽³⁾, according to the diffusion models and classification procedures described in the previous section. Tables 4, 5 and 6 show the results. A zero value of χ/Q was assigned to those hours not shown as data points, since the wind was out of the critical sector during those hours.

The next step was to accumulate these single-hour values χ/Q in 2 hr, 8 hr and 24 hr sequences, starting at each of the 24 hours in a day. For the 2 hr and 8 hr sequences, values of χ/Q for the odd hours were estimated by arithmetically averaging the adjacent even hour values. Then individual sequence accumulations of χ/Q , designated S_i^{l+n-1} where l = starting hour and n = number of hours in the sequence, were calculated, and a cumulative probability distribution made based on a sample population of $24 \times 60 = 1440$ possible sequence accumulations in the two month period. For the 24 hr sequences, S_i^{l+n-1} was assumed equal to twice the sum of the even-hour χ/Q values for a particular day, and 24 of these equal sums appeared each day.

An element of conservatism was introduced into the above calculation by simply adding the hourly χ/Q values in each sequence. In actuality, these hourly χ/Q values occur only on the plume centerline for steady plumes, although they occur anywhere in the sector for meandering plumes. However, the plume centerlines do not lie in the same direction during each hour of the 60 day period. Therefore, a fixed sampling point at the site boundary or low population zone would experience concentrations varying from the hourly χ/Q shown in Table 3 to zero, depending upon the direction of the steady plume axis.

2.6.L-18

Examination of the 15 useful cases in Fig 11 of N.Y.U. Rep TR 71-3⁽³⁾ shows that the mean wind direction for all data points was 026° and the standard deviation was 4.7° . If the distribution of wind directions were normal, this would correspond to a probability of 96% that the winds would fall in a $\pm 10^\circ$ sector about the mean. Thus, the plume centerlines appear to have been normally distributed in a 20° sector centered on 026° .

The reduction factor for long time plume centerline concentrations with short time centerline fluctuations may be estimated by Eq 3.120 in “Meteorology and Atomic Energy” by D. H. Slade, ed, 1968⁽⁶⁾, as $Y^2/(Y^2 + D^2)$, where Y^2 may be taken as the lateral variance of the steady inversion plume and D^2 — the variance of the centerline fluctuations. These quantities are given for the inversion case by:

$$\overline{Y^2} \approx \sigma_y^2 = C_y^2 (X + X_o)^{2-n} / 2 = 0.08 (X + 430)^{1.5}$$

and

$$\overline{D^2} = (4.7 X / 57.3)^2 = 0.0067 X^2$$

the reduction factor is tabulated below for several distances:

dist X (m)	350	520	1100
reduction factor	0.67	0.56	0.37

Figs 1 and 2 show the cumulative probability distribution of for three time periods and $\bar{a} c / Q$ three distances from the source. They represent the simple addition of plume centerline values for the steady plumes, and sector average values for the meandering plumes. Application of the centerline fluctuation factor described in the preceding paragraph would lower the $\bar{a} c / Q$ values at the

2.6.L-19

same probability levels. The amount of the reduction would be somewhat less than the values shown because only 75% of the plumes were steady.

2.3 Accident Diffusion Model Conservatism Estimates

When the Con Edison and AEX-DRL accident model $\bar{a} c / Q$ values from Table 3 are marked on the appropriate curves of Figs 1 and 2, one may estimate the probability levels and factors of safety which were described in Sec 2.1. Table 7 lists these values.

For the 0-2 hr period, the Con Edison model $\bar{a} c / Q$ is exceeded about 0.7% of the time at the average site boundary distance. The AEC-DRL model $\bar{a} c / Q$, being lower, is exceeded about 1.1% of the time. At the low population zone, $x = 1100m$, both model $\bar{a} c / Q$ values are exceeded at about the 0.5% probability level.

For the 0-8 hr period at the low population zone boundary, the Con Edison model $\bar{a} c / Q$ is exceeded 0.7% of the time, whereas the AEC-DRL model is never exceeded. This is due primarily to the AEC-DRL specification of a 1 m/s wind speed during the 2-8 hr period.

For the 0-24 hr period, neither the Con Edison nor the AEC-DRL model $\bar{a} c / Q$ values are ever exceeded. This is due primarily to the omission in both models of the diurnal wind direction reversal which removes the plume from the design sector for a large part of each day. According to Fig 11 of N.Y.U. Rep. TR 71-3⁽³⁾, the longest occasion of wind duration in the sector during a given day was 10 hours, with an average of 7.0 hrs and a standard deviation of 2.65 hrs. Thus the observed 10 hr maximum duration may be expected to occur 75% of the time, and a maximum duration of 14 hrs may be expected to occur 99% of the time if the durations are assumed to be normally distributed.

2.6.L-20

The factors of safety in Table 7 are defined by

$$\text{factor of safety} = \frac{\text{model } \Sigma \gamma / Q}{\text{observed } \Sigma \gamma / Q \text{ at specified probability level}}$$

The two models show about the same factors of safety at the 1% probability level for all distances and time periods, except that the AEC-DRL model shows more conservatism in the 0-8 hr period, due to its use of a 1 m/s wind speed in the 2-6 hr interval while the Con Edison model uses a 2 m/s speed for the same interval. Similar points of similarity and disagreement between the models occur at the 5% probability level.

At the 5% probability level, the two models show about the same agreement and disagreement with respect to factors of safety as appears at the 1% probability level. However, the factors of safety are higher by about 6-10 times for the 0-2 hr period. This reduces to about 2.5 times for the 0-8 hr period and 1.5 times for the 0-24 hr period.

It should be remembered that these factors of safety apply to χ/Q values, or to concentrations if the source strength remains constant throughout the sampling period and no decay occurs in transit from source to sample point. In theory, the source strength will be a rapidly decreasing function of time, due to operations within containment, initiated at the time of occurrence of the accident. Therefore, if the curves of Fig 2 and the corresponding data in Table 7 are to be used for predicting probabilities and factors of safety for cumulative concentration $\sum\chi$, appropriate adjustment must be made for the behavior of Q with time.

2.6.L-21

3. Building Wake Effects in Diffusion

3.1 Physical Appearance of Diffusion Model Wake Plumes

It is often useful to visualize plume behavior by determining the plume boundary in space. This is particularly helpful in wake diffusion estimates. The Con Edison and AEC-DRL accident meteorology models both incorporate wake diffusion parameters whose effect on the plume shape is not immediately seen. In this section, the wake plumes as described by the diffusion models, and as observed in wind tunnel and field tests, will be compared.

The Con Edison wake diffusion model employed a virtual displacement of the point source to a location upwind of the building. This has the effect of increasing the distance available for the plume to grow laterally and vertically before it reaches a given station downwind of the building. The increased transverse dimensions allow the matter in the plume to be distributed over a wider cross-sectional area, and the average concentration is thereby reduced at that station.

The calculation of the vertical point displacement distance for the Con Edison diffusion model is described on Pgs 14.3.5-8 and 14.3.5-9 of the Unit 2 FSAR⁽¹⁾. Analytically its value is given by

$$X_o = (A/8 C_y C_z)^{1/(2-n)} \quad (5)$$

where A is the building area projected in the direction of the wind and C_y , C_z and n are the Sutton diffusion parameters.

The shape of the plume boundary between the virtual source and the building is irrelevant since the plume is non-existent in this region. The shape of the boundary at large distances downwind of the building is that of a simple plume from a ground level continuous point source, i.e. elliptical in cross-section with the horizontal axis at the ground surface. At the building location

2.6.L-22

the real plume boundary must be that of the building wake. Between the building and some distance downwind, the plume boundary changes shape gradually from that of the building wake to that of the undisturbed plume.

The virtual source displacement method does not define the plume boundary at the building, and its characterization of the boundary shape takes on increasing reality with distance downwind from the building. However, it is interesting to compare the hypothetical elliptical plume dimensions with the building dimensions at the building location.

Although the Con Edison diffusion model utilizes the Sutton equations, the concentration distribution in any cross-section is bi-gaussian, and the Sutton parameters are related to the gaussian plume parameters by

$$\sigma_y = C_y X^{(2-n)/2} \quad (6)$$

and

$$\sigma_z = C_z X^{(2-n)/2}$$

Eq (5) derives from Eq (6) when the assumption

$$4\sigma_y = 4\sigma_z = \sqrt{A} \quad (7)$$

is made. However, the equality of σ_y and σ_z implied by (7) indicates that the plume boundary at the building is a circle, as a special case of an ellipse. Since no specification is made of the building shape, one may assume that the projected cross-section of the building is an approximate semi-circle, with radius R_B equal to the building height. This leads to $A = \pi R_B^2/2$ and

$$\sqrt{A} = \quad 2.6.L-23$$

$\sigma_y = \sigma_z = \sqrt{A}/4 = 0.31R_B$. Now assuming as is commonly done, that a gaussian plume boundary lies at 2.5 σ , the plume boundary radius becomes $R_P = 2.5 (0.31/R_B) \cong 0.08R_B$.

This result is not far from reality for a hemispherical building, as may be seen by examining the photographs in Fig 5.23 of Meteorology and Atomic Energy.⁽⁶⁾ For rounded building surfaces, the wake seems to form downwind of the building centerline, especially so for high Reynolds Numbers, and the effective wake radius is smaller than the building radius.

For sharp-edged buildings, however, the wake boundary is larger than the building radius. For example, Fig 5.18 of Meteorology and Atomic Energy shows the cavity and wake downwind of a sharp-edged square plate with the cavity boundary at about 2 plate half-widths above the plate half-widths above the plate centerline. Other experiments described in the same chapter of Meteorology and Atomic Energy⁽⁶⁾ show that the wake boundary for a sharp edged building is about 1.5 building heights above the ground. If considerable roughness exists around the base of the building so that flow is retarded in the lower layers near the ground, the wake height is reduced.

Therefore, it seems that the virtual point source displacement calculation given by Eq (1) is realistic for rounded buildings and conservative for sharp-edged buildings, with respect to replication of the plume dimensions at the building.

The AEC-DRL⁽²⁾ wake model sets $\sigma_y \sigma_z = cA/\pi$ at the building. If $A =$

$\pi R_B^2/2$ and $\sigma_y = \sigma_z$ as before, $\sigma_y = \sigma_z = \sqrt{c/2} R_B$ and $R_p = 2.5 \sqrt{c/2} R_B = 1.77 \sqrt{c} R_B$.

Using the AEC- DRL⁽²⁾ shape $c = 0.5$, we obtain $R_p = 1.25 R_B$.

Therefore, the AEC-DRL wake plume boundary at the building appears to be less conservative but more realistic than the Con Edison wake plume boundary at the same location.

2.6.L-24

The greatest element of conservatism in both wake models is the use of the cross-sectional area of the reactor building alone as the numerical value of A . At a real site, the reactor building may have contiguous auxiliary buildings and lie in a complex of other buildings. Matter released into the atmosphere from the reactor building will diffuse into the composite wake of the reactor and auxiliary buildings, and may disperse laterally and even upwind into the wakes of other buildings in the complex. Therefore, the effective cross-sectional area which characterizes the wake at the building should be based on the probable plume boundary dimensions near the reactor building rather than the area of the building alone. Unfortunately, no systematic study of this aspect is available as a basis for formulating a more liberal rule.

3.2 Wind Tunnel Test of Diffusion in the Indian Point Complex.

Some information regarding the behavior of gas released in a building complex with restricted vertical diffusion potential was obtained in a wind tunnel test of a topographical model of the Indian Point reactor complex. The study was reported in

“Wind Tunnel Test of Gas Dispersion From Indian Point Unit 1” by James Halitsky, June 29, 1971,⁽⁷⁾

and was submitted to the AEC-DRL in connection with a safety analysis of the Unit 1 stack under tornado wind loadings.

In this test, the model was oriented in the 020° wind direction, the tunnel wind stream was isothermal, and had low turbulence (<1%) and uniform mean velocity everywhere except in the floor, ceiling and wall boundary layers. Tests were conducted at prototype wind speeds of 6.7 and 11.1 m/s which, with

2.6.L-25

Froude Number scaling and model linear scale of 1:360, mandated tunnel velocities of 0.35 m/s and 0.58 m/s, respectively. SO₂ tracer gas was released at ground level just downwind of the Unit 1 reactor shell, and sampled on the tunnel centerline at prototype downwind distances of 305m, 610m, and 1100m from the Unit 1 Stack, and at prototype elevations of 2m, 16m, 30 m, 45m, 74m, 103m, 131m, and 160m above local ground at each downwind location.

From the vertical concentration traverses (fig 18 of the reference) it was found that the gas had diffused upward through the entire surface boundary layer by the time it reached the first longitudinal station (305m), and did not diffuse farther vertically with additional distance downwind. The boundary layer height (and plume depth) was about 90m above local ground. Suppression of further upward diffusion was caused by the existence of very low turbulence (equivalent to Pasquill Type E stability) in the free stream.

The lateral plume boundary distance may be calculated from knowledge of the measured value of $\chi \bar{u}/Q$ at the ground and the value of σ_z , which may be assumed to have been $90/2.5 = 36\text{m}$ since the vertical concentration profiles were approximately gaussian in shape. The observed data for the test, and the corresponding σ_y values, calculated with

$$\chi \bar{u}/Q = [\pi \sigma_y \sigma_z]^{-1} \quad (8)$$

are shown below:

distance (m)	305	610	1100
$\chi \bar{u}/Q \text{ (m}^{-2}\text{) (observed)}$	2.2×10^{-4}	1.0×10^{-4}	0.8×10^{-4}
$\sigma_z (= 90/2.5)\text{m (observed)}$	36	36	36
$\sigma_y \text{ (m) calculated}$	39	38	111

2.6.L-26

The above observed values may be replicated by calculation with fair accuracy by using Eq (8) with a fixed σ_z , and assuming a Pasquill stability class slightly more unstable than C, for σ_y . The following table shows the calculated values:

distance (m)	305	610	1100
$\chi \bar{u}/Q \text{ (m}^{-2}\text{) (calculated)}$	2.3×10^{-4}	1.2×10^{-4}	0.7×10^{-4}
$\sigma_z \text{ (m) (assumed)}$	36	36	36
$\sigma_y \text{ (m) (assumed C}^+\text{)}$	39	73	130

The plume behavior in this test is an example of the mixed type of diffusion process which takes place in the atmosphere when vertical diffusion is suppressed by inversion temperature gradients while horizontal diffusion is uninhibited and, in fact, may be augmented by slope density currents and mechanical turbulence generated by wind passage between buildings and other structures in a reactor complex.

Attempts were made to fit the Con Edison and AEC-DRL wake models to the observed tunnel plume behavior, but were unsuccessful. It appears that neither the vertical source displacement nor the volume wake correction, which work well for discrete buildings, is applicable to diffusion in building complexes.

2.6.L-27

4. Turbulence Characteristics Under Low Wind Speed Inversion Conditions.

4.1 Observations at the IP 2 Tower in 1969

IP3
FSAR UPDATE

From September 1968 to May 1969, wind data were measured at three locations in the Hudson River Valley at and near Indian Point, to aid in selection of a site for proposed new nuclear power units. A report of this investigation is contained in NYU Report TR 70-3⁽⁸⁾.

The locations of the three towers, designated by the symbols IP2, MP and BP respectively, are shown in Figs 1-5 of TR 70-3. Of particular significance to the present study is an analysis, contained in TR 70-3, of the wind behavior at the IP 2 tower during periods of upper air stagnation.

The IP2 tower was located 305m southwest of Unit 3 on a cleared strip of ground which sloped down in a westerly direction to the Hudson River. The base of the 100 ft tower was at elevation 60 ft above river elevation. The tower was equipped with sensitive wind speed and direction sensors at 100 ft above local ground, and temperature difference sensors at 95 ft and 5 ft above local ground.

Figs 11-13 of TR 70-3 show simultaneous measurements of hourly mean wind speed, wind direction, temperature difference and wind direction range/4.3 for three periods of upper air stagnation during April and May 1969. During seven nights of these periods, the wind behavior approached the type assumed in both the Con Edison and AEC-DRL 2-hr accident meteorology models, exhibiting low wind speed and temperature inversion, but did not exhibit directional steadiness either within an hour or from hour to hour.

Directional steadiness within an hour is usually identified by a

2.6.L-28

small standard deviation of 15-sec average directional angles about the hourly mean direction. It has been observed by Slade in "Meteorology and Atomic Energy, 1968", Sec. 3-3.4.1, ⁽⁶⁾ that the Pasquill stability categories may be associated with typical numerical values of the standard deviation as follows:

<u>Pasquill Stability Class</u>	<u>Std. Deviation σ_θ</u>
A	25°
B	20°
C	15°
D	10°
E	5°
F	2.5°

Applying Slade's classification system to observations of direction range/ 4.3 . σ_θ) during the seven night periods under consideration, it was found that the observed hourly stabilities varied from A to F, with an average of about C or D, even though a temperature inversion was always present. Thus, on the average, a considerable amount of unsteadiness was present during an average hour.

The effect of wind unsteadiness (high σ_θ) on dispersion is to reduce concentrations to values below those which would occur under steady conditions (low σ_θ). For example, using Slade's Fig A.2, it is readily seen that a change from F stability to D stability would increase σ_y by a factor of 2 at a distance of 1100 m and thereby decrease, $\chi u / Q = [\pi \sigma_y \sigma_z]^{-1}$ a factor of 2, even

2.6.L-29

if σ_z should remain unchanged. By comparing σ_z values in F and D stabilities, it is seen that an additional reduction in concentration by a factor of 2 would occur if the vertical unsteadiness changed in proportion to the lateral unsteadiness.

Thus, it is important in evaluating conservatism to establish realistic stability classifications in both the vertical and horizontal directions.

4.2 Observations at the IP 3 Tower in 1970

4.3

When the Indian Point meteorology tower was moved from the IP 2 location to the IP 3 location in late 1969, a bivane was added at IP 3 to provide additional data on low speed inversion stability characteristics. Data were reported in NYU Report TR 71-10⁽⁹⁾.

The bivane was equipped with a switching device which allowed the strip chart recorder to run at 3 in/min for 10 minutes each hour, and at 3 in/hr during the remainder of the hour. The recorder was operated at various intervals from May to December 1970. The intervals, which were 30 hours long, were determined according to the expectation of low wind speeds and by the availability of personnel. A total of 153 hours for which concurrent speed, direction and vertical temperature difference were available, and the speed was less than 2 m/s, formed the data base.

The most important conclusions of the study were:

IP3
FSAR UPDATE

a) Under inversion conditions, the standard deviation of azimuth angles (σ_θ) increased with wind speed to 1.4 m/s and then decreased, with the following values of σ_θ and equivalent Pasquill stability class according to Slade's system: (from Fig 1 of TR 71-10):

2.6.L-30

No. of Observ.	Speed	5-Sec Smoothing		200-Sec Smoothing	
	Range (m/s)	σ_θ (deg)	Stability	σ_θ (deg)	Stability
3	0-0.4	9	D	7	DE
5	0.4-0.8	12	CD	10	D
12	0.8-1.2	16	C	15	C
17	1.2-1.6	18	BC	13	CD
17	1.6-2.0	9	D	4	E

The 5-sec smoothing period better approximates Slade's procedure than the 200 sec smoothing period.

b) Under the same inversion and speed categories as above, the standard deviation of elevation angles, σ_θ , remained about constant at 6-7° over the entire range of speeds.

c) A breakdown of the above according to wind direction sectors showed a minimum σ_θ of 8° (DE stability) to occur in the 340° - 040° wind sector, with a corresponding σ_ϕ of 6°, for 5 sec smoothing.

d) Under inversion conditions, both σ_θ and s_f increased with $\Delta T = T_{95} - T_5$ (°F) in the 340° - 040° wind sector as follows:

No. of Observ.	ΔT Range (°F)	σ_θ (deg)	5-Sec Smoothing	
			Stability Class	σ_ϕ (deg)
10	0-1	8	DE	6
7	1-2	9	D	7

6 2-3 20 B 9

2.6.L-31

e) A calculation of $\chi \bar{u}/Q$ by the method of Hay and Pasquill in Advances in Geophysics (6) Academic Press pp 345-365⁽¹⁰⁾, using data for the 340° - 040° wind sector, shows the following at a distance of 1100 m and $\bar{u} = 1.85$ m/s:

$\Delta T(^{\circ}\text{F})$	Values of $10^4 \chi \bar{u}/Q$	
	Steady	Meander
0	0.7	0.4
0.5	0.8	0.4
1.0	0.7	0.4
1.5	0.4	0.3
2.0	0.2	0.2

A concentration maximum occurs at a ΔT of 0.5°F .

4.4 Interpretation of Bivane Observations

The behavior of the bivane can be attributed to the development of katabatic winds, or down-slope currents, under inversion conditions. These currents are caused by cooling of slope air near the ground. This air becomes more dense than air over the floor of the valley, resulting in local pressure differences which cause drainage of air down the slopes.

Over irregular terrain, non-parallel descending currents impinge on one another, creating irregular motions in both the horizontal and vertical directions. However, the horizontal motions are unconstrained, while the vertical motions are suppressed by the inversion. Therefore the effects of the slope currents show up strongly in enhanced horizontal turbulence (σ_{θ}) but have only a small effect on vertical turbulence (σ_{ϕ}).

2.6.L-32

The bivane observations show that, in the 340° - 040° sector, maximum turbulence levels of $\sigma_\phi \approx 18^\circ$ and $\sigma_\phi \approx 9^\circ$ occur with wind speeds near 1.4 m/s and vertical temperature differences of about 2.5 ° F. Turbulence levels fall off at wind speeds above and below 1.4 m/s. The temperature difference accompanying speeds greater than 1.4 m/s must have been equal to or less than 2.5 ° F since Table IV of TR 71-10 shows no observations >3.0 ° F in this sector. This may indicate the existence of extra-valley influences in creating higher wind speeds that are not thermally-generated.

The high turbulence level at a wind speed of 1.4 m/s and $\Delta T = 2.5^\circ$ produces a $\chi \bar{u}/Q$ equivalent to a Pasquill type A-B stability (See Table XI).

As ΔT reduces, \bar{u} , σ_θ and σ_ϕ also reduce, causing an increase in $\chi \bar{u}/Q$ to a maximum at $\Delta T = 0.5^\circ$ where the equivalent Pasquill stability is C-D.

Thus, the bivane data confirm the applicability of the Pasquill C-D stability class at near-neutral temperature stratification, even in irregular terrain. However, the customary increase of stability class with increasing temperature gradient, which is valid for level ground, is not valid at this site. On the contrary, the effective stability decreases with increasing temperature gradient at least up to a $\Delta T = 3^\circ$ F. Similar behavior was observed at the IP 2 tower during the previous year.

It appears that the assignment of I stability to those hours which exhibited inversion temperature stratification in the calculation of hourly average χ/Q from observed data in Sec 2.23 is extremely conservative, and that a more realistic rule would be to use N stability instead.

2.6.L-33

5. Wind Persistence

Wind persistence is a measure of steadiness of wind direction with increasing time. It is important in accident meteorology because invariance of wind direction exposes a stationary subject on the plume centerline to the highest concentration for the longest period, under given conditions of source strength and wind speed.

Both the Con Edison and AEC-DRL accident meteorology models postulate that the hypothetical accident occurs at the onset of a 24-hr period of strong wind persistence. Both models assume a steady hourly mean wind direction for the first 8 hours. For the next 16 hours, the Con Edison model retains steadiness, while the AEC-DRL model permits uniform direction meander within a 22½ ° wind sector. Although the Con Edison model is more stringent with respect to direction in the latter period, it also assumes a higher wind speed, thereby making the hourly average χ/Q values about the same for both models.

It is generally recognized that a correlation exists between strong wind speeds and long periods of persistence.⁽¹⁵⁾ However, the accident models assume light wind speeds (<2 m/s) and inversion conditions during the 0-24 hr period. The probability of occurrence of long periods of persistence under these conditions is examined in the following sections.

5.1 Persistence Data Taken in 1955

On Pg 2.6-4 of the Unit 2 FSAR, experiments are cited to show that “... a consecutive 24 hour down-valley flow with light wind speeds and inversion conditions is extremely improbable ...”, that the “... duration of the down-valley flow is about 12 hours rather than 24 hours, ...” and

that "... it must be concluded that the safety analysis for the first 24 hours is conservative to within a factor of about two ...", since the average speeds assumed in the model are about the same as those observed at the site.

2.6.L-34

The experiments referred to above were measurements taken in Sept.-Oct. 1955 with an Aerovane mounted 70 ft above the Hudson River on the mast of a ship, the Jones, whose location is shown in Figs 1-3 of NYU Rep TR 71-3⁽³⁾ at the point marked J. The data taken during the experiments were presented in Figs 2.6-1, 2.6-2 and 2.6-3 of the Unit 2 FSAR.

Figs 2.6-1 and 2.6-2 are wind hodographs, or polar coordinate representations of the behavior of the wind velocity vector during a 24 hour diurnal cycle. Fig 2.6-3 is a graph of wind steadiness, defined as the ratio (mean vector wind speed)/(mean scalar wind speed) vs time of day.

All three Figures present the averages of measurements taken on 12 days and 35 days during the test period. The procedure of basing the accident meteorology model on the average condition rather than on some less frequent but more severe condition has been criticized as not being sufficiently conservative (see Appendix C to the AEC-DRL Safety Evaluation for the Unit 2 Operational License hearing, and Appendix C to the AEC-DRL Safety Evaluation for the Unit 3 Construction License Hearing).⁽¹¹⁾

Also somewhat misleading is the placement of the coordinate center for the hodographs in Figs 2.6-1 and 2.6-2 at the Unit 2 reactor building, rather than at the Jones, which was located about a mile to the north.

The questions regarding individual, rather than average, wind characteristics, and possible differences between characteristics at the Jones and at the plant site, could not be resolved because the original data were no longer available.

2.6.L-35

5.2 Persistence Data Taken in 1970

5.2.1 Hodographs

In 1970, experiments were undertaken to duplicate as closely as possible the 1955 experiments at the Jones and to obtain concurrent data for the ship and plant locations. Results were presented in NYU Report TR 71-3.⁽³⁾

An Aerovane was mounted on the Cape Charles, which was anchored about 350 m SW of the former location of the Jones (at point CC in Figs 2-4 of Report TR 71-3). A sensitive Climet cup and vane anemometer was mounted on the IP 3 tower.

It was found that the average wind hodograph at the ships, separated by 14 years in time, were very similar, exhibiting the same diurnal reversal pattern and the same 2.5 m/sec nighttime downvalley speed in both years. It seems clear that the diurnal reversal of direction is a characteristic of the site and can be expected to occur every year.

The average wind hodograph at IP 3 showed a similar pattern of diurnal reversal, but the average nighttime downvalley speed was somewhat less than 2 m/s.

All sixteen daily wind hodographs at IP 3 showed the diurnal reversal, and exhibited considerable variability in speed and direction from day to day through a complete cycle. The

longest period of direction persistence was 8 hrs, occurring on each of 5 nights, and the average wind speed during each period was least 2 m/s.

Further analysis of wind behavior during these and other low speed inversion days is presented in Sections 2.23 and 4.2 of this report.

2.6.L-36

5.22 numeration of Occurrences of Persistence

Also presented in Report TR 71-3 is a listing of the number of occurrences that wind of specified characteristics persisted for a specified number of consecutive hours during the entire 10-month test period in 1969-70. The data of Table 1 of Report TR 71-3, showing persistence under inversion conditions for the 002° - 022° and 022° - 042° sectors* taken separately, are shown combined in Table 8 of this report. Also shown are comparable data taken during 12 months of calendar year 1971 (previously unpublished).

The two sets of data show that:

- a) persistence increases with wind speed,
- b) the probability of finding 2 consecutive hours when the wind speed is 1 m/s or less in the 40° wide sector under inversion conditions is extremely small (2 hours in 5989 or 0.03% during 1969-70 and 0 in 1971),
- c) the probability of finding 2 consecutive hours when the wind speed is 2 m/s or less under the same conditions as above was 7 hours in 5989 or 0.11% during 1969-70, and 60 hours in 5560 or 1.1% in 1971,
- d) no persistences longer than 7 consecutive hours occurred in either year, for wind speeds less than 3 m/s.

The above figures are based on occurrences of wind direction somewhere in a 40° sector. It is likely that a more stringent definition of steadiness would reduce the probabilities even further.

*Wind direction sectors are identified in this report by the wind angles at the sector boundaries; the difference between these boundary angles is the sector width of 20° . In the Unit 2 FSAR and early NYU reports, sectors are identified according to the range of wind observations as read to the nearest 5° from wind charts. Thus, wind sector 002° - 022° in this report corresponds to wind sector 005° - 020° in FSAR.

2.6.L-37

6. Recurrence of Annual Wind Statistics

Fig 3 shows the annual distribution of wind direction for 1956, 1957 (from NYU Report 372.4, Pg R-6 of Sec 2.6 of the Unit 2 FSAR) and for 1970 and 1971 (unpublished).

The bi-modal character of the distribution occurs in each of the years, and the fraction of time that the wind is in the critical 002° - 022° sector remains relatively constant in all four years.

The most noticeable change is a re-distribution of some southerly (160° - 200°) and north-westerly (290° - 360°) winds to the easterly and westerly sectors. Neither of these changes is a matter for concern since easterly winds carry releases over the river and westerly winds carry them toward a more distant site boundary.

Fig 4 shows the wind direction distribution in each temperature gradient class for 1956, 1970 and 1971. The 1956 curves represent data in Table 3.3 of NYU Rep. 372.3, (Pgs Q-39 and 40 of Sec 2.6 of the Unit 2 FSAR). The 1970 and 1971 data have not been published as yet. The 1956 wind statistics appear to be representative of a typical year. Therefore the stability mix used in the 1-30 day period of the accident model, which was selected on the basis of the 1956 statistics, is still valid.

Fig 5 shows a small decrease in the frequency of light wind speeds (02- m/s) in the critical sector. The shift of southerly winds toward the southeast seems to be accompanied by an increase in wind speed.

2.6.L-38

7. Plume Behavior Beyond the Site Boundary

7.1 Steady Wind

Material released as a leak at the surface of a building under non-zero wind speed conditions will diffuse initially around the building surfaces in a complicated pattern determined by the building shape and the location of the leak. Typical dispersion pattern around a wind tunnel model of a reactor building having rounded surfaces are shown in Figs 5.29a-c of Meteorology and Atomic Energy⁽⁶⁾.

It is seen that concentrations decrease rapidly with distance from the release point, although the direction of the minimum rate of decrease is not always readily foreseen. This results in irregular, non-gaussian concentration distributions in planes normal to the mean wind direction at stations within several building diameters downwind from the building.

However, at about 5 building diameters downwind, the concentration profiles become more-or-less regular in that a concentration maximum occurs at the ground on the building centerline and concentrations decrease radially outward in the y-z plane to zero at the wake boundary. With increasing distance downwind, atmospheric turbulence acts to further smooth the profiles in an asymptotic approach to the familiar bi-gaussian distribution.

A non-dimensional distance of 5 diameters is equivalent to $5 \times 43 = 215$ meters for the Unit No. 2 reactor building. Since the site boundary distance is 350 m from Unit No 2, it seems reasonable to assume that the maximum concentration in a plane normal to the wind at the site boundary will indeed be at the ground. If this is so, then ground level concentrations beyond the

2.6.L-39

site boundary will always be lower than at the boundary by virtue of continued plume expansion with distance downwind.

7.2 Wind Reversal

If the wind should reverse 180° after a steady plume has been established, the time history of concentration at the former downwind site boundary after reversal will be a continued reduction of concentration with time because successively more diffuse portions of the plume will cross the boundary as the plume "backs up."

If the wind reversal persists long enough, the backed-up plume will become the ambient environment within which a new plume has formed in the opposite direction from the original. The total plume concentrations will then be the sum of the residual old plume concentrations plus the new plume concentrations. The critical site boundary will be located 180° from the previous one.

At the Indian Point site, 180° wind reversals occur occasionally during periods of upper air stagnation, between about 1000 and 1200 hours and between 2000 and 2200 hours (see individual hodographs in Figs 10a-d of NYU Report TR 71-3⁽³⁾).

In the daytime reversal, the wind has been in the downvalley direction with inversion conditions, but the change to the upvalley direction is accompanied by a change to a lapse temperature gradient. Therefore both the newly-established plume and the residual old plume have light concentrations compared to those assumed in the accident model.

In the nighttime reversal, the accident meteorology must be assumed to occur at some time prior to the reversal in order to create the residual old plume. This old plume is generated under lapse conditions during the period of greatest source strength. After reversal, these concentrations pass over the downvalley site boundary, but the source strength is now weaker. Therefore the

2.6.L-40

sum of the new and residual concentrations is probably not greater than obtained with the accident model.

2.6.L-41

List of References

1. Con Edison Final Facility Description and Safety Analysis Report (FSAR), as Amended, for Indian Point Nuclear Generating Unit No 2 (U.S.A.E.C. Docket 50-247).
2. U.S.A.E.C.-D.R.S. (1970): Safety Guides for Water Cooled Nuclear Power Plants.
3. Halitsky, J., E. J. Kaplin and J. Laznow (1971): Wind Observations at Indian Point, 26 November 1969-1 October 1970. N.Y.U. Dept of Met. and Ocean. GLS Report TR 71-3.

IP3
FSAR UPDATE

4. U.S.A.E.C.-D.R.L. (1970): Safety Evaluation of Con Edison Indian Point Nuclear Generating Unit No. 2 (Docket 50-247), with Appendix C prepared by Air Resources Environmental Laboratory, Environmental Science Services Administration, Nov. 29, 1968 and Feb. 17, 1970.
5. Turner, D. B. (1969): Workbook of Atmospheric Dispersion Estimates, Air Resources Field Research Office, ESSA.
6. Slade, D. H., ed. (1968): Meteorology and Atomic Energy. U.S.A.E.C. Div. Of Tech. Inform. CFST1 TID-24190.
7. Halitsky, J. (1971): Wind Tunnel Test of Gas Dispersion from Indian Point Unit 1. Unpublished report prepared for Con Ed dated June 29, 1971.
8. Halitsky, J., J. Laznow and D. M. Leahey (1970): Wind Observations at Indian Point, Montrose and Bowline Point, 31 Aug 1968-30 June 1969. NYU Dept. of Met. and Ocean. GSL Report TR 70-3.
9. Leahey, D. M. and J. Halitsky (1971): Low Wind Speed Turbulence and Related Diffusion Estimates for Indian Point, N. Y. N.Y.U. Dept. of Met. and Ocean. GSL Report TR 71-10. Also Atmospheric Environment Vol. 7 page 49-61 January, 1973.
10. Hay, J.S. and F. Pasquill (1959): Diffusion from a Continuous Source in Relation to the Spectrum and Scale of Turbulence. Advances in Geophysics 6. Academic Press pp. 345-365.
11. U.S.A.E.C.-D.R.L. (1969): Safety Evaluation of the Con Edison Indian Point Nuclear Generating Unit No. 3 (Docket No. 50-286), with Appendix C prepared by Air Resources Environmental Laboratory, ESSA January 2, 1968.
12. DiNunno, J. J., R. E. Baker, F. D. Anderson and R. L. Waterfield (1962): Calculation of Distance Factors for Power and Test Reactor Sites, U.S.A.E.C. DTI document TID-14844.
13. Con Edison PSAR for Indian Point Nuclear Generating Unit No. 1 (U.S.A.E.C. Docket 50-3).

2.6.L-42

14. U.S.A.E.C.- Atomic Safety and Licensing Board (1969): Transcript of Testimony in the Matter of Con Edison Application for a Construction License for Indian Point Nuclear Generating Unit No. 3.

15. Van der Hoven, I. (1969): Wind Persistence Probability ESSA Tech. Mem. ERLTM-ARL 10.

2.6.L-43

Table 1. The Con Edison Meteorological Model

Period	Wind Direction U					Building** Wake Effect
	Wind Speed \bar{u}	Variability in 20 ° Sector	Frequency in 20 ° Sector	Stability*		
				Class	Frequency	
0-2 hrs	1 m/s	steady	100%	Inversion, I	100%	yes
2-24 hrs	2 m/s	steady	100%	Inversion, I	100%	yes
1-30 days	1.74 m/s			Lapse, L ₁	13.7%	
	5.23 m/s			Lapse, L ₂	6.1%	
	2.79 m/s			Neutral, N	37.8%	
	2.03 m/s			Inversion, I	42.4%	
	all	meander	35%	all	100%	no

*Sutton parameters C_y , C_z and n for stability classes L₁, L₂ and N were derived from site meteorological experiments. For stability class I, the model adopted the Inversion parameters from USAEC TID-14844 "Calculation of Distance Factors for Power and Test Reactor Sites" by J. J. di Nunno, F. D. Anderson, R. E. Baker and R. L. Waterford, dated March 23, 1962.⁽¹²⁾

**Employs virtual point source displacement $X_o = (A/8 C_y C_z)^{1/(2-n)}$ where A = building area of 2,000 m² for periods 0-2 hrs and 1-30 days.

2.6.L-44

IP3
FSAR UPDATE

**Table 2. The AEC-DRL Meteorological Model
for Pressurized Water Reactors**

Period	Wind Speed \bar{u}	Wind Direction, U		Stability *		Building Wake Effect
		Variability in 22.5 ° Sector	Frequency in 22.5 ° Sector	Class	Frequency	
0-8 hrs	1 m/s	steady	100%	Pasquill F	100%	yes
8-24 hrs	1 m/s	meander	100%	Pasquill F	100%	no
1-4 days	3 m/s			Pasquill D	40%	
	2 m/s			Pasquill F	60%	
	all	meander	100%	all	100%	no
4-30 days	3 m/s			Pasquill C	33.3%	
	3 m/s			Pasquill D	33.3%	
	2 m/s			Pasquill F	33.3%	
	all	meander	33.3%	all	100%	no

*Volumetric building wake correction as defined in Section 3-3.5.2 of AEC TID-24190

Meteorology and Atomic Energy 1968⁽⁶⁾ with shape factor $c = 0.5$ and minimum across
sectional area of reactor building only.

IP3
FSAR UPDATE

Table 3. Values of $10^4 \sum \chi/Q$ (sec/m³)

According to the Con Edison and AEC-DRL Models
for Various Time Periods and Distances

	Con Edison			AEC-DRL		
Distance from Source (m)	350	520	1100	350	520	1100
<u>Time Period</u>						
0-2 hr	20.8	15.8	7.6	25.6	13.2	7.2
2-8 hr	--	--	11.4	--	--	21.6
8-24 hrs	--	--	30.4	--	--	19.6
0-8 hrs	--	--	19.0	--	--	28.8
0-24 hrs	--	--	49.4	--	--	48.4

Values of $\sum \chi/Q$ for sequences longer than 2 hours at x = 350 and 520 are not given because standards at the site boundary are specified for the 0-2 hr period only.

2.6.L-46

IP3
FSAR UPDATE

**Table 4. Values of Hourly Average $10^4 \gamma/Q$ at 350 m from the Source
During 15 Selected Light Wind Days, July 15 – Sept 15, 1970**

	Hour					
Date	<u>22</u>	<u>24</u>	<u>02</u>	<u>04</u>	<u>06</u>	<u>08</u>
7/23-24		3.5	4.7	0.6		
7/24-25		21.7	13.5	1.5	0.3	
7/25-26	0.7	1.2	0.3	1.0	0.4	
7/26-27				1.0		
7/27-28		9.8	8.3		0.5	
7/28-29			0.8	1.0	0.3	
8/8-9	5.1	1.1	1.0	0.7	0.6	
8/13-14	5.9	7.2	2.9	0.4	0.9	
8/14-15		2.4	21.7	5.2	0.6	
8/15-16		12.8	4.7		1.0	6.4
8/25-26	5.5	0.9	.8			
8/26-27				15.4	10.8	
8/27-28		5.5	0.9	0.6		
9/12-13	3.7	7.2	6.8	7.7	0.5	
9/13-14	15.4	9.9	0.7	0.4	0.8	

2.6.L-47

IP3
FSAR UPDATE

**Table 5. Values of Hourly Average $10^4 \gamma/Q$ at 520 m from the Source
During 15 Selected Light Wind Days, July 15 – Sept 15, 1970**

	Hour					
Date	<u>22</u>	<u>24</u>	<u>02</u>	<u>04</u>	<u>06</u>	<u>08</u>
7/23-24		2.2	3.4	0.4		
7/24-25		15.7	9.8	0.9	0.1	
7/25-26	0.3	0.7	0.1	0.6	0.2	
7/26-27				0.6		
7/27-28		7.1	6.1		0.2	
7/28-29			0.4	0.6	0.2	
8/8-9	3.2	0.6	0.6	0.4	0.3	
8/13-14	3.6	5.2	2.1	2.5	0.5	
8/14-15		1.5	15.2	3.7	0.3	
8/15-16		7.9	3.4		0.6	4.6
8/25-26	3.4	0.5	0.5			
8/26-27				9.5	7.9	
8/27-28		3.4	0.5	0.4		
9/12-13	2.3	5.2	4.9	0.5	0.3	
9/13-14	9.5	7.1	0.4	0.3	0.5	

2.6.L-48

IP3
FSAR UPDATE

Table 6 Values of Hourly Average $10^4 \gamma/Q$ at 1100 m from the Source

During 15 Selected Light Wind Days, July 15 – Sept 15, 1970

	Hour					
Date	22	24	02	04	06	08
7/23-24		0.8	1.7	0.1		
7/24-25		7.8	4.8	0.3	0	
7/25-26	0.1	0.3	0	0.2	0.1	
7/26-27				0.2		
7/27-28		3.5	3.0		0.1	
7/28-29			0.1	0.2	0	
8/8-9	1.1	0.2	0.2	0.2	0.1	
8/13-14	1.3	2.6	1.1	0.1	0.2	
8/14-15		0.5	7.8	1.9	0.1	
8/15-16		2.8	1.7		0.2	2.3
8/25-26	1.2	0.2	0.2			
8/26-27				3.4	3.9	
8/27-28		1.2	0.2	0.1		
9/12-13	0.8	2.6	2.4	0.2	0.1	
9/13-14	3.4	3.5	0.1	0.1	0.2	

2.6.L-49

IP3
FSAR UPDATE

**Table 7. Probabilities and Safety Factors in the
Con Edison and AEC-DRL Accident Meteorology Models**

	Con Edison Model			AEC-DRL Model		
	350m	520m	1100 m	350m	520m	1100m
% Probability of Exceeding Accident Model $\Sigma\gamma/Q$						
0-2 hr	0.8	0.68	0.4	1.3	1.0	0.5
0-8 hr	-	-	0.7	-	-	0
0-24 hr	-	-	0	-	-	0
Factor of Safety at 1% Probability Level						
0-2 hr	1.1	1.2	1.3	1.3	1.0	1.2
0-8 hr	-	-	1.2	-	-	1.8
0-24 hr	-	-	2.0	-	-	1.9
Factor of Safety at 5% Probability Level						
0-2 hr	7.0	7.9	12.6	8.5	6.6	12.0
0-8 hr	-	-	3.2	-	-	4.8
0-24 hr	-	-	3.1	-	-	3.0

Note

350m = distance from Unit 3 to site boundary

520m = distance from Unit 2 to site boundary

1100m = distance from Units 2 and 3 to low population zone.

2.6.L-50

IP3
FSAR UPDATE

Table 8. Wind Persistence at IP 3 under Inversion Conditions

In Combined Sectors 002° - 022° - 042°**

(The body of the table shows number of hourly occurrences of the
designated duration and speed class)

Number of Consec. Hours	Maximum Speed in Sequence (m/s)*					
	0.3	0.5	1.0	1.5	2.0	3.0
During 10 months (26 Nov 1969 – 1 Oct 1970)						
1	1	2	38	83	139	270
2			2	5	7	23
3				3	1	4
4				1	0	2
7						1

During 12 months (1 Jan 1971 – 31 Dec 1971)

1	1	6	66	115	217	431
2				18	60	181
3				2	23	89
4					4	39
5					2	19
6					1	5
7						1

*mph notation for speed in Table 1 of Rep TR 71-3⁽³⁾ should be m/s.

**see note on page 32 regarding sector notations.

IP3
FSAR UPDATE

Appendix A

Chronological Review of Events Relating to the Accident Meteorology Models

The Con Edison meteorological model was developed by Dr. Ben Davidson of New York University, using meteorological data collected at Indian Point during the period 1955-1957. That meteorological investigation, conducted in support of the licensing application for Indian Point Unit No. 1, yielded three reports which contained not only the meteorological summaries, but various dose calculations for postulated releases at stack height and at ground level. These reports were submitted to the AEC in their entirety as Exhibits L-1, L-5 and L-6 of Docket 50-3, Indian Point Unit No. 1⁽³⁾

Exh. L-1: N.Y.U. Tech. Rep. 372.1 "A Micrometeorological Survey of the Buchanan, N.Y. Area", dated Nov. 1955,

Exh. L-5: N.Y.U. Techn. Rep. 372-3 "Evaluation of Potential Radiation Hazard Resulting from Assumed Release of Radioactive Wastes to the Atmosphere from Proposed Buchanan Nuclear Power Plant", dated April 1957, and

Exh. L-6: N.Y.U. Tech. Rep. 372.4 "Summary of Climatological Data at Buchanan, N.Y., 1956-1957", dated March 1958.

The meteorological data acquired during the foregoing study were synthesized into the Con Edison meteorological model which first appeared in the PSAR for Indian Point Unit No. 2 (Docket No. 50-247). The supporting documentation for the model included:

2.6.L-57

IP3
FSAR UPDATE

Exhibits L-1 and L-6 (described above) in their entirety,

Meteorology Sections 2 and 3 of Exhibit L-5 (described above),

U.S.W.B. Tech. Paper No. 15: Maximum Station Precipitation for 1, 2, 3, 6, 12 and 24 Hours, Part X: New York, dated Dec. 1954, and

Additional meteorological data concerning wind behavior at an elevation of 70 ft above the Hudson River near the Indian Point site when the wind speed above the valley ridge lines fell into two classes; virtually zero and less than 16 mph. Those data had been collected during 1955, and had been used in generating the dose calculations in Exhibit L-5, but had not been presented previously in this form (low speed hodographs).

The Con Edison meteorological model postulated the sequence of wind condition shown in Table 1, beginning at the time of the postulated accident. The AEC did not comment directly as to the acceptability of the Con Edison model. It did request justification for the inversion frequency used in the 1-30 day period (question No. 16 in letter to Applicant dated Feb 28, 1966). This was provided in the First Supplement to the PSAR for I.P. 2 (Docket No. 50-247, Exhibit B-1).

The Con Edison meteorological model was used again in the PSAR for Indian Point Unit No. 3 (Docket 50-286). During evaluation of the dose calculations, the AEC-DRL made known its own meteorological model which has subsequently been published formerly in Safety Guide No. 4 of:

U.S. A.E.C.-D.R.S.: "Safety Guides for Water Cooled Nuclear Power Plants",
dated Nov. 2, 1970.

The meteorological sequence in the AEC-DRL model is shown in Table 2.

2.6.L-58

IP3
FSAR UPDATE

When the AEC-DRL model became known to Con Edison, the latter compared the two models for comparable time periods, and it was found that the Con Edison model yielded higher χ/Q values than did the AEC-DRL model in all periods except 2-8 hrs after the postulated accident. However, in a submittal to the AEC in the Fifth Supplement to the I.P. 3 PSAR, it was argued in Item 8 that the AEC-DRL assumption of a 1 m/s wind speed during this six-hour period did not in fact occur, and that the Con Edison assumption of 2 m/s for the same period was adequately conservative. This factor of 2 on wind speed, if applied with the AEC-DRL model in the 2-8 hr period, would reduce the AEC-DRL value of χ/Q for the period to below the Con Edison value, thereby rendering the Con Edison model more conservative in all categories. The argument also called upon experimental evidence to show that the wind meandered during the 2-8 hr period, following a directional pattern of wind rotation. The omission of wind meander in both the AEC and Con Edison models during this period introduces conservatism into each model.

In preparation for the I.P. 3 Construction Permit hearings, Con Edison submitted to the AEC Licensing Board:

- (1) Summary of Application (Docket 50-286) dated Feb. 20, 1969, and the AEC-DRL Technical Staff submitted:
- (2) AEC-DRL Safety Evaluation dated Feb. 20, 1969,
- (3) Appendix C to AEC-DRL Safety Evaluation: Comments on PSAR and Fifth Supplement for I.P.3, dated May 24, 1968 and Jan. 2, 1969 (included as Pgs. 75 and 76 of (2) above).
- (4) AEC-DRL Summary Statement dated March 20, 1969.

2.6.L-59

IP3 FSAR UPDATE

During the pre-hearing conference for I.P. 3 on March 11, 1969, Board Member Pigford requested clarification from both AEC-DRL and Con Edison regarding (a) the statement in Document 2 (above) that Con Edison did not have long-term data on stability-speed-direction persistence, and (b) the differences between the Con Edison and AEC-DRL meteorological models (transcript pgs. 70-71).

During the I.P. 3 Construction Permit hearings, on March 27, 1969, oral testimony was given by both Con Edison and AEC-DRL representatives in response to Dr. Pigford's questions. It was established that "the absence of long-term data" referred to the fact that the original experimental data, taken in 1955, 1956 and 1957, were no longer available (transcript pg. 170), leaving only the statistical summaries in the various reports and submittals previously cited. The details of the Con Edison and AEC-DRL accident meteorologies, shown in Table 1 and 2, were also enumerated, and major points of discrepancy between the models were discussed.

Of particular interest to the Board was the rationale behind the AEC-DRL statement that the 0-8 hr meteorology used in the AEC model was conservative (pg. 660). This led to an extended discussion of the low wind speed hodographs shown in Figs. 2.6-1 and 2.6-2 of Section 2 of the Unit 3 PSAR, which provide the justification for both the Con Edison and AEC-DRL 0-8 hr meteorology models.

These hodographs show the progression of wind speed and direction during a typical day when the wind speed above ridge elevation is zero or small. The hodographs were constructed by averaging the measurements taken on 12 days (zero wind speed) and 35 days (small wind speed) during September and October, 1955.

The Con Edison position was that the combination of average hodographs plus conservative assumptions regarding the persistence of wind speed, direction and

2.6.L-60

stability provide adequate conservatism in its 0-24 hr meteorology model.

The AEC-DRL position was that an average hodograph implied the existence of some individual hodographs which might exhibit longer persistence of lower speed winds in the critical direction with strong stability, and that a more conservative model was called for in the absence of evidence to the contrary. In its Safety Evaluation, Document (2) above, the AEC-DRL stated that its standard meteorological model, given in Table 2, "conservatively characterizes the meteorology of the Indian Point site" in the absence of long-term data "on the specific joint frequency of stability-wind speed-wind direction persistence." The AEC-DRL consultant (ESSA Air Resources Environmental Laboratory) concurred in Document (3) above that the 1-8 hr meteorology in the AEC-DRL model was a " --reasonably conservative meteorological assumption..." in view of the absence of joint-frequency data.

Board member Pigford then attempted to obtain a numerical estimate of the probability of occurrence of the Con Edison and AEC-DRL 0-8 hr models in the critical wind direction sector by questioning AEC-DRL staff meteorologist Spickler and Con Edison consultant Halitsky. Mr. Spickler reasoned that it would probably be less than 1%, since the combination of inversion stability and 1 m/s wind speed occurred approximately 5% of the time for all directions combined. However, in view of the lack of persistence data for individual cases, Mr. Spickler characterized his estimate of 1% as an "educated guess" (page 67).

Dr. Pigford then requested that Dr. Halitsky estimate the probability of occurrence of the 0-8 hr meteorological sequences as defined by AEC-DRL and Con Edison (pgs. 675-676). Dr. Halitsky requested some time to consider his reply. Further questioning was directed toward the validity of diffusion coefficients

2.6.L-61

(pg 677), the need for diffusion testing to validate the Sutton diffusion model (pg 678ff and 745ff), plans for continued meteorological testing to generate the data needed to clarify the 0-8 hr assumptions (pg 682ff) and topographical effects on diffusion (pgs 749ff).

Prior to adjournment the Board posed several questions of a meteorological nature to both Con Edison and the AEC-DRL staff (pg 1671). Those were responded to at a resumption of the hearings on 13 May 1969. Mr. Spickler placed into the record the AEC-DRL standard meteorological model as shown in Table 2 (pg 1756). Two questions were directed to Dr. Halitsky (pgs. 1671 and 1672):

a) Present a technical justification for the conclusion that the frequency spectrum of wind speeds and the range of air and low wind speeds is now and will continue to be the same as that measured in 1956.

b) Present a technical justification for the meteorological conditions used in the applicant's accident analysis indicating the estimated probability of occurrence of these conditions.

Question (a) was answered by reviewing the substance of NYU Report 372.4 which compared 1956 and 1957 meteorological data. Question b) was answered in part, but the discussion veered toward temperature gradients and plume rise, not returning to probabilities that day. Mr. Jensch raised the question again of conducting diffusion tests. Dr. Halitsky recommended against such test as being unnecessary.

On the following day Dr. Halitsky continued his reply to Question b) (pgs. 1795ff). He stated that the Con Edison 30-day meteorology was conservative because inversions were assumed to occur twice as frequently as the average for

2.6.L-62

the year, and the meander was assumed to occur in a 20° sector whereas the actual meander angle was more like 40° . The combination of those two effects introduced a factor of about 4 in the χ/Q calculation.

Turning to the first day meteorology, considerable discussions then ensued regarding the interpretation of the hodographs in Figs. 2.6-1 and 2.6-2, particularly with respect to lapse rates during different hours of the day. Dr. Halitsky pointed out that the Con Edison model ignored meander and reversal during the first day, each of which would introduce a factor of 2 for a total of 4 on the calculated χ/Q . Furthermore, the increase of wind speed from 1 m/s to 2 m/s during the 2-24 hr period appeared justified according to the average hodograph.

Dr. Pigford then brought the questioning back to the probability of occurrence of the Con Edison assumed meteorology (pg 1815). Dr. Halitsky offered an opinion of the probabilities of the first-day meteorology specified in the AEC-DRL and Con Edison models, based on Mr. Spickler's previous estimate (pg 670) of "probably less than 1%" and Dr. Halitsky's estimate of two orders of magnitude less than Mr. Spickler's for the same model; i.e., assuming that the average hodograph occurs 100 days/yr, the AEC-DRL "anomalous" hodographs would occur $.01 \times 100 = 1$ day/yr according to Spickler and 1 day/100yrs according to Halitsky. The Con Edison "anomalous" hodograph, which is not as severe as the AEC-DRL version, would have an intermediate frequency, say 1 day/10yrs.

Dr. Pigford then requested a statement of probability for each of the three time periods in the Con Edison model. Dr. Halitsky was unable to furnish this information.

Dr. Pigford subsequently questioned Mr. Grob regarding the possibility of return flows over the site causing an accumulation of concentrations (pg 1846).

the possibility of accumulation of concentrations due to simultaneous operation of Units 1, 2 and 3 (pg 184) and the possibility of plumes leaving the Unit 1 stack and/or the tops of the Units 2 and 3 containment structures and impinging upon a local rise in terrain beyond the site boundary (pg 1853). Mr. Grob and Dr. Halitsky responded by giving qualitative descriptions of plume behavior and concluding that the postulated conditions would not yield higher concentrations than in the assumed accident meteorology.

Mr. Jensch then queried Mr. Spickler on wake effects with cylindrical structures at low wind speeds (pg 1862). Mr. Spickler cited various references, none of which reported tests in wind speeds as low as 1 m/s. Mr. Spickler concurred with Mr. Jensch as to the desirability of having wake concentration data at low wind speeds to justify inclusion of the wake factor in the meteorological model (pg 1864).

Dr. Halitsky completed his statement on the probability of occurrence of the Con Edison meteorological model by specifying a substantially zero probability since the first two periods in the model do not provide for wind meander which always occurs (pg 1914).

After conclusion of the hearings, both Con Edison and the AEC-DRL submitted written answers to the questions posed by Dr. Pigford at the pre-hearing conference. Con Edison concurred that data were lacking to prove that 8 hr wind persistence under low speed conditions could not occur. It also showed that the AEC-DRL value of \overline{Xu}/Q during the 2-8 hr period, while twice as high as the Con Edison value for the same period, would produce only a 20% increase in dose. The AEC-DRL contended that relaxation of their long-term model is not justified until joint probability of persistence with speed and stability can be examined. It

also stated that their model showed a 40% increase in dose over the Con Edison model.

The AEC-DRL also provided written comments on Dr. Halitsky's hearing testimony, i.e.: (a) they agreed with his testimony, (b) they believe that the Sutton equations are valid for this type of terrain and that smoke photography and wind measurements are adequate experimental techniques in lieu of direct concentration measurements, and (c) they believe that year to year variations in meteorology will be small and that accident meteorological assumptions would still be quite conservative.

In its Initial Decision granting a Construction Permit (Aug 13, 1969) the Board took note that Con Edison had undertaken a new meteorological program in the Indian Point area, and had stated that the new data would be used in connection with the proposed operations for Unit No. 3. The Board strongly urged that

- a) Definitive criteria should be developed for judging the adequacy of the meteorological program (pg 12),
 - b) the present continuing study should be made as comprehensive as possible (pg 13),
- and
- c) the possibility that ground concentrations higher than those at the site boundary might occur beyond the site boundary should be given detailed consideration (pg 16).

In response to the Board's recommendations, Con Edison revised its ongoing meteorological program in the Fall of 1969 to serve two functions; one was to acquire data which could be used for the scheduling of operational releases, the other was to acquire data which would help to resolve the unanswered questions, which arose during the hearings, regarding the 0-8 hr accident meteorology models.

IP3
FSAR UPDATE

The portion of the revised program relating to accident meteorology included experiments to obtain data on:

- a) annual wind statistics
- b) low wind speed hodographs
- c) turbulence characteristics under low wind speed inversion conditions
- d) persistence statistics
- e) building wake effects on diffusion

The results of experiments in the above categories were submitted to Con Edison in three reports. These are

- 1) N.Y.U. Tech. Rep. TR 71-3 "Wind Observations at Indian Point, 26 November 1969 – 1 October 1970" by J. Halitsky, E.J. Kaplin, and J. Laznow 17 May 1971.
- 2) N.Y.U. Tech. Rep. TR 71-10 "Low Wind Speed Turbulence Statistics and Related Diffusion Estimates for Indian Point, N.Y." by D. M. Leahey and J. Halitsky 15 September 1971.
- 3) "Wind Test of Gas Dispersion from Indian Point Unit 1", by J. Halitsky 29 June 1971.

Item 1) was submitted to the AEC-DRL in Supplement 1, pgs Y-1 to Y-32 of the Unit No. 3 FSAR.

Item 3) was submitted to the AEC-DRL in support of an application to reduce the stack height of Unit No. 1 to meet structural safety requirements under tornado loadings. In preparation for the I.P.2. Operational Permit hearings, Con Edison submitted to the AEC Licensing Board:

2.6.L-66

IP3
FSAR UPDATE

(1) Summary of Application (Docket 50-247) dated Nov. 12, 1970, and the AEC-DRL Technical Staff submitted:

(2) AEC-DRL Safety Evaluation dated Nov. 16, 1970,

(3) Appendix C to AEC-DRL Safety Evaluation; Comments on FSAR and Amendments 12 and 14 for I.P.2., dated Nov. 29, 1969 and Feb. 17, 1970 (included as Pgs 93, 94 and 95 of (2) above).

In Item (2) pg 9, the AEC-DRL stated that the two years of (new) meteorological data presented by the applicant provide an adequate basis for selecting the meteorological parameters for both routine and accident meteorology calculations.

In Item (3), ESSA-AREL acknowledged the existence of the diurnal reversal of valley winds at the site but stated that in the absence of joint frequency data, an appropriately conservative assumption would be a steady wind of 1 m/s speed for the first 8 hrs followed by a $22\frac{1}{2}^{\circ}$ meandering wind of 1 m/s speed for the next 16 hrs in the same sector. ESSA characterized the latter assumption as "very conservative". It also stated that the Con Edison correction for building wake effect agreed well with the AEC-DRL method, but disagreed with the Con Edison procedure of including a virtual source displacement in the long term average diffusion model.

2.6.L-67

IP3
FSAR UPDATE

February 1973

A STUDY OF ATMOSPHERIC DIFFUSION CONDITION PROBABILITIES
USING THE COMPOSITE YEAR OF
INDIAN POINT SITE WEATHER DATA [Historical Information]

by:

Keith Woodard

Pickard, Lowe and Associates, Inc.
1200 18th Street, N.W., Washington, D. C. 20036

2.6.M-1

IP3
FSAR UPDATE

Introduction

A study is presented below which compares atmospheric diffusion condition probabilities for the Indian Point site computed using various models. Several of these models realistically take into account characteristics of the Indian Point site. The cases studied account for the following: (1) effect of allowing diffusion for the distance to the nearest land not owned or controlled by Consolidated Edison in each direction (i.e., the effluent is assumed to diffuse for the real distance to the boundary, not just to the minimum site boundary radius), (2) effect of using the "split sigma" model to account for lateral wind meander, and (3) effect of averaging diffusion conditions over a two-hour period. Use of these realistic assumptions result in significant reductions in diffusion estimates.

Background

Meteorological data have been taken on a 100 ft tower at the Indian Point site for several years. To provide the most representative one-year period of data, a "composite year" was constructed using the most complete month from the total period of record available. Following is a summary of the data used.

Parameter	Measured Height	Percent Data Recovery
Wind Speed	100 ft	97.6
Wind Direction	100 ft	98.8
Temperature Difference	95 ft-7 ft	95.5

2.6.M-2

Basis Diffusion Model

From these data, centerline values of X/Q were computed for each hour of data using the following relationship:

$$Q / X = \frac{1}{\bar{u}(\pi \sigma_y \sigma_z + cA)}$$

where:

X = concentration ($\mu Ci / m^3$)

Q = release rate ($\mu Ci / sec$)

$\bar{u}_{\bar{a}}$ = average wind speed for the hour measured at 100 ft and extrapolated to 33 ft (m/sec)

σ_y = horizontal diffusion coefficient (m)

σ_z = vertical diffusion coefficient (m)

cA = building wake factor (assumed to be c = 0.5, A = 2000 m³).

The building wake effect is limited such that no more than a factor of 3.0 reduction in dilution is obtained for any condition. The wind speed is extrapolated to the 33 ft level in accordance with recent AEC practice. The method of extrapolation is according to the following relationship:

$$\bar{u}_{33} = \bar{u}_{100} \left(\frac{h_{33}}{h_{100}} \right)^n$$

where:

\bar{u}_{33} = extrapolated wind speed (m/sec)

\bar{u}_{100} = measured speed (m/sec)

h_{33} = height extrapolated to (ft)

h_{100} = measured height (ft)

n = exponent based on diffusion as follows

2.6.M-3

Pasquill Diffusion Group	Value of n
--------------------------	------------

IP3
FSAR UPDATE

A	0.25
B	0.25
C	0.25
D	0.33
E	0.5
F	0.5
G	0.5

Since ground effects influenced the lower sensor at 7 ft, measured values of ΔT are multiplied by a factor as suggested by AEC. The method used to determine this factor assumes an exponential relationship between temperature and height such that measured temperature difference between any two heights can be represented as a temperature difference between two other heights according to the following relationship:

$$f(\Delta T \text{ correction factor}) = \frac{\ln\left(\frac{h_{ue}}{h_{le}}\right)}{\ln\left(\frac{h_{um}}{h_{lm}}\right)}$$

where:

h_{ue} = height of upper extrapolated temperature (ft)

h_{le} = height of lower extrapolated temperature (ft)

h_{um} = height of upper measured temperature (ft)

h_{lm} = height of lower measured temperature (ft)

For Indian Point the factor is computed as follows:
$$f = \frac{\ln \frac{150}{33}}{\ln \frac{95}{7}} = \frac{1.51}{2.60} = 0.58$$

2.6.M-4

IP3
FSAR UPDATE

Thus, all vertical temperature difference values are multiplied by this factor.

In this study, either vertical temperature difference (ΔT) is used or wind direction range (R) is used to determine values of s_z in the diffusion equations. The following table gives the values assumed for each Pasquill Diffusion Category.

Pasquill Category	(1) AEC ΔT Model* (°F/100')	(2) Wind Direction Range (s)
A	$\Delta T < -1.0$	$135 < R$
B	$-1.0 \leq \Delta T < -0.9$	$135 \leq R < 105$
C	$-0.9 \leq \Delta T < -0.8$	$105 \leq R < 75$
D	$-0.8 \leq \Delta T < -0.3$	$75 \leq R < 45$
E	$-0.3 \leq \Delta T < -0.2$	$45 \leq R < 22$
F	$0.2 \leq \Delta T < 2.2$	$22 \leq R < 12$
G	$2.2 \leq \Delta T$	$12 \leq R$
*In conversion from °C/100 m (Safety Guide 23) to °F/100 ft, values were rounded to nearest tenth of a degree.		

Two basic models are used. One is referred to as the "AEC ΔT Model" which utilizes the Safety Guide ΔT values to determine Pasquill category for use in determining both s_y and s_z . The "Split Sigma Model" determines the diffusion coefficients in the diffusion equation based on both ΔT and wind direction range. In this model the X/Q values are computed assuming that s_z (controlling vertical diffusion) is related to ΔT as before, however,

2.6.M-5

IP3
FSAR UPDATE

s_y (the horizontal diffusion coefficient) is determined using the wind direction range categories given above. The validity of decoupling s_y and s_z has been demonstrated in diffusion tests at Three Mile Island, Pennsylvania (Amendment 24 to FSAR) Docket No. 50-289).

As mentioned previously, one of the models used for this study ("Site Shape") assumes that the site boundary is not circular. Consolidated Edison owns or controls land in certain directions out to a distance significantly greater than the minimum assumed radius of 330 m. Additionally, for bodies of water where there are no permanent residents, it is reasonable to assume that when winds blow toward these directions the X/Q values can be computed for a distance corresponding to that of the opposite shore. The following table lists the distances used for each direction in the "Site Shape" model calculations.

<u>Direction</u>	<u>Assumed Distance (meters)</u>
N	1775
NNE	2375
NE	825
ENE	575
E	1195
ESE	585
SE	1165
SSE	1165
S	1285
SSW	1685
SW	330
WSW	1575
W	1575
WNW	1275
NW	1275
NNW	1275

2.6.M-6

Calculational Technique

Probability distributions of the X/Q values computed as described above are constructed by connecting all hours which have X/Q values equal to or greater than a selected value. The numbers of hours so obtained are then divided by the total hours in the year of data to obtain the probability that the selected X/Q value would be equaled or exceeded. This procedure is repeated for a number X/Q values which are then plotted to form a probability distribution.

For AEC licensing it is customary to pick the 5% probable hourly (0-1 hr) X/Q for use in the 0-2 hour period of loss-of-coolant accident evaluations. However, in reality, if the wind direction or diffusion conditions change during the two-hour period, a stationary receptor would not receive a dose at the same rate for the full two-hour period. To account for this effect, probability distributions have also been made using two-hour averaging of the X/Q values.

The method of averaging over longer periods is as follows. Starting with each hour of data, the computed X/Q values are added in each of 16 assumed direction sectors for the duration of the release time period being evaluated (2 hours). The maximum integrated value of all the 16 directions is stored and a new integration period is started spaced one hour later. Again, the maximum value for this next integration period is stored regardless of the direction sector in which it occurred, and so on. After processing all hours of data, cumulative probability plots are made for each release time period considered, 2 hours in this

2.6.M-7

case.

IP3
FSAR UPDATE

Results

Four cases were run using the composite year of Indian Point data. Each case was run to obtain probability distributions using hourly data (0-1 hr) and using the two-hour averaging technique. Figure 1 attached shows the probability distributions for the one-hour cases and Figure 2 shows the results for the two-hour averaging cases. The following table gives the assumptions and results for each case.

Case #	Model	Site Boundary	5% Probable X/Q (sec/m ³)* (1 hr only)	5% Probable X/Q (sec/m ³)* (2 hr averaging)
1	AEC ΔT	Circular	1.8×10^{-3}	1.3×10^{-3}
2	AEC ΔT	Site Shape	6.8×10^{-4}	5.0×10^{-4}
3	Split s	Circular	9.5×10^{-4}	6.5×10^{-4}
4	Split s	Site Shape	3.7×10^{-4}	2.9×10^{-4}
*Note: For Pasquill F and 1 m/sec wind at 330 m, X/Q = 1.3×10^{-3} sec/m ³ .				

Evaluation

Case 1 (1 hour only) is the typical model used by the AEC for the two-hour portion of the LOCA. As shown, the X/Q value is 1.8×10^{-3} sec/m³. If the actual distance to the site boundary is used as in Case 2, the value reduces to a X/Q of 6.8×10^{-4} sec/ m³ resulting in a factor of reduction of 2.65. If the lateral meander is accounted for as in the "Split Sigma" Case 3 for a circular site,

2.6.M-8

IP3
FSAR UPDATE

a X/Q value of 9.5×10^{-4} results. Another meaningful comparison is between the one-hour and two-hour averaging results for Case 1. Here there is a factor of 1.4 reduction for this effect alone.

There are many combinations which can be compared using this table, however, the thrust of this study is to demonstrate that the typical AEC model (Case 1) is not appropriate for this particular site, since it does not account for inherent site characteristics.

2.6.M-9

IP3
FSAR UPDATE

Department of Meteorology and Oceanography

NEW YORK UNIVERSITY

COLLEGE OF ENGINEERING



RESEARCH DIVISION

SUMMARY OF CLIMATOLOGICAL DATA AT BUCHANAN, NEW YORK

1956-1957

By

Ben Davidson

Technical Report No. 372.4

Prepared for

Consolidated Edison Co. of N. Y., Inc.

March, 1958

R-1

IP3
FSAR UPDATE

RESEARCH DIVISION
COLLEGE OF ENGINEERING
NEW YORK UNIVERSITY

Department of Meteorology and Oceanography

Technical Report No. 372.4
SUMMARY OF CLIMATOLOGICAL DATA AT BUCHANAN, NEW YORK
1956-1957

Prepared by
Ben Davidson
Project Director

Prepared for
Consolidated Edison Co. of N. Y., Inc.
March 1958

R-2

Table of Contents

	Page
1. Introduction	1
2. Comparison of 1956-1957 data	2
3. Variation of wind direction with height	4
4. Wind rose presentation	6
References.....	8

List of Figures

Fig. 1.	Comparison of wind direction distribution for all stability classes.....	3
Fig. 2.	Comparison of wind direction distribution for all stability classes, summer 1956	4
Fig. 3.	Wind rose at 300 ft tower level for inversion, neutral and lapse conditions, based upon 1956-1957 data	7

1. Introduction

A detailed summary of climatological data collected during 1956 is contained in Technical Report No. 372.3 – Evaluation of Potential Radiation Hazard, April 1957. The tower was run on a skeleton basis during 1957. Wind observations were made at 100 and 300 feet (200 and 400 feet above river level), while temperature was observed at 7, 150, and 300 feet above ground. Because of the relative infrequency of calibration and general maintenance during 1957 the 1956 data are considered far more accurate. The 300 ft 1957 data were processed in the same manner as the 1956 data. In the present report we summarize:

- (a) The effect of climatological differences between 1956 and 1957 on the radiation calculations of Report 372.3
- (b) The local wind rose as a function of height above river, and
- (c) The combined 1956-1957 wind rose at 300 feet as a function of stability and wind speed.

2. Comparison of 1956-1957 data

In Table I the essential features of the 1956 and 1957 300 ft data are summarized as a function of stability class. All definitions remain the same as in the previous report. In particular, Inversion conditions (I) are defined to occur when $T_{300} - T_7 \geq 0$; Isothermal-adiabatic conditions (N) when $0 > T_{300} - T_7 \geq -1.8^\circ F$; and Lapse conditions (L) when $T_{300} - T_7 < -1.8^\circ F$.

Table I. Frequency of Inversion (I), Neutral (N), and Lapse (L) conditions with associated mean wind speeds, \bar{V} (mph) for 1956 and 1957.

Summer	I	\bar{V}	N	\bar{V}	L	\bar{V}
1956	0.38	6.5	0.31	10.4	0.31	11.6
1957	0.35	6.2	0.33	12.8	0.32	9.7
Winter						
1956	0.25	7.6	0.54	12.6	0.20	8.5
1957	0.33	7.1	0.48	13.1	0.19	9.0
All seasons						
1956	0.315	6.9	0.425	11.8	0.255	10.4
1957	0.340	6.6	0.405	13.0	0.255	9.4

There are minor differences, but on the whole, the data seem compatible. There were slightly more inversion hours in 1957 than in 1956 with a slightly lower wind speed. The yearly frequency for each temperature gradient condition does not vary more than 10 percent whilst the mean wind speed for each class is also within 10 percent of the 1956 figure. Almost all of the radiation calculations are inversely proportional to the mean wind speed or to the harmonic mean. There is not too great a difference between the two years and for this reasons the total integrated dosage for the area should not vary too greatly, say within 10 to 20 percent,

R-5

which is well within the range of uncertainty of the original calculations.

IP3
FSAR UPDATE

The areal distribution of radiation contained in Figs. 1.1. and 1.2 of the earlier report depends in the mean on the distribution of wind direction. Fig. 1 is a comparison of the annual distribution of wind direction for 1956 and 1957. Again the differences are not great; the 1957 distribution seems a bit more peaked than the 1956 data. This may be due in part to systematic individual differences in reading the charts. Whatever the cause, the differences in the distribution are well within the limits of accuracy of the initial calculations.

R-6

3. Variation of wind direction with height

Some idea of the variation of wind direction with height may be gained from the 100 and 300 ft summer wind rose (Figs. 3.1 and 3.2 of the original report). To supplement this information, we compare in Fig. 2 the distribution of wind direction for the 1956 summer season at 400 ft (300 ft tower level), 200 ft (100 ft tower level) and 70 ft above river. The 70 ft data were obtained from an anemometer mounted on the "Jones," a ship anchored in mid-river. The ship site is about 0.8 mile northwest of the tower (see map in Report 372.1). It is evident that there are systematic differences in the three distributions. The most obvious is the build-up of southerly winds with height. The Jones distribution is flat from 150° to 250°, while the 100 and 300 ft tower

distributions peak fairly at 170°. On the down valley side of the distribution (about 020°), The Jones and 100 ft tower level distributions are fairly well matched. The 300 ft tower level distribution does not reach nearly the same frequency at 030° as do the other two distributions. Some of the essential differences in the two distributions are summarized in the following table.

Percent time indicated wind direction ranges were observed at

<u>Direction Range</u>	<u>Jones</u>	<u>100 ft Tower</u>	<u>300 ft Tower</u>
340-040	38	37	30
360-040	28	30	19
160-220	16	23	27
160-200	10	18	22

Part of the difference between the distributions can be explained by the tendency for light southerly winds to be observed at the 300 ft tower level when the nocturnal NNE winds have set in at the Jones and 100 ft tower locations. The remainder appears to be a daytime phenomenon and indicates that The Jones distribution is affected by the proximity of the valley walls in a rather complicated fashion.

4. Wind rose presentation

In Fig. 3 we present wind roses based upon two years of data for inversion, neutral, and lapse conditions at the 300 ft level. The bars here are flying with the wind and pointing to the indicated meteorological wind direction. The length of the bar is proportional to the average frequency of occurrence per year of the appropriate wind direction and stability condition. For convenience in interpretation we indicate the general location of populated areas surrounding the site.

An interesting feature of the wind rose is the elongation along the axis of the valley during inversion hours. Wind trajectories towards Peekskill, the most densely populated area near the site, are relatively infrequent during neutral and lapse conditions. There is a sizeable frequency of 210° winds during inversion hours. This trajectory would just about brush the northern outskirts of Peekskill, but it is probable that terrain effects would tend to curve the trajectory so that it follows the river. In general, the inversion wind rose shows a high frequency of up and down valley wind directions.

During lapse and neutral conditions, the wind rose indicates a substantial frequency of northwest winds which are the prevailing winds over flat land in this area. Under these temperature gradient conditions, one may expect effluent concentrations on the ground. There are a substantial number of wind trajectories toward the villages of Buchanan, Montrose and Verplank during neutral and lapse conditions, and towards the village of Verplank during inversion conditions.

References

Davidson, B., and J. Halitsky, 1955: A micrometeorological survey of the Buchanan, N.Y. area. - Summary of progress to 1 December 1955. Technical Report No. 372.1, Research Division, New York University, College of Engineering.

Davidson, B., and J. Halitsky, 1957: Evaluation of potential radiation hazard resulting from assumed release of radioactive wastes to atmosphere from the proposed Buchanan nuclear power plant. Technical Report No. 372.3, Research Division, New York University, College of Engineering.

IP3
FSAR UPDATE

Station: BEAR MOUNTAIN, NEW YORK

Drainage basin: HUDSON

County: ORANGE

Lat. 41° 19' N Long. 74° 00' W

Elev. (ft.) 1301

Period of record: 1941-1950

Month		Duration (hours)					
		1	2	3	6	12	24
Jan.	Amt. Date	0.38 7/1946	0.60 31/1942	0.85 31/1942	1.29 1/1945	1.49 31/1942	1.51 5-6/1949
Feb.	Amt. Date	0.26 14/1944	0.41 14/1944	0.56 14/1944	0.80 14-15/1944	1.12 20-21/1947	1.42 20-21/1947
Mar.	Amt. Date	0.35a 21/1948	0.57 3/1942	0.78 3/1942	0.99 3/1942	1.19 6-7/1944	1.41 2-3/1947
Apr.	Amt. Date	0.61 30/1947	0.89 30/1947	1.06 1/1948	1.51 1/1948	1.71 1/1948	2.08 18-19/1949
May	Amt. Date	0.70 6/1949	1.21 20/1949	1.35 30/1948	1.77 27/1946	2.51 27/1946	2.87 27/1946
Jun.	Amt. Date	0.67 21/1945	0.83 21/1945	0.88 21/1945	1.01 23/1942	1.50 2/1946	1.82 1-2/1946
July	Amt. Date	1.57 20/1945	1.72 22/1946	1.85 22/1946	2.47 22-23/1945	2.74 22-23/1945	3.98 18-19/1945
Aug	Amt. Date	1.25 26/1947	1.44 16/1942	1.71 16/1942	1.93 16/1942	2.30 9/1942	2.47 24-25/1945
Sep.	Amt. Date	0.81 30/1946	1.21 24/1946	1.71 24/1946	2.08 24/1946	2.28 24/1946	2.80 26-27/1942
Oct.	Amt. Date	0.59 10/1950	0.86 26/1943	1.03 26/1942	1.53b 26/1942	2.83 26-27/1943	3.95 26-27/1943
Nov.	Amt. Date	1.18 8/1947	1.97 8/1947	2.22 8/1947	3.14 8/1947	3.65 8/1947	3.65 8/1947
Dec.	Amt. Date	0.63 25/1945	1.17 25/1945	1.48 25/1945	1.99 25/1945	2.09 25-26/1945	3.33 30-31/1948

IP3
FSAR UPDATE

Annual	Amt.	1.57	1.97	2.22	3.14	3.65	3.98
Date	7/20/45	11/8/47	11/8/47	11/8/47	11/8/47	11/8/47	7/18-19/45
^a Also 23/1949		^b Also 26/1943.					

R-13 ¹⁴

U.S. DEPARTMENT OF COMMERCE, WEATHER BUREAU

Station, Bear Mountain County, Orange State, New York

Latitude, 41.19 Longitude, 74.00 Elevation, 1300 feet.

Data, Precipitation, Monthly and Annuals

Year	January	February	March	April	May	June	July	August	September	October	November	December	Annual
1939	3.81	3.62	3.16	5.90	1.30	5.32	3.04	3.36	3.04	4.20	1.69	3.39	41.83
1940	5.58	3.87	5.72	6.68	6.53	3.12	3.68	4.05	2.82	3.38	4.48	3.87	53.78
1941	2.77	2.87	2.22	2.00	1.79	4.46	6.31	3.33	0.25	2.35	3.18	4.47	36.00
1942	3.98	1.85	5.67	0.92	3.20	3.80	5.79	5.51	4.44	3.61	4.79	4.62	48.18
1943	2.36	1.19	2.00	3.47	4.56	3.80	3.73	2.56	2.99	12.64	4.18	1.01	44.49
1944	1.93	2.05	5.60	5.30	2.54	3.06	2.03	2.42	5.99	2.12	5.09	2.37	40.50
1945	2.97	2.46	1.79	3.79	7.18	4.28	16.87	4.73	5.36	2.13	6.53	4.46	62.55
1946	1.79	1.65	2.97	1.97	8.91	3.11	8.10	4.93	6.24	2.13	1.03	2.48	45.31
1947	2.85	3.39	3.48	4.76	9.49	6.55	7.38	2.78	1.90	2.69	8.51	3.68	57.46
1948	3.05	1.21	3.29	5.28	7.30	4.84	3.52	2.76	0.68	1.92	4.90	6.14	44.89
1949	5.08	2.27	1.88	5.47	6.53	0.96	3.45	2.94	5.60	2.52	1.91	2.79	41.40
1950	2.81	4.46	3.40	2.97	6.02	3.77	5.16	2.94	2.26	2.45	5.39	6.24	47.87
1951	4.60	4.14	8.40	2.94	4.11	3.87	5.07	5.19	2.06	5.13	7.55	5.96	59.02
1952	4.53	3.22	5.46	8.54	5.29	5.92	5.13	8.13	5.01	0.52	4.48	5.84	62.07
1953	6.75	1.89	5.71	4.72									
Sums													
Means													

REMARKS

R-14

U. S. DEPARTMENT OF COMMERCE
WEATHER BUREAU
NATIONAL WEATHER RECORDS CENTER

JOB NO. 6729

SURFACE WIND SPEEDS VERSUS
DIRECTION WHEN SOME
FORM OF PRECIPITATION
IS OCCURRING

STATION: BEAR MOUNTAIN, NEW YORK

PERIOD: JANUARY 1944 – DECEMBER 1948

Sponsored by: Consolidated Edison Company of New York,

Date October 28, 1965

FEDERAL BUILDING
ASHEVILLE, N.C.

Book 2 of 2

USCOMM. WB-ASHVILLE

R-15

U. S. DEPARTMENT OF COMMERCE
WEATHER BUREAU
NATIONAL WEATHER RECORDS CENTER

JOB NO. 6729

**OCCURRENCE OF WIND SPEED
AND DIRECTION DURING
THUNDERSTORMS**

STATION: BEAR MOUNTAIN, NEW YORK

PERIOD: JANUARY 1944 – DECEMBER 1948

Sponsored by: Consolidated Edison Company of New York,

Date October 28, 1965

**FEDERAL BUILDING
ASHEVILLE, N.C.**

Book 1 of 2

USCOMM. WB-ASHVILLE

R-18

IP3
FSAR UPDATE

New York University
School of Engineering and Science
Department of Meteorology and Oceanography
Geophysical Sciences laboratory
Technical Report No. TR 71-3

Wind Observations at Indian Point
26 November 1969-1 October 1970

Prepared by

James Halitsky, Project Director
Edward J. Kaplin
Joseph Laznow

for

Consolidated Edison Co. of N. Y., Inc.
4 Irving Place, New York, N. Y. 10003

17 May 1971

Y-1

Summary

Wind observations made at a 100 ft meteorological tower at Indian Point and at a ship anchored in the Hudson River northwest of Indian Point in 1969-70 were compared with observations made at similar installations in 1955-56. It was found that

- 1) Annual average statistics of wind speed, direction and vertical temperature difference were substantially the same for 1956 and 1970. Points of difference were increased frequencies of lapses and low wind speeds and a shift in the southerly frequency maximum to the southeast in 1969-70. The low-speed inversion frequency was unchanged.
- 2) Average wind hodographs at the ships exhibited the same diurnal reversal pattern and the same 2.5 m/sec nighttime downvalley speed in both years. The average wind hodograph at the tower showed a similar pattern of reversal but the nighttime downvalley speed was about 2m/sec.
- 3) All sixteen daily wind hodographs used for calculating the average hodograph at the tower showed the diurnal reversal and exhibited considerable variability in speed and direction from day to day through a complete cycle.
- 4) Maximum persistences of low-speed inversion winds in the critical 005° - 020° sector were 2 hrs, 4 hrs and 3 hrs for 1, 1.5 and 2 m/s speeds, respectively, during the entire 10-month data record.

Y-2

1. Introduction

This is the second of two progress reports covering meteorological investigations in the Hudson River valley near Indian Point from August 1968 to the present.

The first report [Halitsky, Laznow and Leahev (1970)] described wind measurements at Indian Point, Bowline Point and Montrose until 30 June 1969, and provided details of changes in tower location and instrumentation introduced during the period July-November 1969.

This report presents an analysis of measurements taken at the present tower at Indian Point (IP 3) and at a ship, the Cape Charles (CC) anchored in the Hudson River, and compares them with similar measurements taken in 1955-1957 at approximately the same locations. The focus of this report is to evaluate whether site meteorology has changed significantly during the intervening years, and to elucidate aspects of the meteorology not reported previously.

In order to clarify the various tower locations and periods of operation, the following nomenclature was established in the first report and will be continued.

<u>Date Period</u>	<u>Station Symbol</u>	<u>Station Location</u>
1955	J	Ship "Jones" in Hudson River
1956-1957	I P 1	Indian Point, southeast of plant
1968-1969	I P 2	Indian Point, southwest of plant
1968-	B P	Bowline Point
1968-	M P	Montrose Point
1969-	I P 3	Indian Point (close to I P 1)
1970	C C	Cape Charles (close to J)

Figs 1, 2 and 3 show the station locations and local topography.

2. Data Log

Fig 4 shows the periods of data acquisition for all of the stations which were in operation in 1970. Station 3 P is included, even though its operation is now being funded by Orange and Rockland Utilities, Inc., order to show the total store of data for the region. The net radiometer (R) and ambient temperature (T) at I P 3, and the Aerovane (A) at the Cape Charles are supplementary instruments provided by N. Y. University.

All of the instruments except the bivane produced continuous records on slow-speed strip charts 91 inch, 2 inch or 3 inch per hour). The bivane chart drive was modified to run 50 minutes at 3 inch per hour followed by 10 minutes at 3 inches per minute and repeat. Thus, each chart (indicated by a dot in Fig 3) contained a 36-hr record of fast-and slow-speed data for each hour.

IP3
FSAR UPDATE

3

The statistical data presented in this report represent periods when simultaneous wind speed, wind direction and temperature difference were available at I P 3. The overall period selected for analysis was 26 November 1969-1 October 1970. The degree of completeness of record is as follows:

	<u>Hours all data present</u>	<u>Total Hours in period</u>	<u>% completeness</u>
Climet	5989	7440	80.5
Aerovane	6164	7440	82.8

Y-8

3. Annual Average Wind Statistics at the I P 1 and I P 3 Stations

The annual average wind statistics at I P 3 for the 10-month measurement period in 1969-1970 are shown in graphical form in Figs 5 (a-h), 6 and 7. Also included in these figures, for comparison purposes, are the equivalent I P 1 statistics originally reported by Davidson and Halitsky (9157), Table 3.3 and subsequently incorporated into Se 2.6 of the Unit 2 FSAR.

The two sets of Aerovane statistics represent observations taken about 13 years apart with similar or identical instruments at almost the same locations. As seen in Fig 1, the two towers are about 200 ft apart, and the base of the I P e tower is about 15 ft lower in elevation. The present site topography has fewer trees, more pavement, and new steel and concrete structures in the quadrant northwest of the tower.

Wind speed and direction were measured at the 100 ft elevation on each tower; therefore the absolute elevation of the I P e instrument is about 15 ft lower than that of the I P 1 instruments.

Temperature differences were measured between 95 ft and 7 ft on the 100 ft high I P 3 tower whereas 150 ft and 7 ft were used on the 310 ft high I P 1 tower. However, the isothermal and adiabatic lapse rates were used to separate the lapse, neutral and inversion categories in both cases. This was accomplished by using an adiabatic ΔT of -0.5 F for I P 3 in place of the -0.9 F used for I P 1.

Fig 5 shows the frequency distribution of wind directions as measured by the Aerovanes in 1956 and 1970.

Fig 5a represents all winds irrespective of speed and temperature gradient class. The shapes of the curves are quite similar, the most important difference being a shift of the 1956 southerly maximum toward the southeast in 1970.

Fig 5 (b0d) shows the dependence on temperature gradient class. No major change is apparent in the neutral class, but the 1970 data show more frequent lapses and less frequent inversions in all directions.

Fig 5 (e-h) shows the dependence on speed class. The southeasterly shift observed in Fig 5a is seen to occur in the 5-8 mph and 9-13 mph speed classes. Low-speed winds in the 1-4 mph class were more frequent in 1970, especially for the 000°-045° direction range.

None of the above differences are sufficiently large to invalidate the 1956 wind statistics reported in Davidson and Halitsky (1957). Of the three noticeable differences, the decrease in frequency of inversions and the increase in southeasterly winds both contribute to reducing the concentrations in inhabited regions contiguous to the site. However, the increase frequency of low-speed winds from the northeasterly sector bears further examination.

Fig 6 shows a comparison of cumulative frequencies of wind speed for the two years. The 1956 curves can not be extended below 2 m/s because the published data show only two categories below that speed, i.e., calm and 1-4 mph, covering speeds from 0 – 4.5 mph. The cumulative frequency shown at a speed of 2 m/s is the sum of these two categories. The 1970 data were classified in finer groupings and yielded well-defined curves in the low speed range. The 1970 data in Fig 6 were uncorrected for speed calibration. It is not known if corrections were applied to the 1956 data.

The upper curves, representing all temperature gradients and directions, show good agreement for the two years. The inversion curves show good agreement during calms and near 2-3/m/s, but the 1970 inversion frequencies were smaller than the 1956 frequencies at the higher speeds. This discrepancy in high speed inversions is in the direction of enhancing the atmospheric diffusion potential over that which was postulated on the basis of the 1956 data. It is not known how much of the difference between the two years is due to the absence of October and November data in 1970.

Because of the high starting speed of the Aerovane, the curves of Fig 6 show spuriously high frequencies of low wind speeds. When the 1970 data are corrected for speed calibration (see Fig 6 of Halitsky et al (1970)], the data appear as in Fig 7.

In order to check the Aerovane data, we have included in Fig 7 the corresponding curves obtained from the more sensitive Climet instrument at the same location during the same period, corrected for speed calibration.

The difference between the Aerovane and Climet curves may be attributed to the poor behavior of the aerovane at low speeds. A true speed of 1 m/s is near the starting threshold of the Aerovane. The corresponding indicated speed may be anything in the range 0-2 mph or one division of the chart. At the same time, a one-division indication may be simply a zero setting error. For these reasons, it is believed that the Climet data should be regarded as more reliable.

4. Valley Wind Hodographs During Virtually-Zero Pressure Gradient Conditions

4.1 Average Hodographs

Average wind hodographs taken during the months of September and October 1955 are presented in FSAR Sec 2.6, Figs 2.6-1 and 2.6-2, to demonstrate that the wind reverses diurnally when the upper air (geostrophic) wind is zero or weak, thereby precluding the occurrence of protracted periods of calm or light wind.

The 1955 data were taken with an Aerovane mounted 70 ft above river elevation on the mast of a ship, the Jones, anchored in the Hudson River about one mile northwest of the tower (see Fig 2). Thirty-five days, during which weak pressure gradient conditions existed over the area, were selected for study. Of these 35 days, 12 days had virtually zero pressure gradient. The two Figures represent the average of wind vectors over the 12 or 35 day period, for each even-numbered hour during the day.

Both of the 1955 hodographs show a well-defined steady flow toward the SSW (030° winds) during the night 92000-0800 hrs), and a somewhat less steady flow toward the NNE (210° winds) during the day (1200-1600). During the transition hours (1000 and 1800 hrs) the flow was weak and variable. The average wind speeds during the night were about 2.5 m/s.

On the basis of these data, it was concluded that the accident meteorology model calling for a wind sequence of 1 m/s steady for two hours followed by 2 m/s steady in the same direction for 24 hours was conservative since the hodograph showed a wind reversal after 12 hours. However, it has been pointed out that individual hodographs for each of the days may have exhibited lower wind speeds and may have failed to show the diurnal reversal.

Y-12

8

To explore this aspect, an Aerovane was installed 100 ft above river level on the mast of another ship, the Cape Charles, anchored in the Hudson River close to the former location of the Jones. The instrument was in operation from March 17, 1970 to Sept. 17, 1970. It had been hoped that the period could be extended to the end of October to gather test data for the same months that were used in the 1955 study, but the instrument had to be removed prematurely because the ship was being prepared for removal.

Using the available record, we selected the two-month period July 15-Sept. 15 as having the closest seasonal correspondence to the 1955 study, and found 17 days during which virtually-zero pressure gradient conditions existed, as determined from surface weather maps for 0700 EST. The hourly wind velocity vector was determined for each even-numbered hour and a vector average was taken over the 17 days for those hours. The average hodograph is shown in Fig 8, together with the 1955 Jones hodograph.

The important characteristics of the 1955 hodograph were confirmed by the 1970 data. A predominant, diurnally-reversing circulation exists along the 030° - 210° axis. The nighttime down-valley flow was slightly weaker (~ 2.0 m/s vs ~ 2.4 m/s) and began about an hour later (2100 vs 2000 hrs) in 1970 but both terminated at ~ 0900 hrs. The up-valley daytime flow was also somewhat weaker (~ 1.5 m/s vs ~ 2 m/s), and did not show the strong southerly wind at 1400 and 1600 hrs. The latter effect may be due to the more northerly locations of the Jones, near the nose of Dunderberg Mtn., where the flow direction changes rapidly (see Fig 2).

Y-13

9

Before analyzing the individual hodographs for each day, it should be noted that the Jones and Cape Charles are located very close to the steep southerly side of Dunderberg Mtn. (peak el. 1120 ft), and are therefore exposed to air currents which tend to flow parallel to the hillside. This topographic influence is not present at the plant site.

To determine what differences, if any, exist between the winds at the ships and the plant site, an average hodographs for 16 of the 17 days was calculated from the records of the Climet speed and direction instrument at the 100 ft elevation on the I P 3 tower (Fig 9). The Climet instrument was inoperative on 1 of the 17 days). The most significant change from the Cape Charles hodograph is the appearance of a southeasterly wind component during the afternoon and evening hours. This component also appeared at the Jones in 1955. Apparently this is an integral part of the valley circulation, causing the hodograph vector to rotate counterclockwise with increasing time, and was not experienced at the Cape Charles due to the deflecting influence of the hillside. A northwesterly down-slope wind may also have been present during the afternoon and evening at the Cape Charles, since the hillside is in shadow at that time.

4.2 Daily Hodographs

Fig 10 (a-d) shows the 16 daily hodographs from which the average hodograph at the I P 3 tower, shown in Fig 9, was calculated. The nighttime down-valley flow appears in all 16 cases. The daytime up-valley flow is quite variable in both speed and direction, and is characterized by generally higher wind speeds and wider direction swings.

Y-14

5. Persistence of Low-Speed Winds

Fig 11 contains a time history of each of the wind conditions during the night hours of the days corresponding to the hodographs of Fig 10 (a-d). The graphs are the variation of the wind speed with time for those hours when the wind direction was between 000° and 045°. We shall assume that the wind direction was steady if it remained in this 45° sector. (This is quite conservative, since a wind which meanders uniformly in a 45° sector of 500 m radius under inversion conditions produces an average concentration about 8 times smaller than the steady wind axial concentration.)

The observed wind angle » and temperature differences $\Delta T = T_{95} - T_7$ are noted under each observation. Positive values of ΔT indicate inversions. ΔT values between – 0.5 and 0 indicate neutral. ΔT values smaller than – 0.5 designate lapses.

The longest period of direction persistence was 8 hrs, occurring on July 25-26, Aug. 8-9, Aug. 13-14, Sept. 12-13 and Sept. 13-14. The average winds speed in each case was at least 2 m/s. ΔT was recorded only 3 of these days, and an inversion occurred only during the first two hours of one of the days.

The period of poorest dispersion potential occurred on July 24-25. It lasted 6 hours with a gradual increase of wind speed from 0.2 to 2.0 m/s, a gradual decrease of temperature gradient from $\Delta T = 1.7$ to – 0.8, and a gradual direction change from 007° to 043°. The occurrence of the strongest inversion during the early part of the night and its subsequent weakening and change to neutral or lapse beyond 0200 hrs seems to be a common phenomenon at the site.

IP3
FSAR UPDATE

11

Wind persistence may also be examined by listing the number of occurrences that wind of specified characteristics persisted for a specified number of consecutive hours during the entire 10 month test period in 1969-70. The following table shows these data for inversion condition only.

Table 1. Wind Persistence at I P 3 Under Inversion Conditions 91969-1970)

Wind Sector	No. of Consec. Hrs.	Maximum speed in sequence (mph)							
		0.3	0.5	1.0	1.5	2.0	3.0	4.0	6.0
005°-020°	1	1	2	22	41	64	115	141	151
	2			1	3	2	7	5	2
	3				3		2	2	3
4				1					
	10								1
005°-020°	1			16	42	75	155	189	198
	2			1	2	5	16	7	3
	3					1	2	2	1
	4						2	3	
	5						2	1	
	6							1	
	7						1		

It is seen that very light winds do not persist beyond one hour, and high persistences begin to appear at about 3 m/s. For both sectors combined, the longest persistences for 11.0, 1.5 and 2.0 m/s winds were 2 hrs, 4 hrs and 3 hrs, respectively.

Y-16

References

Davidson, B. and J. Halitsky (1957): Evaluation of Potential Radiation Hazard Resulting from Assumed Release of Radioactive Wastes to Atmosphere from Proposed Buchanan Nuclear Power Plant. N. Y. University Dep't. of Meteorology and Oceanography Tech. Rep't. No 372.3

Halitsky, J., J. Laznow and D. Leahey (1970): Wind Observations at Indian Point, Montrose and Bowline Point. 31 August 1968 to 30 June 1969. N. Y. University Dep't. of Meteorology and Oceanography Tech. Rep't. TR-70-3.

FSAR: Final Facility Description and Safety Analysis Report. Consolidated Edison Co. of N. Y., Inc. Nuclear Generating Unit No. 2. Exhibit B-8.

IP3
FSAR UPDATE

[Historical Information]

New York University
School of Engineering and Science
Department of Meteorology and Oceanography
Geophysical Sciences Laboratory
Technical Report No. TR-73-1

Meteorological Observations at Indian Point,
Trap Rock, Montrose Point and Cape Charles
1 January 1970-31 December 1971

Prepared by

Joseph Laznow
Edward J. Kaplin, Project Director

for

Consolidated Edison Company of New York, Inc.
4 Irving Place, New York, N.Y. 10003

15 December 1972

Z-1

IP3
FSAR UPDATE

Summary

Meteorological data collected at Indian Point 3, Trap Rock, Montrose Point and the Cape Charles in 1970 and 1971 were analyzed annually, seasonally and diurnally. The results were compared with observations made by Davidson in 1955-57 at similar installations.

Results

A) Comparison between two years of Indian Point 3 (1970 and 1971) data with Indian Point 1 (1956) confirm the findings of Halitsky, et al. (1970) that any apparent meteorological differences during the intervening years are such that they favor an increase in the diffusion potential at the Indian Point site. Improvements include: a) a substantial decrease of the occurrence of inversions and b) a decrease in the probability of low wind speeds in the critical quadrant during inversion conditions.

B) A shift of the secondary maximum direction to a more southeasterly orientation was found in the annual direction frequency density distribution.

C) Seasonal differences included a binodal distribution of the summer wind directions with SSE and NNE peaks. The winter curve is tri-nodal with N, WNW-NW and SSE peaks in descending order of magnitude. The percentage of low wind speeds is highest during the summer when neutral and lapse conditions are most prevalent.

D) The seasonal variation of the diurnal mean wind direction and speed is clearly defined. A direction shift occurs during the summer with upvalley winds during the day and downvalley winds at night. The IP3 diurnal curves can be expected to rotate through 360°.

E) The seasonal diurnal persistence of the wind is maximum at night and minimum during the day. The winter

IP3
FSAR UPDATE

persistence values are approximately twice those of the summer.

The winter has a single minimum occurring between 1800-2100 while the summer minimum is binodal: 1000-1300 and 1900-2000.

The winter maximum persistence occurs between 0500-0900 while the summer maximum generally occurs between 0500-0600.

Z-3

IP3
FSAR UPDATE

Table of Contents

	<u>Page</u>
Summary	ii
List of Tables	vi
List of Figures	viii
Acknowledgment.....	x
1. Introduction	1
2. Instrumentation Characteristics	2
2.1 Sensors	2
2.2 Recorders	4
3. Data Log.....	4
4. Analytical Procedure.....	5
4.1 Wind Direction	5
4.2 Wind Speed	9
4.3 Stability Categories	10
4.31 Atmospheric Stability Categories Defined in Terms of Temperature Difference	10
4.32 Classification of Atmospheric Stability According to U. S. A. E. C. Safety Guide 23.....	10
4.4 Seasonal Distributions	11
4.5 Diurnal Analysis	11
4.6 Spatial Variation.....	11
5. Discussion of Data.....	12
5.1 Joint Frequency Distribution of Wind Direc- tion, Wind Speed and Temperature Difference	12
5.1.1 Inversion – Neutral – Lapse Temperature Difference Classification	12
5.1.2 Pasquill Stability Classification	12
5.2 Joint Frequency Distribution of Wind Direction and Temperature Difference	12
5.2.1 Monthly Distribution of Temperature Difference.....	21
5.2.2 Annual Joint Frequency Distribution of Wind Direction and Wind Speed.....	22

Z-4

Table of Contents (continued)

	Page
5.4 Frequency of Distribution of Wind Direction	26
5.4.1 Annual	26
5.4.2 Seasonal	26
5.4.3 Comparison Between IP3 and Cape Charles for a Summer Season.....	27
5.5 Cumulative Probability Distribution for Wind Speed	29
5.5.1 Annual	29
5.5.2 Seasonal	32
5.6 Diurnal Variation of the Mean Wind Direction.....	32
5.7 Diurnal Variation of the Mean Wind Speed.....	34
5.8 Diurnal Variation of Wind Persistence	34
5.9 Spatial Variability of Wind Velocity Between Tower Sites	35
References	35
Figures.....	41
Appendix.....	65

Z-5

List of Tables

<u>Tables</u>	<u>Titles</u>	<u>Page</u>
1	Instrumentation Data.....	3
2	Missing Data Log	6
3	Record of Data Recovery	7
4	Indian Point 3 Frequency Distribution of Wind Speed and Direction at 100 ft. Tower Level According to Temperature Gradient Class - 1 January 1971-31 December 1970	13
5	Indian Point 3 Frequency Distribution of Wind Speed and Direction at 100 ft Tower Level According to Temperature Gradient Class - 1 January 1971-31 December 1971	17
6	Trap Rock Frequency Distribution of Wind Speed and Direction 1 January 1970-31 December 1970	23
7	Trap Rock Frequency Distribution of Wind Speed and Direction 1 January 1971- 31 December 1971	24
8	Montrose Point Frequency Distribution of Wind Speed and Direction 1 January 1970- 31 December 1970	25
9	Annual and Seasonal Median Wind Speeds	29
10	Annual Spatial Variability of Wind Direc- tion Between Indian Point 3 and Trap Rock	35
11	Seasonal Spatial Variability of Wind Direc- tion Between Indian Point 3 and Trap Rock (1970)	36

IP3
FSAR UPDATE

12	Seasonal Spatial Variability of Wind Direction Between Indian Point 3 and Trap Rock (1971)	36
13	Annual Spatial Variability of Wind Speed (m/s) Between Indian Point 3 and Trap Rock	37
14	Seasonal Spatial Variability of Wind Speed (m/s) Between Indian Point 3 and Trap Rock	37
15	Annual Spatial Variability of Wind Direction and Speed (m/s) Between Montrose Point and Trap Rock	38

Z-6

List of Tables (continued)

<u>Tables</u>	<u>Titles</u>	<u>Page</u>
16	Annual Spatial Variability of Wind Direction and Speed (m/s) Between Indian Point 3 and Montrose Point	38
17	Summer (1970) Spatial Variability of Wind Direction and Speed (m/s) Between Cape Charles and Indian Point 3	39

Z-7

IP3
FSAR UPDATE

List of Figures

<u>Tables</u>	<u>Titles</u>	<u>Page</u>
1	Indian Point and Environs	42
2	Monthly Distribution of Temperature Dif- ference at Indian Point 3	43
3	Annual Frequency Distribution of Wind Direction According to Temperature Dif- ference Category at Indian Point 1 (1956) and Indian Point 3 (1970-1971).....	44
4	Annual Frequency Distribution of Wind Direction According to Wind Speed Category at Indian Point 1 (1956) and Indian Point 3 (1970-1971)	45
5	Annual Frequency Distribution of Wind Dir- ection at Indian Point 1 (1956), Indian Point 3 (1970-1971), Trap Rock and Montrose Point.....	46
6	Seasonal Frequency Distribution of Wind Direction at Indian Point 3	47
7	Seasonal Frequency Distribution of Wind Direction at Trap Rock	48
8	Seasonal Frequency Distribution of Wind Direction at Montrose Point.....	49
9	Frequency Distribution of Wind Direction at Cape Charles and Indian Point 3, Summer 1970.....	50
10	Annual Cumulative Probability Distribution of Wind Speed at Indian Point 3 (1970 and 1971)	51
11	Annual Cumulative Probability Distribution of Wind Speed at Indian Point 1 and Indian Point 3	52
12	Annual Cumulative Probability Distribution of Wind Speed at Trap Rock and Indian Point 3	53
13	Annual and Seasonal Cumulative Probability Distribution of Wind Speed at Montrose Point	54

IP3
FSAR UPDATE

14	Seasonal Cumulative Probability Distribution of Wind Speed at Indian Point 3	55
----	--	----

Z-8

List of Figures (continued)

<u>Tables</u>	<u>Titles</u>	<u>Page</u>
15	Seasonal Cumulative Probability Distribution of Wind Speed at Trap Rock	56
16	Cumulative Probability Distribution of Wind Speed at Cape Charles and Indian Point 3, Summer 1970	57
17	Seasonal Diurnal Mean Wind Direction at Indian Point 3.....	58
18	Seasonal Diurnal Mean Wind Direction at Trap Rock	59
19	Seasonal Diurnal Mean Wind Direction at Montrose Point.....	60
20	Diurnal Mean Wind Direction at Cape Charles and Indian Point 3, Summer 1970.....	61
21	Seasonal Diurnal Mean Wind Speed.....	62
22	Seasonal Diurnal Persistence at Indian Point 3 and Trap Rock	63
23	Seasonal Diurnal Persistence at Montrose Point and Cape Charles and Indian Point 3, Summer 1970	64

Z-9

IP3
FSAR UPDATE

Acknowledgment

Appreciation is expressed to those people who helped in the development and preparation of this report:: Assistant Research Scientists – Mitchell M. Wurmbrand, Jack Kirschner, Michael Kozenko and Michael Bono; Research Technician – Mark J. Makower; Drafting – Charles Tessmer, and Patricia Twomey, Secretary.

Z-10

1. Introduction

This is the third of three progress reports covering the continuous meteorological data collection program in the Hudson River Valley at Consolidated Edison's Indian Point nuclear generating complex in Buchanan, New York (Figure 1).

The first report (Halitsky, Laznow and Leahey (1970)) covered wind observations at the Indian Point 2 (IP2), Montrose Point (MP) and Bowline Point (BP) meteorological tower sites, and temperature difference observations at Indian Point 2 and Bowline Point for the period 31 August 1968-30 June 1969.

The second report (Halitsky, Kaplin and Laznow (1970)) covered wind and temperature difference observations at Indian Point 3 (IP3) for the period 26 November 1969-1 October 1970, and wind observations from the U.S.S. Cape Charles for the period 16 March 1970-18 September 1970. The data were compared with similar measurements taken in 1955-1957 by Davidson ((Davidson and Halitsky (1957) and FSAR)) at approximately the same locations. The analysis was made to determine if significant changes had occurred in onsite meteorology during the intervening years.

The function of the present study was to provide meteorological data to support analyses for nuclear units at Indian point as specified by the following items:

- a) Turbulence analysis at Indian Point;
- b) Analysis of spatial variability of winds between Indian Point 3, Trap Rock (TR) and Montrose Point;
- c) Acquisition of wind statistics at Indian Point 3 and Trap Rock; and
- d) Additional instrumentation at Trap Rock to develop annual wind statistics and turbulence measurements comparable to those being collected at Indian Point 3.

Item (a) was satisfied, in part by Leahey and Halitsky (1971) whose study developed the techniques and procedures for the analysis of diffusion parameters at Indian Point and

provided initial results.

Items (b) and (c) are covered in this report. Seasonal, diurnal and annual analyses are provided and the comparison with the 1955-57 data has been extended through December 1971.

The instrumentation required to satisfy item (d) was obtained but due to de-emphasis of the Verplank site (TR) it was never installed.

2. Instrumentation Characteristics

Meteorological station locations, tower base elevations and information pertaining to instrumentation, parameter of measurement, elevation of sensor above tower base and period of record are presented in Table 1.

2.1 Sensors

- a) Climet Wind Speed: threshold, 0.6 MPH; accuracy, \pm % or \pm 0.15 MPH; distance constant, 5 feet. (Distance constant is defined as the feet of air required to pass through the transmitter to give 63% of a sharp change.)
- b) Climet Wind Direction: threshold, < 1 MPH; damping ratio, 0.4; accuracy, \pm 3°.
- c) Aerovane Wind Speed: threshold, 2.5 MPH; distance constant, 15 feet.
- d) Aerovane Wind Direction: distance constant, 34 feet.
- e) Net Exchange Thermal Radiometer: temperature compensation to an accuracy of \pm 1% over a range of -20 to \pm 160° F.
- f) R. M. Young-Gill Bivane: threshold, 0.3-0.5 MPH for both azimuth and elevation.
- g) Honeywell-Brown Resistance Bulb: when placed in specially designed wells, the time constant is about 3 minutes in a wind of 20 fps, the bulbs are in shielded gold leafed cylinders and aspirated at

4.

about 20 fps (Davidson and Halitsky (1955)).

h) Rosemount Nickel Resistance Bulb (Temperature Difference): response time 63%

< 90 sec. With 15 fps air flow; accuracy, $\pm 0.5\%$ at icepoint, linear to 0.05% of full

scale; overall accuracy, $< \pm 0.1^\circ \text{ F}$.

i) Rosemount Nickel Resistance Bulb (Ambient Temperature): same as (h) except

overall accuracy, $\pm 0.1^\circ \text{ F}$.

j) Foxboro Dewcel: if ambient temperature $\geq 32^\circ \text{ F}$, dew point accuracy, $\pm 0.5^\circ \text{ F}$; if

ambient temperature $0^\circ \text{ F} < 32^\circ \text{ F}$, dew point accuracy, $\pm 1.0^\circ \text{ F}$; if ambient

temperature $< 0^\circ \text{ F}$, dew point accuracy, $\pm 1.5^\circ \text{ F}$.

Items (h), (i), and (j) are mounted in Climet aspirated shields.

IP3
FSAR UPDATE

Table 1. Instrumentation Data

Meteorological Station (ft)	Base Elev. (ft) Above				Elev.
<u>Location</u>	<u>River</u>	<u>Operating Period</u>	<u>Parameter</u>	<u>Instruments</u>	<u>Above</u> <u>Base</u>
Indian Point 3 (IP3)	120	1 Jan 70-Present	Wind Speed	Climet	100
			Wind Direction	Climet	100
		1 Jan 70-20 July 71 & 24 July 72-Present	Wind Speed	Aerovane	100
			Wind Direction	Aerovane	100
		14 Aug 70-Present	Net Radiation	Thermal Radiometer	30
		May 70-Dec 70 (Intermittent)	Turbulence	Bivane	100
		1 Jan 70-25 Oct 71	Temperature Difference	Honeywell- Brown Resis-	95-7
				tance Bulb	
		14 Aug 72-Present	Temperature Difference	Rosemount	10-100
				Nickle Resis-	10-30
				tance Bulb	
			Ambient Temperature	Rosemount	30
				Nickle Resis-	
				tance Bulb	
			Dew Point	Foxboro Dew- cel	100, 30, 10
Trap Rock (TR)	90	1 Jan 70-27 July 72	Wind Speed	Climet	100
			Wind Direction	Climet	100
Montrose Point (MP)	60	1 Jan 70-7 June 71	Wind Speed	Climet	100
			Wind Direction	Climet	100
Cape Charles (CC)	0	16 Mar 70-18 Sept 70	Wind Speed	Aerovane	100
			Wind Direction	Aerovane	100

Z-13

IP3
FSAR UPDATE

Table 4. Indian Point 3 Frequency Distribution of Wind Speed and Direction at 100 ft Tower Level
According to Temperature Gradient Class-January 1, 1970-December 31, 1970

Wind Direction	Temp. Grad.	Wind Speed (m/s)										Miss	Total
		0.0- 0.5	>0.5- 1.0	>1.0- 1.5	>1.5- 2.5	>2.5- 3.5	>3.5- 4.5	>4.5- 5.5	>5.5- 8.5	>8.5- 11.0	>11.0		
349- 11	I	.0016	.0031	.0046	.0042	.0038	.0019	.0002	.0005	.0000	.0000	.0001	.0200
	N	.0009	.0010	.0018	.0063	.0093	.0086	.0063	.0045	.0006	.0001	.0015	.0408
	L	.0000	.0007	.0010	.0056	.0104	.0071	.0043	.0050	.0003	.0000	.0001	.0346
	M	.0003	.0008	.0007	.0021	.0040	.0047	.0029	.0019	.0002	.0000	.0000	.0176
	T	.0029	.0056	.0081	.0182	.0274	.0223	.0137	.0119	.0011	.0001	.0017	.1131
12- 33	I	.0003	.0022	.0047	.0125	.0102	.0050	.0013	.0002	.0000	.0000	.0002	.0366
	N	.0002	.0016	.0033	.0091	.0131	.0085	.0021	.0022	.0008	.0001	.0018	.0429
	L	.0001	.0006	.0015	.0067	.0073	.0034	.0018	.0025	.0000	.0000	.0001	.0241
	M	.0001	.0010	.0018	.0080	.0085	.0049	.0022	.0006	.0000	.0000	.0000	.0271
	T	.0008	.0054	.0113	.0364	.0391	.0218	.0073	.0055	.0008	.0001	.0022	.1307
34-56	I	.0007	.0031	.0050	.0090	.0041	.0010	.0003	.0000	.0000	.0000	.0006	.0239
	N	.0002	.0006	.0023	.0043	.0032	.0011	.0003	.0003	.0005	.0000	.0011	.0141
	L	.0002	.0009	.0016	.0048	.0043	.0009	.0006	.0007	.0001	.0000	.0002	.0144
	M	.0002	.0009	.0015	.0051	.0048	.0018	.0007	.0001	.0000	.0000	.0000	.0152
	T	.0014	.0055	.0104	.0233	.0165	.0049	.0019	.0011	.0006	.0000	.0019	.0676
57-78	I	.0009	.0017	.0022	.0019	.0007	.0001	.0001	.0000	.0000	.0000	.0000	.0077
	N	.0003	.0006	.0016	.0011	.0007	.0002	.0000	.0001	.0000	.0000	.0005	.0051
	L	.0001	.0005	.0007	.0014	.0003	.0003	.0000	.0005	.0001	.0000	.0002	.0041
	M	.0001	.0001	.0010	.0018	.0013	.0007	.0005	.0000	.0000	.0000	.0000	.0055
	T	.0015	.0029	.0055	.0063	.0030	.0014	.0006	.0006	.0001	.0000	.0007	.0224
79-101	I	.0001	.0013	.0011	.0016	.0007	.0001	.0000	.0002	.0000	.0000	.0000	.0051
	N	.0002	.0005	.0014	.0016	.0011	.0009	.0006	.0000	.0000	.0000	.0002	.0065
	L	.0000	.0006	.0007	.0008	.0005	.0001	.0000	.0003	.0000	.0000	.0000	.0030
	M	.0000	.0005	.0005	.0018	.0007	.0001	.0003	.0001	.0000	.0000	.0000	.0040
	T	.0003	.0027	.0037	.0058	.0030	.0013	.0009	.0007	.0000	.0000	.0002	.0186

IP3
FSAR UPDATE

Table 4 (continued)

Wind Direction	Temp. Grad.	Wind Speed (m/s)										Miss	Total
		0.0-0.5	>0.5-1.0	>1.0-1.5	>1.5-2.5	>2.5-3.5	>3.5-4.5	>4.5-5.5	>5.5-8.5	>8.5-11.0	>11.0		
102-123	I	.0005	.0008	.0011	.0011	.0011	.0000	.0001	.0000	.0000	.0000	.0001	.0049
	N	.0005	.0015	.0009	.0014	.0015	.0007	.0006	.0003	.0000	.0000	.0003	.0077
	L	.0001	.0005	.0006	.0018	.0002	.0008	.0002	.0002	.0000	.0000	.0000	.0045
	M	.0003	.0006	.0007	.0006	.0010	.0006	.0008	.0001	.0000	.0000	.0000	.0047
	T	.0014	.0033	.0033	.0049	.0039	.0021	.0017	.0007	.0000	.0000	.0005	.0217
124-146	I	.0003	.0014	.0023	.0019	.0014	.0006	.0000	.0000	.0001	.0000	.0001	.0081
	N	.0003	.0010	.0014	.0032	.0027	.0018	.0006	.0006	.0003	.0000	.0001	.0121
	L	.0001	.0006	.0016	.0018	.0015	.0026	.0009	.0017	.0002	.0000	.0000	.0111
	M	.0003	.0009	.0005	.0015	.0022	.0007	.0001	.0002	.0000	.0000	.0000	.0064
	T	.0011	.0039	.0057	.0085	.0078	.0057	.0016	.0025	.0007	.0000	.0002	.0377
147-168	I	.0007	.0015	.0027	.0047	.0040	.0014	.0002	.0002	.0003	.0001	.0000	.0159
	N	.0002	.0008	.0011	.0039	.0064	.0037	.0022	.0035	.0003	.0000	.0002	.0224
	L	.0003	.0003	.0022	.0050	.0098	.0081	.0080	.0110	.0001	.0000	.0001	.0450
	M	.0001	.0005	.0011	.0043	.0057	.0027	.0015	.0003	.0000	.0000	.0000	.0163
	T	.0014	.0031	.0072	.0179	.0260	.0159	.0119	.0151	.0008	.0001	.0003	.0997
169-191	I	.0003	.0013	.0021	.0058	.0047	.0014	.0010	.0002	.0002	.0003	.0000	.0174
	N	.0001	.0005	.0013	.0043	.0049	.0026	.0014	.0005	.0000	.0000	.0001	.0157
	L	.0002	.0010	.0022	.0106	.0101	.0046	.0046	.0027	.0000	.0000	.0003	.0364
	M	.0002	.0005	.0014	.0037	.0065	.0034	.0009	.0007	.0000	.0000	.0000	.0173
	T	.0009	.0032	.0069	.0245	.0262	.0120	.0079	.0041	.0002	.0003	.0005	.0867
192-213	I	.0002	.0021	.0032	.0071	.0040	.0022	.0011	.0002	.0000	.0000	.0002	.0203
	N	.0003	.0006	.0016	.0025	.0013	.0013	.0013	.0008	.0000	.0000	.0000	.0096
	L	.0001	.0002	.0022	.0065	.0039	.0023	.0019	.0008	.0000	.0000	.0001	.0181
	M	.0001	.0003	.0007	.0041	.0032	.0021	.0003	.0002	.0000	.0000	.0000	.0111
	T	.0008	.0032	.0077	.0202	.0123	.0078	.0047	.0021	.0000	.0000	.0003	.0591

Z-24

14.

IP3
FSAR UPDATE

Table 4 (continued)

Wind Direction	Temp. Grad.	Wind Speed (m/s)										Miss	Total
		0.0- 0.5	>0.5- 1.0	>1.0- 1.5	>1.5- 2.5	>2.5- 3.5	>3.5- 4.5	>4.5- 5.5	>5.5- 8.5	>8.5- 11.0	>11.0		
214-236	I	.0011	.0022	.0027	.0062	.0032	.0009	.0008	.0005	.0001	.0000	.0002	.0179
	N	.0002	.0010	.0008	.0014	.0009	.0007	.0003	.0002	.0001	.0001	.0001	.0059
	L	.0000	.0014	.0010	.0042	.0010	.0007	.0010	.0014	.0000	.0000	.0002	.0110
	M	.0001	.0002	.0011	.0031	.0015	.0003	.0002	.0002	.0000	.0000	.0000	.0069
	T	.0015	.0048	.0057	.0149	.0066	.0026	.0024	.0023	.0002	.0001	.0006	.0417
237-258	I	.0007	.0018	.0021	.0021	.0017	.0008	.0013	.0006	.0006	.0000	.0002	.0118
	N	.0000	.0003	.0005	.0010	.0010	.0003	.0003	.0008	.0002	.0001	.0000	.0047
	L	.0003	.0011	.0010	.0014	.0006	.0007	.0007	.0009	.0000	.0000	.0001	.0069
	M	.0000	.0005	.0005	.0007	.0006	.0002	.0001	.0007	.0000	.0000	.0000	.0032
	T	.0010	.0038	.0040	.0051	.0039	.0021	.0024	.0030	.0008	.0001	.0003	.0265
259-281	I	.0009	.0017	.0013	.0008	.0015	.0014	.0006	.0008	.0007	.0003	.0001	.0101
	N	.0001	.0009	.0005	.0008	.0009	.0016	.0009	.0021	.0010	.0002	.0000	.0090
	L	.0001	.0003	.0007	.0017	.0016	.0023	.0018	.0027	.0006	.0001	.0007	.0127
	M	.0000	.0005	.0005	.0006	.0007	.0005	.0008	.0007	.0001	.0000	.0000	.0042
	T	.0011	.0034	.0029	.0039	.0047	.0057	.0041	.0063	.0024	.0007	.0008	.0360
282-303	I	.0005	.0013	.0011	.0003	.0005	.0009	.0014	.0022	.0016	.0010	.0000	.0107
	N	.0001	.0003	.0006	.0003	.0010	.0019	.0033	.0114	.0070	.0011	.0000	.0272
	L	.0006	.0006	.0002	.0011	.0014	.0029	.0015	.0101	.0042	.0017	.0011	.0254
	M	.0000	.0003	.0001	.0005	.0010	.0006	.0009	.0023	.0002	.0003	.0000	.0063
	T	.0011	.0025	.0021	.0023	.0039	.0063	.0071	.0260	.0130	.0042	.0011	.0696
304-326	I	.0005	.0014	.0009	.0006	.0009	.0008	.0007	.0018	.0006	.0002	.0000	.0083
	N	.0003	.0006	.0001	.0010	.0022	.0026	.0047	.0162	.0048	.0016	.0001	.0343
	L	.0001	.0002	.0006	.0010	.0014	.0030	.0033	.0088	.0064	.0025	.0005	.0278
	M	.0000	.0005	.0002	.0010	.0006	.0007	.0026	.0056	.0015	.0003	.0000	.0130
	T	.0009	.0026	.0018	.0037	.0050	.0071	.0113	.0325	.0133	.0047	.0006	.0835

IP3
FSAR UPDATE

Table 4 (continued)

Wind Direction	Temp. Grad.	Wind Speed (m/s)										Miss	Total
		0.0- 0.5	>0.5- 1.0	>1.0- 1.5	>1.5- 2.5	>2.5- 3.5	>3.5- 4.5	>4.5- 5.5	>5.5- 8.5	>8.5- 11.0	>11.0		
327-348	I	.0009	.0015	.0015	.0016	.0011	.0009	.0006	.0010	.0000	.0000	.0001	.0093
	N	.0001	.0005	.0008	.0034	.0033	.0034	.0049	.0083	.0015	.0000	.0002	.0265
	L	.0002	.0005	.0005	.0026	.0043	.0027	.0031	.0077	.0016	.0002	.0000	.0234
	M	.0000	.0005	.0008	.0008	.0011	.0022	.0027	.0053	.0009	.0001	.0000	.0144
	T	.0013	.0029	.0035	.0085	.0099	.0093	.0113	.0223	.0040	.0003	.0003	.0736
Calm	I	.0000										.0000	.0000
	N	.0000										.0000	.0000
	L	.0000										.0000	.0000
	M	.0000										.0000	.0000
	T	.0000										.0000	.0000
Miss	I	.0001	.0003	.0007	.0005	.0003	.0002	.0001	.0003	.0000	.0000	.0017	.0043
	N	.0000	.0000	.0000	.0000	.0000	.0001	.0005	.0010	.0009	.0000	.0010	.0035
	L	.0000	.0000	.0000	.0000	.0000	.0000	.0000	.0000	.0002	.0001	.0024	.0027
	M	.0000	.0000	.0001	.0000	.0006	.0002	.0002	.0000	.0000	.0000		.0011
	T	.0001	.0003	.0008	.0005	.0009	.0006	.0008	.0014	.0011	.0001	.0051	.0118
Total	I	.0104	.0285	.0393	.0620	.0439	.0197	.0098	.0088	.0042	.0021	.0038	.2324
	N	.0043	.0122	.0199	.0458	.0536	.0401	.0302	.0529	.0181	.0034	.0074	.2881
	L	.0027	.0099	.0182	.0573	.0586	.0425	.0338	.0570	.0139	.0047	.0063	.3051
	M	.0021	.0085	.0131	.0397	.0439	.0264	.0178	.0191	.0030	.0009	.0000	.1743
	T	.0195	.0591	.0905	.2048	.2001	.1287	.0917	.1379	.0392	.0110	.0175	1.0000

IP3
FSAR UPDATE

Table 5. Indian Point 3 Frequency Distribution of Wind Speed and Direction at 100 ft Tower Level
According to Temperature Gradient Class-January 1, 1971-December 31, 1971

Wind Direction	Temp. Grad.	Wind Speed (m/s)										Miss	Total
		0.0-0.5	>0.5-1.0	>1.0-1.5	>1.5-2.5	>2.5-3.5	>3.5-4.5	>4.5-5.5	>5.5-8.5	>8.5-11.0	>11.0		
349- 11	I	.0007	.0023	.0041	.0071	.0063	.0041	.0013	.0019	.0003	.0007	.0000	.0288
	N	.0001	.0005	.0009	.0041	.0065	.0050	.0018	.0046	.0008	.0002	.0002	.0248
	L	.0000	.0005	.0010	.0050	.0067	.0047	.0033	.0037	.0011	.0000	.0001	.0262
	M	.0002	.0021	.0031	.0078	.0121	.0074	.0067	.0031	.0000	.0006	.0008	.0439
12- 33	T	.0010	.0053	.0091	.0240	.0317	.0213	.0132	.0133	.0023	.0015	.0011	.1237
	I	.0005	.0033	.0039	.0150	.0169	.0053	.0016	.0018	.0000	.0000	.0000	.0483
	N	.0001	.0011	.0010	.0037	.0070	.0047	.0032	.0016	.0001	.0000	.0000	.0225
	L	.0001	.0002	.0007	.0045	.0043	.0021	.0003	.0007	.0000	.0000	.0001	.0130
34- 56	M	.0002	.0023	.0041	.0136	.0145	.0096	.0040	.0022	.0006	.0000	.0002	.0513
	T	.0009	.0070	.0097	.0367	.0428	.0216	.0091	.0063	.0007	.0000	.0003	.1352
	I	.0002	.0030	.0051	.0070	.0045	.0008	.0001	.0000	.0000	.0000	.0000	.0207
	N	.0001	.0010	.0017	.0025	.0023	.0010	.0001	.0006	.0001	.0000	.0010	.0105
57- 78	L	.0001	.0005	.0013	.0022	.0009	.0008	.0001	.0000	.0000	.0000	.0001	.0059
	M	.0002	.0018	.0048	.0096	.0080	.0024	.0009	.0003	.0002	.0000	.0000	.0284
	T	.0007	.0063	.0129	.0213	.0157	.0050	.0013	.0009	.0003	.0000	.0011	.0655
	I	.0001	.0017	.0027	.0023	.0005	.0003	.0001	.0000	.0000	.0000	.0000	.0078
79-101	N	.0001	.0005	.0006	.0010	.0007	.0016	.0002	.0001	.0000	.0000	.0002	.0050
	L	.0002	.0003	.0001	.0009	.0001	.0002	.0006	.0002	.0000	.0000	.0000	.0027
	M	.0002	.0017	.0022	.0035	.0032	.0006	.0000	.0000	.0000	.0000	.0000	.0114
	T	.0007	.0042	.0056	.0078	.0045	.0027	.0009	.0003	.0000	.0000	.0002	.0270
	I	.0002	.0009	.0017	.0016	.0002	.0000	.0000	.0000	.0000	.0000	.0000	.0047
	N	.0001	.0005	.0009	.0013	.0008	.0005	.0001	.0000	.0000	.0000	.0000	.0041
	L	.0000	.0003	.0002	.0000	.0005	.0007	.0001	.0000	.0000	.0000	.0000	.0018
	M	.0003	.0021	.0016	.0024	.0013	.0003	.0000	.0000	.0000	.0000	.0000	.0080
	T	.0007	.0038	.0045	.0053	.0027	.0015	.0002	.0000	.0000	.0000	.0000	.0186

IP3
FSAR UPDATE

Table 5 (continued)													
Wind Direction	Temp. Grad.	Wind Speed (m/s)										Miss	Total
		0.0-0.5	>0.5-1.0	>1.0-1.5	>1.5-2.5	>2.5-3.5	>3.5-4.5	>4.5-5.5	>5.5-8.5	>8.5-11.0	>11.0		
102-123	I	.0002	.0015	.0016	.0024	.0008	.0001	.0000	.0000	.0000	.0000	.0000	.0066
	N	.0000	.0008	.0002	.0010	.0011	.0001	.0001	.0000	.0000	.0000	.0000	.0034
	L	.0001	.0003	.0003	.0010	.0003	.0003	.0003	.0002	.0000	.0000	.0000	.0031
	M	.0000	.0011	.0021	.0019	.0009	.0001	.0000	.0001	.0000	.0000	.0000	.0063
	T	.0003	.0038	.0042	.0064	.0032	.0007	.0005	.0003	.0000	.0000	.0000	.0194
124-146	I	.0003	.0021	.0015	.0046	.0030	.0007	.0000	.0001	.0000	.0000	.0000	.0122
	N	.0000	.0008	.0005	.0015	.0030	.0011	.0008	.0008	.0000	.0000	.0000	.0085
	L	.0000	.0002	.0005	.0011	.0009	.0021	.0015	.0022	.0001	.0000	.0000	.0086
	M	.0001	.0011	.0007	.0029	.0023	.0017	.0014	.0015	.0002	.0002	.0000	.0121
	T	.0005	.0042	.0031	.0101	.0091	.0056	.0037	.0046	.0003	.0002	.0000	.0414
147-168	I	.0005	.0010	.0026	.0051	.0047	.0025	.0007	.0005	.0000	.0000	.0000	.0176
	N	.0000	.0006	.0005	.0032	.0018	.0019	.0022	.0017	.0000	.0000	.0000	.0119
	L	.0000	.0003	.0011	.0047	.0053	.0051	.0048	.0024	.0003	.0000	.0000	.0241
	M	.0000	.0015	.0021	.0071	.0088	.0046	.0022	.0027	.0000	.0002	.0000	.0292
	T	.0005	.0034	.0063	.0201	.0206	.0142	.0098	.0073	.0003	.0002	.0000	.0828
169-191	I	.0002	.0016	.0038	.0070	.0055	.0017	.0001	.0006	.0001	.0000	.0000	.0206
	N	.0000	.0003	.0005	.0018	.0017	.0014	.0006	.0011	.0000	.0000	.0000	.0074
	L	.0000	.0005	.0015	.0055	.0045	.0023	.0019	.0013	.0000	.0000	.0000	.0174
	M	.0001	.0019	.0027	.0090	.0079	.0034	.0030	.0022	.0000	.0000	.0000	.0303
	T	.0003	.0043	.0085	.0233	.0196	.0088	.0056	.0051	.0001	.0000	.0000	.0757
192-213	I	.0005	.0017	.0034	.0051	.0042	.0021	.0007	.0003	.0002	.0000	.0000	.0183
	N	.0001	.0002	.0005	.0010	.0007	.0006	.0006	.0006	.0001	.0000	.0000	.0043
	L	.0000	.0003	.0008	.0032	.0017	.0009	.0014	.0009	.0000	.0000	.0000	.0093
	M	.0000	.0015	.0031	.0061	.0061	.0039	.0013	.0006	.0000	.0000	.0002	.0226
	T	.0006	.0038	.0078	.0154	.0127	.0074	.0039	.0024	.0003	.0000	.0002	.0545

IP3
FSAR UPDATE

Table 5 (continued)													
Wind Direction	Temp. Grad.	Wind Speed (m/s)										Miss	Total
		0.0-0.5	>0.5-1.0	>1.0-1.5	>1.5-2.5	>2.5-3.5	>3.5-4.5	>4.5-5.5	>5.5-8.5	>8.5-11.0	>11.0		
214-236	I	.0001	.0014	.0023	.0033	.0024	.0010	.0003	.0011	.0001	.0000	.0000	.0121
	N	.0000	.0006	.0005	.0007	.0002	.0009	.0005	.0017	.0002	.0001	.0000	.0054
	L	.0001	.0006	.0010	.0018	.0006	.0007	.0002	.0014	.0001	.0000	.0000	.0065
	M	.0002	.0013	.0025	.0046	.0025	.0010	.0008	.0007	.0000	.0000	.0003	.0140
	T	.0005	.0038	.0063	.0104	.0057	.0037	.0018	.0049	.0005	.0001	.0003	.0380
237-258	I	.0005	.0021	.0019	.0024	.0018	.0021	.0007	.0013	.0007	.0002	.0000	.0136
	N	.0001	.0003	.0005	.0002	.0009	.0014	.0013	.0016	.0006	.0001	.0000	.0070
	L	.0000	.0002	.0003	.0018	.0007	.0007	.0011	.0035	.0014	.0006	.0000	.0104
	M	.0002	.0014	.0013	.0015	.0021	.0006	.0006	.0006	.0000	.0000	.0001	.0082
	T	.0008	.0040	.0040	.0059	.0055	.0047	.0037	.0070	.0026	.0009	.0001	.0392
259-281	I	.0003	.0016	.0013	.0017	.0016	.0019	.0016	.0013	.0007	.0001	.0000	.0121
	N	.0001	.0002	.0000	.0000	.0009	.0013	.0024	.0053	.0013	.0001	.0000	.0115
	L	.0000	.0003	.0003	.0005	.0015	.0027	.0021	.0038	.0023	.0003	.0000	.0138
	M	.0005	.0013	.0014	.0016	.0022	.0023	.0016	.0030	.0014	.0000	.0001	.0152
	T	.0009	.0034	.0030	.0038	.0062	.0082	.0077	.0133	.0056	.0006	.0001	.0527
282-303	I	.0008	.0014	.0009	.0010	.0014	.0017	.0024	.0029	.0008	.0001	.0001	.0135
	N	.0001	.0002	.0003	.0002	.0008	.0023	.0030	.0069	.0024	.0013	.0013	.0188
	L	.0001	.0001	.0009	.0009	.0008	.0023	.0035	.0090	.0041	.0010	.0000	.0229
	M	.0006	.0008	.0014	.0014	.0024	.0025	.0030	.0080	.0024	.0009	.0001	.0234
	T	.0016	.0025	.0035	.0035	.0054	.0088	.0119	.0268	.0097	.0033	.0015	.0786
304-326	I	.0001	.0017	.0005	.0010	.0013	.0019	.0023	.0029	.0003	.0001	.0000	.0121
	N	.0000	.0002	.0002	.0003	.0003	.0015	.0032	.0072	.0011	.0003	.0002	.0148
	L	.0001	.0010	.0006	.0007	.0018	.0023	.0015	.0079	.0041	.0005	.0000	.0205
	M	.0005	.0008	.0010	.0006	.0025	.0030	.0040	.0113	.0056	.0008	.0000	.0301
	T	.0007	.0038	.0023	.0026	.0059	.0087	.0110	.0293	.0112	.0017	.0002	.0774

IP3
FSAR UPDATE

Table 5 (continued)													
Wind Direction	Temp. Grad.	Wind Speed (m/s)										Miss	Total
		0.0-0.5	>0.5-1.0	>1.0-1.5	>1.5-2.5	>2.5-3.5	>3.5-4.5	>4.5-5.5	>5.5-8.5	>8.5-11.0	>11.0		
327-348	I	.0006	.0021	.0011	.0017	.0018	.0010	.0014	.0015	.0002	.0000	.0000	.0114
	N	.0001	.0002	.0002	.0003	.0017	.0017	.0023	.0040	.0003	.0001	.0001	.0112
	L	.0000	.0000	.0003	.0017	.0035	.0040	.0019	.0053	.0005	.0002	.0000	.0175
	M	.0000	.0010	.0014	.0025	.0031	.0042	.0039	.0095	.0032	.0003	.0006	.0297
	T	.0007	.0033	.0031	.0063	.0102	.0110	.0095	.0202	.0042	.0007	.0007	.0699
Calm	I	.0000										.0000	.0000
	N	.0000										.0000	.0000
	L	.0000										.0000	.0000
	M	.0000										.0000	.0000
	T	.0000										.0000	.0000
Miss	I	.0000	.0000	.0000	.0000	.0000	.0000	.0000	.0000	.0000	.0000	.0000	.0000
	N	.0000	.0000	.0000	.0000	.0000	.0000	.0000	.0000	.0000	.0000	.0001	.0001
	L	.0000	.0000	.0000	.0000	.0000	.0000	.0000	.0000	.0000	.0000	.0002	.0002
	M	.0000	.0000	.0000	.0000	.0000	.0000	.0000	.0000	.0000	.0000	.0000	.0000
	T	.0000	.0000	.0000	.0000	.0000	.0000	.0000	.0000	.0000	.0000	.0003	.0003
Total	I	.0058	.0293	.0385	.0684	.0568	.0273	.0133	.0161	.0035	.0013	.0001	.2605
	N	.0011	.0081	.0089	.0230	.0305	.0270	.0223	.0377	.0071	.0023	.0032	.1713
	L	.0009	.0058	.0111	.0356	.0342	.0319	.0248	.0424	.0141	.0026	.0006	.2040
	M	.0034	.0237	.0353	.0760	.0798	.0477	.0333	.0457	.0136	.0031	.0025	.3642
	T	.0113	.0669	.0939	.2030	.2014	.1339	.0937	.1420	.0383	.0093	.0064	1.0000

IP3
FSAR UPDATE

Table 6. Trap Rock Frequency Distribution of Wind Speed and Direction
January 1, 1970-December 31, 1970.

			Wind Speed (m/s)											
			0.0- 0.5	>0.5- 1.0	>1.0- 1.5	>1.5- 2.5	>2.5- 3.5	>3.5- 4.5	>4.5- 5.5	>5.5- 8.5	>8.5- 11.0			>11.0
Wind	Direction											Miss	Total	
Z-33	349- 11	N	.0049	.0113	.0146	.0247	.0203	.0155	.0117	.0170	.0030	.0013	.0029	.1271
	12- 33	NNE	.0024	.0101	.0137	.0244	.0215	.0087	.0051	.0034	.0007	.0002	.0022	.0925
	34- 56	NE	.0035	.0088	.0105	.0118	.0086	.0024	.0005	.0009	.0005	.0000	.0007	.0481
	57- 78	ENE	.0021	.0047	.0058	.0052	.0015	.0003	.0001	.0008	.0000	.0000	.0002	.0208
	79-101	E	.0012	.0028	.0036	.0056	.0028	.0012	.0003	.0003	.0000	.0000	.0001	.0178
	102-123	ESE	.0020	.0038	.0039	.0058	.0046	.0022	.0009	.0007	.0001	.0000	.0000	.0241
	124-146	SE	.0012	.0044	.0058	.0146	.0152	.0130	.0081	.0133	.0027	.0002	.0002	.0786
	147-168	SSE	.0019	.0057	.0109	.0210	.0208	.0126	.0075	.0111	.0010	.0007	.0003	.0935
	169-191	S	.0012	.0072	.0084	.0178	.0141	.0084	.0050	.0041	.0001	.0000	.0008	.0671
	192-213	SSW	.0021	.0057	.0088	.0130	.0091	.0036	.0027	.0023	.0002	.0001	.0007	.0483
	214-236	SW	.0029	.0064	.0065	.0075	.0031	.0024	.0013	.0029	.0001	.0005	.0002	.0338
	237-258	WSW	.0028	.0041	.0025	.0045	.0038	.0029	.0028	.0024	.0005	.0005	.0000	.0267
	259-281	W	.0023	.0038	.0027	.0034	.0043	.0051	.0042	.0083	.0030	.0012	.0001	.0383
	282-303	WNW	.0022	.0038	.0031	.0065	.0073	.0089	.0079	.0204	.0091	.0056	.0010	.0758
	304-326	NW	.0023	.0047	.0049	.0081	.0109	.0131	.0087	.0306	.0191	.0076	.0030	.1130
	327-348	NNW	.0038	.0087	.0079	.0145	.0139	.0114	.0076	.0139	.0031	.0030	.0020	.0898
Calm			.0000											.0000
Miss			.0000	.0003	.0005	.0023	.0012	.0001	.0000	.0001	.0001	.0000		.0046
Total			.0385	.0963	.1140	.1905	.1630	.1117	.0743	.1326	.0434	.0208	.0146	1.0000

IP3
FSAR UPDATE

Table 7. Trap Rock Frequency Distribution of Wind Speed and Direction
January 1, 1971-December 31, 1971

			Wind Speed (m/s)											
Wind	Direction		0.0- 0.5	>0.5- 1.0	>1.0- 1.5	>1.5- 2.5	>2.5- 3.5	>3.5- 4.5	>4.5- 5.5	>5.5- 8.5	>8.5- 11.0	>11.0	Miss	Total
Z-34	349- 11	N	.0011	.0105	.0123	.0240	.0217	.0166	.0126	.0266	.0041	.0030	.0002	.1328
	12- 33	NNE	.0015	.0061	.0159	.0375	.0281	.0145	.0046	.0037	.0002	.0001	.0008	.1130
	34- 56	NE	.0012	.0070	.0078	.0231	.0120	.0044	.0013	.0013	.0001	.0000	.0007	.0590
	57- 78	ENE	.0007	.0033	.0055	.0069	.0032	.0012	.0004	.0001	.0001	.0000	.0001	.0214
	79-101	E	.0008	.0033	.0033	.0040	.0025	.0009	.0004	.0000	.0000	.0000	.0001	.0152
	102-123	ESE	.0011	.0027	.0027	.0071	.0046	.0013	.0009	.0002	.0000	.0000	.0001	.0207
	124-146	SE	.0006	.0019	.0036	.0091	.0139	.0099	.0079	.0084	.0007	.0001	.0002	.0565
	147-168	SSE	.0007	.0040	.0084	.0179	.0188	.0122	.0086	.0081	.0009	.0001	.0000	.0797
	169-191	S	.0015	.0033	.0078	.0161	.0124	.0067	.0041	.0043	.0002	.0001	.0001	.0567
	192-213	SSW	.0012	.0047	.0079	.0145	.0099	.0061	.0033	.0027	.0000	.0000	.0008	.0511
	214-236	SW	.0012	.0047	.0068	.0120	.0058	.0029	.0025	.0037	.0000	.0002	.0008	.0407
	237-258	WSW	.0018	.0053	.0044	.0040	.0047	.0033	.0037	.0071	.0027	.0009	.0008	.0387
	259-281	W	.0013	.0040	.0029	.0044	.0053	.0047	.0057	.0106	.0042	.0009	.0016	.0457
	282-303	WNW	.0013	.0044	.0029	.0042	.0088	.0111	.0118	.0261	.0085	.0034	.0027	.0852
	304-326	NW	.0013	.0057	.0037	.0047	.0071	.0129	.0117	.0360	.0161	.0037	.0022	.1052
	327-348	NNW	.0014	.0083	.0077	.0090	.0094	.0113	.0092	.0139	.0026	.0007	.0013	.0748
Z-35	Calm		.0000											.0000
	Miss		.0000	.0000	.0005	.0012	.0005	.0005	.0004	.0005	.0001	.0002		.0037
	Total		.0185	.0790	.1043	.1997	.1685	.1204	.0891	.1535	.0407	.0137	.0127	1.0000

IP3
FSAR UPDATE

Table 8. Montrose Frequency Distribution of Wind Speed and Direction
January 1, 1970-December 31, 1970.

			Wind Speed (m/s)									Miss	Total	
			0.0- 0.5	>0.5- 1.0	>1.0- 1.5	>1.5- 2.5	>2.5- 3.5	>3.5- 4.5	>4.5- 5.5	>5.5- 8.5	>8.5- 11.0			>11.0
Z-35	349- 11	N	.0038	.0072	.0054	.0084	.0143	.0099	.0050	.0067	.0010	.0003	.0123	.0743
	12- 33	NNE	.0033	.0064	.0125	.0294	.0200	.0102	.0077	.0078	.0011	.0000	.0241	.1224
	34- 56	NE	.0024	.0065	.0092	.0203	.0146	.0054	.0016	.0010	.0001	.0000	.0223	.0834
	57- 78	ENE	.0016	.0037	.0052	.0038	.0033	.0009	.0001	.0013	.0001	.0000	.0078	.0278
	79-101	E	.0010	.0027	.0014	.0044	.0009	.0004	.0009	.0007	.0004	.0000	.0065	.0193
	102-123	ESE	.0016	.0028	.0023	.0043	.0021	.0007	.0001	.0006	.0000	.0000	.0047	.0191
	124-146	SE	.0013	.0035	.0060	.0102	.0094	.0054	.0020	.0010	.0000	.0000	.0098	.0485
	147-168	SSE	.0007	.0026	.0082	.0271	.0240	.0184	.0081	.0070	.0001	.0001	.0160	.1123
	169-191	S	.0009	.0030	.0075	.0153	.0133	.0079	.0026	.0011	.0003	.0006	.0140	.0665
	192-213	SSW	.0017	.0037	.0051	.0108	.0092	.0058	.0026	.0016	.0001	.0001	.0148	.0555
	214-236	SW	.0023	.0045	.0072	.0082	.0044	.0033	.0020	.0026	.0006	.0003	.0099	.0452
	237-258	WSW	.0021	.0037	.0045	.0052	.0024	.0013	.0016	.0023	.0007	.0003	.0071	.0312
	259-281	W	.0023	.0028	.0030	.0034	.0035	.0038	.0031	.0058	.0011	.0011	.0070	.0370
	282-303	WNW	.0017	.0026	.0021	.0030	.0047	.0044	.0051	.0148	.0079	.0028	.0068	.0559
	304-326	NW	.0018	.0024	.0020	.0045	.0058	.0067	.0084	.0262	.0148	.0050	.0135	.0911
	327-348	NNW	.0040	.0034	.0031	.0045	.0071	.0065	.0081	.0200	.0047	.0007	.0119	.0740
Calm			.0000											.0000
Miss			.0054	.0060	.0070	.0085	.0058	.0021	.0010	.0003	.0003	.0000		.0363
Total			.0377	.0675	.0918	.1712	.1448	.0932	.0597	.1006	.0335	.0113	.1885	1.000

2.2 Recorders

All instruments produce ink trace records on strip chart analog recorders. Items (a) and (b) use Esterline Angus continuous trace recorders at chart speed of 3 in./hr. Items (c) and (d) use a Bendix-Friez continuous trace recorder at chart speed of 3 in./hr. Item (e) uses a continuous trace recorder at chart speed of 1 in./hr. Item (f) uses a Texas Instrument dual channel continuous trace recorder for elevation and azimuth readings at chart speeds of either 3 in./hr. or 3 in./min. Item (g) uses a 6 channel Honeywell-Brown dot print recorder with a three minute recording cycle. Items (h), (i) and (j) use a common 8 point Bristol recorder which dot prints every 30 seconds at a chart speed of 3 in./hr.

3. Data Log

A monthly tabulation of days in which 12 or more hours of missing data occurred during the period of data collection

Z-14

ts. Complete breakdowns due to lightning strikes on the Montrose Point and Trap Rock towers were another source of data loss.

A special reference must be made to the Honeywell-Brown temperature difference system. One of the initial purposes for data collection at Indian Point was to determine initial data from January 1970-December 1971 is presented in Table 2. Data collected beyond this period is indicated as well as instrumentation activation and termination dates.

Data recovery information is given in Table 3. Most data loss occurred when instruments were out of service for repair or when data were deemed erroneous due to improper functioning of instruments. Major instrumentation difficulties included: for the Climec wind system, speed head bearing failures and hypersensitivity of the directional module; and for the Honeywell-Brown Temperature Difference system, aspirator failures due to corroded connections and loss of calibration due to unobserved deterioration of recorder component. Any climatic changes had occurred since 1955-57 that could be detrimental to the Indian Point accident model. It was felt that the utilization of the exact instruments used in 1955-57 would facilitate the evaluation. The original Honeywell-Brown system was rehabilitated and placed in operation. Because of age factors it became difficult to maintain temperature difference data recovery at greater than 70-80% after July 1970. The amount of valid data output, however, was considered sufficient to meet its original function. As it became apparent that a reliable, continuously operating temperature difference system was a necessity, and with the complete breakdown of the aging system on 25 October 1971, a new system was acquired and subsequently installed on 14 August 1972.

4. Analytical Procedure

4.1 Wind Direction

IP3
FSAR UPDATE

To facilitate the development of the statistical analysis, the parameter categories were standardized on the basis of sixteen compass point (22 1/2° sectors) as opposed to eighteen 20° sectors from 002 1/2° as used by Davidson. IP1 No recovery information indicated.

Table 3. Record of Data Recovery

Station	Parameter	Period	Hours of Valid Data	Total Hours in Period	% Recovery
IP3	Wind Direction (Climet)	Annual 1970	8644	8760	98.68
		Summer 1970	5072	5136	98.75
		Winter 1970	3572	3624	98.57
		Annual 1971	8742	8760	99.80
		Summer 1971	4406	4416	99.77
		Winter 1971	4336	4344	99.82
	Wind Speed (Climet)	Annual 1970	8594	8760	98.11
		Summer 1970	5019	5136	97.72
		Winter 1970	3575	3624	98.65
		Annual 1971	8689	8760	99.19
		Summer 1971	4381	4416	99.21
		Winter 1971	4308	4344	99.17
	Wind Direction (Aerovane)	Summer 1970 (Partial: until Sept. 18)	4003	4104	97.54
	Wind Speed (Aerovane)	Summer 1970 (Partial: until Sept. 18)	4001	4104	97.49
	Temperature Difference	Annual 1970	7222	8760	82.44
		Annual 1971	5560	8760	63.47
TR	Wind Direction	Annual 1970	8600	8760	98.17
		Summer 1970	4983	5136	97.02
		Winter 1970	3617	3624	99.81
		Annual 1971	8524	8760	97.31
		Summer 1971	4242	4416	96.06
		Winter 1971	4282	4344	98.57
	Wind Speed	Annual 1970	8514	8760	97.19
		Summer 1970	5018	5136	97.70
		Winter 1970	3496	3624	96.47
		Annual 1971	8447	8760	96.43

IP3
FSAR UPDATE

	Summer 1971	4243	4416	96.08
	Winter 1971	4204	4344	96.78

Table 3 (continued)

Station	Parameter	Hours of Valid Period	Total Hours in Data	% Period	Recovery
MP	Wind Direction	Annual 1970	6794	8760	77.56
		Summer	4045	5136	78.76
	Wind Speed	Annual 1970	5721	8760	65.31
		Summer	3140	5136	61.14
CC	Wind Direction	Summer 1970	4093	4104	99.73
		Summer 1970	4091	4104	99.68

The frequency density for each wind quadrant is determined by:

$$f = \frac{n}{(N - m)\theta}$$

where:

f = frequency density

n = number of data hours in a specified category

N = total number of hours possible for a selected time period

m = number of hours for which no data was available

U = sector interval (Note: 20.0 ° for 1955-1957 data and 22.5° for 1970-1971 data.)

The sum of the sector frequency densities is equal to 1. Calm and missing data are assumed to be equally distributed throughout the compass and are divided by a sector width of 360°.

4.2 Wind Speed

Wind speeds are presented in m/s. (For conversion to mph, multiply by 2.237)

The number of speed categories were increased at low end to provide more detailing of the speed distribution in this critical range.

For wind speeds, the frequency is defined by

$$F_x = \frac{n_x}{(N - m)}$$

where:

F_x = frequency in a class interval

n_x = number of data hours within a specified interval

N = total number of hours possible for a selected time period

m = number of hours for which no data was available

The percent probability is defined by

$$P_x = \left[\frac{n_x}{(N - m) + 1} \right] \times 100$$

The cumulative percent probability is defined by

$$CP = \sum_{i=1}^i P_i$$

where:

i = number of class intervals.

When CP is plotted, a point on the curve is read as the percent time that the wind speed # indicated value.

4.3 Stability Categories

IP3
FSAR UPDATE

4.31 Atmospheric Stability Categories Defined in Terms of Temperature Difference

	IP1 – 1955-57 (300 ft tower)	IP3 – 1970-71 (100 ft tower)
I = Inversion ("stable")	$T_{150} - T_7 \geq 0$	$T_{95} - T_7 \geq 0$
N = Isothermal-Adiabatic ("neutral")	$0 > T_{150} - T_7 \geq -0.98$	$0 > T_{95} - T_7 \geq -0.58^F$
L = Lapse ("unstable")	$-0.98^F > T_{150} - T_7$	$-0.58^F > T_{95} - T_7$

4.32 Classification of Atmospheric Stability According to U. S. A. E. C. Safety Guide 23

Stability Classification	Pasquill Categories	Temperature Change with Height	
		(8C/100m)	(°F/88 ft) (IP3)
Extremely Unstable	A	< -1.9	< -0.9
Moderately Unstable	B	-1.9 to -1.7	-0.9 to < -0.8
Slightly Unstable	C	-1.7 to -1.5	-0.8 to < -0.7
Neutral	D	-1.5 to -0.5	-0.7 to < -0.2
Slightly Stable	E	-0.5 to 1.5	-0.2 to < +0.7
Moderately Stable	F	1.5 to 4.0	+0.7 to < 1.9
Extremely Stable	G	>4.0	\$1.9

4.4 Seasonal Distributions

After careful examination of individual monthly frequency distributions it was determined that a definite seasonal effect existed. Two distinct seasons emerge: summer and winter, with no distinctive transition months. November-March are always "winter" months and May-September always "summer" months. April and October distribution patterns may appropriately fit either a winter or summer season. There was no means of predicting, in advance, what season was appropriate for these two months until the actual data was analyzed. The seasonal breakdown, as used, is as follows:

	Winter	Summer
1970	January-March, November-December	April-October
	(5 months)	(7 months)
1971	January-April, November-December	May-October
	(6 months)	(6 months)

4.5 Diurnal Analysis

The hourly diurnal mean wind direction and speed were determined by resolving each individual data point into its N-S and E-W components, summing the components within each hourly category and calculating a mean wind direction and speed. When plotting the diurnal direction curve it is assumed that the rotation of the mean between two points will circumvent the smallest arc.

Persistence is defined as,

$$P = \frac{\text{Vector Average Speed} \left(\left| \overline{\vec{V}} \right| \right)}{\text{Magnitude of Scalar Average Speed} \left(\left| \overline{V} \right| \right)}$$

4.6 Spatial Variation

The spatial relationship of wind direction and speed between two tower sites was determined by selecting the category range at one station as the independent variable and calculating a frequency distribution and mean value at the second station for each of the independent variable's categories. This method assumes a gaussian distribution around the mean value at the independent station.

5. Discussion of Data

5.1 Joint Frequency Distribution of Wind Direction, Wind Speed and Temperature Difference

5.1.1 Inversion – Neutral – Lapse Temperature Difference

Classification

Annual frequency distributions of wind speed and direction according to temperature gradient class at Indian Point 3 for 1970 and 1971 are given in Tables 4 and 5, respectively.

5.1.2 Pasquill Stability Classification

Annual joint frequency distributions of wind direction and speed according to the Pasquill stability categories, as established by the U. S. A. E. C. Safety Guide 23, at Indian Point 3 for 1970 and 1971 are given in Appendix Table 1 and 2, respectively.

5.2 Joint Frequency Distribution of Wind Direction and Temperature Difference

5.2.1 Monthly Distribution of Temperature Difference

A monthly distribution of temperature difference at IP3 for 1970 and 1971 is given in Figure 2. The distribution for missing hours of temperature difference data is also presented so that a measure of reliability can be determined.

The frequency of inversions remain relatively constant throughout the year. Neutral conditions are more frequent during the winter months while lapse conditions reach their peak during the summer months. These features seem most apparent during those time periods, in both years, when data collection efficiency was greater than 80%.

5.2.2 Annual Joint Frequency Distribution

The annual frequency distributions of wind direction according to temperature difference category for IP1 (1956) and IP3 (1970 and 1971) are presented in Figure 3.

For inversion conditions, a marked discrepancy is observed between the 1956 and 1970-71 data. Substantial decreases are observed in the frequency of observed inversions during 1970-71 in all quadrants except those between 050 to 160°. The reduction is by a factor of 0.50 in some sectors. The cause of this deviation may be due to one, or more of the following: a) different tower locations; b) different measurement height intervals ((150-7 ft (1956) and 95-7 ft (1970-71)); c) change in the surrounding environs (the area is now more developed); or d) a calibration error ((only 0.9°F (1956) and 0.5°F (1970-71)) separate inversions from lapse conditions).

The distribution for neutral and lapse conditions between 1956 and 1970-71 are generally similar. The neutral maxima are from the same quadrant (NNE) as the inversion for all years. Under lapse conditions, maximums are observed of approximately equal magnitude for winds from the N and SSE quadrants.

Major discrepancies between the 1970 and 1971 data occur in the neutral category from 300° -030° and in the lapse category from 140° -200°. These can be attributed to periods of missing data. The decrease in frequency of neutral condition northerly winds in 1971 may be due to missing data during October-December. A strong northwesterly wind persists during these months resulting in dominating neutral atmospheric conditions. The decrease in frequency of lapse conditions for southerly winds in 1971 may be due to data loss during May-July. These are the months in which lapse conditions normally prevail.

In general, throughout 1970-71 most specific discrepancies are associated with periods of maximum data losses.

5.3 Joint Frequency Distribution of Wind Direction and Wind Speed

The annual joint frequency distribution of wind direction and wind speed for Trap Rock (TR) 1970 and 1971, and Montrose Point (MP) 1970 are given in Tables 6, 7, and 8, respectively.

Wind direction distributions for various speed categories are presented in Figure 4. Discrepancies between 1956 and 1970-71 are less apparent than when classified by temperature difference. The 1970 and 1971 distributions are almost a duplicate of each other.

Halitsky, et al. (1971) found that there was a significant increase in the frequency of occurrence of low speed winds from the critical sector, 000° -040°, for 10 months of 1970 data compared to 1956. With 1970 and 1971 data, the frequencies are nearly the same. The

remaining small discrepancy may be due to alteration of quadrant angles. The improvement can be attributed to the extension of 1970 data to a complete year and the difference in category range, 0.0-1.5 m/s in this report versus 0.4-2.0 m/s in the 1971 report. The generally slight increase of frequency in 1970 through most directions is due to a change in instrumentation. A Climet speed unit (threshold: 0.6 MPH) was used in 1970-71 while an aerovane (threshold: 2.5 MPH) was used in 1956. Thus, data points which were measured as calm by the aerovane in 1956 would now be present within the distribution with speed between 0.27-1.2 m/s (0.6-2.5 MPH) when measured with the Climet.

Figure 4 also indicates a general backing into the NW of the maximum frequency direction as wind speeds increase for all years.

5.4 Frequency Distribution of Wind Direction

5.4.1 Annual

Annual frequency distributions of wind direction for the various meteorological tower sites are given in Figure 5. Obvious differences that exist between IP1 (1956) and IP3 (1970-71) are: a) decrease in magnitude of the maximum direction; and b) shifting of the secondary maximum from 172° backing to 156° in 1970-71.

Comparison between IP3 and TR for the same years show differences which are no doubt caused by local topographical effects. The IP3 NNE maximum has backed to the N at Trap Rock. There is also a marked increase in both NW and SE winds at Trap Rock with the NW direction now becoming the secondary maximum.

The frequency density distribution at Montrose Point closely resembles that at IP3.

5.4.2 Seasonal

A definite seasonal pattern was observed during the analysis of monthly data at each station. The seasonal frequency distributions for IP3, Trap Rock and Montrose Point are given in Figures 6, 7 and 8, respectively.

The winter season wind direction frequency distribution at IP3 is tri-nodal. The primary maximum appears with winds from N-NNE. The secondary maximum appears for winds from WNW-NW. This second maximum is of the same order of frequency of the primary. The binodal maximum for winds from these northern quadrants may be attributed to the effect of blockage by the Dunderberg Mountain (Figure 1). The winds, as is seen, preferentially go around it rather than over its top. The tertiary maximum during the winter season is for winds from SSE at half the frequency of the north-quadrant maxima.

During the summer season the direction frequency distributions are binodal with two well defined peaked regions, one northerly (NNE) and the other southerly (SSE). Over the 1970-71 seasons, the maxima are approximately equal in frequency. The winter season secondary peak (WNW-NW) is completely lacking during the summer.

Seasonal differences can be attributed to the influence or lack of influence of the atmospheric geostrophic wind. A persistent and strong NW winter geostrophic wind is

responsible for the W-N quadrant peaks at the valley stations. The summer distributions reflect the diurnal wind pattern which flows along the valley axis: upvalley during the day and downvalley at night. The diurnal winds dominate the valley flow system during calm and nearly zero atmospheric pressure gradient conditions, which occur primarily during the summer months and account for the increased frequency of SSE-SSW winds.

Comparison between IP3 (Figure 6) and TR (Figure 7) shows that during the winter TR has the same tri-nodal distribution as IP3. At TR, however, the maximum frequency density is for winds from NNW quadrant without a significant change in frequency of NNE or SSE winds. During the summer the IP3 NNE maximum has backed to N at TR as occurs with the annual distribution and becomes binodal. The previously mentioned sharp increase of annual SE winds at TR is seen to occur almost entirely during the summer season. The annual NW increase is divided between the two seasons.

Based on limited data, the seasonal distributions at Montrose Point (Figure 8) are similar to those of IP3 except for a semblance of retention of the tri-nodal aspect during the summer season.

5.4.3 Comparison Between IP3 and Cape Charles for a Summer Season

Cape Charles as compared to IP3 is further indication of the blocking action of the Dunderberg.

Both stations compare relatively well during northerly quadrant winds. The IP3 sharp peak at NNE is spread out at the Cape Charles almost uniformly over the N, NNE and NE quadrants. This disp On 16 March 1970, an aerovane was installed aboard the U.S.S. Cape Charles. The intent of this station was to obtain comparable data to that collected by Davidson in September-October 1955 aboard the U.S. S. Jones in order to produce diurnal hodographs of the mean vector wind for virtually zero and weak pressure gradient conditions. Data retrieval over a lengthy time span could not be achieved because of the "mothball" fleet's disposal operations. However, a hodograph was constructed for July-September 1970 for comparative purposes (Halitsky, et al. (1971).

Frequency distributions of wind direction for Cape Charles and IP3 aerovanes are given in Figure 9. For the record period, SSE winds are most frequent at IP3 and SW at Cape Charles. This variation is related to the dominant valley terrain features that influence each station (Figure 1). The proximity of the Cape Charles to the Dunderberg Mountain is the controlling feature. The prevailing SSE valley wind, as measured at IP3, is forced to veer and flow parallel to the face of Dunderberg Mountain giving the Cape Charles its SW flow. The lack of NW and NNW winds at the ersion probability reflects the vortex generated as the air is deflected by the eastern tip of Dunderberg. In particular the NE peak could also represent nocturnal drainage flow from the Annsville Creek, Sprout Brook and Peekskill Hollow Brook valley complexes.

It should be cautioned that the Cape Charles aerovane was exposed at an elevation of approximately 100 ft MSL while the IP3 aerovane measured at an elevation of 220 ft MSL and some variations may be due to this difference in exposure elevations.

5.5 Cumulative Probability Distribution for Wind Speed

5.5.1 Annual

IP3
FSAR UPDATE

The annual cumulative probability curves for wind speed are presented for IP1, IP3, Trap Rock and Montrose Point in Figures 10-13. A summary of annual and seasonal median wind speeds is given in Table 9.

Table 9. Annual and Seasonal Median Wind Speeds

				Median	
<u>Station</u>				<u>Period</u>	<u>Wind (m/s)</u>
Indian Point 1	1956 - Annual	3.0			
Indian Point 3	1970 - Annual	3.0			
		-Winter	3.4		
		-Summer	2.9		
	1971 - Annual	3.1			
		-Winter	3.7		
		-Summer	2.7		
Trap Rock	1970 - Annual	2.8			
		-Winter	3.3		
		-Summer	2.5		
	1971 - Annual	3.0			
		-Winter	3.6		
		-Summer	2.7		
Montrose Point	1970 - Annual	2.7			
		-Winter	3.3		
		-Summer	2.3		
Cape Charles	1970 - Summer	2.8			
Indian Point 3	1970 - Summer	2.3			
(Aerovane)					

Figure 10 is a comparison of data collected at IP3 in 1970 and 1971. It shows the relationship between the two years for all wind speed data and as functions of temperature gradient categories. When all wind speed data is considered at each of the stations, there is less than 1% probability deviation between the two annual curves. The maximum deviation is observed at 0.5 m/s where the probability of speeds ≥ 0.5 m/s is about 2.0% and 1.1% for 1970 and 1971, respectively.

IP3 FSAR UPDATE

Before discussing the curves in terms of temperature gradient categories, it should be borne in mind that the annual curve contains all hours for which wind speed data was available. The speed data recovery was 98.1% in 1970 and 99.2% in 1971 (Table 3). The curves now to be considered were constructed from those data hours in which both wind speed and temperature gradient were available: 82% in 1970 and 63.5% in 1971.

In the total inversion category, the two years are nearly identical in the speed range 1.0-2.5 m/s with 1970 having the greater probability of low wind speeds at 0.5 m/s, and 1971 the greater probability of low wind speeds > 2.5 m/s with a spread of approximately 4%. From 3 m/s to 11 m/s the probability of lower speeds is increased from 16.5% to 23.0% in 1970, and from 17.5% to 26.0% in 1971.

In 1970 the neutral and lapse probabilities curves were quite similar. Below 2.4 m/s there were more neutral occurrences and above 2.4 m/s more lapse observations. The neutral-lapse conditions were, as can be anticipated, more frequent at wind speeds greater than 5.5 m/s and less frequent at speeds below 5.5 m/s. This is consistent with their normal association as being high speed phenomena while inversions are associated with low wind speeds. In 1971, however, the neutral-lapse curves were significantly lower than in 1970 and did not approach the probability of the 1971 annual inversion curve. These discrepancies may be, in part, real but most probably the explanation lies in the fact that there was about 20% less valid data available in 1971 compared to 1970. These excess losses are distributed as follows (from Table 2) in terms of missing days:

	<u>J</u>	<u>F</u>	<u>M</u>	<u>A</u>	<u>M</u>	<u>J</u>	<u>J</u>	<u>A</u>	<u>S</u>	<u>O</u>	<u>N</u>	<u>D</u>
1970	0	3	3	0	0	3	0	13	17	20	4	0
1971	0	12	2	1	16	11	13	2	7	5	30	31
1971-1970	0	9	-1	1	16	8	13	-11	-10	-15	26	31

The losses during the summer may account for the lack of lapse data and the excessive winter losses can account for the decrease in neutral data since these are the seasons when such gradients normally prevail.

A comparison of the probability curves between IP1 (1956) and IP3 (1970 and 1971) on an annual basis, for total inversions and inversions in the critical sector, is shown in Figure 11. For all available wind speeds, IP3 is nearly identical to IP1 until 4 m/s after which IP1 indicates a higher probability of lower wind speeds. For all inversion data IP1 indicates a significantly higher probability of low winds speeds. When the analysis of inversion data is restricted to the critical quadrants (002.5°-22.5° in 1956, and 011.5°-033.5° in 1970-71), the 1956 curve always indicates a higher probability of low wind speeds than does IP3 (1970 and 1971).

A comparison between IP3 and Trap Rock (figure 12) shows that a greater percent probability of low wind speeds are observed at TR until about 5.5 m/s in 1970 and 3.5 m/s in 1971 after which TR has greater probability of higher wind speeds.

The low wind speed conditions occur mostly as part of the valley diurnal system. Here, where atmospheric influences are negligible the driving force to a crossvalley or diagonal wind is the gravitational drainage of the valley slopes. The IP3 location is more influenced by such a drainage pattern and will therefore exhibit higher wind speeds at the lower range than over leveler terrain as surrounds Trap Rock.

The Montrose Point cumulative probability resembles that of Trap Rock. It has been found previously that the Montrose Point direction distribution most resembles IP3.

The variations merely emphasize the dominant effects of strictly local terrain.

5.5.2 Seasonal

Seasonal cumulative frequency distributions of wind speed for Montrose Point, IP3 and Trap Rock are given in Figures 13, 14 and 15, respectively. The winter curves show a greater probability of high speeds at all stations than during the summer with but two exceptions: at IP3 in 1970 the winter curve shows a greater probability for wind speeds below 0.68 m/s and Trap Rock in 1971 below 0.87 m/s. Overall, however, the probability of low wind speeds is generally greatest during the summer season.

The summer cumulative frequency speed curves for the Cape Charles and IP3 aerovanes are given in Figure 16. The Cape Charles exhibits a greater percentage of higher wind speeds up to 8.8 m/s after which the IP3 percentage is greater. Higher wind speeds exist at Cape Charles because there are fewer local effects and less frictional loss over water than over land. The deviation at the high speed winds is generally associated with strong W-N geostrophic flow and the Cape Charles is shielded from these by the Dunderberg and Buckberg Mountains.

5.6 Diurnal Variation of the Mean Wind Direction

A primary analysis for data collected in a valley is to determine the extent of the diurnal wind pattern. This pattern is generally ignored in diffusion meteorology models used for nuclear generating sites. The models used are based on air flow over level and unobstructed terrain. The diurnal wind direction fluctuations and the ever present motion of air (zero frequency of calms) in the valley is a definite positive affect on the diffusion potential.

Seasonal diurnal variations of the mean wind direction for IP3, TR, MP and CC are presented in Figures 17-20, respectively.

The seasonal differences are clearly evident. The winter means fluctuate over shorter ranges exhibiting only a slight diurnal variation between the night and day hours. The winter mean at IP3 ranges from 352°-302° in 1970, and from 332°-305° in 1971. The TR mean ranges from 341°-308° in 1970, and from 332°-305° in 1971. The winter range at MP for 1970 was 357°-319°.

On a point by point basis, during the night, TR's mean direction tends to be west of that at IP3 while MP is about the same as IP3. During the day, IP3 and TR are similar while MP holds more to the north.

The summer diurnal curves at IP3 shows the direction rotating through a complete circle, being downvalley at night and upvalley during the day. From 2300-0800 the means hold from 20°-40°. Thereafter the wind direction backs; rapidly during the transition hours of 1000-1100 and 2000-2200, and slower during the intervening hours at a rate of approximately 8 degrees per hour.

The TR summer diurnal wind pattern is similar to that at IP3. From 2300-1000 a downvalley wind exists ranging from 006°-034°. Both transition periods are sharp, occurring at 1000-1100 and 2000-2100. In 1970 the wind backed into the upvalley direction during the day and veered into the downvalley direction at night. This pattern was reversed in 1971.

MP (Figure 19) shows a similar diurnal summer pattern for 1970 but unlike TR it veered into an upvalley flow during the transition hours.

The question of backing or veering during transition hours may be somewhat more complex than is nominally indicated. Referring it back to original analog records during the transition period one can find either the backing or the veering on any particular day. The diurnal wind itself, however, is related not only to a primary valley circulation (katabatic-anabatic)

but a locally induced land-sea breeze. It is the strength of this latter feature that will ultimately determine the backing or veering nature of the diurnal wind during transition hours.

The preceding diurnal analyses indicate that there is small likelihood of a wind persisting in the same direction for as much as 24 hours. The valley structure seems to have a built-in natural mechanism which would prevent such a wind condition from existing particularly at low wind speeds.

5.7 Diurnal Variation of the Mean Wind Speed

Seasonal diurnal variations of mean wind speeds for the various stations are given in Figure 21. The curves indicate that the winter mean speeds are greater than the summer speeds for all the stations throughout the day with both winter and summer maximum speeds occurring between 1300-1500 hours.

5.8 Diurnal Variation of Wind Persistence

The wind persistence is used as a measure of the constancy of a wind direction with time. If a wind always blows from the same direction, the persistence is equal to 1. If the wind is equally likely to blow from all directions or blows half the time from one sector and half the time from the opposite sector, the persistence will be zero.

The seasonal diurnal variation of wind persistence for the various stations is given in Figures 22 and 23. It is clearly evident that the higher persistence values are associated with the winter season. This result is however due to atmospheric conditions which enhance the diffusion, mainly high wind speeds.

Both seasons show a diurnal shift with the summer being more pronounced. Maximum persistence occurs between 04-0600 EST. The times of occurrence of the maximum values of persistence correspond to those times at which the nocturnal downvalley flow is a maximum and the daytime upvalley flow reaches its peak. At CC it almost equals the magnitude of the nighttime maximum. The summer minimums occur between 1100-1200 and 1900-2100 which are about the times of the diurnal wind direction transition periods.

5.9 Spatial Variability of Wind Velocity Between Tower Sites

The annual and seasonal spatial variabilities of wind direction and speed between selected stations are presented in Tables 10 through 17.

Table 10. Annual Spatial Variability of Wind

Direction Between Indian Point 3 and							
Trap Rock.							
IP3	TR	TR	IP3	IP3	TR	TR	IP3
1970	1970	1970	1970	1971	1971	1971	1971
000.0	354	000.0	012	000.0	358	000.0	008
022.5	010	022.5	025	022.5	017	022.5	024
045.0	024	045.0	041	045.0	033	045.0	043
067.5	048	067.5	070	067.5	047	067.5	065
090.0	078	090.0	094	090.0	076	090.0	091
112.5	107	112.5	126	112.5	104	112.5	118
135.0	129	135.0	154	135.0	134	135.0	146
157.5	147	157.5	171	157.5	154	157.5	167
180.0	168	180.0	188	180.0	177	180.0	182
202.5	190	202.5	206	202.5	200	202.5	199
225.0	212	225.0	224	225.0	224	225.0	219
247.5	239	247.5	256	247.5	250	247.5	244
270.0	270	270.0	285	270.0	277	270.0	271
292.5	295	292.5	301	292.5	296	292.5	293
315.0	308	315.0	321	315.0	313	315.0	318
337.5	330	337.5	353	337.5	333	337.5	346

Table 11. Seasonal Spatial Variability of Wind

Direction Between Indian Point 3 and							
Trap Rock (1970).							
IP3	TR	TR	IP3	IP3	TR	TR	IP3
1970	1970	1970	1970	1970	1970	1970	1970

IP3
FSAR UPDATE

<u>Wntr</u>	<u>Wntr</u>	<u>Wntr</u>	<u>Wntr</u>	<u>Smmr</u>	<u>Smmr</u>	<u>Smmr</u>	<u>Smmr</u>
000.0	358	000.0	008	000.0	350	000.0	016
022.5	013	022.5	019	022.5	008	022.5	030
045.0	029	045.0	034	045.0	022	045.0	047
067.5	059	067.5	066	067.5	043	067.5	072
090.0	085	090.0	080	090.0	074	090.0	100
112.5	116	112.5	120	112.5	103	112.5	129
135.0	138	135.0	146	135.0	126	135.0	155
157.5	158	157.5	166	157.5	145	157.5	173
180.0	176	180.0	184	180.0	166	180.0	190
202.5	194	202.5	201	202.5	188	202.5	209
225.0	216	225.0	219	225.0	210	225.0	228
247.5	244	247.5	252	247.5	233	247.5	261
270.0	275	270.0	281	270.0	261	270.0	290
292.5	299	292.5	298	292.5	284	292.5	306
315.0	310	315.0	315	315.0	306	315.0	330
337.5	335	337.5	346	337.5	325	337.5	359

Table 12. Seasonal Spatial Variability of Wind

Direction Between Indian Point 3 and

Trap Rock (1971).

<u>IP3</u>	<u>TR</u>	<u>TR</u>	<u>IP3</u>	<u>IP3</u>	<u>TR</u>	<u>TR</u>	<u>IP3</u>
1971	1971	1971	1971	1971	1971	1971	1971
<u>Wntr</u>	<u>Wntr</u>	<u>Wntr</u>	<u>Wntr</u>	<u>Smmr</u>	<u>Smmr</u>	<u>Smmr</u>	<u>Smmr</u>
000.0	359	000.0	007	000.0	358	000.0	009
022.5	014	022.5	022	022.5	018	022.5	025
045.0	030	045.0	048	045.0	034	045.0	040
067.5	046	067.5	070	067.5	049	067.5	062
090.0	076	090.0	091	090.0	076	090.0	091
112.5	109	112.5	112	112.5	102	112.5	119
135.0	136	135.0	143	135.0	132	135.0	148

IP3
FSAR UPDATE

157.5	157	157.5	165	157.5	152	157.5	168
180.0	178	180.0	181	180.0	176	180.0	183
202.5	203	202.5	201	202.5	198	202.5	198
225.0	226	225.0	222	225.0	222	225.0	215
247.5	250	247.5	243	247.5	249	247.5	246
270.0	277	270.0	272	270.0	275	270.0	268
292.5	296	292.5	292	292.5	296	292.5	296
315.0	313	315.0	317	315.0	312	315.0	322
337.5	331	337.5	345	337.5	335	337.5	348

Table 13. Annual Spatial Variability of Wind Speed

(m/s) Between Indian Point 3 and Trap Rock.

IP3	TR	TR	IP3	IP3	TR	TR	IP3
1970	1970	1970	1970	1971	1971	1971	1971

0.25	0.6	0.25	1.0	0.25	0.7	0.25	0.9
0.75	0.9	0.75	1.4	0.75	0.9	0.75	1.1
1.25	1.2	1.25	1.8	1.25	1.3	1.25	1.6
2.0	1.9	2.0	2.5	2.0	2.0	2.0	2.2
3.0	2.8	3.0	3.3	3.0	3.0	3.0	3.1
4.0	3.9	4.0	4.1	4.0	4.0	4.0	4.0
5.0	4.9	5.0	4.9	5.0	5.1	5.0	4.9
7.0	6.8	7.0	6.2	7.0	6.9	7.0	6.5
9.75	9.9	9.75	8.4	9.75	9.7	9.75	9.0

IP3
FSAR UPDATE

Table 14. Seasonal Spatial Variability of Wind

Speed (m/s) Between Indian Point 3
and Trap Rock.

IP3	TR	TR	IP3	IP3	TR	TR	IP3
1970	1970	1970	1970	1970	1970	1970	1970
<u>Wntr</u>	<u>Wntr</u>	<u>Wntr</u>	<u>Wntr</u>	<u>Smmr</u>	<u>Smmr</u>	<u>Smmr</u>	<u>Smmr</u>

0.25	0.5	0.25	0.8	0.25	0.6	0.25	1.1
0.75	0.8	0.75	1.3	0.75	0.9	0.75	1.4
1.25	1.3	1.25	1.8	1.25	1.2	1.25	1.9
2.0	2.0	2.0	2.4	2.0	1.8	2.0	2.6
3.0	3.0	3.0	3.3	3.0	2.8	3.0	3.4
4.0	4.1	4.0	4.1	4.0	3.8	4.0	4.2
5.0	5.1	5.0	5.0	5.0	4.7	5.0	4.8
7.0	7.2	7.0	6.4	7.0	6.4	7.0	6.0
9.75	10.0	9.75	8.5	9.75	9.3	9.75	8.1

IP3	TR	TR	IP3	IP3	TR	TR	IP3
1971	1971	1971	1971	1971	1971	1971	1971
<u>Wntr</u>	<u>Wntr</u>	<u>Wntr</u>	<u>Wntr</u>	<u>Summr</u>	<u>Summr</u>	<u>Summr</u>	<u>Summr</u>

0.25	0.6	0.25	1.0	0.25	0.7	0.25	0.7
0.75	0.8	0.75	1.1	0.75	1.0	0.75	1.1
1.25	1.2	1.25	1.7	1.25	1.3	1.25	1.5
2.0	1.9	2.0	2.4	2.0	2.1	2.0	2.2
3.0	2.9	3.0	3.3	3.0	3.0	3.0	3.0
4.0	3.9	4.0	4.2	4.0	4.1	4.0	3.8
5.0	5.1	5.0	5.1	5.0	5.2	5.0	4.6
7.0	6.9	7.0	6.8	7.0	6.8	7.0	6.0
9.75	9.6	9.75	9.1	9.75	9.9	9.75	8.5

IP3
FSAR UPDATE

Table 15. Annual Spatial Variability of Wind

Direction and Speed (m/s) Between							
Montrose Point and Trap Rock.							
Wind Direction				Wind Speed			
MP	TR	TR	MP	MP	TR	TR	MP
1970	1970	1970	1970	1970	1970	1970	1970
000.0	351	000.0	018	0.25	0.8	0.25	0.7
022.5	009	022.5	033	0.75	1.2	0.75	1.0
045.0	023	045.0	049	1.25	1.7	1.25	1.4
067.5	035	067.5	069	2.0	2.5	2.0	1.9
090.0	054	090.0	096	3.0	3.7	3.0	2.7
112.5	089	112.5	127	4.0	4.9	4.0	3.4
135.0	135	135.0	150	5.0	5.7	5.0	4.1
157.5	151	157.5	166	7.0	7.4	7.0	5.6
180.0	173	180.0	189	9.75	10.0	9.75	8.0
202.5	191	202.5	207				
225.0	214	225.0	229				
247.5	236	247.5	253				
270.0	269	270.0	277				
292.5	289	292.5	302				
315.0	309	315.0	324				
337.5	323	337.5	356				

IP3
FSAR UPDATE

Table 16. Annual Spatial Variability of Wind

Direction and Speed (m/s) Between							
Indian Point 3 and Montrose Point.							
Wind Direction				Wind Speed			
IP3	MP	MP	IP3	IP3	MP	MP	IP3
1970	1970	1970	1970	1970	1970	1970	1970
000.0	011	000.0	358	0.25	0.6	0.25	0.9
022.5	029	022.5	015	0.75	0.8	0.75	1.3
045.0	043	045.0	027	1.25	1.2	1.25	1.8
067.5	067	067.5	040	2.0	1.8	2.0	2.6
090.0	088	090.0	070	3.0	2.6	3.0	3.5
112.5	123	112.5	108	4.0	3.5	4.0	4.5
135.0	142	135.0	153	5.0	4.4	5.0	5.3
157.5	158	157.5	167	7.0	6.2	7.0	6.9
180.0	175	180.0	183	9.75	9.1	9.75	9.1
202.5	198	202.5	198				
225.0	216	225.0	220				
247.5	238	247.5	244				
270.0	272	270.0	275				
292.5	304	292.5	297				
315.0	320	315.0	315				
337.5	338	337.5	330				

IP3
FSAR UPDATE

Table 17. Summer (1970) Spatial Variability of Wind

Direction and Speed (m/s) Between Cape Charles and Indian Point 3.							
CC	IP3	IP3	CC	CC	IP3	IP3	CC
1970	1970	1970	1970	1970	1970	1970	1970
Smmr	Smmr	Smmr	Smmr	Smmr	Smmr	Smmr	Smmr
000.0	001	000.0	007	0.25	0.9	0.25	1.1
022.5	017	022.5	022	0.75	1.1	0.75	1.4
045.0	031	045.0	028	1.25	1.5	1.25	1.9
067.5	049	067.5	044	2.0	1.8	2.0	2.5
090.0	088	090.0	069	3.0	2.5	3.0	3.4
112.5	102	112.5	107	4.0	3.4	4.0	4.5
135.0	122	135.0	153	5.0	4.4	5.0	5.3
157.5	146	157.5	187	7.0	5.4	7.0	6.0
180.0	163	180.0	212	9.75	7.2	9.75	7.3
202.5	180	202.5	221				
225.0	196	225.0	234				
247.5	216	247.5	247				
270.0	285	270.0	268				
292.5	301	292.5	286				
315.0	321	315.0	317				
337.5	346	337.5	355				

The station listed first in each tabular set is the independent variable.

When the role of independent and dependent stations are reversed, the relationships between the mean values are not, a priori, similarly inverted. This discrepancy may be attributed, in part, to the effects of local topography as well as to a reaction time lag engendered by the spatial distance between stations.

The significance of any degree of change in magnitude of speed or wind direction angle between stations are arbitrary. An angular change of $\pm 10^\circ$ and speed change of ± 0.5 m/s may be considered.

The spatial variability analysis indicated:

IP3
FSAR UPDATE

- 1) A general backing of wind direction between IP3 and TR, with TR having a lower speed at the low range and a higher speed at the high range. Seasonal analysis showed the greatest variations occurring during the "summer" months.
- 2) A general backing of wind direction between MP and TR with speeds being greater at TR.
- 3) Based on the comparable data available (1970), the wind directions at IP3 and MP were similar to each other and in the relationship to TR. The magnitude of the wind speeds were similar at IP3 and TR, with each being generally stronger than at MP.

References

Halitsky, J., J. Laznow and D. Leahey (1970): Wind Observations at Indian Point, Montrose and Bowline Point. 31 August 1968 to 30 June 1969. New York University, Department of Meteorology and Oceanography Technical Report TR-70-3.

Halitsky, J., E. J. Kaplin and J. Laznow (1971): Wind Observations at Indian Point 26 November 1969-1 October 1970. New York University Department of Meteorology and Oceanography Technical Report TR-71-3.

Leahey, D. M. and J. Halitsky (1971): Low Wind Speed Turbulence Statistics and Related Diffusion Estimates for Indian Point, N.Y. New York University Department of Meteorology and Oceanography Technical Report TR-71-10.

FSAR: Final Facility Description and Safety Analysis Report. Consolidated Edison Company of New York, Inc. Nuclear Generating Unit No. 2. Exhibit B-8.

Davidson, B. and J. Halitsky (1955): A Micrometeorological Survey of the Buchanan, New York Area, Summary of Program to 1 December 1955. New York University Department of Meteorology and Oceanography Technical Report 372.1.

Davidson, B. and J. Halitsky (1957): Evaluation of Potential Radiation Hazard Resulting from Assumed Release of Radioactive Wastes to Atmosphere from Proposed Buchanan Nuclear Power Plant. New York University Department of Meteorology and Oceanography Technical Report 372.3.

U. S. Atomic Energy Commission Safety Guide 23 – Onsite Meteorological Programs, February 17, 1972.

IP3
FSAR UPDATE

Appendix Table 1. Indian Point B(3) Joint Frequency
Distribution of Wind Speed and Direction
for Pasquill Stability Category A –
January 1, 1970-December 31, 1970.

Wind Direction			Wind Speed (mph)						Miss	Total
			01-03	04-07	08-12	13-18	19-24	>24		
349- 11	N		.0010	.0086	.0097	.0025	.0002	.0000	.0001	.0222
12- 33	NNE		.0008	.0059	.0031	.0010	.0000	.0000	.0001	.0110
34- 56	NE		.0015	.0041	.0008	.0005	.0001	.0000	.0001	.0071
57- 78	ENE		.0005	.0006	.0000	.0003	.0002	.0000	.0000	.0016
79-101	E		.0003	.0005	.0002	.0002	.0000	.0000	.0000	.0013
102-123	ESE		.0005	.0005	.0003	.0002	.0000	.0000	.0000	.0015
124-146	SE		.0013	.0010	.0010	.0016	.0002	.0000	.0000	.0051
147-168	SSE		.0016	.0074	.0109	.0078	.0003	.0000	.0000	.0280
169-191	S		.0016	.0122	.0081	.0015	.0000	.0000	.0000	.0234
192-213	SSW		.0010	.0071	.0033	.0002	.0000	.0000	.0001	.0118
214-236	SW		.0009	.0034	.0016	.0006	.0000	.0000	.0000	.0065
237-258	WSW		.0010	.0010	.0011	.0002	.0000	.0000	.0001	.0035
259-281	W		.0009	.0022	.0030	.0013	.0007	.0001	.0001	.0082
282-303	WNW		.0005	.0014	.0031	.0053	.0024	.0008	.0010	.0144
304-326	NW		.0005	.0016	.0042	.0054	.0035	.0007	.0005	.0163
327-348	NNW		.0007	.0039	.0049	.0041	.0011	.0001	.0000	.0149
Calm				.0000						.0000
Miss				.0000	.0000	.0000	.0000	.0000	.0000	.0022
Total			.0145	.0614	.0554	.0327	.0089	.0017	.0043	.1790

Indian Point B(3) Joint Frequency Distribution of Wind Speed
and Direction for Pasquill Stability Category B – January 1,
1970-December 31, 1970.

Wind Direction			Wind Speed (mph)						Miss	Total
			01-03	04-07	08-12	13-18	19-24	>24		
349- 11	N		.0002	.0007	.0006	.0001	.0000	.0000	.0000	.0016
12- 33	NNE		.0001	.0009	.0006	.0000	.0000	.0000	.0000	.0016
34- 56	NE		.0005	.0008	.0002	.0000	.0000	.0000	.0000	.0015
57- 78	ENE		.0001	.0003	.0000	.0000	.0000	.0000	.0001	.0006
79-101	E		.0002	.0000	.0000	.0000	.0000	.0000	.0000	.0002
102-123	ESE		.0003	.0007	.0000	.0000	.0000	.0000	.0000	.0010
124-146	SE		.0000	.0003	.0001	.0000	.0000	.0000	.0000	.0005
147-168	SSE		.0001	.0002	.0008	.0008	.0001	.0000	.0000	.0021
169-191	S		.0003	.0010	.0005	.0005	.0000	.0000	.0000	.0023
192-213	SSW		.0000	.0005	.0003	.0002	.0000	.0000	.0000	.0010
214-236	SW		.0002	.0001	.0000	.0000	.0000	.0000	.0000	.0003
237-258	WSW		.0007	.0002	.0000	.0001	.0000	.0000	.0000	.0010
259-281	W		.0000	.0000	.0002	.0001	.0000	.0000	.0000	.0003
282-303	WNW		.0001	.0000	.0001	.0003	.0003	.0001	.0000	.0010
304-326	NW		.0001	.0001	.0007	.0007	.0003	.0003	.0000	.0023
327-348	NNW		.0000	.0001	.0005	.0001	.0000	.0001	.0000	.0008
Calm				.0000						.0000

IP3
FSAR UPDATE

Miss	.0000	.0000	.0000	.0000	.0000	.0000	.0000
Total	.0031	.0061	.0046	.0030	.0008	.0006	.0001

Appendix Table 1 (continued)

Indian Point B(3) Joint Frequency Distribution of Wind Speed and Direction for Pasquill Stability Category C – January 1, 1970-December 31, 1970

Wind			Wind Speed (mph)						Miss	Total
Direction			01-03	04-07	08-12	13-18	19-24	>24		
349- 11	N		.0000	.0007	.0008	.0006	.0000	.0000	.0000	.0021
12- 33	NNE		.0001	.0008	.0009	.0003	.0001	.0000	.0000	.0023
34- 56	NE		.0002	.0006	.0003	.0001	.0000	.0000	.0000	.0013
57- 78	ENE		.0002	.0000	.0003	.0000	.0000	.0000	.0000	.0006
79-101	E		.0001	.0001	.0000	.0001	.0000	.0000	.0000	.0003
102-123	ESE		.0000	.0001	.0000	.0000	.0000	.0000	.0000	.0001
124-146	SE		.0002	.0005	.0006	.0001	.0000	.0000	.0000	.0014
147-168	SSE		.0002	.0013	.0018	.0008	.0000	.0000	.0000	.0041
169-191	S		.0002	.0014	.0008	.0001	.0000	.0000	.0000	.0025
192-213	SSW		.0001	.0005	.0003	.0001	.0000	.0000	.0000	.0010
214-236	SW		.0003	.0005	.0002	.0003	.0000	.0000	.0000	.0014
237-258	WSW		.0001	.0000	.0001	.0003	.0000	.0000	.0000	.0006
259-281	W		.0000	.0002	.0003	.0008	.0001	.0000	.0000	.0015
282-303	WNW		.0003	.0005	.0002	.0015	.0010	.0005	.0000	.0040
304-326	NW		.0000	.0000	.0001	.0001	.0010	.0006	.0000	.0018
327-348	NNW		.0003	.0005	.0005	.0007	.0006	.0000	.0000	.0025
Calm			.0000							.0000
Miss			.0000	.0000	.0000	.0000	.0002	.0001		.0006
Total			.0026	.0074	.0074	.0061	.0031	.0011	.0002	.0280

Indian Point B(3) Joint Frequency Distribution of Wind Speed and Direction for Pasquill Stability Category D - January 1, 1970-December 31, 1970.

Wind			Wind Speed (mph)						Miss	Total
Direction			01-03	04-07	08-12	13-18	19-24	>24		
349- 11	N		.0024	.0143	.0173	.0051	.0007	.0001	.0014	.0413
12- 33	NNE		.0042	.0178	.0122	.0029	.0006	.0001	.0014	.0392
34- 56	NE		.0031	.0078	.0026	.0003	.0003	.0000	.0006	.0147
57- 78	ENE		.0022	.0016	.0001	.0001	.0000	.0000	.0006	.0046
79-101	E		.0021	.0021	.0009	.0000	.0000	.0000	.0002	.0053
102-123	ESE		.0026	.0016	.0011	.0002	.0000	.0000	.0003	.0059
124-146	SE		.0025	.0053	.0038	.0003	.0002	.0000	.0001	.0122
147-168	SSE		.0023	.0110	.0098	.0032	.0000	.0000	.0003	.0266
169-191	S		.0025	.0098	.0053	.0010	.0000	.0000	.0003	.0190
192-213	SSW		.0030	.0038	.0021	.0008	.0000	.0000	.0000	.0096
214-236	SW		.0023	.0017	.0009	.0006	.0001	.0000	.0003	.0059
237-258	WSW		.0008	.0016	.0007	.0008	.0000	.0000	.0000	.0039
259-281	W		.0011	.0019	.0019	.0016	.0008	.0001	.0006	.0081
282-303	WNW		.0011	.0010	.0051	.0095	.0062	.0011	.0001	.0242

IP3
FSAR UPDATE

304-326	NW	.0010	.0019	.0061	.0109	.0074	.0026	.0000	.0300
327-348	NNW	.0009	.0054	.0069	.0079	.0022	.0002	.0002	.0237
Calm		.0000							.0000
Miss		.0000	.0000	.0000	.0001	.0005	.0000		.0010
Total		.0342	.0886	.0768	.0454	.0190	.0043	.0070	.2753

Appendix Table 1 (continued)

Indian Point B(3) Joint Frequency Distribution of Wind Speed and Direction for Pasquill Stability Category E – January 1, 1970-December 31, 1970.

Wind		Wind Speed (mph)						Miss	Total
Direction		01-03	04-07	08-12	13-18	19-24	>24		
349- 11	N	.0045	.0067	.0043	.0014	.0001	.0000	.0002	.0173
12- 33	NNE	.0045	.0166	.0080	.0005	.0003	.0000	.0006	.0304
34- 56	NE	.0030	.0078	.0019	.0001	.0001	.0000	.0008	.0137
57- 78	ENE	.0023	.0018	.0003	.0000	.0000	.0000	.0000	.0045
79-101	E	.0011	.0023	.0011	.0001	.0001	.0000	.0000	.0048
102-123	ESE	.0014	.0029	.0016	.0001	.0000	.0000	.0001	.0061
124-146	SE	.0027	.0035	.0017	.0001	.0003	.0000	.0001	.0086
147-168	SSE	.0022	.0053	.0041	.0016	.0005	.0002	.0000	.0138
169-191	S	.0017	.0062	.0043	.0003	.0002	.0003	.0001	.0133
192-213	SSW	.0027	.0063	.0045	.0005	.0000	.0000	.0000	.0139
214-236	SW	.0024	.0045	.0024	.0006	.0001	.0001	.0000	.0101
237-258	WSW	.0019	.0027	.0016	.0008	.0007	.0002	.0000	.0080
259-281	W	.0015	.0015	.0034	.0014	.0008	.0005	.0000	.0090
282-303	WNW	.0010	.0006	.0038	.0054	.0041	.0014	.0000	.0162
304-326	NW	.0008	.0017	.0054	.0071	.0016	.0005	.0001	.0171
327-348	NNW	.0017	.0034	.0046	.0027	.0001	.0000	.0001	.0127
Calm		.0000							.0000
Miss		.0005	.0007	.0009	.0007	.0010	.0000		.0048
Total		.0359	.0744	.0541	.0233	.0102	.0032	.0032	.2043

Indian Point B(3) Joint Frequency Distribution of Wind Speed and Direction for Pasquill Stability Category F – January 1, 1970-December 31, 1970

Wind		Wind Speed (mph)						Miss	Total
Direction		01-03	04-07	08-12	13-18	19-24	>24		
349- 11	N	.0047	.0022	.0008	.0001	.0000	.0000	.0000	.0078
12- 33	NNE	.0030	.0075	.0022	.0000	.0000	.0000	.0000	.0127
34- 56	NE	.0034	.0042	.0009	.0000	.0000	.0000	.0005	.0090
57- 78	ENE	.0015	.0011	.0001	.0000	.0000	.0000	.0000	.0027
79-101	E	.0011	.0005	.0000	.0000	.0000	.0000	.0000	.0016
102-123	ESE	.0010	.0006	.0000	.0000	.0000	.0000	.0000	.0016
124-146	SE	.0009	.0006	.0000	.0000	.0000	.0000	.0000	.0015
147-168	SSE	.0023	.0027	.0005	.0001	.0002	.0000	.0000	.0058
169-191	S	.0016	.0035	.0009	.0000	.0000	.0000	.0000	.0061

IP3
FSAR UPDATE

192-213	SSW	.0013	.0032	.0008	.0000	.0000	.0000	.0000	.0053
214-236	SW	.0024	.0040	.0006	.0000	.0000	.0000	.0001	.0071
237-258	WSW	.0018	.0009	.0009	.0000	.0000	.0000	.0001	.0038
259-281	W	.0011	.0003	.0003	.0000	.0003	.0000	.0001	.0023
282-303	WNW	.0007	.0002	.0003	.0002	.0001	.0001	.0000	.0017
304-326	NW	.0011	.0002	.0001	.0000	.0002	.0000	.0000	.0017
327-348	NNW	.0013	.0007	.0003	.0002	.0000	.0000	.0000	.0025
Calm		.0000							.0000
Miss		.0007	.0001	.0000	.0000	.0000	.0000		.0013
Total		.0300	.0327	.0088	.0007	.0009	.0001	.0013	.0744

Appendix Table 1 (Continued)

Indian Point B(3) Joint Frequency Distribution of Wind Speed and Direction for Pasquill Stability Category C – January 1, 1970-December 31, 1970.

Wind Direction		Wind Speed (mph)						Miss	Total
		01-03	04-07	08-12	13-18	19-24	>24		
349- 11	N	.0019	.0010	.0003	.0000	.0000	.0000	.0000	.0033
12- 33	NNE	.0018	.0037	.0008	.0000	.0000	.0000	.0001	.0064
34- 56	NE	.0030	.0021	.0000	.0000	.0000	.0000	.0000	.0050
57- 78	ENE	.0018	.0006	.0000	.0000	.0000	.0000	.0000	.0024
79-101	E	.0008	.0003	.0000	.0000	.0000	.0000	.0000	.0011
102-123	ESE	.0006	.0002	.0000	.0000	.0000	.0000	.0000	.0008
124-146	SE	.0014	.0007	.0000	.0000	.0000	.0000	.0000	.0021
147-168	SSE	.0013	.0014	.0002	.0000	.0000	.0000	.0000	.0029
169-191	S	.0009	.0015	.0005	.0000	.0000	.0000	.0000	.0029
192-213	SSW	.0024	.0024	.0003	.0000	.0000	.0000	.0002	.0054
214-236	SW	.0019	.0013	.0002	.0000	.0000	.0000	.0001	.0035
237-258	WSW	.0015	.0006	.0003	.0000	.0000	.0000	.0001	.0025
259-281	W	.0018	.0005	.0000	.0000	.0000	.0000	.0000	.0023
282-303	WNW	.0015	.0002	.0000	.0000	.0000	.0000	.0000	.0017
304-326	NW	.0011	.0000	.0000	.0000	.0000	.0000	.0000	.0011
327-348	NNW	.0015	.0005	.0001	.0001	.0000	.0000	.0000	.0022
Calm		.0000							.0000
Miss		.0000	.0000	.0000	.0000	.0000	.0000		.0008
Total		.0253	.0168	.0029	.0001	.0000	.0000	.0014	.0464

Appendix Table 2. Indian Point B(3) Point Frequency Distribution of Wind Speed and Direction for Pasquill Stability Category A - January 1, 1971-December 31, 1971

Wind Direction		Wind Speed (mph)						Miss	Total
		01-03	04-07	08-12	13-18	19-24	>24		
349- 11	N	.0006	.0054	.0057	.0021	.0011	.0000	.0001	.0150
12- 33	NNE	.0003	.0043	.0018	.0005	.0000	.0000	.0000	.0070

IP3
FSAR UPDATE

34- 56	NE	.0008	.0011	.0002	.0000	.0000	.0000	.0000	.0022
57- 78	ENE	.0001	.0008	.0000	.0000	.0000	.0000	.0000	.0009
79-101	E	.0000	.0000	.0002	.0000	.0000	.0000	.0000	.0002
102-123	ESE	.0001	.0005	.0005	.0001	.0000	.0000	.0000	.0011
124-146	SE	.0002	.0005	.0018	.0016	.0001	.0000	.0000	.0042
147-168	SSE	.0006	.0050	.0065	.0015	.0003	.0000	.0000	.0140
169-191	S	.0005	.0062	.0041	.0007	.0000	.0000	.0000	.0114
192-213	SSW	.0003	.0029	.0014	.0006	.0000	.0000	.0000	.0051
214-236	SW	.0003	.0015	.0007	.0005	.0000	.0000	.0000	.0030
237-258	WSW	.0003	.0018	.0011	.0024	.0009	.0003	.0000	.0070
259-281	W	.0003	.0009	.0039	.0022	.0017	.0002	.0000	.0093
282-303	WNW	.0008	.0008	.0042	.0050	.0027	.0009	.0000	.0145
304-326	NW	.0005	.0016	.0031	.0046	.0035	.0006	.0000	.0138
327-348	NNW	.0003	.0033	.0046	.0039	.0007	.0001	.0000	.0129
Calm		.0000							.0000
Miss		.0000	.0000	.0000	.0000	.0000	.0000		.0002
Total		.0062	.0366	.0399	.0255	.0112	.0022	.0003	.1219

Indian Point B(3) Joint Frequency Distribution of Wind Speed and Direction
for Pasquill Stability Category B – January 1, 1971-December 31, 1971.

Wind		Wind Speed (mph)						Miss	Total
Direction		01-03	04-07	08-12	13-18	19-24	>24		
349- 11	N	.0000	.0013	.0009	.0001	.0000	.0000	.0000	.0023
12- 33	NNE	.0000	.0008	.0000	.0000	.0000	.0000	.0000	.0008
34- 56	NE	.0002	.0001	.0001	.0000	.0000	.0000	.0000	.0005
57- 78	ENE	.0002	.0000	.0000	.0000	.0000	.0000	.0000	.0002
79-101	E	.0000	.0000	.0000	.0000	.0000	.0000	.0000	.0000
102-123	ESE	.0000	.0001	.0001	.0001	.0000	.0000	.0000	.0003
124-146	SE	.0000	.0001	.0003	.0002	.0000	.0000	.0000	.0007
147-168	SSE	.0002	.0008	.0014	.0001	.0001	.0000	.0000	.0026
169-191	S	.0002	.0009	.0000	.0000	.0000	.0000	.0000	.0011
192-213	SSW	.0003	.0008	.0002	.0001	.0000	.0000	.0000	.0015
214-236	SW	.0001	.0001	.0002	.0001	.0000	.0000	.0000	.0006
237-258	WSW	.0001	.0002	.0000	.0002	.0001	.0001	.0000	.0007
259-281	W	.0000	.0002	.0005	.0000	.0002	.0001	.0000	.0010
282-303	WNW	.0000	.0001	.0005	.0010	.0003	.0000	.0000	.0019
304-326	NW	.0005	.0002	.0003	.0006	.0003	.0001	.0000	.0021
327-348	NNW	.0000	.0003	.0002	.0006	.0000	.0000	.0000	.0011
Calm		.0000							.0000
Miss		.0000	.0000	.0000	.0000	.0000	.0000		.0000
Total		.0018	.0062	.0048	.0032	.0011	.0003	.0000	.0175

Z-79

70.

Appendix Table 2 (continued)

Indian Point B(3) Joint Frequency Distribution of Wind Speed and

IP3
FSAR UPDATE

Direction for Pasquill Stability Category C – January 1, 1971-
December 31, 1971.

Wind		Wind Speed (mph)						Miss	Total
Direction		01-03	04-07	08-12	13-18	19-24	>24		
349- 11	N	.0003	.0014	.0006	.0002	.0000	.0000	.0000	.0025
12- 33	NNE	.0001	.0006	.0006	.0001	.0000	.0000	.0001	.0015
34- 56	NE	.0001	.0003	.0001	.0000	.0000	.0000	.0000	.0006
57- 78	ENE	.0000	.0000	.0001	.0000	.0000	.0000	.0000	.0001
79-101	E	.0001	.0002	.0001	.0000	.0000	.0000	.0000	.0005
102-123	ESE	.0003	.0001	.0002	.0000	.0000	.0000	.0000	.0007
124-146	SE	.0001	.0003	.0005	.0000	.0000	.0000	.0000	.0009
147-168	SSE	.0001	.0006	.0003	.0002	.0000	.0000	.0000	.0013
169-191	S	.0005	.0011	.0005	.0002	.0000	.0000	.0000	.0023
192-213	SSW	.0000	.0005	.0001	.0000	.0000	.0000	.0000	.0006
214-236	SW	.0003	.0001	.0001	.0001	.0001	.0000	.0000	.0008
237-258	WSW	.0001	.0001	.0003	.0001	.0002	.0001	.0000	.0010
259-281	W	.0001	.0001	.0003	.0003	.0001	.0000	.0000	.0010
282-303	WNW	.0001	.0001	.0006	.0010	.0000	.0001	.0000	.0019
304-326	NW	.0003	.0002	.0002	.0005	.0003	.0000	.0000	.0016
327-348	NNW	.0000	.0007	.0007	.0001	.0001	.0000	.0000	.0016
Calm		.0000							.0000
Miss		.0000	.0000	.0000	.0000	.0000	.0000		.0000
Total		.0027	.0065	.0054	.0030	.0009	.0002	.0001	.0180

Indian Point B(3) Joint Frequency Distribution of Wind Speed and
Direction for Pasquill Stability Category D – January 1, 1971-
December 31, 1971.

Wind		Wind Speed (mph)						Miss	Total
Direction		01-03	04-07	08-12	13-18	19-24	>24		
349- 11	N	.0014	.0079	.0067	.0034	.0005	.0000	.0001	.0200
12- 33	NNE	.0023	.0066	.0050	.0015	.0000	.0000	.0000	.0154
34- 56	NE	.0029	.0026	.0014	.0005	.0000	.0000	.0001	.0074
57- 78	ENE	.0010	.0011	.0018	.0003	.0000	.0000	.0000	.0043
79-101	E	.0015	.0008	.0011	.0000	.0000	.0000	.0000	.0034
102-123	ESE	.0011	.0015	.0002	.0000	.0000	.0000	.0000	.0029
124-146	SE	.0013	.0026	.0026	.0008	.0001	.0000	.0000	.0074
147-168	SSE	.0013	.0040	.0065	.0014	.0001	.0000	.0000	.0133
169-191	S	.0015	.0030	.0014	.0009	.0001	.0000	.0000	.0069
192-213	SSW	.0009	.0017	.0018	.0006	.0000	.0001	.0000	.0051
214-236	SW	.0017	.0013	.0013	.0019	.0001	.0001	.0000	.0064
237-258	WSW	.0008	.0010	.0026	.0018	.0008	.0002	.0000	.0073
259-281	W	.0005	.0005	.0024	.0041	.0023	.0001	.0000	.0098
282-303	WNW	.0008	.0002	.0056	.0051	.0024	.0010	.0003	.0156
304-326	NW	.0009	.0002	.0031	.0055	.0014	.0000	.0001	.0112
327-348	NNW	.0003	.0010	.0039	.0019	.0008	.0001	.0001	.0082
Calm			.0000						.0000
Miss			.0000	.0000	.0000	.0000	.0000	.0000	.0001

IP3
FSAR UPDATE

Total	.0201	.0361	.0476	.0298	.0086	.0017	.0009	.1449
-------	-------	-------	-------	-------	-------	-------	-------	-------

Z-80

71.

Appendix Table 2 (continued)

Indian Point B (3) Joint Frequency Distribution of Wind Speed and Direction for Pasquill Stability Category E – January 1, 1971-December 31, 1971.

Wind			Wind Speed (mph)							
Direction			01-03	04-07	08-12	13-18	19-24	>24	Miss	Total
349- 11	N		.0027	.0072	.0094	.0037	.0013	.009	.0001	.0253
12- 33	NNE		.0029	.0144	.0129	.0019	.0002	.0000	.0000	.0324
34- 56	NE		.0035	.0063	.0019	.0001	.0001	.0000	.0010	.0130
57- 78	ENE		.0021	.0021	.0014	.0000	.0000	.0000	.0002	.0057
79-101	E		.0016	.0021	.0001	.0000	.0000	.0000	.0000	.0038
102-123	ESE		.0015	.0034	.0006	.0000	.0000	.0000	.0000	.0055
124-146	SE		.0019	.0063	.0024	.0002	.0000	.0000	.0000	.0109
147-168	SSE		.0016	.0061	.0058	.0009	.0000	.0000	.0000	.0144
169-191	S		.0019	.0058	.0038	.0009	.0001	.0000	.0000	.0126
192-213	SSW		.0016	.0034	.0031	.0005	.0002	.0000	.0000	.0088
214-236	SW		.0010	.0013	.0015	.0008	.0002	.0000	.0000	.0048
237-258	WSW		.0017	.0014	.0026	.0014	.0005	.0002	.0000	.0078
259-281	W		.0006	.0015	.0050	.0025	.0009	.0001	.0000	.0106
282-303	WNW		.0006	.0015	.0051	.0051	.0024	.0006	.0010	.0164
304-326	NW		.0005	.0010	.0063	.0054	.0013	.0003	.0001	.0149
327-348	NNW		.0008	.0016	.0035	.0030	.0006	.0001	.0000	.0096
Calm			.0000							.0000
Miss			.0000	.0000	.0000	.0000	.0000			.0000
Total			.0265	.0653	.0655	.0264	.0078	.0023	.0025	.1963

Indian Point B(3) Joint Frequency Distribution of Wind Speed and Direction for Pasquill Stability Category F – January 1, 1971-December 31, 1971.

Wind			Wind Speed (mph)							
Direction			01-03	04-07	08-12	13-18	19-24	>24	Miss	Total
349-	11	N	.0019	.0042	.0015	.0001	.0000	.0000	.0000	.0078
12-	33	NNE	.0026	.0113	.0029	.0000	.0000	.0000	.0000	.0168
34-	56	NE	.0024	.0046	.0008	.0000	.0000	.0000	.0000	.0078
57-	78	ENE	.0010	.0009	.0000	.0000	.0000	.0000	.0000	.0019
79-	101	E	.0008	.0003	.0001	.0000	.0000	.0000	.0000	.0013
102-	123	ESE	.0011	.0005	.0000	.0000	.0000	.0000	.0000	.0016
124-	146	SE	.0010	.0023	.0000	.0000	.0000	.0000	.0000	.0033
147-	168	SSE	.0013	.0024	.0005	.0001	.0000	.0000	.0000	.0042
169-	191	S	.0014	.0040	.0002	.0001	.0000	.0000	.0000	.0057
192-	213	SSW	.0016	.0030	.0006	.0001	.0000	.0000	.0000	.0053
214-	236	SW	.0008	.0023	.0005	.0008	.0000	.0000	.0000	.0043
237-	258	WSW	.0010	.0016	.0007	.0001	.0002	.0000	.0000	.0037

IP3
FSAR UPDATE

259-281	W	.0007	.0011	.0008	.0001	.0000	.0000	.0000	.0027
282-303	WNW	.0013	.0005	.0007	.0005	.0001	.0000	.0000	.0030
304-326	NW	.0006	.0008	.0003	.0000	.0000	.0001	.0000	.0018
327-348	NNW	.0010	.0014	.0006	.0001	.0000	.0000	.0000	.0031
Calm		.0000							.0000
Miss		.0000	.0000	.0000	.0000	.0000	.0000		.0000
Total		.0206	.0412	.0101	.0021	.0003	.0001	.0000	.0743

Z-81

72.

Appendix Table 2 (continued)

Indian Point B(3) Joint Frequency Distribution of Wind Speed and Direction for Pasquill Stability Category G – January 1, 1971-December 31, 1971.

Wind		Wind Speed (mph)							Total
Direction		01-03	04-07	08-12	13-18	19-24	>24	Miss	
349- 11	N	.0031	.0034	.0005	.0000	.0000	.0000	.0000	.0070
12- 33	NNE	.0027	.0064	.0008	.0000	.0000	.0000	.0000	.0099
34- 56	NE	.0031	.0026	.0000	.0000	.0000	.0000	.0000	.0057
57- 78	ENE	.0019	.0003	.0000	.0000	.0000	.0000	.0000	.0023
79-101	E	.0009	.0006	.0000	.0000	.0000	.0000	.0000	.0015
102-123	ESE	.0009	.0001	.0000	.0000	.0000	.0000	.0000	.0010
124-146	SE	.0013	.0005	.0000	.0001	.0000	.0000	.0000	.0018
147-168	SSE	.0016	.0019	.0002	.0001	.0000	.0000	.0000	.0039
169-191	S	.0024	.0030	.0000	.0000	.0000	.0000	.0000	.0054
192-213	SSW	.0027	.0027	.0000	.0000	.0000	.0000	.0000	.0055
214-236	SW	.0022	.0016	.0003	.0000	.0000	.0000	.0000	.0041
237-258	WSW	.0019	.0013	.0002	.0001	.0000	.0000	.0000	.0035
259-281	W	.0021	.0007	.0002	.0000	.0000	.0000	.0000	.0030
282-303	WNW	.0014	.0002	.0002	.0000	.0000	.0000	.0000	.0018
304-326	NW	.0013	.0007	.0000	.0000	.0000	.0000	.0000	.0019
327-348	NNW	.0022	.0011	.0002	.0000	.0000	.0000	.0000	.0035
Calm		.0000							.0000
Miss		.0000	.0000	.0000	.0000	.0000	.0000		.0000
Total		.0317	.0272	.0027	.0003	.0000	.0000	.0000	.0620

Z-82